
Analysis of the DNA damage response in living cells

Oliver Mortusewicz



München 2007

Analysis of the DNA damage response in living cells

Oliver Mortusewicz

Dissertation
an der Fakultät für Biologie
der Ludwig-Maximilians-Universität
München

vorgelegt von
Oliver Mortusewicz
aus Giessen

München, den 08. November 2007

Erstgutachter: Prof. Dr. Heinrich Leonhardt
Zweitgutachter: Prof. Dr. Manfred Schliwa

Tag der mündlichen Prüfung: 19.12.2007

CONTENT

CONTENT **1**

SUMMARY **3**

1. INTRODUCTION **7**

- 1.1. DNA lesion detection and signalling 9
- 1.2. Checkpoint activation 12
- 1.3. Repair of genetic information 13
- 1.4. Repair of epigenetic information 16
- 1.5. A new assay to study protein-protein interactions in living cells 18
- 1.6. Technical Background 19

2. RESULTS **23**

- 2.1. Feedback regulated poly(ADP-ribosyl)ation by PARP-1 is required for rapid response to DNA damage in living cells. 23
- 2.2. Recruitment of RNA Polymerase II cofactor PC4 to DNA repair sites. 41
- 2.3. Spatiotemporal dynamics of p21CDKN1A protein recruitment to DNA damage sites and interaction with proliferating cell nuclear antigen. 71
- 2.4. XRCC1 and PCNA are loading platforms with distinct kinetic properties and different capacities to respond to multiple DNA lesions. 87
- 2.5. Differential recruitment of DNA Ligase I and III to DNA repair sites. 99
- 2.6. Recruitment of DNA methyltransferase 1 to DNA repair sites. 119
- 2.7. A fluorescent two-hybrid (F2H) assay for direct visualization of protein interactions in living cells. 129

3. DISCUSSION **159**

- 3.1. DNA lesion detection and signalling 160
- 3.2. The role of p21 in DNA repair 163
- 3.3. Coordination of DNA repair by central loading platforms 164
- 3.4. Maintenance of DNA methylation patterns in DNA repair 167
- 3.5. A new assay to visualize protein-protein interactions in living cells 169

4. ANNEX **171**

- 4.1. Abbreviations 171
- 4.2. Contributions 173
- 4.3. Acknowledgements 177
- 4.4. References 179

5. CURRICULUM VITAE **191**



SUMMARY

DNA lesions arising from environmental and endogenous sources induce various cellular responses including cell cycle arrest, DNA repair and apoptosis. Although detailed insights into the biochemical mechanisms and composition of DNA repair pathways have been obtained from *in vitro* experiments, a better understanding of the interplay and regulation of these pathways requires DNA repair studies in living cells.

In this study we employed laser microirradiation and photobleaching techniques in combination with specific mutants and inhibitors to analyze the real-time accumulation of proteins at laser-induced DNA damage sites *in vivo*, thus unravelling the mechanisms underlying the coordination of DNA repair in living cells.

The immediate and faithful recognition of DNA lesions is central to cellular survival, but how these lesions are detected within the context of chromatin is still unclear. *In vitro* data indicated that the DNA-damage dependent poly(ADP-ribose) polymerases, PARP-1 and PARP-2, are involved in this crucial step of DNA repair. With specific inhibitors, mutations and photobleaching analysis we could reveal a complex feedback regulated mechanism for the recruitment of the DNA damage sensor PARP-1 to microirradiated sites. Activation of PARP-1 results in localized poly(ADP-ribosyl)ation and amplifies a signal for the subsequent rapid recruitment of the loading platform XRCC1 which coordinates the assembly of the repair machinery.

Using similar techniques we could demonstrate the immediate and transient binding of the RNA Polymerase II cofactor PC4 to DNA damage sites, which depended on its single strand binding capacity. This establishes an interesting link between DNA repair and transcription. We propose a role for PC4 in the early steps of the DNA damage response, recognizing and stabilizing single stranded DNA (ssDNA) and thereby facilitating DNA repair by enabling repair factors to access their substrates.

After DNA lesions have been successfully detected they have to be handed over to the repair machinery which restores genome integrity. Efficient repair requires the coordinated recruitment of multiple enzyme activities which is believed to be controlled by central loading platforms. As laser microirradiation induces a variety of different DNA lesions we could directly compare the recruitment kinetics of the two loading platforms PCNA and XRCC1 which are involved in different repair pathways side by side. We could demonstrate that PCNA and XRCC1 show distinct recruitment and binding kinetics with the immediate and fast recruitment of XRCC1 preceding the

slow and continuous recruitment of PCNA. Introducing consecutively multiple DNA lesions within a single cell, we further demonstrated that these different recruitment and binding characteristics have functional consequences for the capacity of PCNA and XRCC1 to respond to successive DNA damage events.

To further study the role of PCNA and XRCC1 as loading platforms in DNA repair, we extended our analysis to their respective interaction partners DNA Ligase I and III. Although these DNA Ligases are highly homologous and catalyze the same enzymatic reaction, they are not interchangeable and fulfil unique functions in DNA replication and repair. With deletion and mutational analysis we could identify domains mediating the specific recruitment of DNA Ligase I and III to distinct repair pathways through their interaction with PCNA and XRCC1. We conclude that this specific targeting may have evolved to accommodate the particular requirements of different repair pathways (single nucleotide replacement vs. synthesis of short stretches of DNA) and thus enhances the efficiency of DNA repair.

Interestingly, we found that other PCNA-interacting proteins exhibit recruitment kinetics similar to DNA Ligase I, indicating that PCNA not only serves as a central loading platform during DNA replication, but also coordinates the recruitment of multiple enzyme activities to DNA repair sites. Accordingly, we found that the maintenance methyltransferase DNMT1, which is known to associate with replication sites through binding to PCNA, is likewise recruited to DNA repair sites by PCNA. We propose that DNMT1, like in DNA replication, preserves methylation patterns in the newly synthesized DNA, thus contributing to the restoration of epigenetic information in DNA repair.

In summary, we found immediate and transient binding of repair factors involved in DNA damage detection and signalling, while repair factors involved in the later steps of DNA repair, like damage processing, DNA ligation and restoration of epigenetic information, showed a slow and persistent accumulation at DNA damage sites. We conclude that DNA repair is not mediated by binding of a preassembled repair machinery, but rather coordinated by the sequential recruitment of specific repair factors to DNA damage sites.

1. INTRODUCTION

DNA repair – a complex response to a lethal threat

Mammalian cells are constantly threatened by multiple types of DNA lesions arising from various sources like irradiation, environmental agents, replication errors or by-products of the normal cellular metabolism. If not readily detected and repaired these lesions can lead to cell death or to the transformation of cells giving rise to serious diseases like cancer. Consequently, multiple specialized repair pathways have evolved to preserve the genetic integrity of a cell (**Figure 1**).

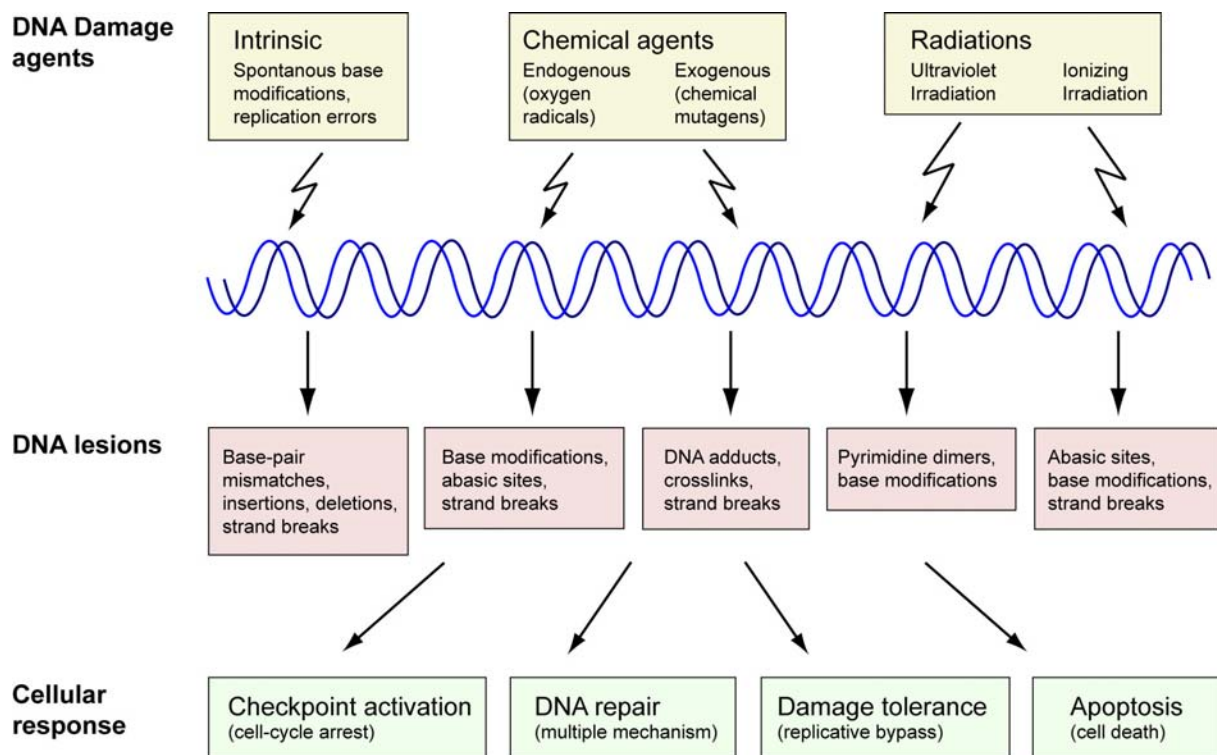


Figure 1 Cellular responses to DNA damage. Different types of DNA damage agents cause different lesions which induce various cellular responses ranging from checkpoint activation to cell death.

The DNA damage response is a multistep process involving lesion detection, processing of repair intermediates, checkpoint activation and finally restoration of the genetic and epigenetic information (**Figure 2**). Given the increasing number of DNA damage sensors, checkpoint regulators and repair factors identified in the numerous interconnected repair pathways raises the question of how DNA repair is coordinated. Furthermore, it is still unclear how specific repair factors gain access to their respective substrates. DNA lesions might be detected through continuous scanning of the genome or by high affinity binding and transient immobilization of freely diffusing proteins (assembly on the spot). It has also been proposed that instead of being directly sensed, DNA lesions might rather be indirectly detected through

changes in chromatin topology (Bakkenist and Kastan, 2003). Once the DNA damage has been successfully detected it has to be handed over to the repair machinery which then restores the genetic information. This could either be achieved through competition between different repair proteins binding at the lesion site, or alternatively, a rapid turnover of repair factors could generate a window of opportunity for every factor to bind, enabling a more flexible access. Finally, after the genetic information has been successfully restored, the epigenetic information including methylation patterns and chromatin states has to be re-established.

We addressed several of these questions using a combination of laser microirradiation, live cell microscopy and photobleaching analysis to gain insights into the spatio-temporal coordination of DNA repair factors ranging from damage detection to restoration of genome integrity.

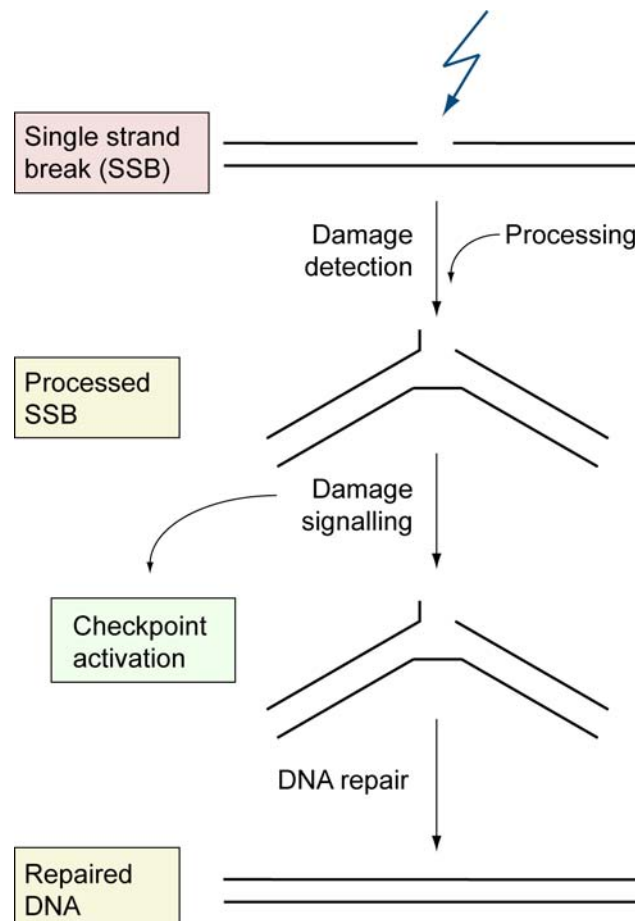


Figure 2 Basic steps in DNA repair, exemplary illustrated for the single strand break repair pathway. DNA lesions are detected by DNA damage sensors which trigger the DNA damage response, resulting in lesion processing, checkpoint activation and finally DNA repair.

1.1. DNA lesion detection and signalling

Lesion detection and signalling by the DNA-damage-dependent Poly(ADP-ribose) polymerases PARP-1 and PARP-2

Cellular survival depends on the immediate recognition of DNA lesions and rapid recruitment of repair factors. A central surveillance factor, which is believed to play an important role in damage recognition and signalling is the poly(ADP-ribose) polymerase-1 (PARP-1). PARP-1 is the founding member of the PARP family encompassing 17 members involved in various biological processes such as DNA repair, transcription, mitotic segregation, telomere homeostasis and cell death (Schreiber et al., 2006). *In vitro* studies indicated that PARP-1 either directly senses single strand breaks (SSBs) or detects DNA breaks, resulting from the processing of damaged bases by the single strand break repair (SSBR) or base excision repair (BER) pathway, through its two zinc fingers (Gradwohl et al., 1990).

Upon binding its substrate, PARP-1 becomes activated and catalyzes the polymerization of ADP-ribose moieties from NAD⁺ on target proteins, a post-translational modification called poly(ADP-ribosyl)ation. Albeit automodifying itself, PARP-1 poly(ADP-ribosyl)ates histones leading to chromatin relaxation. Several proteins were reported to interact with poly(ADP-ribose) (PAR) or poly(ADP-ribosyl)ated PARP-1 suggesting that PAR may serve as a recruiting molecule (Pleschke et al., 2000).

Besides PARP-1, PARP-2 is the only DNA-damage-dependent PARP identified so far. Several lines of evidence obtained from knock-out mice and cells suggest that PARP-1 and PARP-2 have both overlapping and non-redundant functions in DNA repair (de Murcia et al., 1997; Masutani et al., 1999; Menissier de Murcia et al., 2003; Schreiber et al., 2002; Trucco et al., 1998; Wang et al., 1997). Biochemical studies revealed that PARP-2, like PARP-1, interacts with the SSBR/BER repair factors XRCC1, DNA polymerase β and DNA Ligase III (Ame et al., 1999; Schreiber, 2004). PARP-1 and PARP-2 can heterodimerize, but they recognize different targets within DNA (Schreiber, 2004). PARP-2 does not recognize SSBs, but gaps or flap structures, which indicates that PARP-2 is probably involved in the later steps of the repair process (Schreiber et al., 2002). However, the exact cellular function of PARP-2 remains to be elucidated.

As most data on the role and regulation of PARP-1 and PARP-2 are derived from biochemical experiments, we systematically investigated the kinetics, role and

interplay of PARP-1 and PARP-2 in living cells. We found that both PARPs are recruited to DNA damage sites, however with different kinetics and roles. Our data indicate that the initial step of the damage response is mediated by a feedback regulated accumulation of PARP-1 and concomitant local poly(ADP-ribosyl)ation leading to a rapid recruitment of repair factors.

Role of the RNA Polymerase II cofactor PC4 in the early steps of DNA repair

The positive cofactor 4 (PC4) is a multifunctional nuclear protein involved in various cellular processes including transcription, replication and chromatin organization (Das et al., 2006; Ge and Roeder, 1994; Kretzschmar et al., 1994; Pan et al., 1996). Originally, PC4 was identified as a positive cofactor enhancing activator-dependent transcription by RNA polymerase II (Ge and Roeder, 1994; Kretzschmar et al., 1994; Meisterernst et al., 1991). Expression of class II genes in eukaryotes is a complex and highly regulated process mediated by the basic transcription machinery consisting of general transcription factors and RNA Polymerase II. Moreover, transcription is further regulated by additional cofactors (Blazek et al., 2005; Kaiser and Meisterernst, 1996; Malik and Roeder, 2000; Thomas and Chiang, 2006). One of these cofactors is PC4, which has been shown to facilitate the formation of the preinitiation complex (PIC), thereby enhancing the transcriptional activation potential of gene-specific activators (Kaiser et al., 1995). Furthermore, PC4 interacts with TFIIA a component of the basic transcription machinery (Ge and Roeder, 1994; Kretzschmar et al., 1994) and has been shown to bind to TFIIIB in yeast (Knaus et al., 1996). These findings imply that PC4 connects gene-specific regulators and the basal transcription machinery during PIC formation, by direct interaction with the TFIIA-TBP-complex and the activation domains of transcriptional regulators (Ge and Roeder, 1994; Kretzschmar et al., 1994). However, PC4 also seems to function as a transcriptional repressor in a minimal transcription system lacking an activator (Werten et al., 1998; Wu and Chiang, 1998). The complex role of PC4 in transcription is further underlined by recent findings showing that PC4 is also involved in promoter release, transcription elongation (Fukuda et al., 2004) and polyadenylation (Calvo and Manley, 2001).

PC4 has a bipartite structure consisting of an N-terminal regulatory domain (amino acid residues 1-62), which mediates protein-protein interactions and is essential for coactivator functions and a C-terminal domain (CTD, amino acid residues 63-127)

which allows sequence-independent binding to single and double stranded DNA (Kaiser et al., 1995; Kretzschmar et al., 1994; Werten et al., 1998). Structural analysis revealed that PC4 homodimerizes through its CTD and that the dimeric fold provides a binding surface for two anti-parallel single-stranded DNAs (Brandsen et al., 1997; Werten and Moras, 2006). Through comparison with the RPA-ssDNA co-crystal structure (Bochkarev et al., 1997), critical amino acid residues within the CTD of PC4 predicted to be essential for ssDNA binding were identified and mutated. These mutations abolished the binding of PC4 to ssDNA and resulted in the loss of its potential to repress transcription (Werten et al., 1998). The N-terminal domain of PC4 contains a so called SEAC motif, which was shown to be a target of casein kinase II (CKII) phosphorylation (Kretzschmar et al., 1994), regulating the activity of PC4 in mammalian cells (Ge et al., 1994). Phosphorylation of PC4 has been shown to revoke its coactivator and dsDNA binding activities, but maintains its ability to bind to ssDNA to mediate transcriptional repression (Ge et al., 1994; Werten et al., 1998). PC4 was recently identified in a screen for human genes suppressing an oxidative mutagenesis phenotype in *E. coli*. Moreover, it was found that the ssDNA binding capacity of PC4 is required for resistance to hydrogen peroxide (H₂O₂) and prevents spontaneous and induced oxidative mutagenesis in *E. coli* and *S. cerevisiae* (Wang et al., 2004). While this study suggests a role for PC4 in DNA repair, the direct involvement of PC4 in the mammalian DNA damage response remains elusive. To gain further insights into the potential role of PC4 in DNA repair, we studied its recruitment and binding dynamics at laser-induced DNA damage sites in living cells. We found a very rapid and transient accumulation of PC4 at DNA damage sites which depended on its ability to bind ssDNA, which argues for a role of PC4 in the very early steps of DNA repair.

1.2. Checkpoint activation

Recruitment of the cyclin-dependent kinase inhibitor p21 to DNA repair sites

A central mechanism of the DNA damage response is the activation of cell cycle checkpoints to prevent spreading of unrepaired DNA lesions to daughter cells. Depending on the damage extent, different cellular responses can be induced including cell death through apoptosis, induction of cellular senescence or cell survival after successful DNA repair (Bartek and Lukas, 2007). Failure of checkpoint activation can have severe consequences. This is highlighted by the fact that defects in checkpoint components like p53 and ATM are found in nearly all human cancer types (Bartek et al., 2004). The cyclin-dependent kinase inhibitor p21 plays a central role in the DNA damage response by inducing cell cycle arrest and inhibiting DNA replication through stable association with proliferating cell nuclear antigen (PCNA). Additionally, p21 has been shown to be involved in several other cellular pathways like growth arrest, senescence, terminal differentiation and transcription regulation (reviewed in (Coqueret, 2003; Dotto, 2000)). Whether or not p21 is directly involved in DNA repair is still controversial. While some studies indicate that high levels of p21 inhibit DNA repair (Cooper et al., 1999; Pan et al., 1995; Podust et al., 1995) others have shown that p21 has no negative (McDonald et al., 1996; Sheikh et al., 1997; Shivji et al., 1998; Shivji et al., 1994) or even a stimulating effect on DNA repair (Li et al., 1996; Ruan et al., 1998; Savio et al., 1996). Furthermore, it has been shown that p21 must be degraded for S phase entry to prevent binding to PCNA which would inhibit DNA replication (Bornstein et al., 2003; Gottifredi et al., 2004). However, whether p21 inhibits recruitment of PCNA to DNA repair sites or loading of other factors to PCNA is still under debate. We investigated whether p21 induction might inhibit DNA repair by interfering with PCNA accumulation at DNA damage sites and studied the recruitment kinetics of p21 to laser-induced DNA damage sites in living cells. Interestingly, we found that p21 is recruited to DNA damage sites, albeit with slower kinetics than PCNA. These results indicate that p21 is involved in DNA repair.

1.3. Repair of genetic information

Role and dynamics of the loading platforms PCNA and XRCC1 in DNA repair

DNA repair requires the coordinated recruitment of multiple enzyme activities to ensure efficient repair of DNA lesions. So called loading platforms are considered to play a central role by locally concentrating and coordinating repair factors at sites of DNA damage. Loading platforms are characterized as proteins with no intrinsic enzymatic activity and the ability to interact with numerous proteins through highly conserved binding motifs. The two repair factors XRCC1 (X-ray cross complementing factor 1) and PCNA both fulfil these criteria and are therefore considered to act as central loading platforms in DNA replication and repair (Caldecott, 2003; Maga and Hubscher, 2003; Moldovan et al., 2007; Warbrick, 2000). XRCC1 was first identified in a mutant cell line which shows a defect in SSBR and increased sensitivity to alkylating agents and ionizing irradiation resulting in elevated frequency of spontaneous chromosome aberrations and deletions (Thompson et al., 1982). Consistent with these results XRCC1 was found to interact with various proteins involved in SSBR and BER including PARP-1, PARP-2 (Masson et al., 1998; Schreiber et al., 2002), DNA polymerase- β (Caldecott et al., 1994; Kubota et al., 1996) and DNA Ligase III (Caldecott et al., 1994; Wei et al., 1995). Recently, it was reported that XRCC1 interacts with PCNA, another central loading platform involved in DNA repair and replication (Fan et al., 2004).

PCNA forms a homotrimeric ring around the DNA which at the same time allows stable association with and sliding along the DNA double helix. Because of this unique property PCNA is often referred to as a “sliding clamp” which is capable of mediating interactions of various proteins with DNA in a sequence-independent manner. Apart from being a central component of the replication machinery, PCNA is also involved in various repair pathways including nucleotide excision repair (NER) (Shivji et al., 1992), base excision repair (BER) (Gary et al., 1999; Levin et al., 2000), mismatch repair (MMR) (Jiricny, 2006; Johnson et al., 1996; Umar et al., 1996) and repair of double strand breaks (DSBs) (Dorazi et al., 2006; Holmes and Haber, 1999). In addition, PCNA is implicated in the coordination of postreplicative processes such as cytosine methylation and chromatin assembly (Chuang et al., 1997; Moggs et al., 2000). Most of the PCNA-interacting proteins bind to a common site on PCNA through a conserved PCNA-binding domain (PBD). The increasing number of identified PCNA-interacting proteins raises the question of how binding is coordinated

and sterical hindrance avoided in various processes such as DNA replication and repair. Recently, it has been shown that posttranslational modifications such as ubiquitylation and sumoylation target PCNA to different repair pathways (Hoege et al., 2002; Matunis, 2002; Papouli et al., 2005; Pfander et al., 2005; Solomon et al., 2004; Stelter and Ulrich, 2003). In order to gain insights into the spatio-temporal accumulation of PCNA and XRCC1 at DNA repair sites and their ability to respond to successive DNA damage events, we used a combination of repeated microirradiation, live cell microscopy and photobleaching techniques. We found that the two loading platforms XRCC1 and PCNA exhibit distinct recruitment and binding kinetics at repair sites resulting in different capacities to respond to successive DNA damage events.

Recruitment of DNA Ligase I and III to DNA repair sites

To complete repair of the genetic information the integrity of the phosphodiester backbone has to be re-established. This reaction is catalyzed by members of the ATP-dependent DNA Ligase family which consists of three enzymes termed DNA Ligase I, III and IV. Although all three DNA Ligases catalyze the same basic reaction and contain a highly conserved catalytic domain they are not interchangeable and have distinct cellular functions (Martin and MacNeill, 2002; Timson et al., 2000). DNA Ligase I is required for joining of Okazaki fragments during lagging strand synthesis and is implicated in long-patch or replicative BER and NER. DNA Ligase I is targeted to replication sites through its PBD-mediated interaction with PCNA (Cardoso et al., 1997; Montecucco et al., 1995). Loss of DNA Ligase I function leads to abnormal joining of Okazaki fragments during S phase (Mackenney et al., 1997), defective long-patch BER (Levin et al., 2000) and reduced repair of DSBs by homologous recombination (Goetz et al., 2005).

DNA Ligase III is implicated in short-patch BER and SSBR and *in vivo* exists as a preformed complex with XRCC1 (Caldecott et al., 1994; Cappelli et al., 1997; Wei et al., 1995). The interaction of DNA Ligase III with XRCC1 is mediated by the carboxy terminal BRCT (BRCA1 carboxy terminal) domain of DNA Ligase III (Beernink et al., 2005; Dulic et al., 2001; Taylor et al., 1998b). DNA Ligase III possesses a unique N-terminal zinc finger which was suggested to bind SSBs (Mackey et al., 1999) and shows homology with the two zinc finger motifs of PARP-1 which also binds DNA strand breaks. The recent identification of DNA Ligase III as a candidate component of the nonhomologous end joining (NHEJ) backup pathway (B-NHEJ) (Wang et al.,

2005) indicates that DNA Ligase III might also be implicated in double strand break repair (DSBR).

The last member of the ATP-dependent DNA Ligase family, DNA Ligase IV, plays a central role in the NHEJ pathway and forms a complex with XRCC4 (Critchlow et al., 1997; Grawunder et al., 1997). The importance of DNA Ligase IV functions for various cellular processes is highlighted by defects in V(D)J recombination, increased sensitivity to ionizing radiation and embryonic lethality in mice lacking DNA Ligase IV (Barnes et al., 1998; Frank et al., 1998).

To shed light on the mechanisms mediating the unique functions of the highly conserved ATP-dependent DNA Ligases, we compared their recruitment to laser-induced DNA damage sites in living cells. We could detect only a weak accumulation of DNA Ligase IV at laser-induced DNA damage sites. Kinetic studies and deletion analysis indicated that selective recruitment of DNA Ligase I and III to specific repair pathways is mediated through interaction with PCNA and XRCC1, respectively. These results suggest that PCNA and XRCC1 play a central role in the spatio-temporal coordination of repair factors and thereby enhance the specificity and efficiency of DNA repair in eukaryotic cells.

1.4. Repair of epigenetic information

Recruitment of DNA methyltransferase 1 to DNA repair sites

Numerous DNA repair pathways re-establishing the genetic information are known and have been extensively described (Friedberg, 2003; Hoeijmakers, 2001). In contrast, much less is known about enzymes and mechanisms involved in the restoration of the epigenetic information. Epigenetic information is defined as the information which is not contained within the basic sequence of DNA, but is nevertheless maintained over multiple cell divisions. There are two main epigenetic marks, DNA methylation and histone modifications which are essential for cell type specific gene expression (Becker, 2006; Berger, 2007; Bird, 2007; Jaenisch and Bird, 2003; Leonhardt and Cardoso, 2000; Reik, 2007; Robertson, 2002). Recently, it has become more and more evident that during DNA repair chromatin is extensively modified, remodelled and finally restored similar to what has been initially described for chromatin states during transcription (reviewed in: (Downs et al., 2007; Groth et al., 2007; van Attikum and Gasser, 2005)). In contrast, the problem of restoring and thus maintaining the methylation pattern during DNA repair has not been addressed. DNA methylation is a postreplicative modification which occurs mostly at cytosine residues of CpG dinucleotides and is essential for mammalian development (Li et al., 1992), parental imprinting (Li et al., 1993), X inactivation (Panning and Jaenisch, 1996) and genome stability (Brown and Robertson, 2007; Chen et al., 2007; Eden et al., 2003; Espada et al., 2007; Gaudet et al., 2003). In mammalian cells DNA methylation is carried out by members of the DNA methyltransferase family which can be subdivided into maintenance methyltransferases (DNMT1) and *de novo* methyltransferases (DNMT3a, DNMT3b) (Bestor, 2000). The maintenance methyltransferase DNMT1 is ubiquitously expressed and has a preference for hemimethylated sites generated during replication. The association of DNMT1 with the processivity factor PCNA ensures faithful maintenance of the methylation pattern during S phase (Chuang et al., 1997; Leonhardt et al., 1992). In contrast to DNMT1, the two *de novo* methyltransferases DNMT3a and DNMT3b (in concert with DNMT3L) establish new methylation patterns during development and show a low and tissue specific expression (Okano et al., 1999; Okano et al., 1998; Xu et al., 1999). The requirement of maintaining methylation patterns was recently underscored by several studies using DNMT1 knock-out or knock-down approaches. Loss of DNMT1 and accompanying hypomethylation leads to altered gene

expression, development defects, onset of cancer, genome instability and cell death (Brown and Robertson, 2007; Chen et al., 2007; Espada et al., 2007; Gaudet et al., 2003; Gaudet et al., 2004; Spada et al., 2007). These results clearly demonstrate the importance of DNA methylation, and raise the question whether and how this epigenetic information is maintained during DNA repair. We therefore investigated whether and which DNA methyltransferases are present at DNA repair sites. We could show that the maintenance methyltransferase DNMT1 is recruited to laser-induced DNA damage sites in S and non S cells in a PCNA-dependent manner, while the two *de novo* methyltransferases DNMT3a and DNMT3b were not recruited. These results argue for a role of DNMT1 in maintaining methylation patterns in DNA repair.

1.5. A new assay to study protein-protein interactions in living cells

As more and more proteins participating in the various DNA damage response pathways are identified, it becomes essential to reveal their complex interaction network to gain insights into the mechanisms and coordination of DNA repair. A wide variety of different methods to study protein-protein interactions, ranging from biochemical to genetic or cell-based approaches, have been introduced in recent years. The classical genetic yeast two-hybrid (Y2H) assay enables screening of hundreds or even thousands of interactions within the cellular environment but the read out involving transcriptional activation leads to many false positive and false negative results (Parrish et al., 2006; Suter et al., 2006). In contrast, biochemical methods like affinity purification, pull down analyses or immunoprecipitation allow direct detection of protein-protein interactions *in vitro*. Recent advances in fluorescence microscopy and molecular biology lead to the introduction of new fluorescence-based methods for in-cell visualization of protein-protein interactions. Fluorescence resonance energy transfer (FRET) (Miyawaki, 2003; Sekar and Periasamy, 2003) and bimolecular fluorescence complementation (BiFC) (Kerppola, 2006) are two well-established methods which rely on the expression of fluorescently labelled proteins or fragments thereof and allow to study protein-protein interactions in potentially any (living) cell.

We developed a new method for direct visualization of protein-protein interactions in living cells termed fluorescence two-hybrid (F2H) assay. This assay relies on the immobilization of a fluorescent bait protein at a given cellular structure. Interaction of a differently labelled prey protein with the bait protein results in colocalization of the fluorescent signals which can be visualized by microscopy. In our approach we chose a *lac* operator array stably integrated into BHK and U2OS cells (Janicki et al., 2004; Tsukamoto et al., 2000) to immobilize a triple fusion bait protein consisting of a fluorescent protein (FP), the Lac repressor (LacI) and a protein to be tested for interactions. Binding of this fusion protein to the *lac* operator array results in focal enrichment of the fluorescent signal in the nucleus. Interaction with a second differently labelled protein of interest (prey) can then be detected by colocalization of the fluorescent signals at the *lac* operator array. Using this F2H assay we could observe various interactions between different repair factors. In addition, we could show that these interactions occur in the absence of DNA damage.

1.6. Technical Background

Methods to study DNA repair in living cells

In vitro studies of the DNA repair machinery using isolated proteins and cell extracts provided detailed insights into the biochemical mechanisms of DNA repair. However, the complexity of the genome surveillance network and the spatio-temporal coordination of various repair factors require studying DNA repair *in vivo*. The recent development of a variety of different methods to generate DNA lesions together with the introduction of fluorescently tagged proteins opened up new ways to investigate DNA repair mechanisms in living cells. A classical approach, traditionally used to study the repair of DSBs, is ionizing irradiation or the use of radiomimetic drugs. Ionizing irradiation leads to the accumulation of DSB repair factors in so called ionizing radiation-induced foci (IRIF). Using ionizing irradiation in combination with FRAP analysis it has been shown that DSB repair factors rapidly diffuse throughout the nucleus until they encounter a break and become transiently immobilized (Essers et al., 2002). This finding is very reminiscent of what has been originally described for NER repair proteins (Houtsmuller et al., 1999) and allows an efficient and fast recognition of DNA damage and rapid exchange of repair factors. The disadvantage of using ionizing irradiation is that DNA lesions are scattered randomly throughout the genome. Furthermore, it is not possible to visualize the real-time accumulation of repair proteins and IRIF are hardly distinguishable from other nuclear foci like replication sites. Recently, some of these drawbacks have elegantly been circumvented by using focal irradiation with charged particles or heavy ions, which allows specific induction of DSBs along the ion or particle track (Aten et al., 2004; Hauptner et al., 2004; Hauptner et al., 2006; Jakob et al., 2002; Jakob et al., 2003). However, these methods require technical expertise and expensive instrumentation not available in most standard laboratories.

Researchers working on the NER pathway which removes UV-induced photolesions faced a similar problem, as the classical approach to study NER is global irradiation with a UVC lamp (254 nm) which leads to random distribution of UV-lesions throughout the genome. UVC irradiation through an isopore polycarbonate filter confines DNA damage induction to subnuclear regions (Green and Almouzni, 2003; Volker et al., 2001). This local irradiation approach combined with live cell imaging and FRAP analysis can be used to study the dynamics of NER proteins in living cells (Mone et al., 2004; Politi et al., 2005).

An elegant approach to specifically induce DSBs at defined subnuclear sites is the introduction of rare restriction sites into the genome followed by conditional expression of the respective endonuclease. This method was first developed in yeast (Lisby et al., 2003; Melo et al., 2001) but has also been adapted in mammalian cells (Jasin, 1996; Soutoglou et al., 2007). DSBs can even be followed over time *in vivo* by flanking the restriction sites with *tet* or *lac* operator cassettes and expression of fluorescently tagged Tet- and/or Lac-binding fusion proteins (Lisby et al., 2003; Soutoglou et al., 2007). However, the considerable long lag time between induction of the endonuclease and cutting (up to 30 min) does not allow precise kinetics measurements of repair factor assembly at DNA breaks.

In recent years, lasers used in confocal microscopy or microdissection devices have been adapted by various groups to introduce DNA lesions at preselected subnuclear sites in living cells. These microlaser techniques are based on the presensitization of DNA with low levels of halogenated thymidine analogs and/or DNA intercalating dyes (e.g. Hoechst 33258) which render the DNA hypersensitive to light within the UVA spectrum (Bekker-Jensen et al., 2005; Bradshaw et al., 2005; Celeste et al., 2003; Fernandez-Capetillo and Nussenzweig, 2004; Lukas and Bartek, 2004; Rogakou et al., 1999; Tashiro et al., 2000; Walter et al., 2003). Microirradiation with a UV laser leads to a photochemical reaction which is sufficient to induce various DNA lesions including SSBs and DSBs. Interestingly, it has been shown that the number of DSBs can be controlled by level of BrdU substitution, presence of Hoechst and fluence of UVA light (Limoli and Ward, 1993). In addition to SSBs and DSBs other more UVA typical DNA lesions, like thymine dimers, may be introduced by UVA irradiation. To eliminate these side effects some groups used laser microirradiation without sensitization, which requires much higher laser energy and can lead to damage of overall cellular structures (Kim et al., 2002; Lan et al., 2004).

We adapted the microirradiation protocol first introduced by Tashiro et al (Tashiro et al., 2000) using a 405 nm Diode laser coupled into the light path of a Leica SP2 or Leica SP5 confocal microscope. The 405 nm laser is normally used for photoactivation experiments or excitation of DNA dyes such as Hoechst or DAPI. The advantage of this system is that the FRAP wizard module of the Leica software can easily be used to exactly define the laser energy and the sites to be microirradiated. Thus additional laser lines or costly instrumentation, like microdissection devices used in the past, are not needed. The combination of this system with the use of

fluorescently tagged proteins allows the real-time measurement of protein redistribution immediately after damage induction over extended time periods in living cells (**Figure 3**). Several studies indicated that the use of halogenated thymidine analogs in combination with Hoechst 33285 may lead to oversensitization of cells (Lukas and Bartek, 2004; Rogakou et al., 1999; Tashiro et al., 2000). Thus we decided to sensitize cells by preincubation in medium containing moderate levels of BrdU (10 μ M) for a limited time period (about 24-48 h) which is sufficient to increase the sensitivity to UV laser microirradiation leading to the generation of various DNA lesions including SSBs and DSBs.

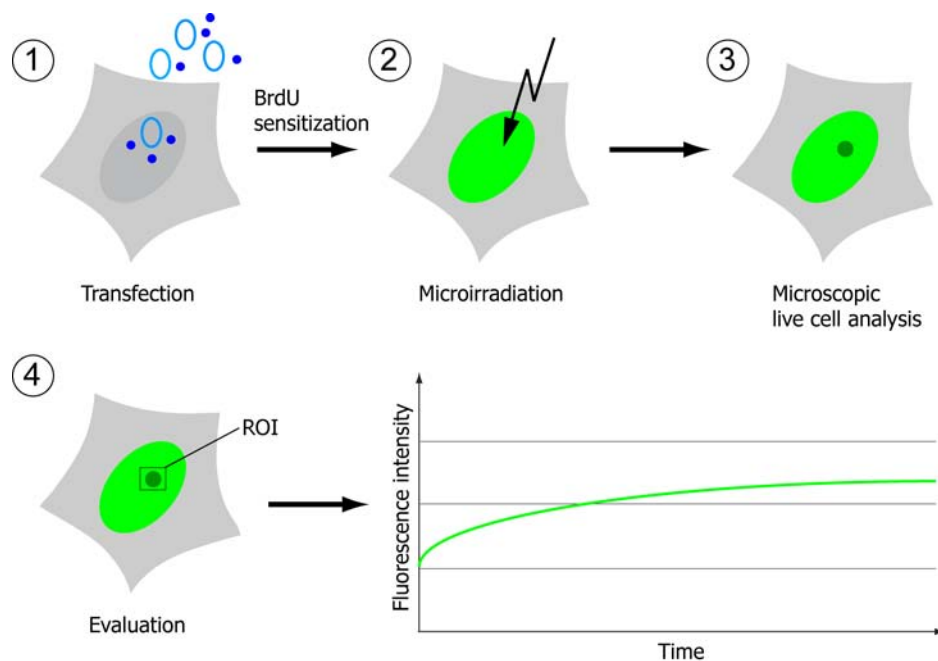


Figure 3 Schematic outline of microirradiation experiments. Cells are transfected with expression constructs (light blue circles) encoding fluorescently tagged fusion proteins and sensitized by incubation in medium containing BrdU (dark blue dots) for 24-48 h (1). Microirradiation is performed with a 405 nm laser (2) and the accumulation of fluorescently labelled proteins at DNA damage sites is monitored in real-time (3). After measuring and normalizing the fluorescence intensity at the microirradiated site, the recruitment kinetics are plotted as a graph (4).



2. RESULTS

2.1. Feedback regulated poly(ADP-ribosylation) by PARP-1 is required for rapid response to DNA damage in living cells.

Feedback-regulated poly(ADP-ribosylation) by PARP-1 is required for rapid response to DNA damage in living cells

Oliver Mortusewicz^{1,2}, Jean-Christophe Amé³, Valérie Schreiber^{3,*} and Heinrich Leonhardt^{1,2,*}

¹Munich Center for Integrated Protein Science CiPS^M, ²Department of Biology, Ludwig Maximilians University Munich, 82152 Planegg-Martinsried, Germany and ³Université Strasbourg 1, Institut Gilbert Laustriat, CNRS - UMR 7175, Département Intégrité du Génome, ESBS, Bld Sébastien Brant, BP 10413, 67412 Illkirch Cedex, France.

Received August 8, 2007; Revised and Accepted October 10, 2007

ABSTRACT

Genome integrity is constantly threatened by DNA lesions arising from numerous exogenous and endogenous sources. Survival depends on immediate recognition of these lesions and rapid recruitment of repair factors. Using laser microirradiation and live cell microscopy we found that the DNA-damage dependent poly(ADP-ribose) polymerases (PARP) PARP-1 and PARP-2 are recruited to DNA damage sites, however, with different kinetics and roles. With specific PARP inhibitors and mutations, we could show that the initial recruitment of PARP-1 is mediated by the DNA-binding domain. PARP-1 activation and localized poly(ADP-ribose) synthesis then generates binding sites for a second wave of PARP-1 recruitment and for the rapid accumulation of the loading platform XRCC1 at repair sites. Further PARP-1 poly(ADP-ribosylation) eventually initiates the release of PARP-1. We conclude that feedback regulated recruitment of PARP-1 and concomitant local poly(ADP-ribosylation) at DNA lesions amplifies a signal for rapid recruitment of repair factors enabling efficient restoration of genome integrity.

INTRODUCTION

Genomic DNA is under constant surveillance and protection from mutagenic or clastogenic insults, which can result from environmental or endogenous threats such as ionizing radiation, genotoxic chemicals and free radicals. Specific proteins inspect the DNA for the presence of particular lesions such as base or nucleotide

damage, single- or double-strand breaks and if necessary trigger appropriate repair mechanisms (1).

A growing number of proteins are known to be involved in these pathways enabling damage recognition, signaling of the damage, recruitment of other repair factors and finally restoration of the genetic and epigenetic information. A central surveillance factor, which is believed to play an important role in damage recognition and signaling is the poly(ADP-ribose) polymerase-1 (PARP-1). PARP-1 is the founding member of the PARP family encompassing 17 members involved in various biological processes such as DNA repair, transcription, mitotic segregation, telomere homeostasis and cell death (2). PARP-1 is a molecular sensor of single-strand DNA breaks (SSB) generated directly or resulting from the processing of damaged bases by the SSB/BER pathway. The two C-X₂-C-X_{28,30}-H-X₂-C zinc fingers of PARP-1 were shown to bind single-strand breaks *in vitro* and define a novel DNA interruptions binding module, present also in the SSB/BER factor DNA ligase III (3,4). Upon binding to its DNA target, PARP-1 catalyzes the polymerization of ADP-ribose moieties from NAD⁺ on target proteins, a post-translational modification called poly(ADP-ribosylation). Major targets of poly(ADP-ribose) (PAR) are PARP-1 itself and histones, mainly H1, leading to chromatin relaxation. In addition, PAR likely serves as a recruiting molecule, since several proteins were reported to interact with PAR or poly(ADP-ribosylated) PARP-1 (5). XRCC1, the non-enzymatic scaffold protein of SSB/BER that interacts with and stimulates most of the SSB/BER enzymes (6) was shown to interact preferentially with poly(ADP-ribosylated) PARP-1 (7). Recent studies demonstrated that XRCC1 is recruited to local damaged sites through a PAR- and PARP-1 dependent manner (8–10). However, the

*To whom correspondence should be addressed. Tel: +1 49 89 2180 74232; Fax: +1 49 89 2180 74236; Email: h.leonhardt@lmu.de

*Correspondence may also be addressed to V. Schreiber. Tel: +33 3 90 24 47 04; Fax: +33 3 90 24 46 86; Email: valerie.schreiber@esbs.u-strasbg.fr

The authors wish it to be known that, in their opinion, the last two authors should be regarded as joint Authors.

© 2007 The Author(s)

This is an Open Access article distributed under the terms of the Creative Commons Attribution Non-Commercial License (<http://creativecommons.org/licenses/by-nc/2.0/uk/>) which permits unrestricted non-commercial use, distribution, and reproduction in any medium, provided the original work is properly cited.

involvement of PARP-1 in DNA repair has been questioned by a study showing that BER is efficient in cells lacking PARP-1 (11).

One additional PARP, PARP-2 has been implicated in the cellular response to DNA damage (12,13). PARP-1 and PARP-2 deficient cellular and animal models indicated redundant but also complementary functions of the two enzymes in the surveillance and maintenance of genome integrity (14,15). PARP-1 and PARP-2 knock out mice are sensitive to ionizing radiation and alkylating agents (14,16–18), and embryonic fibroblasts derived from both genotypes showed a comparable delay in the repair of alkylated DNA (15,19). Yet, a recent report using siRNA suggested that PARP-2 depletion has only a minor impact on global SSB rates (20).

Biochemical studies revealed that PARP-2, like PARP-1, interacts with the SSB/BER repair factors XRCC1, DNA polymerase β and DNA ligase III (12,15). However, whether PARP-2 acts in a similar way as PARP-1 is still under debate. PARP-1 and PARP-2 can heterodimerize, but they recognize different targets within DNA (15). PARP-2 does not recognize SSBs, but gaps or flap structures which indicates that PARP-2 is probably involved in the later steps of the repair process (13).

As most data on the role and regulation of PARP-1 and PARP-2 are derived from biochemical experiments we systematically investigated the kinetics, role and interplay of PARP-1 and PARP-2 in living cells. With microirradiation and live cell microscopy we could show that both PARPs are recruited to DNA damage sites however with different kinetics and roles. Our data indicate that the initial step of the damage response is mediated by a feedback regulated accumulation of PARP-1 and concomitant local poly(ADP-ribosyl)ation leading to a rapid recruitment of repair factors.

MATERIALS AND METHODS

Cell culture and transfection

Hela cells stably expressing GFP-PARP-1 were generated by transfection of pEGFP-C3-hPARP-1 vector and selection of resistant clones with G418 (0.5 μ g/ml). The activity of the recombinant fusion protein was verified by activity blot according to Dantzer *et al.* (21). Wild type, PARP-1 and PARP-2 deficient MEF cells were previously described (15,19). All cell lines were cultured in DMEM containing 50 μ g/ml gentamicin supplemented with 10% FCS. Cells grown on μ -slides (Ibidi) or on gridded coverslips were cotransfected with jetPEI (PolyPlus Transfection) according to the manufacturer's instructions. For microirradiation experiments cells were either sensitized by incubation in medium containing BrdU (10 μ g/ml) for 24–48 h, or incubated with Hoechst 33285 (10 μ g/ml) for 10 min. NU1025 (Sigma) was added to the medium at least 1 h before microirradiation experiments in a final concentration of 200 μ M.

Expression plasmids

Mammalian expression constructs encoding full length or truncated translational fusions of human PARP-2

were previously described (22). The GFP-PARP-1 expression vector was described in Maeda *et al.* (23). Mammalian expression constructs encoding truncated forms of human PARP-1 were generated by subcloning into the PstI site of pEGFP-C3 (Clontech). PstI/PstI fragments were isolated from the following pTG plasmids previously described: PARP-1_{C21G,C125G} (4), PARP-1_{E988} (24), and PARP-1_{1–373} (25). The GFP-XRCC1 expression construct was generated by subcloning the EcoRI/EcoRI fragment from pCD2E-XRCC1 into the EcoRI site of pEGFP-C2. A red variant of XRCC1 was generated by replacing GFP with RFP (26). In all cases expression was under the control of the CMV promoter. We tested all fusion proteins by expression in 293T cells followed by western blot analysis.

Immunofluorescence and detergent extraction

Cells were fixed in 3.7% formaldehyde for 10 min and permeabilized with ice-cold methanol for 5 min. The following primary antibodies (diluted in PBS containing 2% BSA) were used: anti-PAR (Trevigen) and anti-PARP-1 (C2-10) mouse monoclonal antibodies, and anti-PARP-2 rabbit polyclonal antibody (Yuc, Alexis). Primary antibodies were detected using secondary antibodies (diluted 1:400 in PBS containing 2% BSA) conjugated to Alexa Fluor 488, 555 or 647 (molecular probes). Cells were counterstained with DAPI and mounted in Vectashield (Vector Laboratories).

Live-cell microscopy, microirradiation and photobleaching experiments

Live cell imaging, microirradiation and photobleaching experiments were carried out with a Leica TCS SP5/AOBS confocal laser scanning microscope equipped with a UV-transmitting HCX PL 63 \times /1.4 oil objective. Fluorophores were excited using a 488 nm Ar-laser line and a 561 nm DPSS laser line. The microscope was equipped with a heated environmental chamber set to 37°C. Confocal image series were typically recorded with a frame size of 256 \times 256 pixels and a pixel size of 90 nm.

Microirradiation was carried out with a 405 nm diode laser set to 50% transmission. Preselected spots of \sim 1 μ m in diameter within the nucleus were microirradiated for 1 s. Before and after microirradiation confocal image series of one mid z-section were recorded at 2 s time interval (typically six preirradiation and 150 post-irradiation frames). For evaluation of the recruitment kinetics, fluorescence intensities of the irradiated region were corrected for background and for total nuclear loss of fluorescence over the time course and normalized to the preirradiation value. Data from microirradiation of individual cells obtained in at least two independent experiments performed on different days were averaged for evaluation and plotting of corresponding graphs.

For FRAP analysis, a region of interest was selected and photobleached for 300 ms with all laser lines of the Ar-laser and the 561 nm DPSS laser set to maximum power at 100% transmission. Before and after bleaching, confocal image series were recorded at 150 ms time intervals (typically 10 prebleach and 200 post-bleach

frames). Mean fluorescence intensities of the bleached region were corrected for background and for total-nuclear loss of fluorescence over the time course and normalized to the mean of the last four prebleach values.

For the quantitative evaluation of microirradiation and photobleaching experiments, data of at least nine nuclei were averaged and the mean curve as well as the standard error of the mean calculated and displayed using Microsoft Excel software. The half-time of recovery was calculated from the average curves.

Images of fixed cells were taken with a Zeiss Axiophot 2 widefield epifluorescence microscope using a Zeiss Plan-Apochromat 63x/1.40 oil objective and a cooled CCD camera (Visitron Systems).

RESULTS

PARP-1 is recruited to DNA damage sites

Various biochemical studies and knock out experiments have clearly shown the involvement of PARP-1 in DNA repair (2). However, whether and how PARP-1 is recruited to sites of DNA damage is still an open question. To investigate the dynamics of PARP-1 recruitment to DNA damage sites in living cells we generated DNA lesions at preselected subnuclear sites with a long wavelength UV diode laser in BrdU-sensitized cells, as described before (27,28). Immunofluorescence stainings with specific antibodies revealed that endogenous PARP-1 is recruited to microirradiated sites in HeLa and MEF cells (Figure 1B and data not shown). When transiently or stably transfected in MEFs or HeLa cells, GFP-PARP-1 was distributed throughout the nucleus and accumulated in nucleoli as previously described (22). For *in vivo* studies we determined the recruitment kinetics of PARP-1 in living cells by quantifying the amount of GFP-tagged PARP-1 accumulated at microirradiated sites. We observed a rapid accumulation of GFP-PARP-1 at DNA damage sites immediately after microirradiation (Figure 1C and D). Accumulation of PARP-1 at DNA damage sites was rather transient, as the fluorescence intensity gradually declined after reaching a maximum about 1 min after microirradiation (Figure 1C and D). Interestingly, we observed a similar fast recruitment of GFP-PARP-1 in cells undergoing mitosis (Supplementary Figure 1). To test whether PARP-1 recruitment is accompanied by poly(ADP-ribosylation) at microirradiated sites we performed immunostainings with specific antibodies against PAR. We found a strong PAR signal clearly colocalizing with GFP-PARP-1 at microirradiated sites (Figure 1A). Taken together, our results show a rapid but transient accumulation of PARP-1 at DNA damage sites colocalizing with sites of poly(ADP-ribosylation).

PARP activity enhances the recruitment of PARP-1 to DNA damage sites

It has previously been shown that PARP activity is required for the recruitment of the repair factor XRCC1 to DNA lesions (8–10). To address the question whether PARP activity has an effect on its own recruitment

we tested the recruitment of GFP-PARP-1 in the presence of the PARP inhibitor NU1025. As expected, treatment with NU1025 efficiently inhibited poly(ADP-ribosylation) as no PAR signal could be detected after microirradiation of treated cells (Figure 1A). Interestingly, accumulation of endogenous and GFP-tagged PARP-1 at laser-induced DNA damage sites seemed not to be affected by this treatment (Figure 1A and B). Quantitative evaluation of live cell experiments, however, revealed that inhibition of PARP activity lead to a reduced recruitment efficiency in HeLa cells (Figure 1C and D).

We then examined the recruitment of GFP-PARP-1 in MEFs lacking PARP-1. Whereas GFP-PARP-1 was efficiently but transiently recruited, similarly to what was observed in HeLa cells, treatment of these *parp-1*^{-/-} cells with NU1025 lead to a delayed and prolonged accumulation of GFP-PARP-1 (Figure 1E and F).

To further test the influence of the catalytic activity on the recruitment of PARP-1, we generated a catalytic mutant by replacing the central glutamic acid at aa position 988 by lysine (GFP-PARP-1_{E988K}). This mutation, affecting the PAR chain elongation, converts PARP-1 into a mono-ADP-ribosyl-transferase (24). The inability of GFP-PARP-1_{E988K} to synthesize PAR was verified by activity blot (data not shown). To circumvent side effects arising from endogenous PARP-1 dimerizing with the fusion protein, we performed the microirradiation experiments in *parp-1*^{-/-} MEFs. The PARP-1_{E988K} fusion protein showed a delayed accumulation and longer persistence at DNA damage sites in comparison to the wild-type protein (Figure 1E and F) which is in agreement with our data obtained from *parp-1*^{-/-} MEFs treated with NU1025. Altogether, these results indicate that PARP activity is not essential for the initial recruitment of PARP-1 to DNA damage sites, but clearly enhances the recruitment efficiency.

Recruitment of PARP-1 to DNA damage sites is mediated by the DNA-binding domain and the BRCT domain

Having shown that PARP-1 accumulates at DNA damage sites, we determined which domain of PARP-1 mediates this recruitment *in vivo*. First we tested whether the two zinc finger containing DNA-binding domain of PARP-1 [DBD, residues 1–373, (4)] was sufficient for the recruitment to laser-induced DNA damage sites. We observed recruitment of GFP-PARP-1_{1–373} in both *parp-1*^{-/-} (Figure 2) and HeLa cells (data not shown). A direct comparison of the recruitment kinetics of the DBD and the full-length PARP-1 revealed a fast but less efficient recruitment of the DNA binding domain (Figure 2A and B). Using half-nucleus FRAP experiments, we found that the initial, very fast, recruitment of the DBD is supported by an overall higher mobility of the isolated DBD ($t_{1/2} = 3.75$ s) in the nucleus compared to the full-length PARP-1 ($t_{1/2} = 7.20$ s) and PARP-1_{E988} ($t_{1/2} = 7.25$ s) harboring all interaction domains (Supplementary Figure 2).

The reduced and transient accumulation of the DBD suggests that another part of the protein could enhance the recruitment of PARP-1. To further test this hypothesis we mutated key residues within the DBD known to be

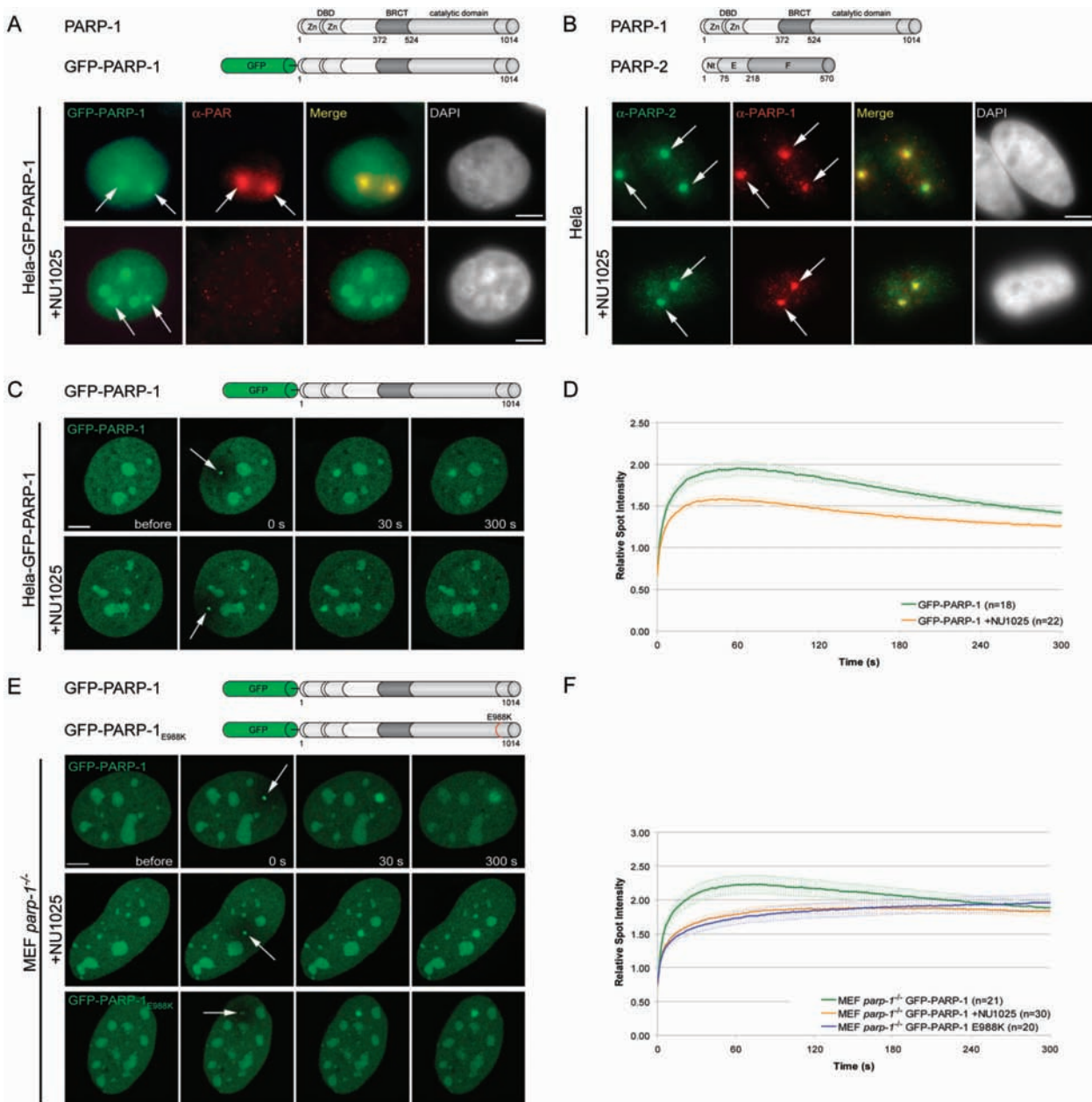


Figure 1. Recruitment of PARP-1 to DNA damage sites. (A) Immunostaining of PAR after microirradiation of HeLa cells stably transfected with GFP-PARP-1. GFP-PARP-1 clearly colocalizes with PAR at microirradiated sites. Treatment of HeLa GFP-PARP-1 cells with the PARP-1 inhibitor NU1025 results in loss of PAR signals at microirradiated sites, while GFP-PARP-1 accumulation is still present. (B) Immunostaining of PARP-1 and PARP-2 after microirradiation of HeLa cells in the absence or presence of NU1025. (C) Live cell imaging of microirradiated HeLa cells stably expressing GFP-PARP-1. Accumulation of GFP-PARP-1 can be observed immediately after microirradiation in untreated cells as well as in cells treated with the PARP inhibitor NU1025. (D) Quantitative evaluation of PARP-1 recruitment kinetics in the absence and presence of the PARP inhibitor NU1025. Inhibition of PARP activity does not prevent recruitment of PARP-1 but leads to a reduced accumulation at microirradiated sites. (E and F) Live cell imaging and quantitative evaluation of PARP-1 recruitment kinetics in the absence and presence of the PARP inhibitor NU1025 compared with the recruitment kinetics of the fluorescence tagged catalytic mutant PARP-1 after microirradiation of PARP-1 knock out cells. Error bars represent the SEM. Scale bar, 5 μ m.

essential for DNA binding, in the context of the full-length PARP-1. The C21G and C125G mutations target cysteine residues involved in zinc binding and abolish the binding to DNA (4). These mutations lead to a dramatically reduced, but still detectable recruitment of GFP-PARP-1_{C21G,C125G} to DNA damage sites (Figure 2C

and D). Interestingly, treatment with the PARP inhibitor NU1025 affected the recruitment of GFP-PARP-1_{C21G,C125G}. (Figure 2C–F), indicating that PAR molecules synthesized at the damaged site by local PARP-1 are involved in this second wave of DBD-independent recruitment of PARP-1. Furthermore, we found that the

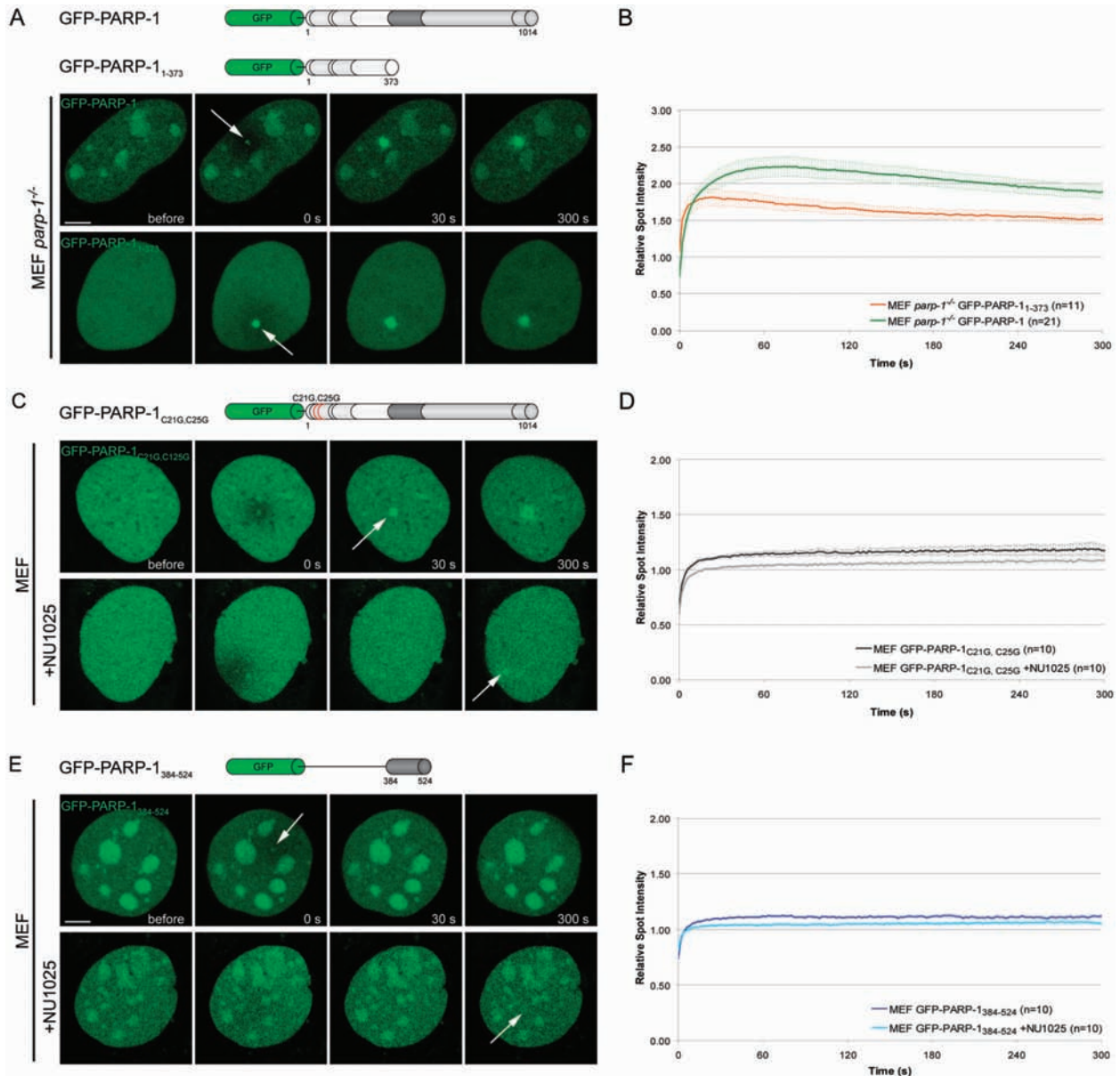


Figure 2. Mechanism of PARP-1 recruitment to DNA damage sites. (A) Live cell imaging of microirradiated PARP-1 knock out MEFs (MEF *parp-1*^{-/-}) expressing either GFP-PARP-1 or the GFP-tagged DNA binding domain of PARP-1 (GFP-PARP-1₁₋₃₇₃). Accumulation of both, GFP-PARP-1 and GFP-PARP-1₁₋₃₇₃ can be observed immediately after microirradiation. (B) Quantitative evaluation of GFP-PARP-1₁₋₃₇₃ recruitment kinetics. For comparison, the recruitment kinetics of GFP-PARP-1 from Figure 1F are displayed. Time-matched controls are shown in Supplementary Figure 3. (C) Live cell imaging of microirradiated MEFs expressing a PARP-1 fusion protein containing two point mutations affecting the DNA binding capacities of PARP-1 (GFP-PARP-1_{C21G,C25G}) in the absence or presence of the PARP inhibitor NU1025. (D) Quantitative evaluation of recruitment kinetics. (E) Live cell imaging of microirradiated MEFs expressing the GFP-tagged BRCT domain of PARP-1 (GFP-PARP-1₃₈₄₋₅₂₄) in the absence or presence of the PARP inhibitor NU1025. (F) Quantitative evaluation of recruitment kinetics. Error bars represent the SEM. Scale bar, 5 μm.

BRCT domain alone (residues 384–524), which is involved in PARP-1 homodimerization (15) and PAR binding (data not shown), showed a weak accumulation at laser-induced DNA damage sites which was reduced in the presence of NU1025 (Figure 2E and F). Taken together, our results indicate that the DBD of PARP-1 is necessary and sufficient for recruitment of PARP-1 to DNA lesions. The catalytic activity of PARP-1 likely enhances the recruitment efficiency by locally generating

PAR polymers, which are then recognized by the BRCT domain, recruiting more PARP-1 molecules.

The enzymatic activity is required for dissociation of PARP-1 from DNA damage sites

The longer persistence of the catalytic PARP-1 mutant at DNA damage sites (Figure 1E and F) was rather unexpected and led us to study this effect in more detail.

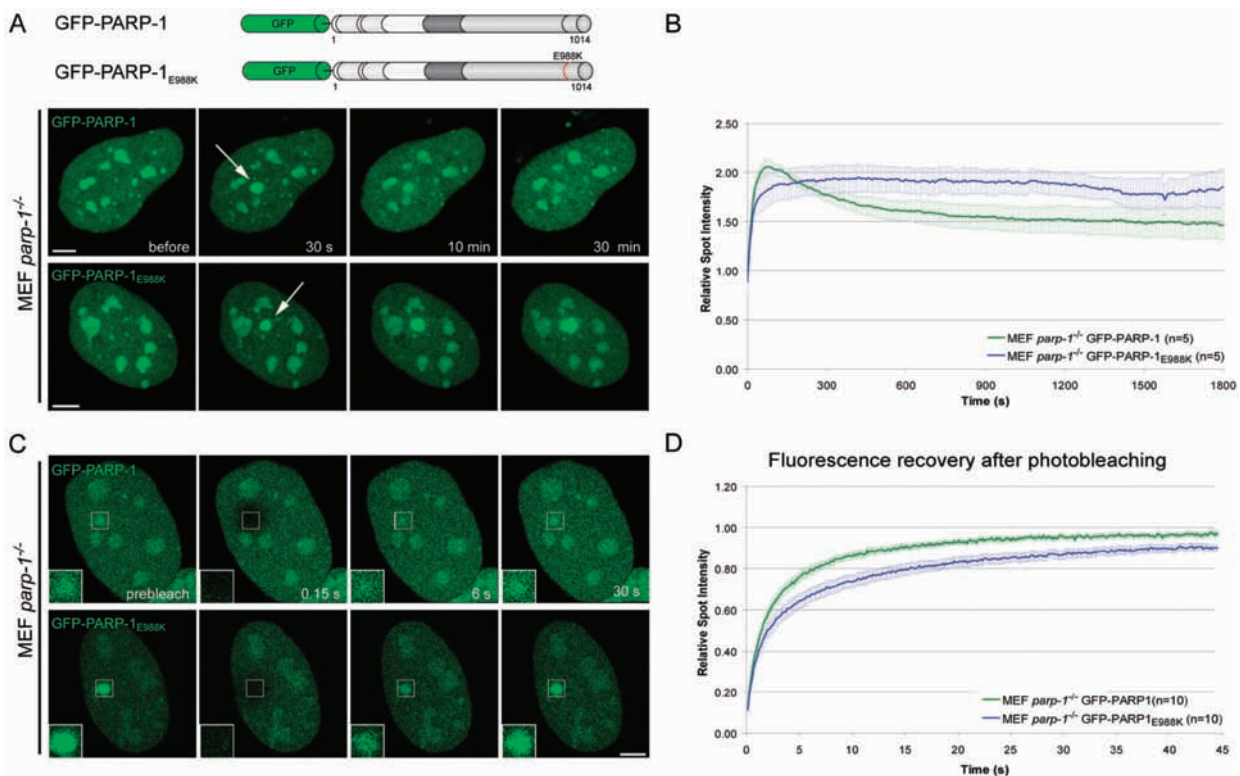


Figure 3. The catalytic activity of PARP-1 is needed for dissociation from DNA damage sites. (A) Long-term observations of microirradiated PARP-1 knock out MEFs (MEF *parp-1*^{-/-}) expressing either GFP-PARP-1 or a GFP-tagged catalytic mutant (GFP-PARP-1_{E988K}). The catalytic mutant shows a prolonged association at DNA damage sites. (B) Quantitative evaluation of recruitment kinetics. (C) Mobility of GFP-PARP-1 and GFP-PARP-1_{E988K} at DNA damage sites. The mobility of accumulated fluorescent fusion proteins was determined by bleaching the microirradiated site 5 min after microirradiation and subsequent recovery measurements. Inset shows the bleached microirradiated site. (D) FRAP data from 10 individual experiments are shown as mean curves. Error bars represent the SEM. Scale bar, 5 μ m.

We performed long-term live cell observations of microirradiated *parp-1*^{-/-} MEFs transiently transfected with either GFP-PARP-1 or GFP-PARP-1_{E988K}. In contrast to the very fast accumulation reaching a maximum about 1 min after microirradiation followed by the dissociation of PARP-1, GFP-PARP-1_{E988K} showed a delayed accumulation and persisted at DNA repair sites during the observation period of 30 min (Figure 3A and B).

To analyze the mechanisms underlying these kinetic differences, we performed FRAP analysis. The irradiated region was bleached with a high-energy laser pulse 5 min after microirradiation and the fluorescence recovery was determined for GFP-PARP-1 and GFP-PARP-1_{E988K}. We found a slower fluorescence recovery of GFP-PARP-1_{E988K} ($t_{1/2} = 2.25$ s) in comparison to GFP-PARP-1 ($t_{1/2} = 1.80$ s), indicating a stronger binding of the catalytic mutant at DNA damage sites (Figure 3C and D). These results show that the catalytic activity of PARP-1 is not only needed for efficient targeting to but also for dissociation from DNA damage sites.

PARP-2 is recruited to DNA damage sites later than PARP-1

Besides PARP-1, PARP-2 is the only DNA-damage dependent PARP identified so far (12). PARP-2 is required for efficient single-strand break repair like PARP-1 (15), but its function(s) in the repair process

are still largely unknown (2). When transiently expressed in MEFs or HeLa cells, GFP-PARP-2 distributes throughout the nucleus and accumulates within the nucleoli, as previously described (22). Microirradiation of MEFs and HeLa cells lead to the recruitment of GFP-PARP-2 to DNA damage sites. However, in comparison to PARP-1, PARP-2 was recruited slower but persisted longer at DNA repair sites (Figure 4A and B and Supplementary Figure 4). In addition, we could demonstrate recruitment of endogenous PARP-2 to laser-induced DNA damage sites (Figure 1B).

We next analyzed whether recruitment of PARP-2 depends on PARP activity or the presence of PARP-1. We found that recruitment of PARP-2 to DNA repair sites was less efficient in cells treated with NU1025 as well as in *parp-1*^{-/-} cells, (Figure 4C and D and Supplementary Figure 4). Altogether, these results indicate that PARP-1 and PARP-2 show distinct recruitment and dissociation kinetics at DNA repair sites and that poly(ADP-ribose)ation enhances the recruitment efficiency of both.

The nucleolus is a storage of PARP-1 and PARP-2 for heavy DNA damage

In the course of this study, we observed that microirradiation in the presence of the photosensitizer Hoechst leads to more DNA damage than sensitization with BrdU,

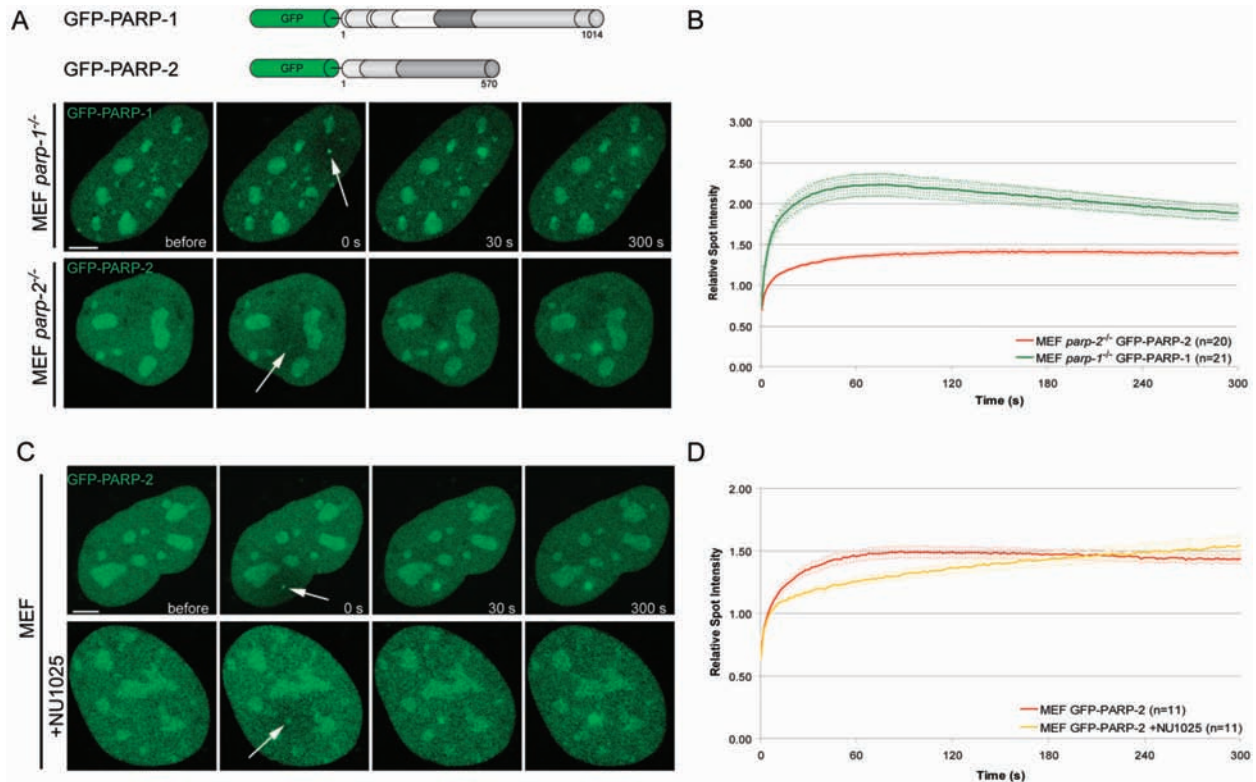


Figure 4. Recruitment of PARP-2 to DNA damage sites in living cells. (A) Live cell imaging of microirradiated MEFs either expressing GFP-PARP-1 or GFP-PARP-2. Accumulation of GFP-PARP-1 and GFP-PARP-2 can be observed immediately after microirradiation. (B) Quantitative evaluation of GFP-PARP-2 recruitment kinetics. For comparison, the recruitment kinetics of GFP-PARP-1 from Figure 1F are displayed. Time-matched controls are shown in Supplementary Figure 3. (C and D) Live cell imaging of microirradiated MEFs reveals a slower accumulation of GFP-PARP-2 in the presence of NU1025. Error bars represent the SEM. Scale bar, 5 μ m.

which is likely due to more efficient absorption of the energy of the 405 nm laser. We therefore used Hoechst to determine the kinetics of GFP-PARP-1 and GFP-PARP-2 in response to heavy DNA damage. Microirradiation of Hoechst-sensitized cells resulted in massive recruitment of GFP-PARP-1 and GFP-PARP-2 from nucleoli to damage sites (Figure 5). This depletion of the nucleolar storage was transient and GFP-PARP-1 and GFP-PARP-2 reappeared in the nucleolus correlating with their dissociation from repair sites (Figure 5). These data suggest that the nucleolus serves as a storage supplying PARP-1 and PARP-2 in response to heavy DNA damage.

Recruitment of XRCC1 to damage sites depends on PARP-1 but not on PARP-2

Recent studies have indicated that the recruitment of SSB/BER factors, like XRCC1 depends on PARP activity (9,10). To analyze the effect of poly(ADP-ribose)ylation on recruitment of XRCC1 in more detail, we microirradiated wild-type, *parp-1*^{-/-} and *parp-2*^{-/-} MEFs expressing GFP-XRCC1. We found a considerably reduced recruitment of GFP-XRCC1 in cells lacking PARP-1, whereas recruitment of GFP-XRCC1 in *parp-2*^{-/-} MEFs was as in wild-type cells (Figure 6A and B). To elucidate the mechanisms underlying these different recruitment kinetics we performed FRAP

analysis, 5 min after microirradiation. In wild-type cells as well as in cells lacking PARP-2 we found a slow turnover of GFP-XRCC1 at microirradiated sites ($t_{1/2} = 3.3$ s and $t_{1/2} = 2.85$ s, respectively) whereas in *parp-1*^{-/-} cells GFP-XRCC1 fluorescence recovered much faster ($t_{1/2} = 1.2$ s), indicating a high mobility of XRCC1 at DNA damage sites (Figure 6C and D).

To test, whether the enzymatic activity of PARP-1 is needed for XRCC1 recruitment we cotransfected *parp-1*^{-/-} MEFs with RFP-XRCC1 and GFP-tagged wild-type (GFP-PARP-1) or catalytically inactive PARP-1 (GFP-PARP1_{E988K}). We found that RFP-XRCC1 is efficiently recruited to laser-induced DNA damage sites in *parp-1*^{-/-} MEFs rescued with GFP-PARP-1 (Figure 7A and C). In contrast, recruitment of RFP-XRCC1 was dramatically reduced in *parp-1*^{-/-} MEFs transfected with GFP-PARP-1_{E988K} (Figure 7B and C). These results show that PARP-1 activity enhances the recruitment of repair factors to DNA damage sites by generating high-affinity binding sites.

DISCUSSION

Genetic studies of knockout mice and cells have demonstrated the requirement of the two DNA-damage dependent PARPs, PARP-1 and PARP-2, for DNA repair

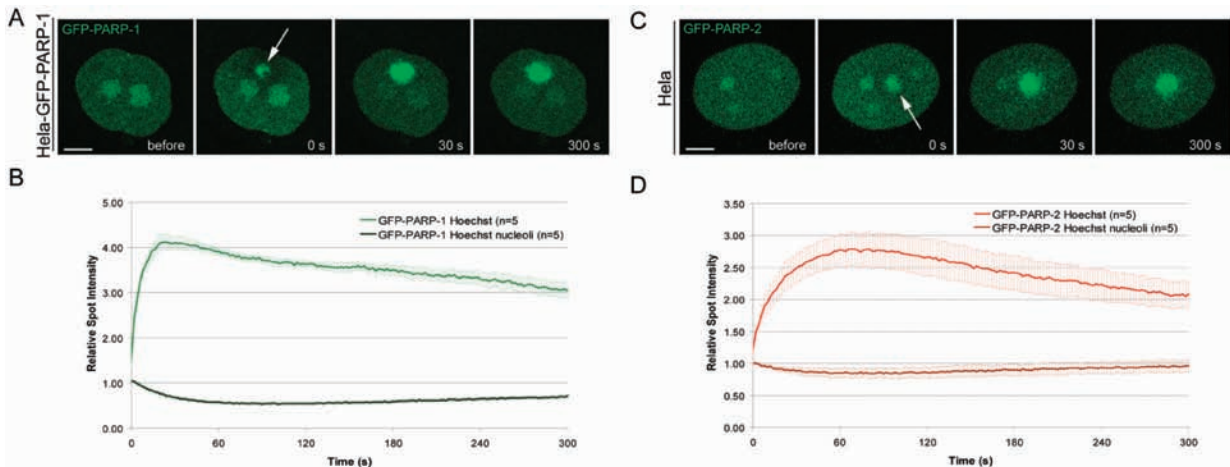


Figure 5. The Nucleolus serves as a storage of PARP-1 and PARP-2 to cope with heavy DNA damage. (A and C) Live cell imaging of microirradiated HeLa cells sensitized with Hoechst 33285. Microirradiation of Hoechst sensitized cells leads to massive recruitment and temporary depletion of PARP-1 and PARP-2 from the nucleolus. (B and D) Quantitative evaluation of recruitment and nucleolar depletion kinetics. Error bars represent the SEM. Scale bar, 5 μ m.

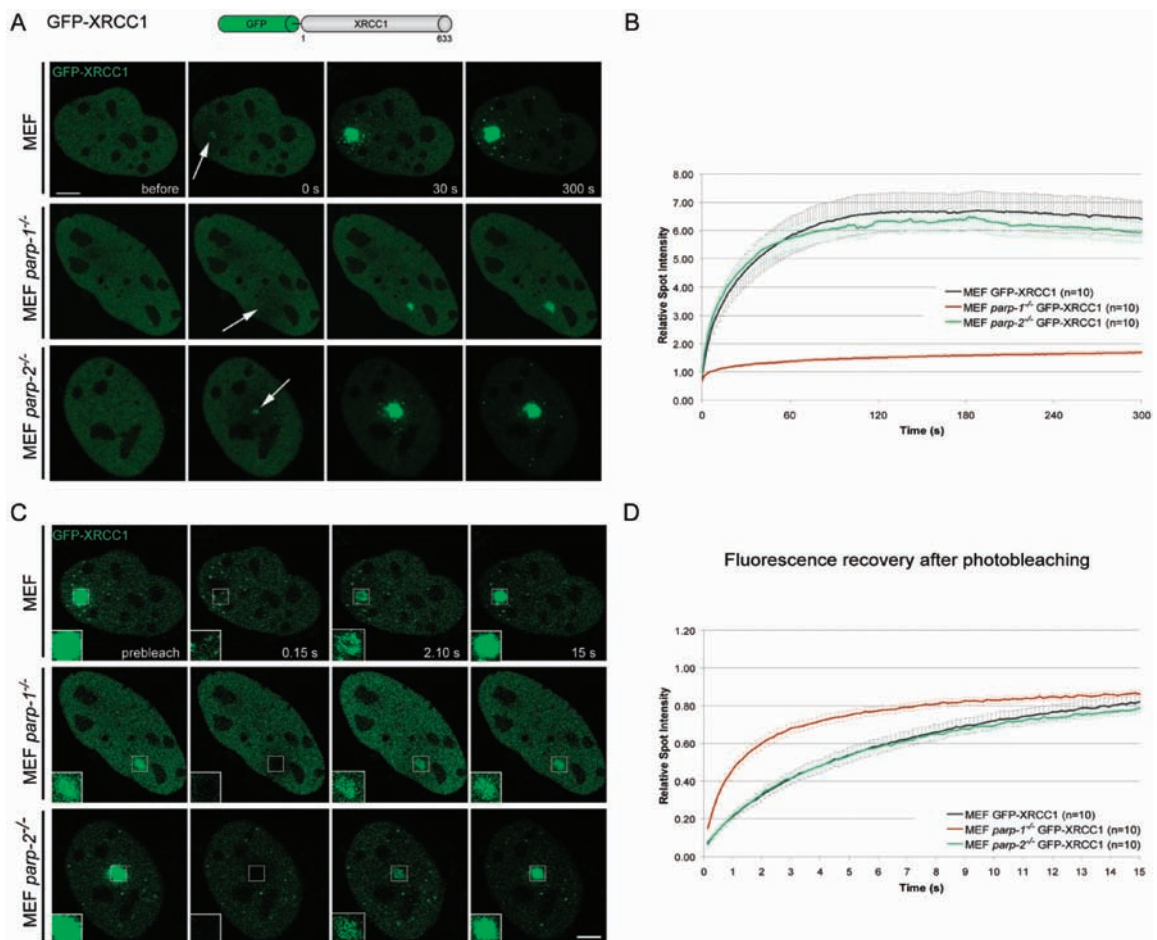


Figure 6. Efficient recruitment of XRCC1 to DNA repair sites depends on the presence of PARP-1. (A) Live cell imaging of microirradiated wild-type, PARP-1 and PARP-2 knock out MEFs (MEF *parp-1*^{-/-}, MEF *parp-2*^{-/-}) expressing GFP-XRCC1. Accumulation of GFP-XRCC1 at DNA damage sites is dramatically reduced in the absence of PARP-1. (B) Quantitative evaluation of recruitment kinetics. (C and D) Mobility of GFP-XRCC1 at DNA damage sites. The mobility of accumulated fluorescent fusion proteins was determined by bleaching the microirradiated site 5 min after microirradiation and subsequent recovery measurements. Inset shows the bleached microirradiated site. FRAP data from 10 individual experiments are shown as mean curves. Error bars represent the SEM. Scale bar, 5 μ m.

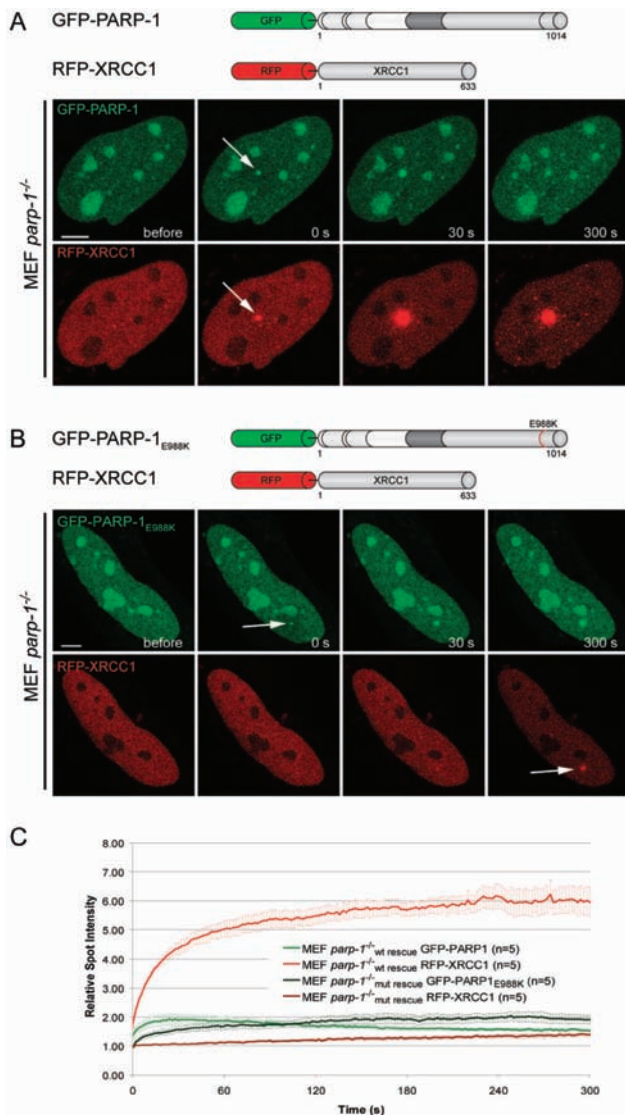


Figure 7. The catalytic activity of PARP-1 is needed for efficient recruitment of XRCC1 to laser-induced DNA damage sites. (A) Live cell imaging of microirradiated PARP-1 knock out MEFs (MEF *parp-1*^{-/-}) coexpressing GFP-PARP-1 and RFP-XRCC1. Expression of GFP-tagged wild-type PARP-1 results in efficient recruitment of RFP-XRCC1. (B) Live cell imaging of microirradiated PARP-1 knock out MEFs (MEF *parp-1*^{-/-}) coexpressing GFP-PARP-1^{E988K} and RFP-XRCC1. Accumulation of RFP-XRCC1 at DNA damage sites is dramatically reduced in PARP-1 knock out MEFs expressing catalytically inactive GFP-PARP-1^{E988K}. (C) Quantitative evaluation of recruitment kinetics. Error bars represent the SEM. Scale bar, 5 μ m.

(14–19). Based on their interaction with common proteins involved in genome restoration and binding to different DNA lesions and substrates, it was suggested that PARP-1 and PARP-2 have both overlapping and non-redundant functions (14,13). However, there have been reports questioning the importance of PARP-1 or PARP-2 for DNA repair (11,20). In this study, we compared the spatio-temporal redistribution of PARP-1 and PARP-2 in response to DNA damage induced by laser

microirradiation in living cells. We observed a clear accumulation of both DNA-damage dependent PARPs at DNA damage sites. Consistent with distinct roles in DNA repair we found different recruitment kinetics for PARP-1 and PARP-2. While PARP-1 accumulated fast and transiently, PARP-2 showed a delayed and persistent accumulation at repair sites. The clear accumulation of PARP-2 at DNA damage sites together with biochemical and genetic data argues for an involvement of PARP-2 in DNA repair. Our kinetic studies suggest a role for PARP-2 in the latter steps of DNA repair, however the precise function of PARP-2 has to be elucidated in future studies.

Recruitment of PARP-1 is mainly mediated by its N-terminal DNA binding domain, as mutations of two cysteine residues within the Zn Finger domain dramatically reduced accumulation at repair sites, whereas the isolated DBD was sufficient for recruitment. Interestingly, the highly homologous Zn Finger domain of DNA ligase III, was neither necessary nor sufficient for recruitment to DNA repair sites, which was instead mediated by its BRCT domain binding to XRCC1 (28). Using a potent PARP inhibitor we could demonstrate that PARP activity is not essential for, but enhances the efficiency of, PARP-1 and PARP-2 recruitment to repair sites. This fits well with our observation that the second wave of PARP-1 recruitment relies on PAR binding via the BRCT domain of PARP-1. Interestingly, we found that the catalytic activity of PARP-1 is not only needed for efficient recruitment, but also for dissociation from DNA repair sites. This observation could be explained with earlier findings showing that automodification of PARP-1 abolishes DNA binding *in vitro* (29). These data argue for three distinct roles of PARP-1 in response to DNA damage: the detection and labeling of the damaged site, the local relaxation of chromatin structure and the recruitment of repair factors.

In summary, we propose the following model for the spatio-temporal accumulation of SSB/BER factors at DNA strand breaks (Figure 8). Single-strand breaks are detected by the DNA binding domain of PARP-1. Poly(ADP-ribosylation) by PARP-1 leads to chromatin relaxation and attracts additional PARP-1 molecules via its BRCT domain. Further poly(ADP-ribosylation) at DNA lesions then leads to the release of PARP-1 through charge repulsion enabling a switch to the next step in DNA repair initiated by recruitment of the versatile loading platform XRCC1. Interestingly, PARP-2, which is required for DNA repair could not replace PARP-1 in the rapid recruitment of repair factors. However, we cannot exclude that PARP-2 could contribute to the slow recruitment of XRCC1 observed in *parp1*^{-/-}MEFs.

This study of PARP-1 recruitment revealed a complex regulation of a repair factor in response to DNA damage. After detection of the DNA damage, PARP-1 activation and poly(ADP-ribosylation) leads to a positive feedback loop accumulating more PARP-1 and thus amplifying the signal for rapid recruitment of repair factors. Further accumulation is countered by a negative feedback resulting in the release of PARP-1 likely to protect against

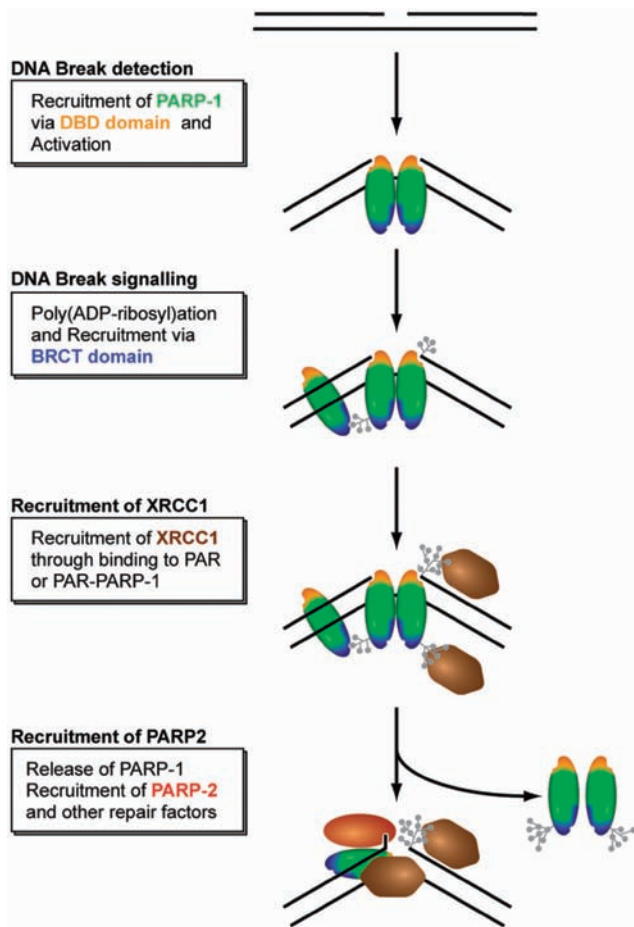


Figure 8. Simplified model for the recruitment of repair factors to SSB. See text for a detailed discussion of the role and regulation of PARPs.

uncontrolled poly(ADP-ribosylation) which would disrupt cellular functions and lead to apoptosis. This feedback regulated recruitment of PARP-1 at DNA lesions thus allows a balance between signal amplification for rapid recruitment of repair factors and protection against extensive poly(ADP-ribosylation).

SUPPLEMENTARY DATA

Supplementary Data are available at NAR Online.

ACKNOWLEDGEMENTS

We would like to thank G. de Murcia for helpful comments and suggestions. V.S. and J.C.A. are supported by funds from Centre National de la Recherche Scientifique, Association pour la Recherche contre le Cancer, Electricité de France, Ligue Nationale contre le Cancer (comité du Haut-Rhin) and Commissariat à l'Énergie Atomique. This work was supported by grants from the Deutsche Forschungsgemeinschaft and the Volkswagenstiftung to H.L. Funding to pay the Open Access publication charges for this article was provided by the DFG.

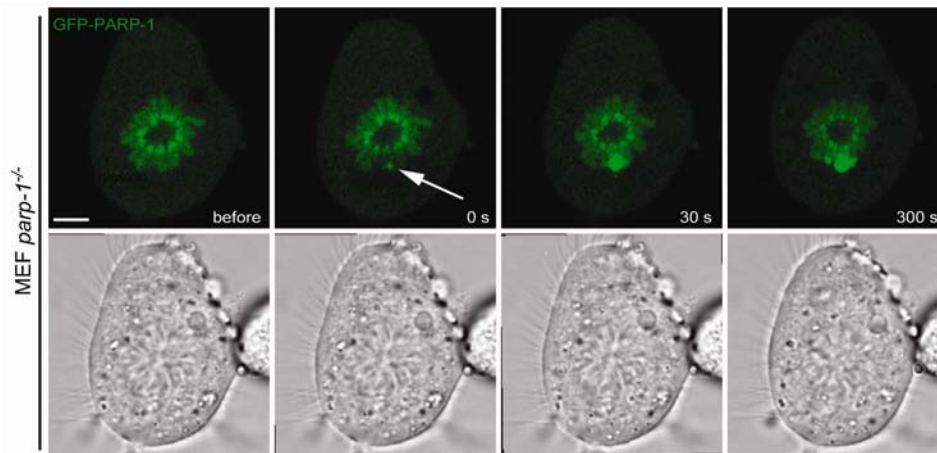
Conflict of interest statement. None declared.

REFERENCES

- Hoeijmakers, J.H. (2001) Genome maintenance mechanisms for preventing cancer. *Nature*, **411**, 366–374.
- Schreiber, V., Dantzer, F., Ame, J.C. and de Murcia, G. (2006) Poly(ADP-ribose): novel functions for an old molecule. *Nat. Rev. Mol. Cell Biol.*, **7**, 517–528.
- Mackey, Z.B., Niedergang, C., Murcia, J.M., Leppard, J., Au, K., Chen, J., de Murcia, G. and Tomkinson, A.E. (1999) DNA ligase III is recruited to DNA strand breaks by a zinc finger motif homologous to that of poly(ADP-ribose) polymerase. Identification of two functionally distinct DNA binding regions within DNA ligase III. *J. Biol. Chem.*, **274**, 21679–21687.
- Gradwohl, G., Menissier de Murcia, J.M., Molinete, M., Simonin, F., Koken, M., Hoeijmakers, J.H. and de Murcia, G. (1990) The second zinc-finger domain of poly(ADP-ribose) polymerase determines specificity for single-stranded breaks in DNA. *Proc. Natl Acad. Sci. USA*, **87**, 2990–2994.
- Pleschke, J.M., Kleczkowska, H.E., Strohm, M. and Althaus, F.R. (2000) Poly(ADP-ribose) binds to specific domains in DNA damage checkpoint proteins. *J. Biol. Chem.*, **275**, 40974–40980.
- Caldecott, K.W. (2003) XRCC1 and DNA strand break repair. *DNA Repair*, **2**, 955–969.
- Masson, M., Niedergang, C., Schreiber, V., Muller, S., Menissier-de Murcia, J. and de Murcia, G. (1998) XRCC1 is specifically associated with poly(ADP-ribose) polymerase and negatively regulates its activity following DNA damage. *Mol. Cell Biol.*, **18**, 3563–3571.
- Okano, S., Lan, L., Caldecott, K.W., Mori, T. and Yasui, A. (2003) Spatial and temporal cellular responses to single-strand breaks in human cells. *Mol. Cell Biol.*, **23**, 3974–3981.
- Lan, L., Nakajima, S., Oohata, Y., Takao, M., Okano, S., Masutani, M., Wilson, S.H. and Yasui, A. (2004) In situ analysis of repair processes for oxidative DNA damage in mammalian cells. *Proc. Natl Acad. Sci. USA*, **101**, 13738–13743.
- El-Khamisy, S.F., Masutani, M., Suzuki, H. and Caldecott, K.W. (2003) A requirement for PARP-1 for the assembly or stability of XRCC1 nuclear foci at sites of oxidative DNA damage. *Nucleic Acids Res.*, **31**, 5526–5533.
- Vodenicharov, M.D., Sallmann, F.R., Satoh, M.S. and Poirier, G.G. (2000) Base excision repair is efficient in cells lacking poly(ADP-ribose) polymerase 1. *Nucleic Acids Res.*, **28**, 3887–3896.
- Ame, J.C., Rolli, V., Schreiber, V., Niedergang, C., Apiou, F., Decker, P., Muller, S., Hoger, T., Menissier-de Murcia, J. and de Murcia, G. (1999) PARP-2, A novel mammalian DNA damage-dependent poly(ADP-ribose) polymerase. *J. Biol. Chem.*, **274**, 17860–17868.
- Schreiber, V., Ricoul, M., Amé, J.C., Dantzer, F., Meder, V.S., Spenlehauer, C., Stiegler, P., Niedergang, C., Sabatier, L. *et al.* (2004) PARP-2, structure-function relationship. In Burkle, A. (ed.), *Poly(ADP-ribose)ylation*, Chapter 2. Landes Bioscience, Georgetown, pp. 13–31.
- Menissier de Murcia, J., Ricoul, M., Tartier, L., Niedergang, C., Huber, A., Dantzer, F., Schreiber, V., Ame, J.C., Dierich, A. *et al.* (2003) Functional interaction between PARP-1 and PARP-2 in chromosome stability and embryonic development in mouse. *Embo. J.*, **22**, 2255–2263.
- Schreiber, V., Ame, J.C., Dolle, P., Schultz, I., Rinaldi, B., Fraulob, V., Menissier-de Murcia, J. and de Murcia, G. (2002) Poly(ADP-ribose) polymerase-2 (PARP-2) is required for efficient base excision DNA repair in association with PARP-1 and XRCC1. *J. Biol. Chem.*, **277**, 23028–23036.
- Masutani, M., Nozaki, T., Nishiyama, E., Shimokawa, T., Tachi, Y., Suzuki, H., Nakagama, H., Wakabayashi, K. and Sugimura, M. (1999) Function of poly(ADP-ribose) polymerase in response to DNA damage: gene-disruption study in mice. *Mol. Cell Biochem.*, **193**, 149–152.
- Menissier de Murcia, J., Niedergang, C., Trucco, C., Ricoul, M., Dutrillaux, B., Mark, M., Olivier, F.J., Masson, M., Dierich, A. *et al.* (1997) Requirement of poly(ADP-ribose) polymerase in recovery from DNA damage in mice and in cells. *Proc. Natl Acad. Sci. USA*, **94**, 7303–7307.

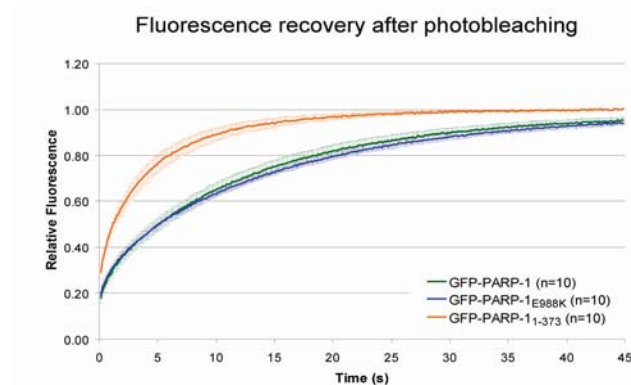
18. Wang,Z.Q., Stingl,L., Morrison,C., Jantsch,M., Los,M., Schulze-Osthoff,K. and Wagner,E.F. (1997) PARP is important for genomic stability but dispensable in apoptosis. *Genes Dev.*, **11**, 2347–2358.
19. Trucco,C., Oliver,F.J., de Murcia,G. and Menissier-de Murcia,J. (1998) DNA repair defect in poly(ADP-ribose) polymerase-deficient cell lines. *Nucleic Acids Res.*, **26**, 2644–2649.
20. Fisher,A., Hohegger,H., Takeda,S. and Caldecott,K.W. (2007) Poly (ADP-ribose) polymerase-1 accelerates single-strand break repair in concert with poly (ADP-ribose) glycohydrolase. *Mol. Cell. Biol.*, **27**, 5597–5605.
21. Dantzer,F., Ame,J.C., Schreiber,V., Nakamura,J., Menissier-de Murcia,J. and de Murcia,G. (2006) Poly(ADP-ribose) polymerase-1 activation during DNA damage and repair. *Methods Enzymol.*, **409**, 493–510.
22. Meder,V.S., Boeglin,M., de Murcia,G. and Schreiber,V. (2005) PARP-1 and PARP-2 interact with nucleophosmin/B23 and accumulate in transcriptionally active nucleoli. *J. Cell Sci.*, **118**, 211–222.
23. Maeda,Y., Hunter,T.C., Loudy,D.E., Dave,V., Schreiber,V. and Whitsett,J.A. (2006) PARP-2 interacts with TTF-1 and regulates expression of surfactant protein-B. *J. Biol. Chem.*, **281**, 9600–9606.
24. Rolli,V., O'Farrell,M., Menissier-de Murcia,J. and de Murcia,G. (1997) Random mutagenesis of the poly(ADP-ribose) polymerase catalytic domain reveals amino acids involved in polymer branching. *Biochemistry*, **36**, 12147–12154.
25. Molinete,M., Vermeulen,W., Burkle,A., Menissier-de Murcia,J., Kupper,J.H., Hoeijmakers,J.H. and de Murcia,G. (1993) Overproduction of the poly(ADP-ribose) polymerase DNA-binding domain blocks alkylation-induced DNA repair synthesis in mammalian cells. *Embo. J.*, **12**, 2109–2117.
26. Campbell,R.E., Tour,O., Palmer,A.E., Steinbach,P.A., Baird,G.S., Zacharias,D.A. and Tsien,R.Y. (2002) A monomeric red fluorescent protein. *Proc. Natl Acad. Sci. USA*, **99**, 7877–7882.
27. Mortusewicz,O., Schermelleh,L., Walter,J., Cardoso,M.C. and Leonhardt,H. (2005) Recruitment of DNA methyltransferase I to DNA repair sites. *Proc. Natl Acad. Sci. USA*, **102**, 8905–8909.
28. Mortusewicz,O., Rothbauer,U., Cardoso,M.C. and Leonhardt,H. (2006) Differential recruitment of DNA ligase I and III to DNA repair sites. *Nucleic Acids Res.*, **34**, 3523–3532.
29. Ferro,A.M. and Olivera,B.M. (1982) Poly(ADP-ribosylation) in vitro. Reaction parameters and enzyme mechanism. *J. Biol. Chem.*, **257**, 7808–7813.

Supplementary Information



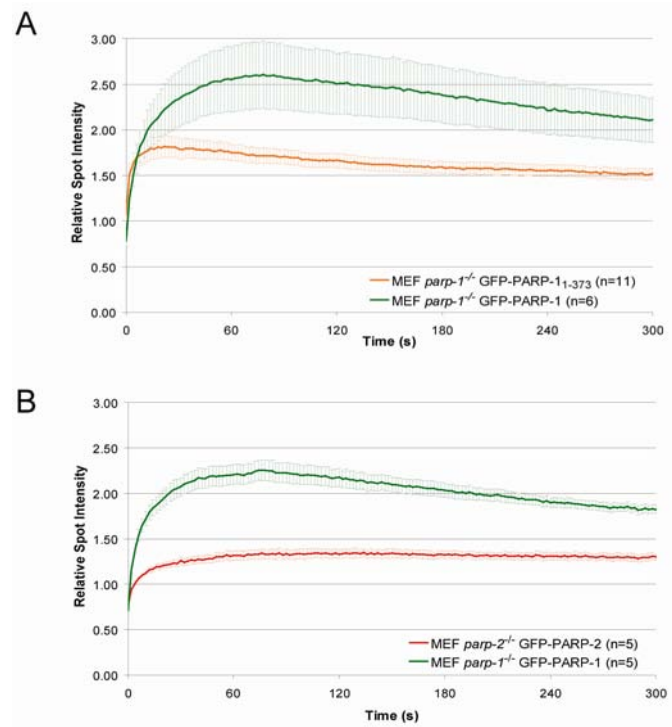
Supplementary Figure 1

Recruitment of GFP-PARP-1 to DNA damage sites during mitosis. Live cell imaging of a microirradiated *parp-1*^{-/-} cell expressing GFP-PARP-1. Accumulation of GFP-PARP-1 can be observed immediately after microirradiation in cells undergoing mitosis. Scale bar, 5 μ m.



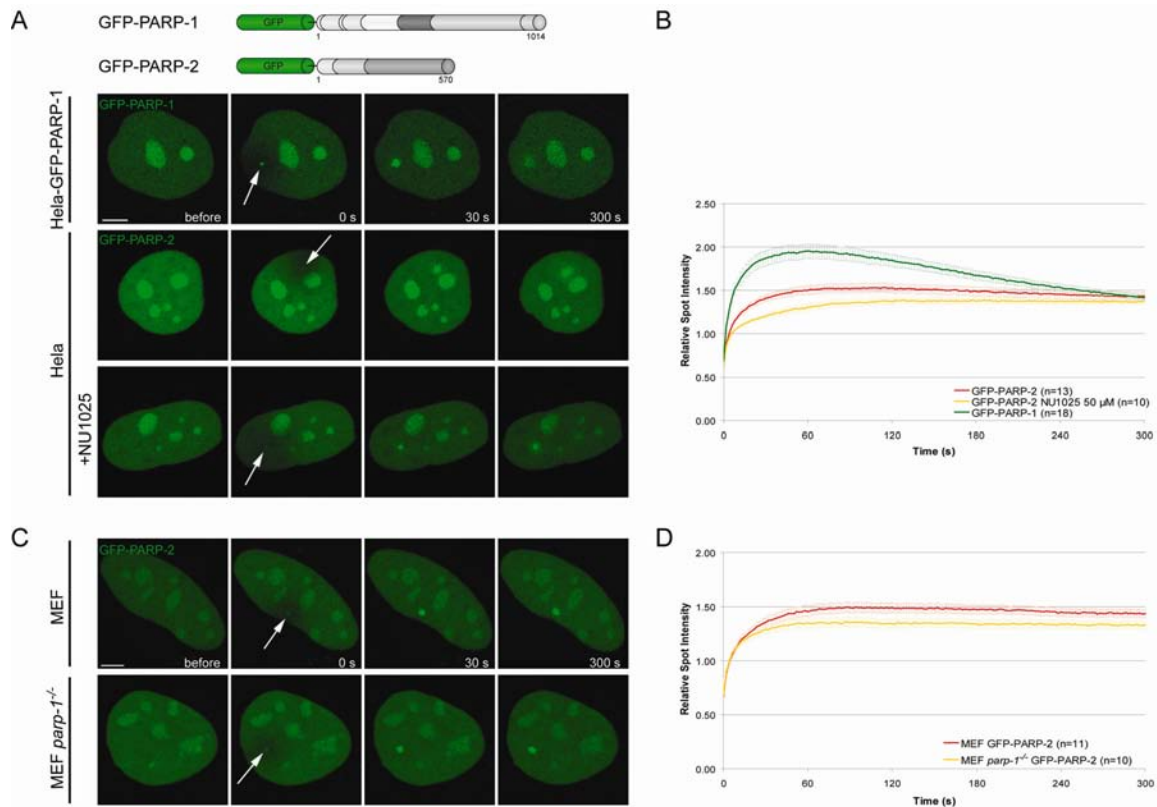
Supplementary Figure 2

Half nucleus FRAP reveals high mobility of the DNA binding domain in comparison to the full length and catalytic PARP-1 mutant. Quantitative evaluation of half nucleus FRAP experiments are shown. The DNA binding domain shows an overall higher mobility compared to the full length PARP-1 or the catalytic mutant PARP-1.



Supplementary Figure 3

Time-matched controls for the recruitment of (A) GFP-PARP-1₁₋₃₇₃ and (B) GFP-PARP-2 in comparison to GFP-PARP-1.



Supplementary Figure 4

Recruitment of PARP-2 to DNA damage sites in living cells. (A) Live cell imaging of microirradiated HeLa cells either expressing GFP-PARP-1 or GFP-PARP-2. Accumulation of GFP-PARP-1 and GFP-PARP-2 can be observed immediately after microirradiation. Live cell imaging of microirradiated HeLa cells reveals a delayed accumulation of GFP-PARP-2 in the presence of NU1025. (B) Kinetics of PARP-2 recruitment in the absence and presence of NU1025. For comparison, the recruitment kinetics of GFP-PARP-1 from Figure 1 D are displayed. (C and D) Comparison of PARP-2 recruitment kinetics in wild type and PARP-1 knock out MEFs. Error bars represent the standard error of the mean. Scale bar, 5 μ m.

2.2. Recruitment of RNA Polymerase II cofactor PC4 to DNA repair sites.

Recruitment of RNA Polymerase II cofactor PC4 to DNA repair sites

Oliver Mortusewicz^{1,2*}, *Wera Roth*^{3,4*}, *M. Cristina Cardoso*⁵,
Michael Meisterernst^{1,3,6†} and *Heinrich Leonhardt*^{1,2†}

¹ Munich Center for Integrated Protein Science CiPS^M

² Ludwig Maximilians University Munich, Department of Biology II, 82152 Planegg-Martinsried, Germany

³ GSF-National Research Center for Environment and Health, Department of Gene Expression, 81377 Munich, Germany

⁴ University of Bonn, Institute of Physiological Chemistry, Division of Cell Biochemistry, 53115 Bonn, Germany

⁵ Max Delbrück Center for Molecular Medicine, 13125 Berlin, Germany

⁶ Wilhelms University Muenster, Institute for Cell- and Tumor Biology (ICTB), Faculty of Medicine, 48149 Muenster, Germany

^{†*} these authors contributed equally to this work

Correspondence should be addressed to:

H. Leonhardt (E-mail: h.leonhardt@lmu.de; Fax +49 89 2180-74236; Tel. +49 89 2180-74232)

Running title: Recruitment of PC4 to DNA repair sites

Abstract

The multifunctional nuclear protein PC4 is involved in various cellular processes including transcription, replication and chromatin organization. Recently, PC4 has been identified as a suppressor of oxidative mutagenesis in *E. coli* and *S. cerevisiae*. To investigate a potential role of PC4 in mammalian DNA repair, we used a combination of live cell microscopy, microirradiation and FRAP analysis. We found a clear accumulation of endogenous PC4 at DNA damage sites introduced by either chemical agents or laser microirradiation. Using fluorescent fusion proteins and specific mutants we could demonstrate that the single strand binding capacity of PC4 is essential for rapid recruitment to laser-induced DNA damage sites. Furthermore PC4 showed a high turnover at DNA damages sites compared to the repair factors RPA and PCNA. We propose that PC4 plays a role in the early steps of the DNA damage response recognizing and stabilizing ssDNA and thereby facilitating DNA repair by enabling DNA repair factors to access their substrates.

Keywords: PC4, RPA, microirradiation, DNA repair, RNA pol II

Introduction

The human positive cofactor 4 (PC4) is an abundant nuclear protein which plays an important role in various cellular processes including transcription, replication and chromatin organization (Das et al., 2006; Ge and Roeder, 1994; Kretzschmar et al., 1994; Pan et al., 1996; Wang et al., 2004). PC4 was originally identified as a transcription cofactor that was minimally needed - in addition to the basal transcription machinery consisting of TFIIA, TFIIB, TFIID, TFIIE, TFIIIF and TFIIH - to mediate the response of RNA polymerase II to transcriptional activators (Ge and Roeder, 1994; Kretzschmar et al., 1994; Meisterernst et al., 1991).

PC4 is thought to facilitate the formation of the preinitiation complex at the level of TFIID-TFIIA binding as well as during promoter opening and the escape of RNA polymerase II through interaction with TFIIH (Fukuda et al., 2004; Kaiser et al., 1995). In addition to its cofactor function PC4 represses transcription through interaction with single stranded DNA at open promoter regions (Werten et al., 1998; Wu and Chiang, 1998). Interestingly, PC4 was found to interact genetically and physically with a component of the polyadenylation complex, CtsF-64/Rna15p, which indirectly supported the hypothesis that transcription, polyadenylation and termination may be closely linked (Calvo and Manley, 2001).

The 127 amino acid protein PC4 consists of two major domains that are critical for distinct functions. The lysine-rich N-terminal regulatory domain (amino acid residues 1-62) is required for protein-protein interactions and is essential for coactivator function *in vitro* (Kaiser et al., 1995; Kretzschmar et al., 1994). The C-terminal domain, comprising amino acid residues 63-127, allows binding to single and double stranded DNA in a sequence-independent manner, mediating both transcriptional repression and coactivation (Kaiser et al., 1995; Werten et al., 1998). Structural analysis of the C-terminal domain (CTD) revealed that PC4 dimerizes and binds single-stranded DNA through the carboxy-terminal domain (Brandsen et al., 1997; Werten and Moras, 2006). Mutation of critical amino acid residues within the CTD of PC4, predicted to be essential for ssDNA binding based on structural comparison analyses using the RPA-ssDNA co-crystal structure (Bochkarev et al., 1997), resulted in the loss of its ability to bind to ssDNA and to repress transcription (Werten et al., 1998). Within its N-terminal regulatory domain PC4 contains the co-called SEAC motif, which is rich in serine and acidic residues and was shown to be a target of casein kinase II (CKII) phosphorylation (Kretzschmar et al., 1994), regulating the

activity of PC4 in mammalian cells (Ge et al., 1994). In proliferating mammalian cells about 95% of PC4 was shown to be phosphorylated, which affects its DNA-binding properties. Phosphorylated PC4 was shown to lose its coactivator and dsDNA binding activities, but maintained its ability to bind to ssDNA mediating transcriptional repression (Ge et al., 1994; Werten et al., 1998).

Recently it has been shown that the ssDNA binding capacity of PC4 is required for resistance to hydrogen peroxide (H₂O₂) and prevents mutagenesis by oxidative DNA damage in *E. coli* and *S. cerevisiae* (Wang et al., 2004). While these genetic studies argue for a role of PC4 in DNA repair, the direct involvement of PC4 in the DNA damage response of mammalian cells remains elusive. We used a combination of live cell microscopy, laser microirradiation and FRAP analysis to study the recruitment of PC4 to DNA damage sites *in vivo*. We found a very rapid and transient accumulation of PC4 at DNA damage sites depending on its ability to bind ssDNA which, together with the suggested helicase activity of PC4, argues for a role of this multifunctional cofactor in the early steps of DNA repair.

Results and discussion

PC4 accumulates at DNA damage sites

To investigate the role of PC4 in DNA repair we examined the redistribution of PC4 in response to DNA damage in human and mouse cells. After treatment with different chemical agents, cells were in situ extracted and subsequently stained for endogenous PC4 and specific DNA damage markers. In untreated cells we found a diffuse distribution of PC4 in the nucleus. Upon treatment with H₂O₂ or Hydroxyurea (HU) PC4 accumulated at discrete subnuclear foci colocalizing with sites of DNA damage visualized by antibodies against poly (ADP)Ribose (PAR) and γ H2AX, respectively (Figure 1 A and B). Replication arrest with HU or Aphidicolin (Aph), resulting in extended stretches of single stranded DNA (ssDNA), as well as treatment with H₂O₂, also lead to a redistribution of PC4 into foci colocalizing with the single strand binding protein RPA (Figure 1 C).

To locally introduce DNA lesions at preselected subnuclear sites we employed microirradiation using a 405 nm diode laser as described previously (Mortusewicz et al., 2006; Mortusewicz et al., 2005). This treatment results in the generation of a mixture of different types of DNA damage, including single strand breaks (SSBs) and double strand breaks (DSBs), which are substrates for different DNA repair pathways. Immunofluorescence stainings with specific antibodies revealed that endogenous PC4 accumulates at sites of DNA damage as early as 5 min after microirradiation in both human and mouse cells (Figure 2 A, B and D). Furthermore we observed colocalization of PC4 with the replication and repair protein PCNA at laser-induced DNA damage sites (Figure 2 C and E). Taken together, these results show that PC4 accumulates at sites of DNA damage generated by chemical agents or laser microirradiation.

Recruitment kinetics and mobility of PC4 at DNA repair sites

Having shown that endogenous PC4 accumulates at DNA damage sites we generated GFP- and RFP-tagged fusion proteins to study the recruitment of PC4 in living cells (supplementary Figure 1 A). As a positive control we chose the processivity factor PCNA, which is involved in various DNA repair pathways including nucleotide excision repair (NER) (Shivji et al., 1992), base excision repair

(BER) (Gary et al., 1999; Levin et al., 2000), mismatch repair (MMR) (Jiricny, 2006; Johnson et al., 1996; Umar et al., 1996) and repair of double strand breaks (DSBs). Using a combination of microirradiation and time-lapse analysis we followed the spatio-temporal accumulation of GFP-PC4 and RFP-PCNA *in vivo*. For quantification, the fluorescence intensity at the irradiated sites were measured, corrected for background and total nuclear loss of fluorescence over the time course and normalized to the preirradiation value as described before (Mortusewicz et al., 2006). We found that GFP-PC4 accumulated at DNA damage sites immediately after microirradiation, preceding recruitment of RFP-PCNA (Figure 3 A). While RFP-PCNA showed a slow and constant increase of accumulation at repair sites during the observation period of 5 min, fluorescence intensities of GFP-PC4 declined after reaching a maximum around 20-40 s after microirradiation (Figure 3 B). To determine whether the recruitment of PC4 to DNA damage sites is cell cycle dependent, we microirradiated cells in different S phase stages using RFP-PCNA as a cell cycle marker. We found that PC4 accumulates at laser-induced DNA damage sites in early, mid and late S phase cells (supplementary Figure 2).

To determine the mobility of PC4 at laser-induced DNA damage sites we performed FRAP analysis 5 min after microirradiation. The irradiated region was bleached with a high energy laser pulse for 300 ms and the fluorescence recovery was determined. After bleaching of the repair foci we observed complete recovery of the PC4 signal within 5-10 s indicating a high mobility of PC4 at repair sites (Figure 3 C and D). In contrast, no recovery of PCNA at repair sites could be observed within the observation period, which is in good agreement with previous studies where DNA damage was induced by chemical agents or irradiation with a UV lamp (Essers et al., 2005; Solomon et al., 2004). As the fluorescence intensity of PC4 already begins to decline during the observation period of 5 min we also performed FRAP analysis 20 s after microirradiation to determine the mobility of PC4 at the peak of accumulation. We could not detect any differences in the mobility of PC4 20 s or 5 min after microirradiation (supplementary Figure 3). The constant increase in RFP-PCNA fluorescence observed when FRAP analysis was performed 20 s after microirradiation can be explained by new RFP-PCNA molecules being recruited during the time course of the FRAP experiment.

Taken together these results show an early and transient binding of PC4 at DNA damage sites suggesting a role for PC4 in the early steps of DNA repair, like damage recognition and/or signaling.

This raises the question of how PC4 gets recruited to DNA lesions. Given that the single strand binding capacity of PC4 is needed for resistance against hydrogen peroxide in repair deficient *E. coli* (Wang et al., 2004), it was tempting to speculate that PC4 is recruited by binding to single stranded DNA generated at microirradiated sites. In addition, the crystal structure of PC4 shows high similarity to the single strand binding domains of RPA70 and RPA34 (supplementary Figure 1B and (Bochkarev et al., 1999; Bochkarev et al., 1997; Brandsen et al., 1997)). Therefore, we directly compared the recruitment kinetics and the mobility of RFP-PC4 with GFP-RPA34. We found that both, PC4 and RPA34, were recruited immediately after microirradiation, with PC4 accumulating slightly faster than RPA34 (Figure 4 A). Like PCNA, RPA34 showed a slow and constant increase in fluorescence intensity at the irradiated site, while the intensity of PC4 gradually declined after reaching a maximum (Figure 4 B). FRAP analysis revealed distinct recovery rates indicating that PC4 exhibits a higher mobility at DNA damage sites than RPA34 (Figure 4 C and D). Taken together we could demonstrate that in comparison to the single strand binding protein RPA34, PC4 shows distinct recruitment and binding properties at laser-induced DNA damage sites.

The C-terminal single strand binding domain of PC4 mediates recruitment to DNA damage sites

The fact that PC4 and RPA show different recruitment kinetics and turnover rates at DNA repair sites raises the question whether PC4 indeed recognizes single stranded DNA generated after microirradiation. Earlier studies revealed a bipartite structure of PC4 comprising an amino-terminal regulatory domain (aa 1 to 62) and a carboxy-terminal ssDNA binding and dimerization domain (CTD, aa 63 to 127). It has also been shown that the ssDNA binding activity is not needed for the coactivator function of PC4 (Werten et al., 1998). To investigate the mechanisms mediating the recruitment of PC4 to DNA damage sites we generated GFP-fusion constructs comprising either the N-terminal regulatory domain (GFP-PC4 1-61) or the C-terminal domain (GFP-PC4 62-127). For direct comparison, we cotransfected the N-terminal domain together with the full length PC4. We found only a minor

accumulation of GFP-PC4 1-61 at microirradiated sites (Figure 5 A). In contrast GFP-PC4 62-127 showed the same recruitment kinetics as the full length protein (Figure 5 B). We conclude that the C-terminal domain of PC4 is necessary and sufficient for recruitment to DNA damage sites.

To further characterize the recruitment of PC4 to DNA damage sites, we generated mutants in the context of the full length and the C-terminal domain (CTD) of PC4. We introduced a point mutation at position 89 replacing Trp by Ala (GFP-PC4W89A and GFP-PC4CTDW89A) and a triple mutation at positions 77, 78 and 80 (GFP-PC4 β 2 β 3 and GFP-PC4CTD β 2 β 3), which were previously described to be essential for ssDNA binding of PC4 (Werten et al., 1998). The results of the microirradiation analysis of the PC4 mutants are summarized in supplementary Figure 1 A and shown in detail in Figure 5. Both mutations lead to a reduced accumulation of PC4 at microirradiated sites in the context of the full length and the CTD of PC4 (Figure 5 C-F) indicating that the single strand binding capacity of PC4 is needed for efficient recruitment of PC4 to DNA repair sites in living cells.

The fast and transient binding of the transcriptional cofactor PC4 at DNA damage sites identified in this study raises several interesting questions concerning potential roles in DNA repair and connections to transcriptional regulation. The observation that the recruitment of PC4 depends on its single strand binding capacity suggests that PC4 might fulfill similar roles in DNA repair as RPA. However, the different binding kinetics and mobility of PC4 and RPA at DNA damage sites would argue for distinct functions in DNA repair. As PC4 has been implicated in the regulation of DNA replication (Pan et al., 1996), it could stop DNA replication near DNA lesions. Similarly, PC4 might also stop transcription as a response to DNA damage which is supported by the fact that PC4 is a potent repressor of transcription at specific DNA structures such as ssDNA, DNA ends and heteroduplex DNA which are generated during DNA repair (Werten et al., 1998). Moreover, PC4 could have a helicase-like function (Werten and Moras, 2006; Werten et al., 1998), which through binding and multimerization along ssDNA is predicted to enable ATP-independent unwinding of duplex DNA.

The crystalization of PC4 in complex with ssDNA revealed that the subunits of the PC4 homodimer cooperate in the sequence-independent binding (Ballard et al.,

1988) of two opposing DNA backbones, exposing the DNA bases to the surrounding environment (Werten and Moras, 2006). These observations together with the rapid recruitment of PC4 to DNA damage sites argue for a role of PC4 in the detection and/or exposure of DNA damages. During the subsequent repair process PC4 may be displaced, as suggested by the observed transient binding at damaged sites.

Materials and Methods

Cell culture and transfection

Mouse C2C12 and human HeLa cells were cultured in DMEM containing 50 µg/ml gentamicin supplemented with 20% and 10% FCS, respectively. Cells grown on µ-slides (Ibidi) or on gridded coverslips were cotransfected with jetPEI (PolyPlus Transfection) according to the manufacturers instructions. For microirradiation experiments cells were sensitized by incubation in medium containing BrdU (10 µg/ml) for 24-48 h. Hydroxyurea, Hydrogen Peroxide and Aphidicolin were obtained from Sigma.

Expression plasmids

The generation of PC4 deletion and point mutants was previously described (Kretzschmar et al., 1994; Werten et al., 1998). Corresponding GFP-PC4 fusion constructs were constructed by ligation of either restriction fragments (NdeI/ClaI for GFP-PC4; EcoRI/ClaI for the constructs GFP-PC4 β 2 β 3, GFP-PC4W89A, GFP-PC4 22-127, GFP-PC4 CTD β 2 β 3, and GFP-PC4 CTDW89A; XhoI/PstI for GFP-PC4 62-127), or PCR products (forward primer 5' GAAGATCTCCGGTTATTCTTCATATGCC 3', reverse primer 5' TGGAATTCTCAATCATCTCTG 3' and BglIII/EcoRI cloning for GFP-PC4 1-61) into matching restriction sites of pEGFP-C1 (Clontech). GFP-PC4 fusion constructs were verified by sequencing and tested by expression in HeLa cells followed by western blot analysis. A red variant of PC4 was generated by replacing GFP with RFP (Campbell et al., 2002) and termed RFP-PC4.

Mammalian expression constructs encoding translational fusions of human RPA34 and PCNA with either green (GFP) or red (RFP) fluorescent protein were previously described (Sporbert et al., 2005). In all cases expression was under the control of the CMV promoter and correct expression of fusion proteins was verified by western blot analysis.

Immunofluorescence and Detergent Extraction

Cells were fixed in 3,7 % formaldehyde for 10 min and permeabilized with 0,5% Triton X-100 or ice-cold methanol for 5 min. The following primary antibodies (diluted in PBS containing 4% BSA) were used: anti- γ H2AX (Ser139) mouse monoclonal

antibodies (Upstate), anti-PAR mouse monoclonal antibodies (Trevigen), anti-RPA34 mouse monoclonal antibodies (Calbiochem), anti-PC4 rabbit polyclonal antibodies (SA2249, generated by standard techniques, Herstal, Belgium) and anti-PCNA rat monoclonal antibodies (Spada et al., 2007). Primary antibodies were detected using secondary antibodies (diluted 1:200 in PBS containing 4% BSA) conjugated to Alexa Fluor 488 or 555 (Molecular Probes). Cells were counterstained with DAPI and mounted in Vectashield (Vector Laboratories). For in situ extraction, cells were permeabilized for 30 s with 0,5 % Triton X-100 in PBS before fixation.

Live-cell Microscopy, microirradiation and photobleaching experiments

Live cell imaging, microirradiation and photobleaching experiments were carried out with a Leica TCS SP2/AOBS confocal laser scanning microscope equipped with a UV-transmitting HCX PL 63x/1.4 oil objective. Fluorophores were excited using a 488 nm Ar laser line and a 561 nm DPSS laser line. The microscope was equipped with a heated environmental chamber set to 37°C. Confocal image series were typically recorded with a frame size of 256x256 pixels and a pixel size of 90 nm.

Microirradiation was carried out as previously described (Mortusewicz et al., 2006). In brief, a preselected spot of ~1 µm in diameter within the nucleus was microirradiated for 1 s with a 405 nm diode laser set to maximum power at 100% transmission. Before and after microirradiation confocal image series of one mid z-section were recorded at 2 s time interval (typically 6 pre-irradiation and 150 post-irradiation frames). For evaluation of the recruitment kinetics, fluorescence intensities at the irradiated region were corrected for background and for total nuclear loss of fluorescence over the time course and normalized to the pre-irradiation value.

For FRAP analysis, a region of interest was selected and photobleached for 300 ms with all laser lines of the Ar-laser and the 561 nm DPSS laser set to maximum power at 100% transmission. Before and after bleaching, confocal image series were recorded at 150 ms time intervals (typically 10 prebleach and 200 postbleach frames). Mean fluorescence intensities of the bleached region were corrected for background and for total nuclear loss of fluorescence over the time course and normalized to the mean of the last 4 prebleach values.

For the quantitative evaluation of microirradiation and photobleaching experiments, data of at least 9 nuclei were averaged and the mean curve and the standard error of the mean calculated and displayed using Microsoft Excel software.

Images of fixed cells were taken with a Zeiss Axiophot 2 widefield epifluorescence microscope using a Zeiss Plan-Apochromat 63x/1.40 oil objective and a cooled CCD camera (Visitron Systems).

Online supplemental material

Fig.S1 shows a schematic outline of the fusion proteins used in this study and a comparison of the crystal structure of PC4 (Brandsen et al., 1997) with RPA70 (Bochkarev et al., 1997) and RPA34 (Bochkarev et al., 1999). Fig.S2 shows that recruitment of PC4 to laser-induced DNA damage sites occurs in all S phase stages. Fig.S3 shows that PC4 displays a high turnover at DNA damage sites 20 s and 5 min after microirradiation.

.

Acknowledgements

We are indebted to Dr R. Tsien for providing the mRFP1 expression vector. We are grateful to Na Li for help in the construction and testing of the PC4 constructs. This work was supported by grants from the Deutsche Forschungsgemeinschaft to H.L., M.M. and M.C.C.

Abbreviations:

PC4: positive cofactor 4

PCNA: proliferating cell nuclear antigen

RPA: replication protein A

HU: Hydroxyurea

Aph: Aphidicolin

PAR: poly (ADP)ribose

SSB: single strand breaks

TFII: transcription factor II

TBP: TATA-binding protein

TAF: TBP-associated factor

RNA pol II : RNA polymerase II

PIC: preinitiation complex

CTD: C-terminal domain

ssDNA: single-stranded DNA

dsDNA: double-stranded DNA

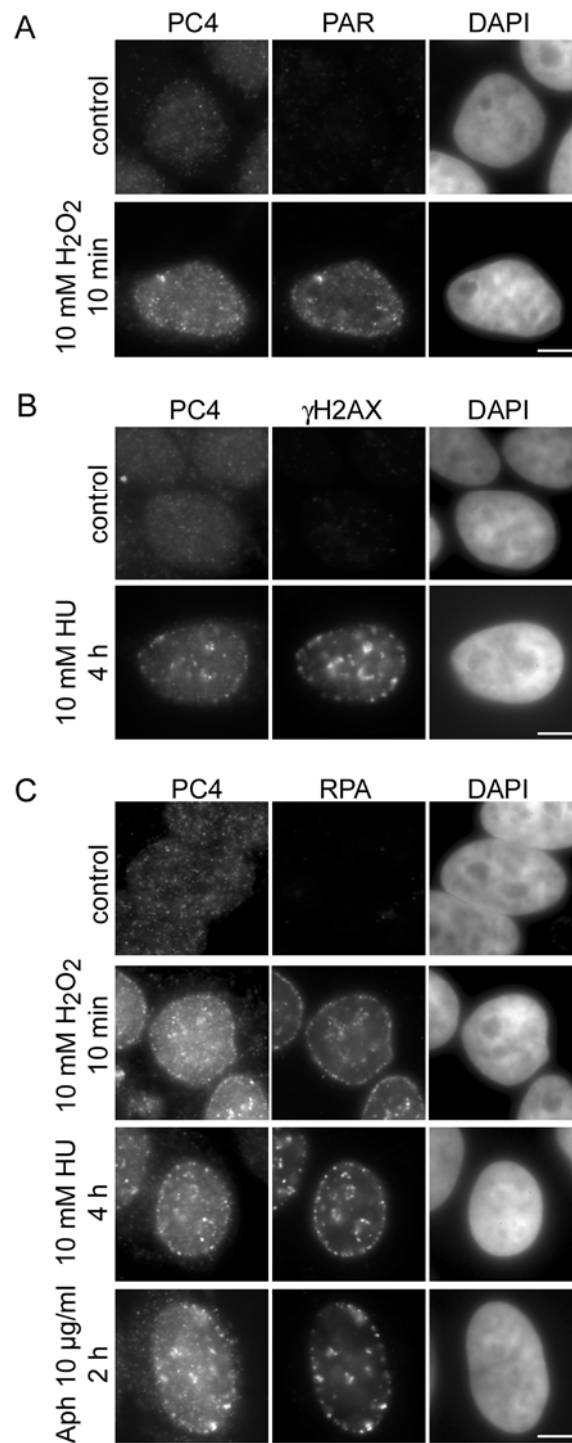
RPA: replication protein A

References

- Blazek, E., and G. Mittler, and M. Meisterernst. 2005. The Mediator of RNA polymerase II. *Chromosoma* 113:399-408.
- Ballard, D.W., W.M. Philbrick, and A.L. Bothwell. 1988. Identification of a novel 9-kDa polypeptide from nuclear extracts. DNA binding properties, primary structure, and in vitro expression. *J Biol Chem.* 263:8450-7.
- Bochkarev, A., E. Bochkareva, L. Frappier, and A.M. Edwards. 1999. The crystal structure of the complex of replication protein A subunits RPA32 and RPA14 reveals a mechanism for single-stranded DNA binding. *Embo J.* 18:4498-504.
- Bochkarev, A., R.A. Pfuetzner, A.M. Edwards, and L. Frappier. 1997. Structure of the single-stranded-DNA-binding domain of replication protein A bound to DNA. *Nature.* 385:176-81.
- Brandsen, J., S. Werten, P.C. van der Vliet, M. Meisterernst, J. Kroon, and P. Gros. 1997. C-terminal domain of transcription cofactor PC4 reveals dimeric ssDNA binding site. *Nat Struct Biol.* 4:900-3.
- Calvo, O., and J.L. Manley. 2001. Evolutionarily conserved interaction between CstF-64 and PC4 links transcription, polyadenylation, and termination. *Mol Cell.* 7:1013-23.
- Campbell, R.E., O. Tour, A.E. Palmer, P.A. Steinbach, G.S. Baird, D.A. Zacharias, and R.Y. Tsien. 2002. A monomeric red fluorescent protein. *Proc Natl Acad Sci U S A.* 99:7877-82.
- Das, C., K. Hizume, K. Batta, B.R. Kumar, S.S. Gadad, S. Ganguly, S. Lorain, A. Verreault, P.P. Sadhale, K. Takeyasu, and T.K. Kundu. 2006. Transcriptional coactivator PC4, a chromatin-associated protein, induces chromatin condensation. *Mol Cell Biol.* 26:8303-15.
- Essers, J., A.F. Theil, C. Baldeyron, W.A. van Cappellen, A.B. Houtsmuller, R. Kanaar, and W. Vermeulen. 2005. Nuclear dynamics of PCNA in DNA replication and repair. *Mol Cell Biol.* 25:9350-9.
- Fukuda, A., T. Nakadai, M. Shimada, T. Tsukui, M. Matsumoto, Y. Nogi, M. Meisterernst, and K. Hisatake. 2004. Transcriptional coactivator PC4 stimulates promoter escape and facilitates transcriptional synergy by GAL4-VP16. *Mol Cell Biol.* 24:6525-35.

- Gary, R., K. Kim, H.L. Cornelius, M.S. Park, and Y. Matsumoto. 1999. Proliferating cell nuclear antigen facilitates excision in long-patch base excision repair. *J Biol Chem.* 274:4354-63.
- Ge, H., and R.G. Roeder. 1994. Purification, cloning, and characterization of a human coactivator, PC4, that mediates transcriptional activation of class II genes. *Cell.* 78:513-23.
- Ge, H., Y. Zhao, B.T. Chait, and R.G. Roeder. 1994. Phosphorylation negatively regulates the function of coactivator PC4. *Proc Natl Acad Sci U S A.* 91:12691-5.
- Jiricny, J. 2006. The multifaceted mismatch-repair system. *Nat Rev Mol Cell Biol.* 7:335-46.
- Johnson, R.E., G.K. Kovvali, S.N. Guzder, N.S. Amin, C. Holm, Y. Habraken, P. Sung, L. Prakash, and S. Prakash. 1996. Evidence for involvement of yeast proliferating cell nuclear antigen in DNA mismatch repair. *J Biol Chem.* 271:27987-90.
- Kaiser, K., G. Stelzer, and M. Meisterernst. 1995. The coactivator p15 (PC4) initiates transcriptional activation during TFIIA-TFIIID-promoter complex formation. *Embo J.* 14:3520-7.
- Kretzschmar, M., K. Kaiser, F. Lottspeich, and M. Meisterernst. 1994. A novel mediator of class II gene transcription with homology to viral immediate-early transcriptional regulators. *Cell.* 78:525-34.
- Levin, D.S., A.E. McKenna, T.A. Motycka, Y. Matsumoto, and A.E. Tomkinson. 2000. Interaction between PCNA and DNA ligase I is critical for joining of Okazaki fragments and long-patch base-excision repair. *Curr Biol.* 10:919-22.
- Meisterernst, M., A.L. Roy, H.M. Lieu, and R.G. Roeder. 1991. Activation of class II gene transcription by regulatory factors is potentiated by a novel activity. *Cell.* 66:981-93.
- Mortusewicz, O., U. Rothbauer, M.C. Cardoso, and H. Leonhardt. 2006. Differential recruitment of DNA Ligase I and III to DNA repair sites. *Nucleic Acids Res.* 34:3523-32.
- Mortusewicz, O., L. Schermelleh, J. Walter, M.C. Cardoso, and H. Leonhardt. 2005. Recruitment of DNA methyltransferase I to DNA repair sites. *Proc Natl Acad Sci U S A.*

- Pan, Z.Q., H. Ge, A.A. Amin, and J. Hurwitz. 1996. Transcription-positive cofactor 4 forms complexes with HSSB (RPA) on single-stranded DNA and influences HSSB-dependent enzymatic synthesis of simian virus 40 DNA. *J Biol Chem.* 271:22111-6.
- Shivji, K.K., M.K. Kenny, and R.D. Wood. 1992. Proliferating cell nuclear antigen is required for DNA excision repair. *Cell.* 69:367-74.
- Solomon, D.A., M.C. Cardoso, and E.S. Knudsen. 2004. Dynamic targeting of the replication machinery to sites of DNA damage. *J Cell Biol.* 166:455-63.
- Spada, F., A. Haemmer, D. Kuch, U. Rothbauer, L. Schermelleh, E. Kremmer, T. Carell, G. Langst, and H. Leonhardt. 2007. DNMT1 but not its interaction with the replication machinery is required for maintenance of DNA methylation in human cells. *J Cell Biol.* 176:565-71.
- Sporbert, A., P. Domaing, H. Leonhardt, and M.C. Cardoso. 2005. PCNA acts as a stationary loading platform for transiently interacting Okazaki fragment maturation proteins. *Nucleic Acids Res.* 33:3521-8.
- Umar, A., A.B. Buermeyer, J.A. Simon, D.C. Thomas, A.B. Clark, R.M. Liskay, and T.A. Kunkel. 1996. Requirement for PCNA in DNA mismatch repair at a step preceding DNA resynthesis. *Cell.* 87:65-73.
- Wang, J.Y., A.H. Sarker, P.K. Cooper, and M.R. Volkert. 2004. The single-strand DNA binding activity of human PC4 prevents mutagenesis and killing by oxidative DNA damage. *Mol Cell Biol.* 24:6084-93.
- Werten, S., and D. Moras. 2006. A global transcription cofactor bound to juxtaposed strands of unwound DNA. *Nat Struct Mol Biol.* 13:181-2.
- Werten, S., G. Stelzer, A. Goppelt, F.M. Langen, P. Gros, H.T. Timmers, P.C. Van der Vliet, and M. Meisterernst. 1998. Interaction of PC4 with melted DNA inhibits transcription. *Embo J.* 17:5103-11.
- Wu, S.Y., and C.M. Chiang. 1998. Properties of PC4 and an RNA polymerase II complex in directing activated and basal transcription in vitro. *J Biol Chem.* 273:12492-8.

**Figure 1**

PC4 accumulates at DNA damage sites. HeLa cells were treated with Hydroxyurea (10 mM), H₂O₂ (10 mM) or Aphidicolin (10 μ g/ml) for indicated time points and in situ extracted with 0,5 % Triton-X-100 for 30 s before fixation. (A and B) Widefield fluorescence images of human HeLa cells treated with H₂O₂ or Hydroxyurea (HU) show accumulation of PC4 at subnuclear sites colocalizing with the DNA damage markers PAR and γ H2AX, respectively.

(C) Replication arrest with Hydroxyurea or Aphidicolin, as well as DNA damage induction with H₂O₂ results in relocalization of PC4 to subnuclear foci colocalizing with the single strand binding protein RPA34. Scale bar, 5 μm.

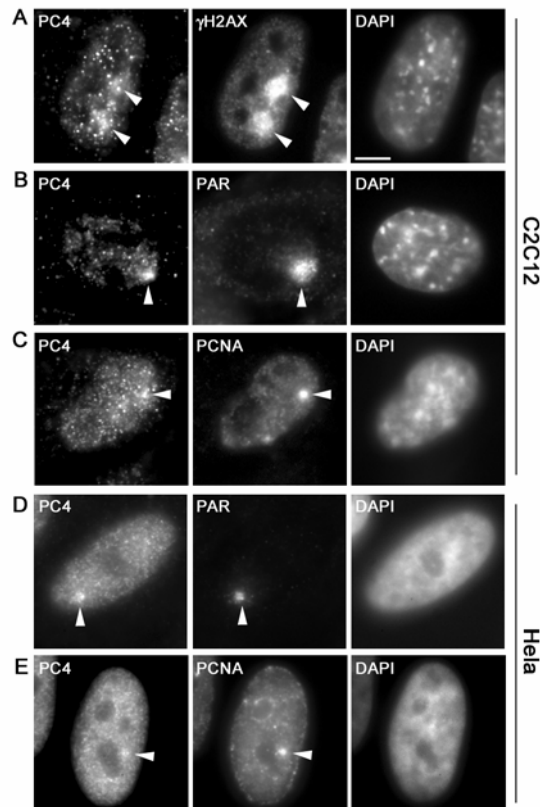


Figure 2

PC4 accumulates at laser-induced DNA damage sites. Widefield fluorescence images of mouse C2C12 and human HeLa cells are shown. Fixation and immunostaining was performed ~5 min after laser microirradiation. Arrows mark sites of irradiation. Laser microirradiation results in local generation of DSBs and SSBs (A, B and D) detected by antibodies against γ H2AX and PAR, respectively. Endogenous PC4 accumulates at DNA damage sites in mouse (A and B) and human cells (D) and colocalizes with PCNA (C and E). Scale bar, 5 μm.

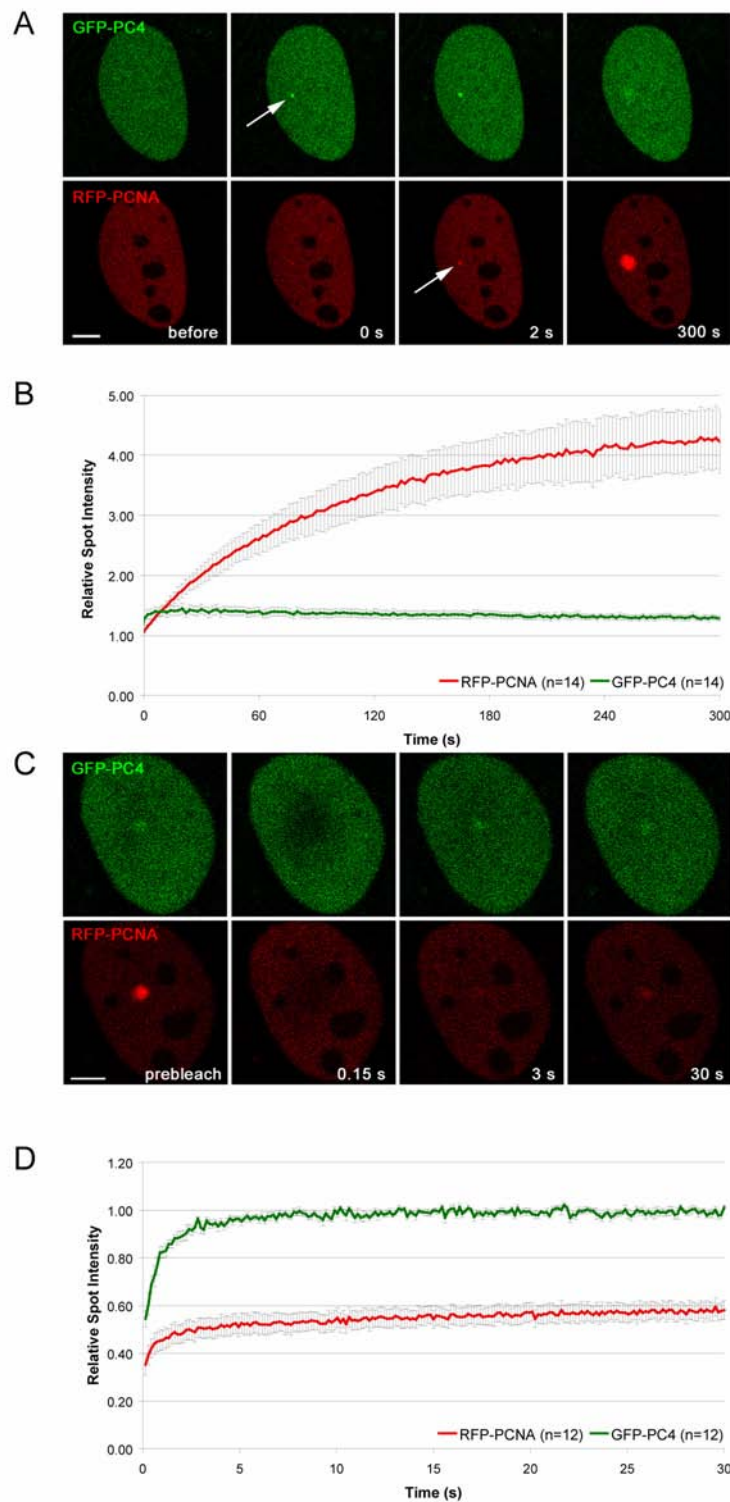


Figure 3

Recruitment and mobility of PC4 and PCNA at DNA damage sites in living cells.

(A) Live cell imaging of a microirradiated C2C12 cell coexpressing GFP-PC4 and RFP-PCNA. Accumulation of GFP-PC4 can be observed immediately after microirradiation, while RFP-PCNA accumulates with a short delay of about 2-10 s.

(B) Quantitative evaluation of recruitment kinetics showing mean curves. (C) To

analyze the mobility of PC4 and PCNA at DNA damage sites, the microirradiated region was bleached 5 min after microirradiation and the fluorescence recovery was measured. Quantitative evaluation of FRAP data showing mean curves. Error bars represent the standard error of the mean. Scale bar, 5 μm .

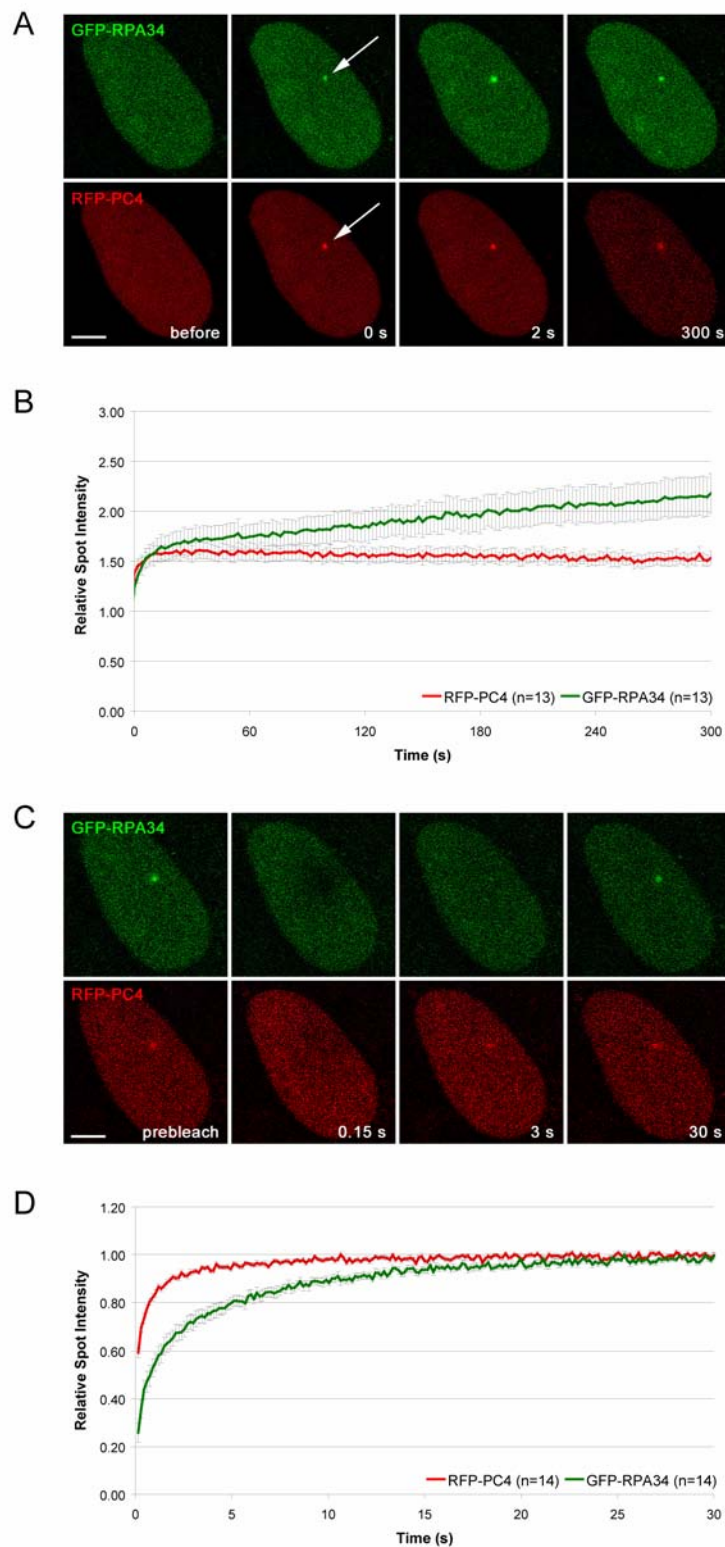


Figure 4

Comparison of recruitment and binding capacities of PC4 with RPA34 in living cells.

(A) Live cell imaging of a microirradiated C2C12 cell coexpressing GFP-RPA34 and RFP-PC4. Both, GFP-RPA34 and RFP-PC4 accumulate immediately after microirradiation (at sites of DNA damage). (B) Quantitative evaluation of recruitment kinetics showing mean curves. (C) Mobility of PC4 and RPA34 at DNA damage sites. (D) Quantitative evaluation of FRAP data showing mean curves. The Error bars represent the standard error of the mean.

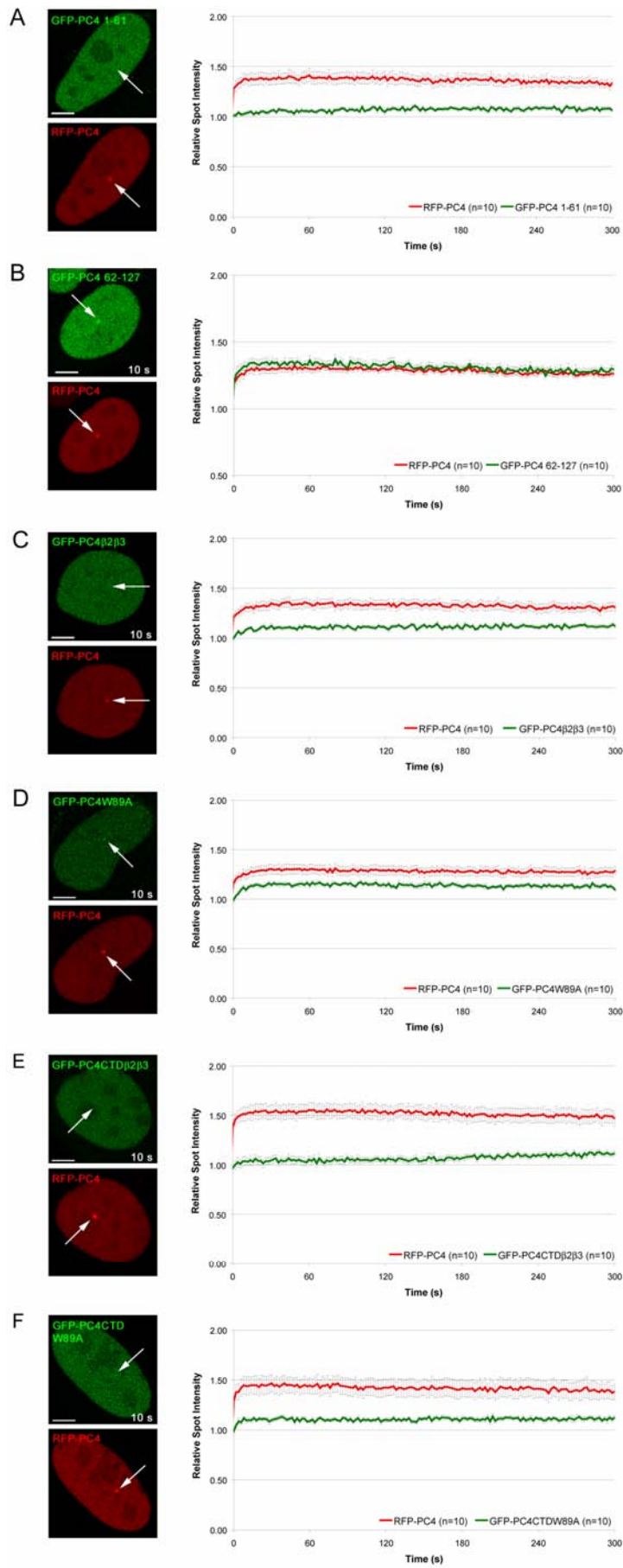
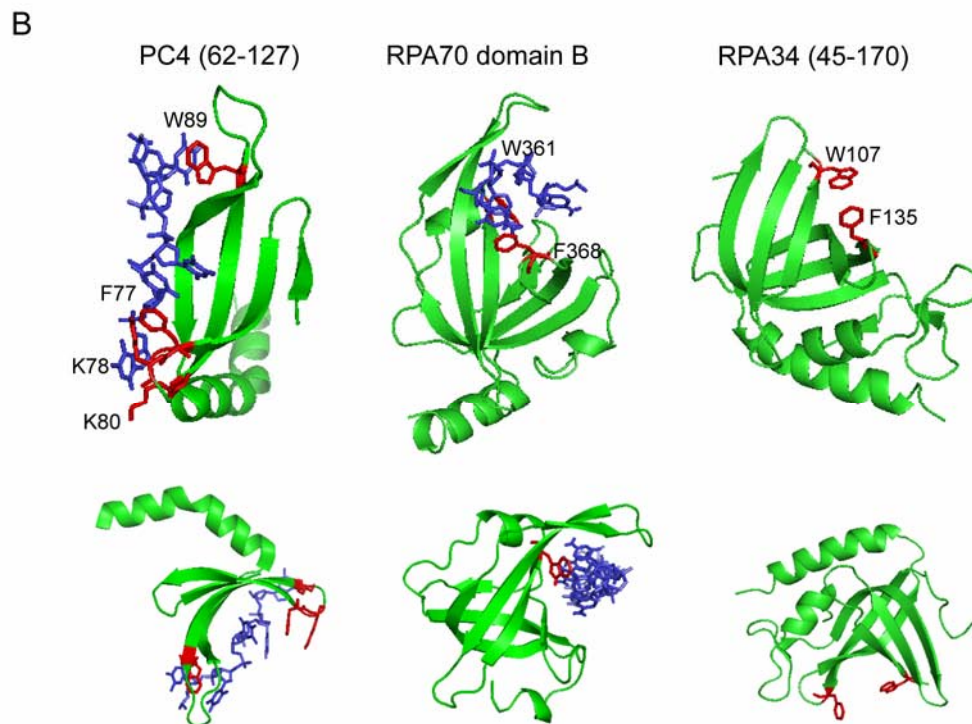
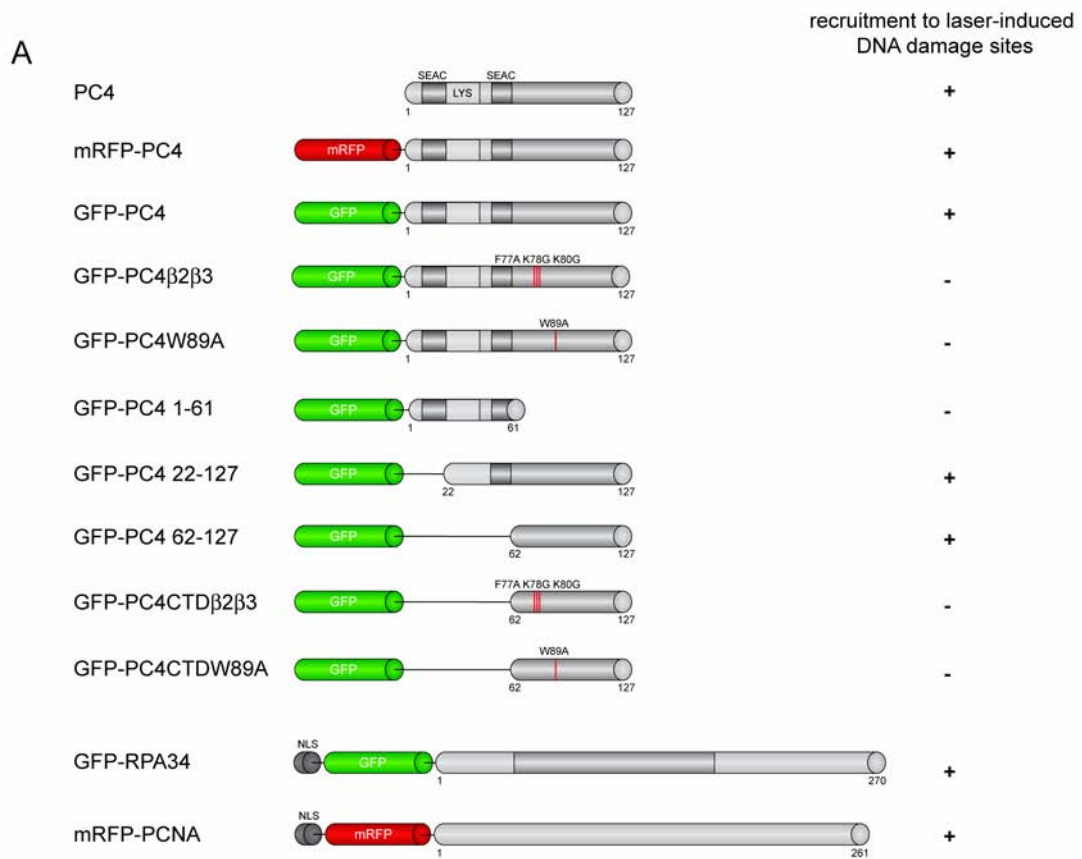


Figure 5

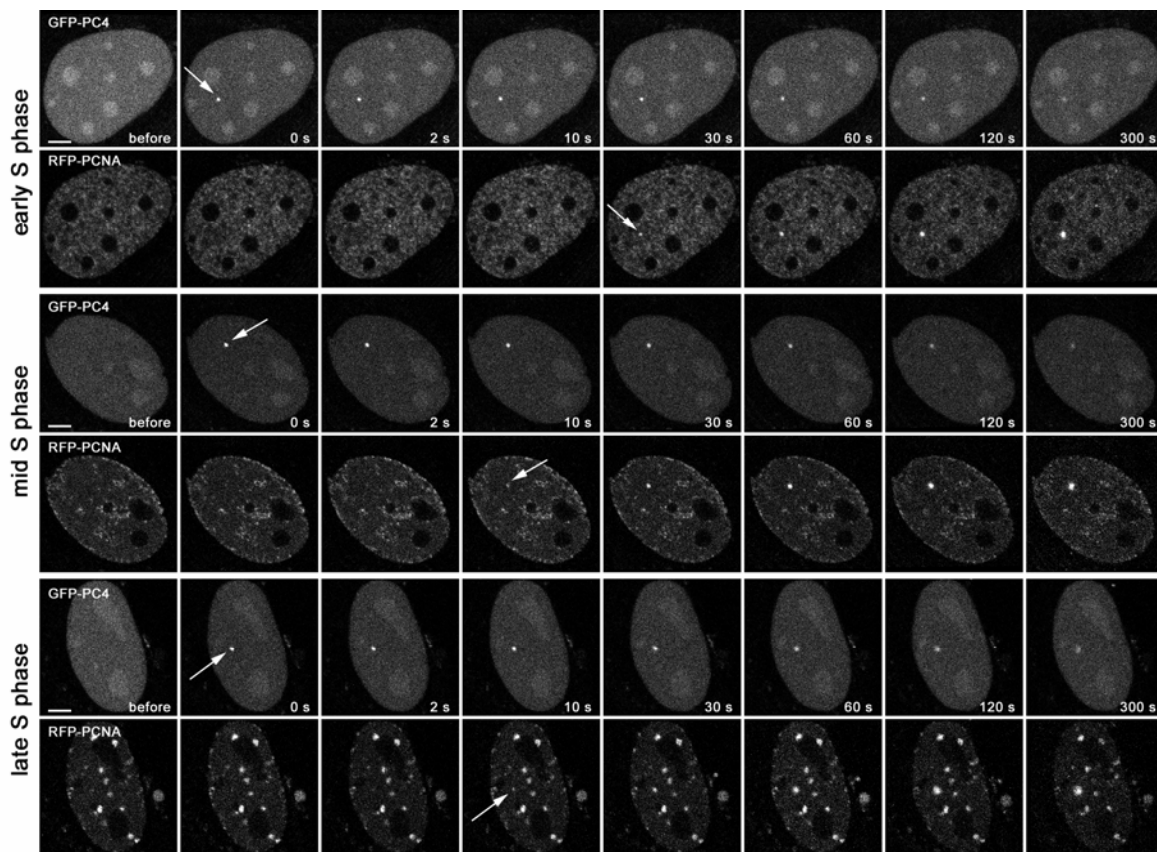
The single strand binding capacity of PC4 is needed for efficient recruitment to DNA damage sites. Deletion constructs containing either the N-terminal (1-61) or the C-terminal domain (62-127) of PC4 were tested for *in vivo* recruitment to DNA damage sites. While the N-terminal domain shows only a minor accumulation at microirradiated sites (A), the C-terminal domain is recruited with similar kinetics like the full length PC4 (B). For further analysis key residues essential for single strand binding within the full length or CTD of PC4 were mutated (outlined in Figure 3A). Recruitment of mutated fusion proteins to DNA damage sites is greatly reduced (C-F). Scale bar, 5 μm .

Supplementary Information



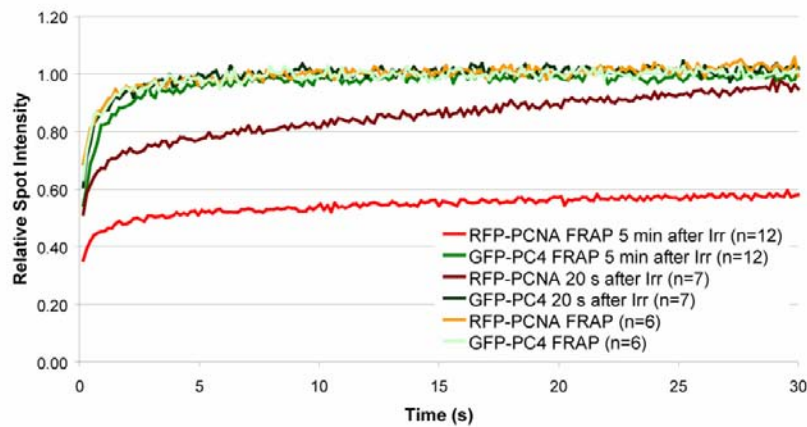
Supplementary Figure 1

(A) Schematic outline of fusion proteins used in this study. Mutated amino acid positions are indicated in red. (B) Comparison of the crystal structure of PC4 (Brandsen et al., 1997) with RPA70 (Bochkarev et al., 1997) and RPA34 (Bochkarev et al., 1999). Shown are two conformations indicating the OB fold and the binding curvature. PC4, RPA70 and RPA43 are shown as green ribbon models. The ssDNA is represented as a blue stick model. Key residues involved in binding of single stranded DNA are indicated in red.

**Supplementary Figure 2**

Recruitment of PC4 to laser-induced DNA damage sites occurs in all S phase stages. Live cell imaging of microirradiated C2C12 cells coexpressing GFP-PC4 and RFP-PCNA. The cell cycle stage was determined using the characteristic S phase

pattern of RFP-PCNA. Recruitment of GFP-PC4 to laser-induced DNA damage sites can be observed in early, mid and late S phase cells. Scale bar, 5 μm .



Supplementary Figure 3

PC4 displays a high turnover at laser-induced DNA damage sites. To analyze the mobility of GFP-PC4 and RFP-PCNA at the peak of GFP-PC4 accumulation, the microirradiated region was bleached 20 sec after microirradiation and the fluorescence recovery was measured. As a control a similar sized region in non-irradiated cells cotransfected with GFP-PC4 and RFP-PCNA was bleached and the fluorescence recovery was measured. The recovery curves obtained from FRAP analysis 5 min after microirradiation (Figure 4 B) are also displayed as a reference. Quantitative evaluation of FRAP data showing mean curves.

2.3. Spatiotemporal dynamics of p21CDKN1A protein recruitment to DNA damage sites and interaction with proliferating cell nuclear antigen.

Spatiotemporal dynamics of p21^{CDKN1A} protein recruitment to DNA-damage sites and interaction with proliferating cell nuclear antigen

Paola Perucca¹, Ornella Cazzalini¹, Oliver Mortusewicz², Daniela Necchi³, Monica Savio¹, Tiziana Nardo³, Lucia A. Stivala¹, Heinrich Leonhardt², M. Cristina Cardoso⁴ and Ennio Prosperi^{3,*}

¹Dipartimento di Medicina Sperimentale, sez. Patologia generale, Università di Pavia, 27100 Pavia, Italy

²Ludwig Maximilians University Munich, Department of Biology II, 82152 Planegg-Martinsried, Germany

³Istituto di Genetica Molecolare-CNR, sez. Istochimica e Citometria, Dipartimento di Biologia Animale, Università di Pavia, 27100 Pavia, Italy

⁴Max Delbrück Center for Molecular Medicine, 13125 Berlin, Germany

*Author for correspondence (e-mail: prosperi@igm.cnr.it)

Accepted 4 January 2006

Journal of Cell Science 119, 1517-1527 Published by The Company of Biologists 2006
doi:10.1242/jcs.02868

Summary

The cyclin-dependent kinase inhibitor p21^{CDKN1A} plays a fundamental role in the DNA-damage response by inducing cell-cycle arrest, and by inhibiting DNA replication through association with the proliferating cell nuclear antigen (PCNA). However, the role of such an interaction in DNA repair is poorly understood and controversial. Here, we provide evidence that a pool of p21 protein is rapidly recruited to UV-induced DNA-damage sites, where it colocalises with PCNA and PCNA-interacting proteins involved in nucleotide excision repair (NER), such as DNA polymerase δ , XPG and CAF-1. In vivo imaging and confocal fluorescence microscopy analysis of cells coexpressing p21 and PCNA fused to green or red fluorescent protein (p21-GFP, RFP-PCNA), showed a rapid relocation of both proteins at microirradiated nuclear spots, although dynamic measurements suggested that p21-

GFP was recruited with slower kinetics. An exogenously expressed p21 mutant protein unable to bind PCNA neither colocalised, nor coimmunoprecipitated with PCNA after UV irradiation. In NER-deficient XP-A fibroblasts, p21 relocation was greatly delayed, concomitantly with that of PCNA. These results indicate that early recruitment of p21 protein to DNA-damage sites is a NER-related process dependent on interaction with PCNA, thus suggesting a direct involvement of p21 in DNA repair.

Supplementary material available online at
<http://jcs.biologists.org/cgi/content/full/119/8/1517/DC1>

Key words: p21^{waf1/cip1}, PCNA, DNA repair, Nucleotide excision repair, UV irradiation

Introduction

The cyclin-dependent kinase (CDK) inhibitor p21^{CDKN1A} (also known as p21^{WAF1/Cip1}) plays an important role in several cellular pathways in response to intracellular and extracellular stimuli. In particular, p21 is involved in growth arrest induced by cell-cycle checkpoints, senescence, or terminal differentiation (Dotto, 2000). In addition, p21 has been shown to interact directly, or indirectly with proteins regulating gene expression, thus suggesting a role for p21 in regulation of transcription (Coqueret, 2003).

Although its activity is usually associated with CDK inhibition, p21 is also able to interact directly with proliferating cell nuclear antigen (PCNA), thereby inhibiting DNA replication (Gulbis et al., 1994). PCNA is a cofactor of DNA polymerases δ and ϵ , that is necessary both for DNA replication and repair (Tsurimoto, 1999; Warbrick, 2000). However, PCNA plays a major role in coordinating DNA metabolism with cell-cycle control (Prosperi, 1997) by interacting with other DNA replication and repair factors, as well as with cell-cycle proteins (Paunesku et al., 2001; Vivona and Kelman, 2003). The binding of p21 to PCNA results in competition and displacement of PCNA-interacting proteins,

thereby inhibiting DNA synthesis (Oku et al., 1998). Given that PCNA is also involved in DNA repair, the effects of p21 on this process are more controversial. In fact, biochemical studies suggest that high p21 levels inhibit DNA repair (Pan et al., 1995; Podust et al., 1995), and similar results are obtained on electroporated cells (Cooper et al., 1999). However, other studies showed that nucleotide excision repair (NER) was insensitive to p21 in vitro (Shivji et al., 1994; Shivji et al., 1998), and that p21 did not inhibit NER in vivo (McDonald et al., 1996; Sheikh et al., 1997). In particular, cells expressing a p21 mutant form unable to bind PCNA were deficient in NER, but when the wild-type protein was expressed, cells became proficient for repair (McDonald et al., 1996). A positive role for p21 in NER, was also suggested by the colocalisation and interaction of p21 and PCNA in actively repairing normal fibroblasts (Li et al., 1996; Savio et al., 1996), and by cell resistance to cytotoxic drugs after p21 expression (Ruan et al., 1998). Other studies performed on p21-null murine fibroblasts, or on tumour cell lines lacking p21 protein, report that the NER process is not significantly affected (Smith et al., 2000; Adimoolan et al., 2001; Wani et al., 2002). However, deletion of p21 gene in human normal fibroblasts results in reduced

DNA repair capacity (Stivala et al., 2001). Thus, although p21 is required for the successful cellular response to DNA damage, its participation in NER is still debated. It is known that p21 must be degraded for S-phase entry (Bornstein et al., 2003; Gottifredi et al., 2004), to prevent PCNA binding and consequent inhibition of DNA replication. Similarly, it has been recently shown that ubiquitin-dependent proteolysis of p21 is triggered after UV-induced DNA damage, and that this degradation is required for PCNA recruitment to DNA-repair sites (Bendjennat et al., 2003). However, it is well known that PCNA is also recruited to DNA-damage sites with fast kinetics in quiescent cells (Toschi and Bravo, 1988; Prospero et al., 1993; Aboussekhra and Wood, 1995; Savio et al., 1998), which show delayed p21 proteasomal degradation (Bendjennat et al., 2003). Thus, p21 removal may not be directly required for this step of the repair process.

In this study we have investigated whether the induction of p21 may inhibit DNA repair by preventing PCNA recruitment, and analyzed the spatiotemporal dynamics of p21 recruitment to DNA-damage sites directly on living cells. We show that a pool of p21 was rapidly recruited to, and colocalised with PCNA and other DNA-repair proteins at DNA-damage sites. By coexpressing p21 fused to green fluorescent protein (p21-GFP) and PCNA fused to red fluorescent protein (RFP-PCNA), we further show by dynamic fluorescence measurements that p21-GFP was recruited to damaged sites with slower kinetics than that of RFP-PCNA. Relocation of p21 was found to depend on prior recruitment of PCNA to DNA-damage sites.

Results

p21 protein is not completely degraded after UV irradiation

To investigate to what extent removal of p21 protein was required for DNA repair, human fibroblasts were exposed to different UV-C doses, and collected at various periods of time after irradiation. Fig. 1A shows that 6 hours after irradiation, p21 levels were unchanged in samples exposed to a relatively low dose (2.5 J/m²). By contrast, the protein was significantly degraded (by about 55% as quantified by band densitometry versus actin loading), at a high dose (10 J/m²). These doses corresponded to clonogenic survivals of about 80% and 10%, respectively. A more significant decrease in p21 protein (by about 85%) was observed after a dose of 30 J/m². The time-course study (Fig. 1B) showed that after an initial reduction (by about 60%) observed 30 minutes after exposure to 2.5 J/m² UV-C, p21 levels increased, reaching at 24 hours, about twice the amount of the untreated control samples. A consistent decrease was observed at each time point after irradiation with 10 J/m², though p21 was not completely degraded, because about 20% of the protein was still detected 24 hours after irradiation.

p21 is recruited together with PCNA to DNA repair sites
Previous studies on the involvement of p21 in NER focus only on a time scale of hours after DNA damage (Li et al., 1996; Savio et al., 1996). Thus, we first asked whether p21 protein surviving degradation could relocate to DNA-damage sites within a short interval after UV irradiation, similarly to PCNA. Fibroblasts were synchronised in G1 phase, to avoid the presence of S-phase cells containing high levels of chromatin-bound PCNA. Samples collected 30 minutes after irradiation

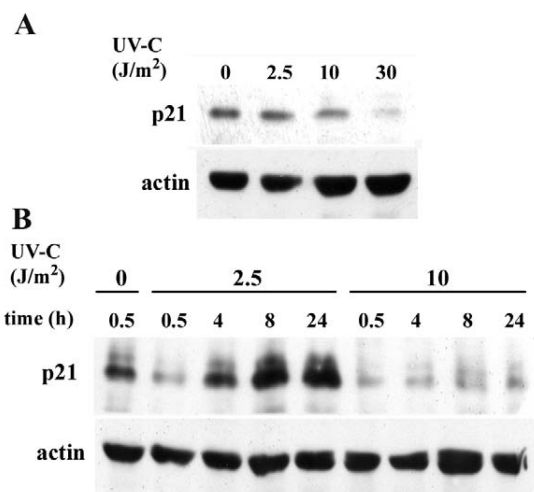


Fig. 1. p21 is not completely degraded after UV-induced DNA damage. (A) Dose response analysis of p21 degradation after UV-induced DNA damage in LF1 human fibroblasts. Cells were lysed directly in loading buffer 6 hours after UV-C irradiation at the indicated doses. Samples were analysed by western blot for p21 protein levels versus actin as a loading control. (B) Time-course analysis of p21 degradation after UV irradiation at 2.5 or 10 J/m². Samples were analysed for p21 and actin, as above.

were processed for indirect immunostaining of chromatin-bound PCNA, and three-step amplification with streptavidin-Texas-Red for detection of p21. The results clearly indicate that after DNA damage, early recruitment of p21 occurs similarly to PCNA (Fig. 2A).

To further test that this was an active process induced by exposure to UV-C radiation, p21 and PCNA were coexpressed in HeLa cells as GFP and RFP fusion proteins, p21-GFP and RFP-PCNA respectively. Coexpression levels of the two fusion proteins were similar in a high proportion (60–80%) of transfected cells. Previous analysis showed that p21-GFP arrested HeLa cells mainly in G1, and partly in G2 phase (Cazzalini et al., 2003). Thus, in nonirradiated control samples chromatin-binding of fluorescent proteins was dependent on the cell-cycle phase. About 65% of transfected cells showed chromatin-bound p21-GFP, whereas RFP-PCNA was chromatin-bound (in about 30% of cells), only in S phase (Leonhardt et al., 2000), as verified by BrdU incorporation (not shown). The concomitant presence of the two proteins bound to chromatin, was found in a very low number of cells (about 4%), that were probably at the G1-S transition, as previously observed for p21-GFP and endogenous PCNA (Cazzalini et al., 2004). By contrast, after UV irradiation, both proteins were chromatin-bound in about 70% of transfected cells (Fig. 2B). In these cells, the two proteins were already colocalised 30 minutes after irradiation, as indicated by the yellow colour of the merged confocal images (Fig. 2C). To further test the recruitment of both p21-GFP and RFP-PCNA at DNA repair sites, cotransfected HeLa cells were also exposed to local UV irradiation (10 J/m²) through 3- μ m-pore filters. Fig. 2D shows confocal sections of green and red fluorescence signals that are localised to the exposed areas. The merged image shows the distribution of the two proteins in the nucleus, as visualised by DNA staining.

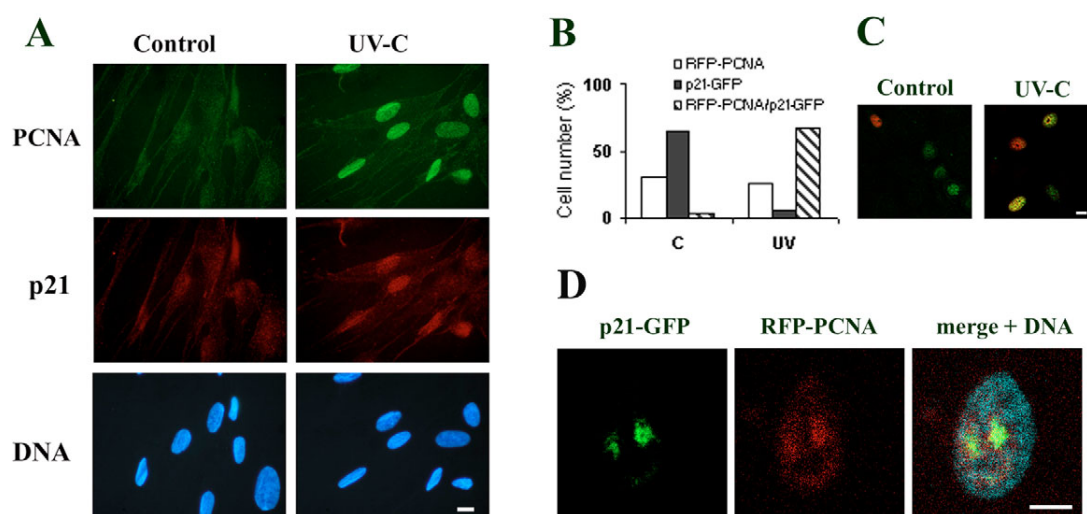


Fig. 2. Early recruitment of p21 to DNA repair sites. (A) LFI human fibroblasts were irradiated with UV-C (10 J/m^2) and 30 minutes later samples were extracted in situ and fixed for indirect immunofluorescence determination, or biotin-streptavidin amplification of chromatin-bound PCNA (green fluorescence) and p21 (red fluorescence), respectively. DNA (blue fluorescence) was stained with Hoechst 33258. (B) HeLa cells were cotransfected with p21-GFP and RFP-PCNA expression vectors, and 24 hours later exposed to UV-C radiation (10 J/m^2). After 30 minutes, control (C) and irradiated (UV) cells were extracted in situ and fixed for detection and counting of cells showing only chromatin-bound RFP-PCNA (empty bars), p21-GFP (solid bars), or both (dashed bars). The percentages of cells in a representative experiment are shown. (C) Confocal sections of merged green and red fluorescence signals, of untreated control and UV-C-irradiated cells. (D) HeLa cells expressing p21-GFP and RFP-PCNA were exposed to local UV-C radiation (10 J/m^2) through $3 \mu\text{m}$ pores. Confocal sections of green (p21-GFP) and red (RFP-PCNA) fluorescence signals are displayed, together with the merged image showing also the blue fluorescence (Hoechst) of DNA counterstaining. Bars, $10 \mu\text{m}$ (A,C); $5 \mu\text{m}$ (D).

Spatiotemporal dynamics of p21-GFP recruitment to DNA-damage sites

To directly compare p21 relocation with that of PCNA, and to demonstrate that this process occurred independently of the cell type, we analysed the recruitment kinetics of p21-GFP and RFP-PCNA in living C2C12 myoblasts, after inducing cyclobutane pyrimidine dimers (CPDs) DNA damage with a 405 nm laser (supplementary material Fig. S1). The dynamics of p21-GFP and RFP-PCNA fluorescent signals observed at DNA-damage sites in single C2C12 living cells, is shown in Fig. 3A. The irradiated spot shows maximal fluorescence intensities of both proteins within 2-15 minutes of irradiation, and then a decrease reaching basal levels 1-2 hours later. A detailed analysis showed that both proteins started to accumulate at the irradiated spot within a few seconds, but p21-GFP fluorescence appeared with a short delay after that of RFP-PCNA (Fig. 3B). Also, a direct comparison of fluorescence intensities at irradiated spots revealed a slightly but consistent faster recruitment of RFP-PCNA than p21-GFP (Fig. 3C). A similar behaviour was also observed in HeLa cells (supplementary material Fig. S2).

p21 is recruited to UV-damaged sites together with DNA-repair proteins

In order to clarify whether the levels of p21 may be a crucial determinant negatively influencing the recruitment of PCNA to DNA-damage sites, human fibroblasts were treated with trichostatin (TSA), a histone deacetylase inhibitor that is known to induce transcription of the p21 gene thereby increasing p21 protein levels (Richon et al., 2000). TSA-treated and mock-treated cells were exposed to UV-C irradiation, and

30 minutes later were collected for determination of total and chromatin-bound levels of PCNA and p21, as well as of other proteins participating in DNA repair. Western blot analysis shows that the total amount of PCNA, DNA ligase I (Lig I), or DNA polymerase δ (pol δ), were not appreciably modified by TSA or UV-C exposure, either alone or in combination (Fig. 4A). As expected, TSA induced an increase in p21 protein levels (by about 35%), whereas UV-C reduced the levels to about 15% of the untreated control sample. Interestingly, cells treated with TSA and then irradiated with UV-C also showed reduced levels (about 20% of the TSA-treated sample), indicating that p21 was degraded to a similar extent, notwithstanding the higher starting levels. The levels of the above proteins in the chromatin-bound fraction were undetectable in the control and in the TSA-treated cells, whereas UV-C induced a significant relocation of all proteins, including p21 itself. Pre-treatment with TSA did not induce any significant decrease in the amount of chromatin-bound PCNA, or of the other proteins, even if the levels of chromatin-bound p21 were apparently increased (Fig. 4B).

To further test whether p21 relocation occurred concomitantly with PCNA, and did not interfere with the recruitment of other repair factors, HeLa cells transfected with p21-GFP expression vector, were exposed to UV-C irradiation through filters with $3 \mu\text{m}$ pores. Thirty minutes later, cells were processed for in situ hypotonic lysis, fixed and immunostained with antibodies to pol δ , XPG, or CAF-1. Fig. 5A shows confocal sections of p21-GFP fluorescence (green) and immunofluorescence (red) signals relative to pol δ , and the merged image of both signals, together with that of DNA. Similarly, Fig. 5B,C shows the presence of XPG or CAF-1, respectively, together with that of p21-GFP, at

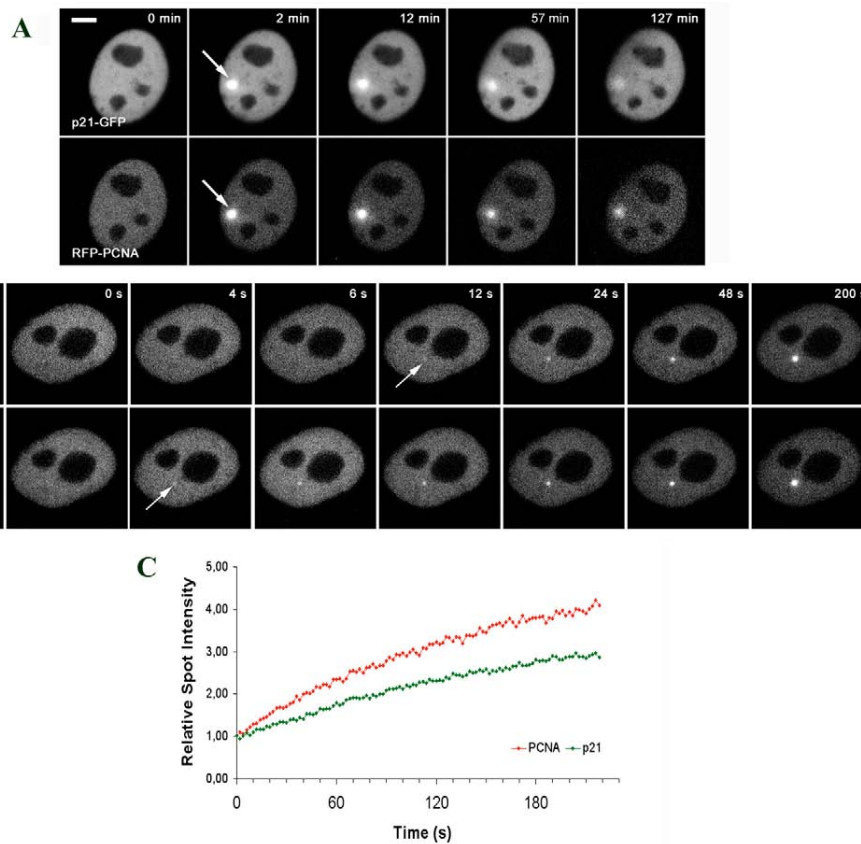


Fig. 3. Dynamics of p21 recruitment to DNA-repair sites in living cells. (A) C2C12 myoblasts expressing both p21-GFP and RFP-PCNA were exposed to 405 nm laser microirradiation and fluorescence signals were acquired after the indicated times. Maximum projections of confocal mid sections show the accumulation of p21-GFP and RFP-PCNA fluorescence signals at sites of DNA damage (arrows). (B) Short-term kinetic analysis of p21-GFP and RFP-PCNA fluorescence after 405 nm laser microirradiation. Signals were acquired every 2 seconds and confocal sections are shown of images taken at the indicated times. The arrows indicate the site of irradiation. (C) Plot of the relative fluorescence intensity of p21-GFP (green) and RFP-PCNA (red) at the irradiated spot. Fluorescence intensities acquired every 2 seconds at the irradiated region, were corrected for background, and for total nuclear loss of fluorescence over the time course, and normalised to the pre-irradiation value. Bars, 5 μ m (A,B).

locally irradiated sites. Each protein analysed was detected (though with variable intensity) at virtually every spot containing p21-GFP. These results indicate that in addition to PCNA, p21-GFP also colocalises with these proteins involved in different steps of DNA repair.

Interaction of p21 with PCNA and DNA pol δ after UV-C irradiation

Previous studies showed that p21 does not influence the RFC-mediated PCNA loading to DNA replication sites, yet it prevents or destabilises further binding of PCNA-interacting proteins, such as pol δ (Waga and Stillman, 1998; Cazzalini et al., 2003). To understand whether this was also the case during DNA repair, native p21 or p21-GFP were immunoprecipitated from normal fibroblasts, or from HeLa cells, respectively using antibodies to p21 or to GFP. After immunoprecipitation, bound peptides were analysed by western blot for the presence of PCNA and pol δ (p125 subunit). Fig. 6A shows the results of

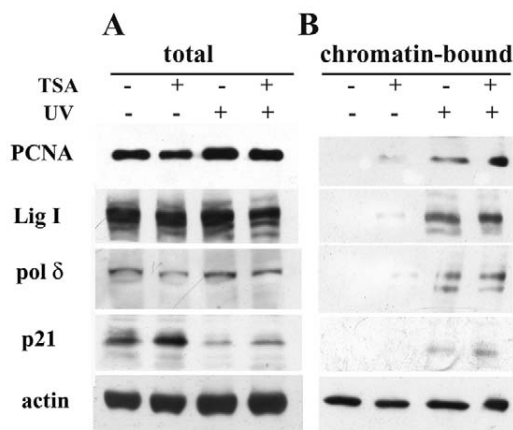


Fig. 4. Induction of p21 expression does not inhibit recruitment of PCNA and DNA repair proteins. LF1 fibroblasts were treated for 16 hours with TSA to induce expression of p21, as described in the Materials and Methods. 30 minutes after exposure to UV-C radiation (10 J/m²), cells were directly lysed in loading buffer, for determination by western blot of total cellular content (total) of p21, PCNA, pol δ (p125 subunit) and Lig I. (A). Parallel samples were fractionated for western blot analysis of proteins in the chromatin-bound fraction (B). Actin was also determined as a loading control.

p21 immunoprecipitation from fractionated cell extracts (detergent-soluble or chromatin-bound fractions) of LF1 fibroblasts. It can be seen that in the detergent-soluble fraction, PCNA was coimmunoprecipitated with p21 from both control and UV-treated samples. Interestingly, the pol- δ -p125 subunit was also present, being immunoprecipitated to a higher extent in UV-treated cells than in the control samples, though protein levels in the input soluble extracts were not significantly different. For a positive control, an aliquot of the soluble fraction was immunoprecipitated with a polyclonal antibody anti-p125 subunit. As expected, PCNA was coimmunoprecipitated with p125 (Riva et al., 2004).

No detectable signal of PCNA or p125 could be observed in the immunoprecipitation from the chromatin-bound fraction of untreated control cells, in which p21 levels were not detectable. By contrast, PCNA and pol δ were clearly immunoprecipitated by p21 antibody from the chromatin-bound fraction of UV-treated samples, in which p21 levels before immunoprecipitation were readily detected.

To investigate the kinetics of the p21-PCNA interaction, HeLa cells expressing p21-GFP or pEGFP, were UV irradiated

and collected at various periods of time. After fractionation, immunoprecipitation was performed with anti-GFP antibody on chromatin-bound extracts. Fig. 6B shows that both PCNA and pol δ could be immunoprecipitated from the chromatin-bound fraction of cells transfected with the p21-GFP expression vector, but not from that of cells transfected with empty vector (pEGFP). In particular, PCNA coimmunoprecipitated with p21-GFP from untreated control and from UV-irradiated samples, whereas pol δ was found only in the immunoprecipitates from UV-irradiated cells. The levels of PCNA and pol δ immunoprecipitating together with p21-GFP decreased with time. This result may be attributed to a reduction in the levels of pol δ in the chromatin-bound extract. The levels of PCNA were not concomitantly reduced, probably because they represent the sum of chromatin-

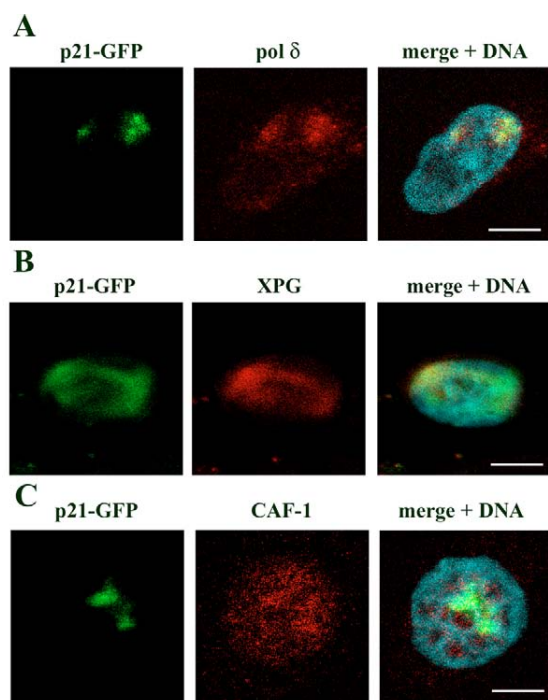


Fig. 5. Colocalisation of p21-GFP with DNA repair proteins recruited to DNA-damage sites. HeLa cells expressing p21-GFP were locally irradiated with UV-C (10 J/m^2) through $3 \mu\text{m}$ pores. After 30 minutes, cells were extracted in situ and fixed for determination of chromatin-bound p21-GFP and immunofluorescence staining of DNA repair proteins. (A) Confocal sections of p21-GFP (green) and pol δ (red) fluorescence signals are displayed together with the merged image also showing DNA counterstaining with Hoechst 33258 (blue). (B) confocal sections showing the single and merged images of p21-GFP (green), and XPG (red) at the irradiated sites. DNA was counterstained with Hoechst 33258 (blue). (C) Confocal sections showing the recruitment of p21-GFP (green) and CAF-1 (red), and DNA counterstaining (blue). Bars, $5 \mu\text{m}$.

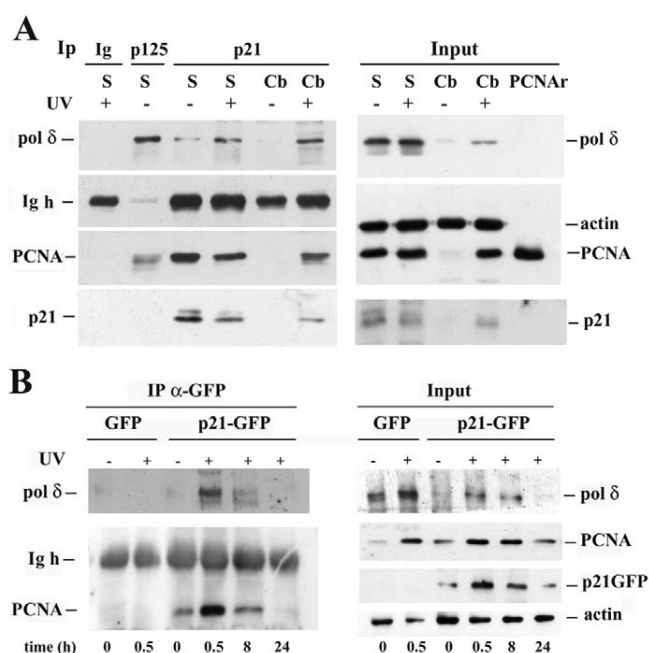


Fig. 6. p21 does not displace pol δ from binding to PCNA after UV-C DNA damage. (A) Immunoprecipitation (Ip) was performed on detergent-soluble (S), or chromatin-bound fraction (Cb) obtained from LF1 fibroblasts irradiated or not with UV-C (10 J/m^2), and harvested after 30 minutes. Samples were immunoprecipitated with anti-p21, or with anti-p125 (pol δ) polyclonal antibodies, or with purified rabbit immunoglobulins (Ig) for specificity control. The immunoprecipitated material was analysed by western blot for the presence of PCNA, pol δ (p125 subunit), and p21. The position of each protein is shown together with Ig heavy chains (Ig h). Fractionated extracts (Input) were loaded (1/30 and 1/15 for S and Cb fractions, respectively) together with recombinant PCNA (PCNAr), and analysed by western blot for pol δ , PCNA, p21, and actin as a loading control. (B) Immunoprecipitation (IP) was performed on HeLa chromatin-bound extracts with anti-GFP antibody. Cell extracts were obtained from cells expressing pEGFP (GFP), or p21-GFP, irradiated or not with UV-C (10 J/m^2) and harvested at times indicated below each panel. Western blot analysis of PCNA and pol δ , was performed on immunoprecipitated material. The position of each protein is shown together with Ig heavy chains (Ig h). Chromatin-bound extracts (Input) were loaded (1/15) on a parallel gel for western blot analysis of pol δ , PCNA, p21-GFP, and actin as a loading control.

bound PCNA in transfected and non-transfected cells (see Discussion).

Relocation of p21 to DNA-damage sites depends on the interaction with PCNA

Although it had been suggested that p21 interaction with PCNA is important for DNA repair (MacDonald, 1996; Stivala et al., 2001), the mechanism underlying this aspect was not previously elucidated. Thus, we investigated whether the presence of p21 at DNA-damaged sites was dependent on the interaction with PCNA. To this purpose, HeLa cells were transfected with constructs for the expression of HA-tagged wild-type p21 (p21^{wt}-HA), or a mutant form unable to bind PCNA (p21^{PCNA-}-HA) (Cayrol and Ducommun, 1998). These constructs were chosen because a similar p21 mutant protein

fused to GFP was previously found to be unstable (Cazzalini et al., 2003). After localised UV irradiation, cells were immunostained with anti-PCNA and anti-HA antibodies for detection of chromatin-bound PCNA and p21-HA, respectively. Analysis by fluorescence confocal microscopy showed that p21^{wt}-HA colocalised with PCNA at the locally irradiated sites, as shown by the merged images of p21-HA (green fluorescence) and PCNA (red fluorescence). By contrast, the p21^{PCNA-}-HA mutant form showed a heterogeneous, punctuate distribution, but was not recruited with PCNA to the irradiated areas (Fig. 7A). Whole-cell exposure to UV-C was also performed for immunoprecipitation analysis with anti-HA antibody, after cell fractionation. Fig. 7B shows that PCNA and pol δ were immunoprecipitated from both the soluble and chromatin-bound fractions, obtained from UV-exposed cells expressing p21^{wt}-HA. In the immunoprecipitate obtained from the soluble fraction of cells expressing p21^{PCNA-}-HA, a faint band was detected at the position relative to pol δ or PCNA, probably because of an interaction with CDK2 (Cazzalini et al., 2003). Remarkably, no band corresponding to PCNA or pol δ could be detected in the immunoprecipitate performed on the chromatin-bound fraction, despite the presence of both proteins together with p21^{PCNA-}-HA, in the extract. Immunoprecipitation with anti-HA antibody from non-transfected cells showed the absence of any of these proteins in the immunoprecipitate, indicating the specificity of the antibody reaction.

As a further step to understand whether p21 recruitment was dependent on the DNA-repair process, and not a consequence of checkpoint activation, we used NER-deficient XP-A fibroblasts (DeLaat et al., 1999). These cells do not recruit PCNA with the fast kinetics shown by normal cells (Aboussekhra and Wood, 1995; Miura, 1999). Fig. 8 shows that

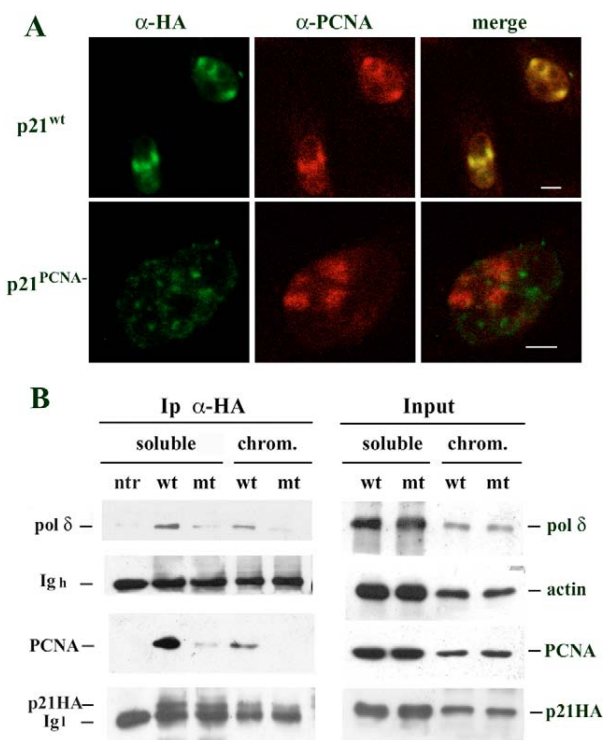


Fig. 7. p21 recruitment to DNA repair sites requires interaction with PCNA. HeLa cells were transfected with HA-tagged constructs for expression of wild-type p21 (p21^{wt}-HA) or a mutant form (p21^{PCNA-}-HA) unable to bind PCNA (p21^{PCNA-}-HA). (A) 24 hours after transfection, cells were exposed to local UV irradiation (15 J/m²) through filters with 3 μ m pores, extracted in situ 30 minutes later and fixed for immunofluorescence staining with anti-HA (green fluorescence) or anti-PCNA (red fluorescence) antibody. Confocal sections of each signal, together with the merged images, are shown. Bars, 5 μ m. (B) Immunoprecipitation was performed with anti-HA antibody on detergent-soluble (soluble), and chromatin-bound (chrom.) fractions obtained from non-transfected (ntr) cells, and from cells expressing p21^{wt} (wt), or p21^{PCNA-} (mt) proteins. Immunoprecipitated material was analysed by western blot with anti-pol δ , anti-PCNA, and anti-HA antibodies. The position of each protein is shown together with Ig heavy (Ig h), and light (Ig l) chains. For detergent-soluble and chromatin-bound extracts, 1/30 and 1/15 respectively, were loaded (Input) on a parallel gel for western blot analysis of pol δ , PCNA, p21HA-tagged proteins, and actin as a loading control.

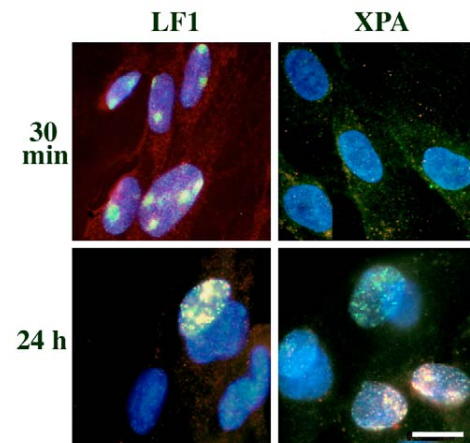


Fig. 8. p21 recruitment to DNA-damage sites depends on DNA repair activity. LF1 and XP20PV (XPA) fibroblasts were exposed to local UV-C irradiation (15 J/m²) through filters with 3 μ m pores, extracted in situ, and fixed at the indicated times for determination of chromatin-bound PCNA and p21. Samples were immunostained with anti-PCNA polyclonal, and anti-p21 monoclonal antibody, detected respectively with secondary antibody conjugated with Alexa Fluor 488 (green fluorescence) or Alexa Fluor 594 (red fluorescence); DNA was counterstained with Hoechst 33258 (blue fluorescence). Bar, 10 μ m.

30 minutes after local exposure to UV-C irradiation, immunofluorescence signals related to PCNA (green) and p21 (red) were present at damaged sites in normal (LF1), but not in XPA fibroblasts, as indicated by the yellow spots (merged green and red signals). This result was not dependent on the lack of lesions at the irradiated areas, since CPDs were detected with a specific antibody (supplementary material Fig. S3). Chromatin-bound PCNA and p21 associated to DNA-repair sites could be detected in XPA cells, 24 hours after irradiation.

p21 does not inhibit PCNA-dependent DNA-repair synthesis

In order to test whether the presence of p21 did not inhibit DNA repair, unscheduled DNA synthesis (UDS) was assessed in normal LF1 fibroblasts, as well as in p21-GFP-expressing HeLa cells. In normal fibroblasts, UDS can be visualised by BrdU incorporation and discriminated from DNA replication, in which much higher levels of BrdU are normally incorporated (Nakagawa et al., 1998). Fig. 9A shows the spots of BrdU incorporation detected in LF1 fibroblasts after exposure to UV-C (10 J/m^2) and further incubated for 3 hours in medium containing $100 \mu\text{M}$ BrdU. For comparison, samples containing high levels of p21 induced by TSA treatment (see Fig. 4A)

were also included (TSA and TSA+UV). An overexposed S-phase cell is visible in the control sample. UDS in irradiated samples is denoted by the presence of fluorescent nuclear foci. Quantification by flow cytometry revealed that G1-phase cells treated with TSA before irradiation (TSA+UV) showed BrdU incorporation levels 1.5 times higher than untreated but UV-irradiated cells (Fig. 9B). In HeLa cells, UDS was assessed by autoradiography of [^3H]thymidine incorporation in cells transfected with p21-GFP, or pEGFP, and detected by immunoperoxidase staining (brown colour) with anti-GFP antibody (Fig. 9C). The results showed that the number of autoradiographic granules relative to UDS, detected after UV irradiation in p21-GFP transfected cells, was not significantly different from that in pEGFP, or in non-transfected cells (Fig. 9D).

Discussion

Fast recruitment of p21 and PCNA to DNA repair sites independently of p21 degradation

In this study we provide evidence showing that UV-induced DNA damage elicits two different immediate responses regarding p21 protein. In normal fibroblasts, UV irradiation induced a drastic reduction (~60-80%) in p21 protein levels.

However, a detectable pool (~5-10%) of the remaining protein was rapidly recruited together with PCNA at the irradiated sites. It was recently reported that p21 was degraded by the proteasome within hours after UV irradiation, in order to promote PCNA-dependent DNA repair (Bendjennat et al., 2003). In our system, p21 protein was not completely degraded either at low (2.5 J/m^2) or high (10 J/m^2) UV doses. In fact, other mechanisms regulating gene expression after UV damage (Barley et al., 1998; McKay et al., 1998), or after other types of DNA lesions (Frouin et al., 2003), may influence p21 turnover. An important factor limiting p21 proteasomal degradation is the interaction with PCNA, because the C8 proteasome subunit binds p21 at its C-terminal region, where the PCNA binding site is located (Touitou et al., 2001). In fact, a p21 mutant protein unable to bind PCNA showed proteasomal degradation faster than wild-type protein (Cayrol and Ducommun, 1998).

Dose-response and time-course studies previously showed that low levels of p21 become chromatin-bound within 2 hours of UV damage (Pagano et al., 1994; Savio et al., 1996). Here we have clearly detected chromatin association of p21 as an immediate response to DNA damage. The time course of p21-GFP and RFP-PCNA accumulation in living murine and human cells, showed that both proteins were recruited within seconds of UV irradiation and persisted for more than 2 hours, consistent with in vivo dynamics of

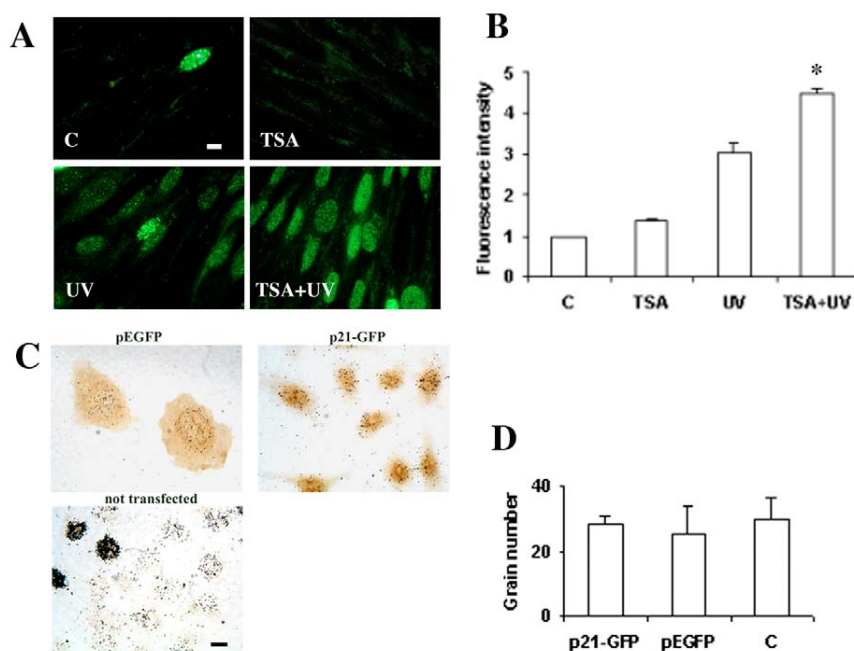


Fig. 9. p21 does not inhibit UDS repair activity. (A) Untreated or TSA-treated LF1 fibroblasts were irradiated with UV-C (10 J/m^2), and incubated with $100 \mu\text{M}$ BrdU for 3 hours. Cells were then fixed and immunostained with anti-BrdU antibody, a secondary biotinylated antibody followed by streptavidin-FITC. Fluorescence images of untreated (C), or TSA-treated cells (TSA) are shown together with samples exposed to UV radiation (UV), or exposed after TSA treatment (TSA+UV). (B) Normalised fluorescence intensity of BrdU immunofluorescence in G1-phase cells, measured by flow cytometry. Mean values \pm s.d. ($n=3$) are reported. * $P<0.05$ compared with levels in the UV sample (Student's t -test). (C) HeLa cells expressing pEGFP, or p21-GFP, were UV-C irradiated (20 J/m^2), incubated for 2 hours in [^3H]thymidine and then fixed. Cells were immunostained with anti-GFP primary antibody and HRP-conjugated secondary antibody, and detected by immunoperoxidase staining (brown precipitate). UDS is denoted by the presence of nuclear autoradiographic granules. (D) Quantification of UDS grains in non-S-phase nuclei. Mean values of grain number (\pm s.d.) in duplicate samples, are reported. Bars, $10 \mu\text{m}$ (A,C).

other repair factors, such as ERCC1-XPF or TFIIH (Houtsmuller et al., 1999; Hoogstraten et al., 2002; Rademakers et al., 2003; Moné et al., 2004). This time period is in agreement with estimated repair time under local irradiation conditions (Houtsmuller et al., 1999), with the time course of endogenous PCNA recruitment (Toschi and Bravo, 1988; Prospero et al., 1993), and with the evidence that PCNA recruited to sites of DNA damage shows a very low turnover (Solomon et al., 2004). Initial measurements indicated that RFP-PCNA was relocated slightly faster than p21-GFP, suggesting that p21 binding to DNA-damage sites followed that of PCNA.

Rapid recruitment of p21 was previously observed after heavy-ion-induced DNA damage in human fibroblasts, supporting a role for p21 in early processing of double-strand breaks (Jakob et al., 2002). We also observed rapid p21 relocation with irradiation conditions (337 nm laser) producing double-strand breaks (not shown). However, we used 405 nm laser irradiation to induce CPDs, a typical NER substrate (supplementary material Fig. S1). Although it cannot be excluded that under these conditions other DNA lesions were also produced, our results were confirmed by microirradiation experiments with UV-C. Thus, the p21 response seems to be independent of the type of lesion, but related to PCNA-dependent repair pathways.

Interaction of p21 with PCNA at DNA repair sites does not displace PCNA-interacting proteins

Our results also showed that p21 relocation after DNA damage occurred concomitantly with the recruitment of other proteins directly involved in DNA repair, such as pol δ and Lig I (Aboussekhra et al., 1995). This relocation was not affected in TSA-treated fibroblasts, which after DNA damage exhibited chromatin-bound p21 levels higher than those in samples exposed only to UV irradiation. In addition, in HeLa cells we found that p21-GFP was not significantly degraded (not shown), and colocalised with pol δ , and with factors known to interact with PCNA, required at different steps of the NER process, such as XPG (Gary et al., 1997), and CAF-1 (Green and Almouzni, 2003). These results indicate that p21 does not inhibit the recruitment of repair factors to DNA-damage sites.

In the present study, immunoprecipitation experiments have shown that in UV-irradiated samples, pol δ could interact with chromatin-bound p21 and PCNA. These results are in contrast to previous findings showing that p21 disrupts the interaction of PCNA-associated proteins involved both in DNA replication and repair, such as FEN-1 (Chen et al., 1996), Lig I (Levin et al., 1997), DNA methyltransferase (Chuang et al., 1997), XPG (Gary et al., 1997), or pol δ (Cazzalini et al., 2003; Riva et al., 2004). However, in those studies the interaction was mainly assessed with purified proteins, or by overexpressing p21 in cells not exposed to DNA damaging agents. Thus, although high p21 levels may saturate PCNA binding, this condition may not have occurred in repairing normal cells. We have also shown that in UV-damaged cells, chromatin-bound pol δ remained associated with PCNA, even in cells expressing exogenous p21 (either as GFP- or HA-tagged proteins). Moreover, a p21 mutant form (p21^{PCNA-}) unable to bind PCNA (Cayrol and Ducommun, 1998), was not able to coimmunoprecipitate detectable levels of chromatin-bound PCNA, or pol δ , further supporting the evidence that

p21 binds in vivo to PCNA complexed with pol δ at DNA-damage sites.

The role of a p21-PCNA-pol- δ complex during DNA repair is still unclear. It could be hypothesised that p21 is required for PCNA-pol- δ interaction during DNA repair. From this point of view, p21-null human fibroblasts showed substantially normal recruitment of PCNA after UV irradiation, whereas the repair efficiency was significantly reduced (Stivala et al., 2001). Alternatively, this complex could represent a transition state in which p21 binding to PCNA will enable the disassembly of pol δ , thereby promoting the next PCNA-dependent steps (Riva et al., 2004). In fact, in p21-null human fibroblasts, or in cells with mutant p53, an accumulation of chromatin-bound PCNA was observed at late repair times (Stivala et al., 2001; Riva et al., 2001). Similar behaviour of PCNA was observed here in p53-deficient HeLa cells (Fig. 6B).

p21 recruitment depends on binding to PCNA involved in NER activity

The evidence that p21^{PCNA-} mutant protein was not able to relocate to DNA-damage sites strongly suggests that interaction with PCNA is responsible for p21 recruitment. Thus, the slightly slower kinetics of p21-GFP accumulation may indicate that PCNA is recruited first, and soon after p21 follows. In NER-deficient XPA cells, PCNA recruitment was previously described only at late times after DNA damage (Miura, 1999). In agreement with these findings, we also observed a delayed relocation of p21 concomitant with that of PCNA. The lack of early recruitment of both proteins in XP-A cells supports the conclusion that p21 interacts with PCNA in a process dependent on ongoing DNA repair, and not as an immediate consequence of checkpoint activation. Accordingly, early p21 recruitment after UV damage was also observed in normal quiescent fibroblasts (not shown), which have p21 levels higher than those in proliferating cells (Itahana et al., 2002).

p21 does not inhibit DNA-repair activity in living cells

The presence of p21 did not inhibit DNA repair, as determined by the UDS assay, because both TSA-treated human fibroblasts and HeLa cells containing detectable levels of p21, showed UDS activity equivalent to that of cells containing low physiological levels (untreated fibroblasts), or low-to-undetectable amounts (untransfected or pEGFP-transfected HeLa cells) of endogenous p21. Thus, it is possible that only relatively high p21 levels, such as those reached in cells expressing a p21 mutant protein not degraded after UV irradiation, may reduce or abolish the recruitment of PCNA (Bendjennat et al., 2003). Interestingly, an increase in UDS activity was observed after UV exposure in fibroblasts treated with TSA, an inducer of p21 (Richon et al., 2000). It is known that TSA also increases histone acetylation, thereby favouring the accessibility of DNA-repair machinery to DNA-damage sites (Rubbi and Milner, 2003), which was not hindered by higher p21 levels.

We have shown that, as an immediate response to DNA damage, cells do not completely degrade p21, and that low p21 levels interacting with PCNA accumulate at DNA-damage sites, without inhibition of DNA repair. Possible effects of p21 on the composition and/or activity of PCNA complexes in DNA repair remain to be clarified by future studies.

Materials and Methods

Cells, transfections and treatments

HeLa S3 cell line was grown in Dulbecco's modified Eagle's medium (DMEM, Sigma) supplemented with 10% foetal bovine serum (FBS, Gibco BRL), 4 mM L-glutamine (Gibco BRL), 100 U/ml penicillin, 100 µg/ml streptomycin in a 5% CO₂ atmosphere. Expression constructs coding for p21 wt or a C-terminal mutant (p21^{PCNA}) protein deficient for PCNA interaction (Cayrol and Ducommun, 1998) were cloned in pEGFP-N1 (Clontech), or pCDNA3 vectors, for expression of p21-GFP or p21-HA fusion proteins respectively, as previously described (Cazzalini et al., 2003). The expression construct encoding mRFP-PCNAL2 was obtained by replacing EGFP with mRFP1 (Sporbert et al., 2005). Cells seeded on coverslips or Petri dishes, were transiently transfected with Effectene transfection reagent (Qiagen) 24 hours after seeding (70% confluence), and irradiation was usually performed 24 hours after transfection.

Mouse C2C12 myoblasts were cultured in DMEM supplemented with 25 mM HEPES, 50 µg/ml gentamicin and 20% FBS (Sporbert et al., 2002). Cells grown on gridded coverslips, or on Lab-Tek® chamber slides (Nunc), were either microinjected with plasmid DNA using an automated microinjection system (Eppendorf), or cotransfected with TransFectin® transfection reagent (Bio-Rad), according to manufacturers instructions. Cells were subsequently incubated overnight before microirradiation and live-cell analyses.

Human embryonic lung fibroblasts (LF1), kindly provided by J. Sedivy (Brown University, Providence, RI), were grown in Earle's minimal essential medium (Invitrogen) supplemented with 10% FBS (Invitrogen), 100 U/ml penicillin and 100 µg/ml streptomycin in a 5% CO₂ atmosphere. The XP20PV (XPA) primary fibroblasts were provided by M. Stefanini (IGM-CNR, Pavia, Italy), and grown in HAM F-10 medium, supplemented with 10% FBS.

For cell synchronisation in G1 phase, fibroblasts were serum starved (0.5% FBS) for 72 hours, and then re-incubated in complete medium for 8 hours. In some experiments, cells were treated for 16 hours with trichostatin A (TSA) at the final concentration of 200 ng/ml (Rubbi and Milner, 2003). Cell exposure to UV-C was performed with a lamp (Philips TUV-9) emitting mainly at 254 nm, at doses ranging from 2.5 to 30 J/m², as measured with a DCRX radiometer (Spectronics). Localised irradiation was performed by laying Isopore polycarbonate filters (Millipore) with 3-µm pores (Katsumi et al., 2001) on top of the cells.

Laser microirradiation and time-lapse microscopy

Microirradiation experiments were essentially performed as described (Mortusewicz et al., 2005). In brief, C2C12 cells were seeded on coverslips and sensitised for microirradiation by incubation in medium containing BrdU (10 µg/ml) for 20 hours. For live-cell microscopy and irradiation, coverslips were mounted in FCS2 (Bioprotechs), or in POC (Visitron Systems) live-cell chambers and maintained at 37°C. In some experiments, microirradiation was carried out with a microdissection system (P.A.L.M.) using a pulsed N₂ laser (337 nm) coupled to a Zeiss LSM410 confocal laser-scanning microscope. However, to induce the formation of cyclobutane pyrimidine dimers (CPDs), microirradiation was carried out with a 405 nm Diode laser coupled to a Leica TCS SP2/AOBS confocal laser scanning microscope. The laser was set to maximum power at 100% transmission, and cells were irradiated for 1 second. For evaluation of the recruitment kinetics, fluorescence intensities of the irradiated region were corrected for background and for total nuclear loss of fluorescence over the time course and normalised to the pre-irradiation value.

For long time-lapse analysis, light optical sections were acquired with a Zeiss LSM410 confocal laser-scanning microscope using the 488 nm Ar laser line and the 543 nm HeNe laser line. Six mid z-sections at 0.5 µm intervals were taken every 3–10 minutes and cells were followed up to several hours. Focus drift over time was compensated with a macro, as described (Mortusewicz et al., 2005). After image acquisition, a projection of all six z-sections was performed from each time point using ImageJ 1.34. Short time series were taken with a Leica TCS SP2/AOBS confocal laser-scanning microscope using the 488 nm Ar laser line and the 561 nm DPSS laser line. Before and after microirradiation, confocal image series of one mid z-section were recorded every 2 seconds.

Immunofluorescence and confocal microscopy

HeLa cells seeded on coverslips were transfected as described above. After 24 hours, cells were locally irradiated, and re-incubated in whole medium for the required period of time. Cells on coverslips were then washed twice in PBS, dipped in cold physiological saline and lysed for 10 minutes at 4°C in hypotonic buffer: 10 mM Tris-HCl (pH 7.4), 2.5 mM MgCl₂, 0.1% Nonidet NP-40, 0.2 mM phenylmethylsulfonyl fluoride (PMSF) and 0.2 mM Na₃VO₄. Thereafter, samples were washed in PBS, fixed in 2% formaldehyde for 5 minutes at room temperature (RT), and then post-fixed in 70% ethanol. After re-hydration, samples were blocked in PBST buffer (PBS, 0.2% Tween 20) containing 1% bovine serum albumin (BSA), and then incubated for 1 hour with specific monoclonal antibodies. anti-PCNA (PC10, Dako), anti-DNA polymerase δ (pol δ) p125 subunit (clone 22, BD Biosciences), anti-CAF-1 (Ab-2, Oncogene Research), or anti-XPG (Ab-1, NeoMarkers), all diluted 1:100 in PBST buffer/BSA. After washing, each reaction was followed by incubation for 30 minutes with anti-mouse antibody conjugated

with Alexa Fluor 594 (Molecular Probes). Cells expressing p21-HA fusion proteins were incubated with anti-HA monoclonal antibody (clone H7, Sigma), and with FL261 rabbit polyclonal antibody to PCNA (Santa Cruz Biotech.), diluted 1:500 or 1:100, respectively. After three washes with PBST buffer, coverslips were incubated for 30 minutes with goat anti-rabbit and anti-mouse antibodies labeled with Alexa Fluor 488 or 594 (Molecular Probes), respectively. After immunoreactions, cells were incubated with Hoechst 33258 dye (0.5 µg/ml) for 2 minutes at RT and washed in PBS. Slides were mounted in Mowiol (Calbiochem) containing 0.25% 1,4-diazabicyclo-[2,2,2]-octane (Aldrich) as antifading agent. LF1 fibroblasts grown on coverslips were irradiated as above, dipped in cold double-distilled H₂O before lysis in hypotonic buffer, and fixation as above (Savio et al., 1998). Samples were incubated for 1 hour in FL261 polyclonal antibody to PCNA, and with monoclonal antibody to p21 (clone DCS 60.2, NeoMarkers), both diluted 1:100. After washing, samples were incubated for 30 minutes in goat anti-rabbit and anti-mouse antibodies conjugated with Alexa Fluor 488 (1:200), and Alexa Fluor 594 or biotin, respectively. In the latter case, incubation with streptavidin-Texas-Red (Amersham Biosciences) diluted 1:100 was performed.

For determination of laser-induced CPDs, C2C12 cells were fixed with 3.7% formaldehyde in PBS and permeabilised with 0.2% Triton X-100 for 4 minutes. DNA was denatured by incubation in 0.5 M NaOH for 5 minutes, and then coverslips were stained with anti-CPDs monoclonal antibody (Kamiya Biomedical) diluted 1:1000 in PBS containing 2% BSA, and detected with Cy3-conjugated goat anti-mouse antibody (Amersham) diluted 1:400. Cells were counterstained with DAPI and mounted in Vectashield (Vector Laboratories).

Fluorescence signals were acquired with a Leica TCS SP2 confocal microscope, at 0.3 µm intervals. Image analysis was performed using the LCS software. Images of fixed cells were taken with a Zeiss Axiophot 2 widefield epifluorescence microscope equipped with a cooled CCD camera (Visitron Systems), or with a BX51 Olympus fluorescence microscope equipped with a C4040 digital camera.

Immunoprecipitation and western blot analysis

For western blot analysis, cells were directly lysed in SDS sample buffer (65 mM Tris-HCl pH 7.5, 1% SDS, 30 mM DTT, 10% glycerol, 0.02% Bromophenol Blue), or fractionated in soluble and chromatin bound fraction, as previously described (Riva et al., 2004) with minor modifications. Cells were lysed in hypotonic buffer containing 10 mM Tris-HCl (pH 7.4), 2.5 mM MgCl₂, 1 mM PMSF, 0.5% Nonidet NP-40, 0.2 mM Na₃VO₄ and a mixture of protease and phosphatase inhibitor cocktails (Sigma). After 10 minutes on ice, cells were pelleted by low-speed centrifugation (200 g, 1 minute), and the detergent-soluble fraction was recovered. Lysed cells were washed once in hypotonic buffer, followed by a second wash in 10 mM Tris-HCl buffer (pH 7.4), containing 150 mM NaCl, and protease/phosphatase inhibitor cocktails. Cell pellets were then incubated with DNase I (20 U/10⁶ cells) in 10 mM Tris-HCl (pH 7.4), 5 mM MgCl₂ and 10 mM NaCl for 15 minutes at 4°C. After a brief sonication on ice, samples were again centrifuged (13,000 g, 1 minute), and the supernatant containing the chromatin-bound fraction was collected.

For immunoprecipitation, about 10⁷ cells were re-suspended in 1 ml lysis buffer and fractionated as above. Equal amounts of each extract were incubated with anti-GFP rabbit polyclonal antibody (Molecular Probes), N-19 rabbit polyclonal antibody to p21 (Santa Cruz), or with H7 anti-HA antibody pre-bound to protein A Sepharose CL-4B (Pharmacia). Half the amount of each antibody was used for chromatin-bound fractions. In some experiments, C20 polyclonal antibody to pol δ p125 subunit (Santa Cruz) was also used. Reactions were performed for 3 hours at 4°C under constant agitation. The samples were then centrifuged at 14,000 g (30 minutes, 4°C), and immunocomplexes were washed with ice-cold 50 mM Tris-HCl (pH 7.4) containing 150 mM NaCl, 0.5% Nonidet NP-40. Immunoprecipitated peptides were eluted in SDS sample buffer and resolved by 7.5% or 12% SDS-polyacrylamide gel electrophoresis (SDS-PAGE). Proteins were electrotransferred to nitrocellulose, then membranes were blocked for 30 minutes in 5% non-fat milk in PBST buffer, and probed with primary antibodies anti-PCNA, or anti-HA (H7) diluted 1:1000. Anti-pol δ p125 (clone 22), and anti-DNA ligase I (1A9, NeoMarkers) were diluted 1:500. Membranes were then washed in PBST, incubated for 30 minutes with appropriate HRP-conjugated secondary antibodies (Amersham), and revealed using enhanced chemiluminescence.

Analysis of DNA repair by UDS determination

DNA repair was assessed by determination of unscheduled DNA synthesis (UDS). After irradiation, LF1 fibroblasts were incubated for 3 hours in medium containing 100 µM BrdU, then fixed in 70% ethanol (Nakagawa et al., 1998). After DNA denaturation in 2 N HCl for 30 minutes, and neutralisation for 15 minutes in 0.15 M Na₂B₄O₇, samples were blocked in TBST/BSA. Incubation (1 hour) in anti-BrdU antibody (Amersham) was followed by a biotinylated anti-mouse antibody, and streptavidin-FITC (Amersham). Immunofluorescence of G1-phase cells was measured with an Epics XL flow cytometer, as described (Stivala et al., 2001).

In p21-GFP, or pEGFP-expressing HeLa cells, UDS was determined after irradiation (20 J/m²), by incubating cells for 2 hours in medium containing 1 ml [³H]-thymidine (NEN, 10 µCi/ml specific activity), then chased for 1 hour in medium containing 10 µM each cold thymidine and cytidine. Cells were then fixed

in 4% formaldehyde and post-fixed in 70% ethanol. Detection of cells expressing p21-GFP or pEGFP was performed by incubation in anti-GFP antibody, followed by immunoperoxidase staining with diaminobenzidine. Samples were processed for autoradiography using an Ilford K2 emulsion, exposed for 4 days at 4°C, and then developed and fixed before mounting on microscope slides. Autoradiographic granules were counted in 50 non-S phase cells showing GFP staining, in duplicate experiments.

We are grateful to J. M. Sedivy (Brown University, Providence) for LFI fibroblasts, M. Stefanini (IGM-CNR, Pavia) for XP-A cells, B. Ducommun for p21^{PCNA}-HA construct, A.I. Scovassi for discussion, and P. Vaghi (Centro Grandi Strumenti, Pavia University) for help in confocal microscopy. This work was in part supported by CNR grant (E.P.), MIUR grant (FIRB project RBNE0132MY) and grants from the 'Deutsche Forschungsgemeinschaft' (M.C.C and H.L.).

References

- Aboussekhra, A. and Wood, R. D.** (1995). Detection of nucleotide excision repair incision in human fibroblasts by immunostaining for PCNA. *Exp. Cell Res.* **221**, 326-332.
- Aboussekhra, A., Biggerstaff, M., Shivji, M. K. K., Vilpo, J. A., Moncollin, V., Podust, V. N., Protic, M., Hübscher, U., Egly, J. M. and Wood, R. D.** (1995). Mammalian DNA nucleotide excision repair reconstituted with purified components. *Cell* **80**, 859-868.
- Adimoolam, S., Lin, C. X. and Ford, J. M.** (2001). The p53 regulated cyclin-dependent kinase inhibitor, p21 (cip1,waf1,sdi1), is not required for global genomic and transcriptional coupled nucleotide excision repair of UV-induced DNA photoproducts. *J. Biol. Chem.* **278**, 25813-25822.
- Barley, R. D. C., Enns, L., Peterson, M. C. and Mirzayans, R.** (1998). Aberrant p21^{WAF-1}-dependent growth arrest as the possible mechanism of abnormal resistance to ultraviolet light cytotoxicity in Li-Fraumeni syndrome fibroblast strains heterozygous for TP53 mutations. *Oncogene* **17**, 533-543.
- Bendjennat, M., Boulaire, J., Jascur, T., Brickner, H., Barbier, V., Sarasin, A., Fotedar, A. and Fotedar, R.** (2003). UV irradiation triggers ubiquitin-dependent degradation of p21^{WAF1} to promote DNA repair. *Cell* **114**, 599-610.
- Bornstein, G., Bloom, J., Sitry-Ahevah, D., Nakayama, K., Pagano, M. and Hershko, A.** (2003). Role of the SCF^{Skp2} ubiquitin ligase in the degradation of p21^{Cip1} in S phase. *J. Biol. Chem.* **278**, 25752-25757.
- Cayrol, C. and Ducommun, B.** (1998). Interaction with cyclin-dependent kinases and PCNA modulates proteasome-dependent degradation of p21. *Oncogene* **17**, 2437-2444.
- Cazzalini, O., Perucca, P., Riva, F., Stivala, L. A., Bianchi, L., Vannini, V., Ducommun, B. and Prosperi, E.** (2003). p21^{CDKN1A} does not interfere with loading of PCNA at DNA replication sites, but inhibits subsequent binding of DNA polymerase δ at the G1/S phase transition. *Cell Cycle* **2**, 596-603.
- Cazzalini, O., Perucca, P., Valsecchi, F., Stivala, L. A., Bianchi, L., Vannini, V. and Prosperi, E.** (2004). Intracellular localization of the cyclin-dependent kinase inhibitor p21^{CDKN1A}-GFP fusion protein during cell cycle arrest. *Histochem. Cell Biol.* **121**, 377-381.
- Chen, J., Chen, S., Saha, P. and Dutta, A.** (1996). p21^{Cip1/Waf1} disrupts the recruitment of human Fen1 by proliferating-cell nuclear antigen into the DNA replication complex. *Proc. Natl. Acad. Sci. USA* **93**, 11597-11602.
- Chuang, L. S.-H., Ian, H.-I., Koh, T.-W., Ng, H.-H., Xu, G. and Li, B. F. L.** (1997). Human DNA-(Cytosine-5) methyltransferase-PCNA complex as a target for p21^{WAF1}. *Science* **277**, 1996-2000.
- Cooper, M. P., Balajee, A. S. and Bohr, V. A.** (1999). The C-terminal domain of p21 inhibits nucleotide excision repair in vitro and in vivo. *Mol. Biol. Cell* **10**, 2119-2129.
- Coqueret, O.** (2003). New roles for p21 and p27 cell-cycle inhibitor: a function for each cell compartment? *Trends Cell Biol.* **13**, 65-70.
- De Laat, W. L., Jasper, N. G. J. and Hoeijmakers, H. J.** (1999). Molecular mechanism of nucleotide excision repair. *Genes Dev.* **13**, 768-785.
- Dotto, G. P.** (2000). p21^{WAF1/Cip1}: more than a break to the cell cycle?. *Biochim. Biophys. Acta* **1471**, M43-M56.
- Frouin, I., Maga, G., Denegri, M., Riva, F., Savio, M., Spadari, S., Prosperi, E. and Scovassi, I.** (2003). Human proliferating cell nuclear antigen, poly (ADP-ribose) polymerase-1, and p21^{WAF1/Cip1}: a dynamic exchange of partners. *J. Biol. Chem.* **278**, 39265-39268.
- Gary, R., Ludwig, D. L., Cornelius, H. L., MacInnes, M. A. and Park, M. S.** (1997). The DNA repair endonuclease XPG binds to proliferating cell nuclear antigen (PCNA) and shares sequence elements with the PCNA-binding regions of FEN-1 and cyclin dependent kinase inhibitor p21. *J. Biol. Chem.* **272**, 24522-24529.
- Gottifredi, V., McKinney, K., Poyurovsky, M. V. and Prives, C.** (2004). Decreased p21 levels are required for efficient restart of DNA synthesis after S phase block. *J. Biol. Chem.* **279**, 5802-5810.
- Green, C. M. and Almouzni, G.** (2003). Local action of the chromatin assembly factor CAF-1 at sites of nucleotide excision repair in vivo. *EMBO J.* **22**, 5163-5174.
- Gulbis, J. M., Kelman, Z., Hurtwitz, J., O'Donnel, M. and Kuriyan, J.** (1996). Structure of the C-terminal region of p21^{waf1/cip1} complexed with human PCNA. *Cell* **87**, 297-306.
- Hoogstraten, D., Nigg, A. L., Heath, H., Mullenders, L. H. F., van Driel, R., Hoeijmakers, J. H. J., Vermeulen, W. and Houtsmuller, A. B.** (2002). Rapid switching of TFIIH between RNA polymerase I and II Transcription and DNA repair in vivo. *Mol. Cell* **10**, 1163-1174.
- Houtsmuller, A. B., Rademakers, S., Nigg, A. L., Hoogstraten, D., Hoeijmakers, J. H. J. and Vermeulen, W.** (1999). Action of DNA repair endonuclease ERCC1/XPF in living cells. *Science* **284**, 958-961.
- Itahana, K., Dimri, G. P., Hara, E., Itahana, Y., Zou, Y., Desprez, P.-Y. and Campisi, J.** (2002). A role for p53 in maintaining and establishing the quiescence growth arrest in human cells. *J. Biol. Chem.* **277**, 18206-18214.
- Jakob, B., Scholz, M. and Taucher-Scholz, G.** (2002). Characterization of CDKN1A (p21) binding to sites of heavy-ion-induced damage: colocalization with proteins involved in DNA repair. *Int. J. Radiat. Biol.* **78**, 75-88.
- Katsumi, S., Kobayashi, N., Imoto, K., Nakagawa, A., Yamashina, Y., Muramatsu, T., Shirai, T., Miyagawa, S., Sugiura, S., Hanaoka, F. et al.** (2001). *In situ* visualization of ultraviolet-light-induced DNA damage repair in locally irradiated human fibroblasts. *J. Invest. Dermatol.* **117**, 1156-1161.
- Leonhardt, H., Rahn, H. P., Weinzierl, P., Sporberr, A., Cremer, T., Zink, D. and Cardoso, M. C.** (2000). Dynamics of DNA replication factories in living cells. *J. Cell Biol.* **149**, 271-279.
- Levin, D. S., Bai, W., Yao, N., O'Donnell, M. and Tomkinson, A. E.** (1997). An interaction between DNA ligase I and proliferating cell nuclear antigen: implications for Okazaki fragment synthesis and joining. *Proc. Natl. Acad. Sci. USA* **94**, 12863-12868.
- Li, R., Hannon, G. J., Beach, D. and Stillman, B.** (1996). Subcellular distribution of p21 and PCNA in normal and repair-deficient cells following DNA damage. *Curr. Biol.* **6**, 189-199.
- McDonald, E. R., III, Wu, G. S., Waldman, T. and El-Deiry, W. S.** (1996). Repair defect of p21^{waf1/cip1}- human cancer cells. *Cancer Res.* **56**, 2250-2255.
- McKay, B. C., Ljungman, M. and Rainbow, A. J.** (1998). Persistent DNA damage induced by ultraviolet light inhibits p21^{waf1} and bax expression: implications for DNA repair, UV sensitivity and the induction of apoptosis. *Oncogene* **17**, 545-555.
- Miura, M.** (1999). Detection of chromatin-bound PCNA in mammalian cells and its use to study DNA excision repair. *J. Radiat. Res.* **40**, 1-12.
- Moné, M. J., Bernas, T., Dinant, C., Goedvree, F. A., Manders, E. M. M., Volker, M., Houtsmuller, A. B., Hoeijmakers, J. H. J., Vermeulen, W. and van Driel, R.** (2004). *In vivo* dynamics of chromatin-associated complex formation in mammalian nucleotide excision repair. *Proc. Natl. Acad. Sci. USA* **101**, 15933-15937.
- Mortusewicz, O., Schermelleh, L., Walter, J., Cardoso, M. C. and Leonhardt, H.** (2005). Recruitment of DNA methyltransferase I to DNA repair sites. *Proc. Natl. Acad. Sci. USA* **102**, 8905-8909.
- Nakagawa, A., Kobayashi, N., Muramatsu, T., Yamashina, Y., Shirai, T., Hashimoto, M. W., Ikenaga, M. and Mori, T.** (1998). Three-dimensional visualization of ultraviolet-induced DNA damage and its repair in human cell nuclei. *J. Invest. Dermatol.* **110**, 143-148.
- Oku, T., Ikeda, S., Sasaki, H., Fukuda, K., Morioka, H., Ohtsuka, E., Yoshikawa, H. and Tsurimoto, T.** (1998). Functional sites of human PCNA which interact with p21 (Cip1/Waf1), DNA polymerase δ and replication factor C. *Genes Cells* **3**, 357-369.
- Pagano, M., Theodoras, A. M., Tam, S. W. and Draetta, G. F.** (1994). Cyclin D1-mediated inhibition of repair and replicative DNA synthesis in human fibroblasts. *Genes Dev.* **8**, 1627-1639.
- Pan, Z.-Q., Reardon, J. T., Li, L., Flores-Rozas, H., Legerski, R., Sancar, A. and Hurwitz, J.** (1995). Inhibition of nucleotide excision repair by cyclin-dependent kinase inhibitor p21. *J. Biol. Chem.* **270**, 22008-22016.
- Paunesku, T., Mittal, S., Protic, M., Oryhon, J., Korolev, S. V., Joachimiak, A. and Woloschak, G. E.** (2001). Proliferating cell nuclear antigen (PCNA): ringmaster of the genome. *Int. J. Radiat. Biol.* **77**, 1007-1021.
- Podust, V. N., Podust, L., Goubin, E., Ducommun, B. and Hübscher, U.** (1995). Mechanism of inhibition of proliferating cell nuclear antigen-dependent DNA synthesis by the cyclin-dependent kinase inhibitor p21. *Biochemistry* **34**, 8869-8875.
- Prosperi, E.** (1997). Multiple roles of the proliferating cell nuclear antigen: DNA replication, repair and cell cycle control. *Prog. Cell Cycle Res.* **3**, 193-210.
- Prosperi, E., Stivala, L. A., Sala, E., Scovassi, A. I. and Bianchi, L.** (1993). Proliferating cell nuclear antigen complex-formation induced by ultraviolet irradiation in human quiescent fibroblasts as detected by immunostaining and flow cytometry. *Exp. Cell Res.* **205**, 320-325.
- Rademakers, S., Volker, M., Hoogstraten, D., Nigg, A. L., Moné, M. J., van Zeeland, A. A., Hoeijmakers, J. H. J., Houtsmuller, A. B. and Vermeulen, W.** (2003). Xeroderma pigmentosum group A protein loads as a separate factor onto lesions. *Mol. Cell Biol.* **23**, 5755-5767.
- Richon, V. M., Sandhoff, T. W., Rifkind, R. A. and Marks, P. A.** (2000). Histone deacetylase inhibitor selectively induces p21^{WAF1} expression and gene-associated histone acetylation. *Proc. Natl. Acad. Sci. USA* **97**, 10014-10019.
- Riva, F., Zucco, V., Vink, A. A., Supino, R. and Prosperi, E.** (2001). UV-induced DNA incision and proliferating cell nuclear antigen recruitment to repair sites occurs independently of p53-replication protein A interaction in p53 wild type and mutant ovarian carcinoma cells. *Carcinogenesis* **22**, 1971-1978.
- Riva, F., Savio, M., Cazzalini, O., Stivala, L. A., Scovassi, I. A., Cox, L. S., Ducommun, B. and Prosperi, E.** (2004). Distinct pools of proliferating cell nuclear antigen associated to DNA replication sites interact with the p125 subunit of DNA polymerase δ or DNA ligase I. *Exp. Cell Res.* **293**, 357-367.
- Ruan, S., Oku, M. F., Ren, J. P., Chiao, P., Andreoff, M., Levin, V. and Zhang, W.** (1998). Overexpressed WAF1/Cip1 renders glioblastoma cells resistant to chemotherapy agents 1,3-Bis(2-chloroethyl)-1-nitrosourea and cisplatin. *Cancer Res.* **58**, 1538-1543.

- Rubbi, C. P. and Milner, J.** (2003). p53 is a chromatin accessibility factor for nucleotide excision repair of DNA damage. *EMBO J.* **22**, 975-986.
- Savio, M., Stivala, L. A., Scovassi, A. I., Bianchi, L. and Prosperi, E.** (1996). p21^{waf1/cip1} protein associates with the detergent-insoluble form of PCNA concomitantly with disassembly of PCNA at nucleotide excision repair sites. *Oncogene* **13**, 1591-1598.
- Savio, M., Stivala, L. A., Bianchi, L., Vannini, V. and Prosperi, E.** (1998). Involvement of the proliferating cell nuclear antigen (PCNA) in DNA repair induced by alkylating agents and oxidative damage in human fibroblasts. *Carcinogenesis* **19**, 591-596.
- Sheikh, M. S., Chen, Y. Q., Smith, M. L. and Fornace, A. J., Jr** (1997). Role of p21^{waf1/cip1/sdi1} in cell death and DNA repair as studied using a tetracycline-inducible system in p53-deficient cells. *Oncogene* **14**, 1875-1882.
- Shivji, M. K. K., Grey, S. J., Strausfeld, U. P., Wood, R. D. and Blow, J. J.** (1994). Cip1 inhibits DNA replication but not PCNA-dependent nucleotide excision repair. *Curr. Biol.* **4**, 1062-1068.
- Shivji, M. K. K., Ferrari, E., Ball, K., Hübscher, U. and Wood, R. D.** (1998). Resistance of human nucleotide excision repair synthesis in vitro to p21^{CDKN1}. *Oncogene* **17**, 2827-2838.
- Smith, M. L., Ford, J. M., Hollander, M. C., Bortnick, R. A., Amounson, S. A., Seo, Y. R., Deng, C., Hanawalt, P. C. and Fornace, A. J.** (2000). p53-mediated DNA repair responses to UV radiation: studies of mouse cells lacking p53, p21, and/or gadd45 genes. *Mol. Cell. Biol.* **20**, 3705-3714.
- Solomon, D. A., Cardoso, M. C. and Knudsen, E. S.** (2004). Dynamic targeting of the replication machinery to sites of DNA damage. *J. Cell Biol.* **166**, 455-463.
- Sporbert, A., Gahl, A., Ankerhold, R., Leonhardt, H. and Cardoso, M. C.** (2002). DNA polymerase clamp shows little turnover at established sites but sequential de novo assembly at adjacent origin clusters. *Mol. Cell* **10**, 1355-1365.
- Sporbert, A., Domaing, P., Leonhardt, H. and Cardoso, M. C.** (2005). PCNA acts as a stationary loading platform for transiently interacting Okazaki fragment proteins. *Nucleic Acids Res.* **33**, 3521-3528.
- Stivala, L. A., Riva, F., Cazzalini, O., Savio, M. and Prosperi, E.** (2001). p21^{waf1/cip1}-null human fibroblasts are deficient in nucleotide excision repair downstream the recruitment of PCNA to DNA repair sites. *Oncogene* **20**, 563-570.
- Toschi, L. and Bravo, R. R.** (1988). Changes in cyclin/proliferating cell nuclear antigen distribution during DNA repair synthesis. *J. Cell Biol.* **107**, 1623-1628.
- Toutou, R., Richardson, J., Bose, S., Nakanishi, M., Rivett, J. and Allday, M. J.** (2001). A degradation signal located in the C-terminus of p21^{WAF1/CIP1} is a binding site for the C8 α -subunit of the 20S proteasome. *EMBO J.* **20**, 2367-2375.
- Tsurimoto, T.** (1999). PCNA binding proteins. *Front. Biosci.* **4**, 849-858.
- Vivona, J. B. and Kelman, Z.** (2003). The diverse spectrum of sliding clamp interacting proteins. *FEBS Lett.* **546**, 167-172.
- Volker, M., Moné, M. J., Karmakar, P., van Hoffen, A., Schul, W., Vermeulen, W., Hoeijmakers, J. H. J., van Driel, R., van Zeeland, A. A. and Mullenders, L. H. F.** (2001). Sequential assembly of the nucleotide excision repair factors in vivo. *Mol. Cell* **8**, 213-224.
- Waga, S. and Stillman, B.** (1998). Cyclin-dependent kinase inhibitor p21 modulates the DNA primer-template recognition complex. *Mol. Cell. Biol.* **18**, 4177-4187.
- Wani, M. A., Wani, G., Yao, J., Zhu, Q. and Wani, A.** (2002). Human cells deficient in p53 regulated p21^{waf1/cip1} expression exhibit normal nucleotide excision repair of UV-induced DNA damage. *Carcinogenesis* **3**, 403-410.
- Warbrick, E.** (2000). The puzzle of PCNA's many partners. *BioEssays* **22**, 997-1006.

Supplementary Information

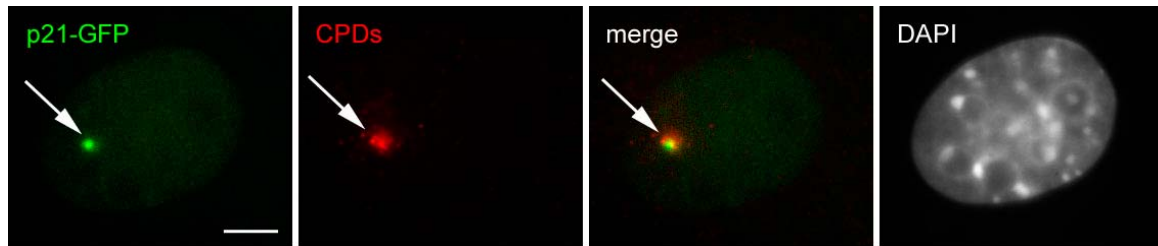


Fig. S1. Colocalization of p21-GFP and CPDs at the micro irradiated spot in a C2C12 myoblast. p21 transfected C2C12 cells were fixed 25 min after 405 nm laser microirradiation. CPDs were detected with monoclonal antibody. Arrow marks site of irradiation. p21-GFP accumulates at sites of DNA damage and co-localizes with CPDs. Bar, 5 μ m.

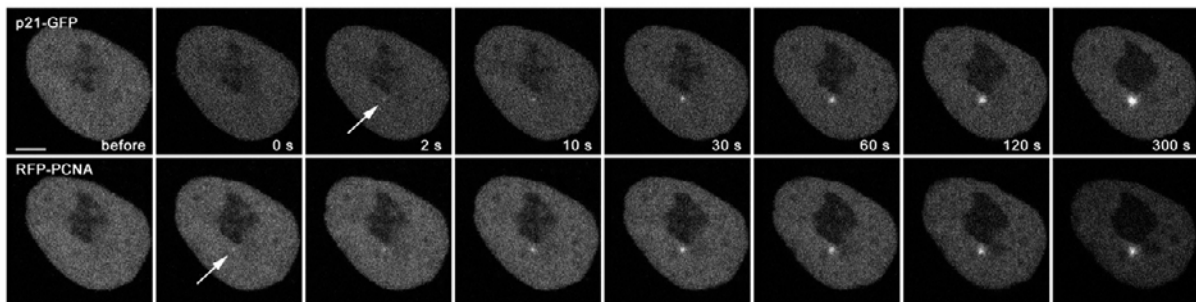


Fig. S2. Short term kinetics analysis of p21-GFP and RFP-PCNA fluorescence after 405 nm laser microirradiation in HeLa cells. Signals were acquired every 2 seconds and confocal sections are shown of images taken at the indicated times. The arrows indicate the site of irradiation. Bar, 5 μ m.

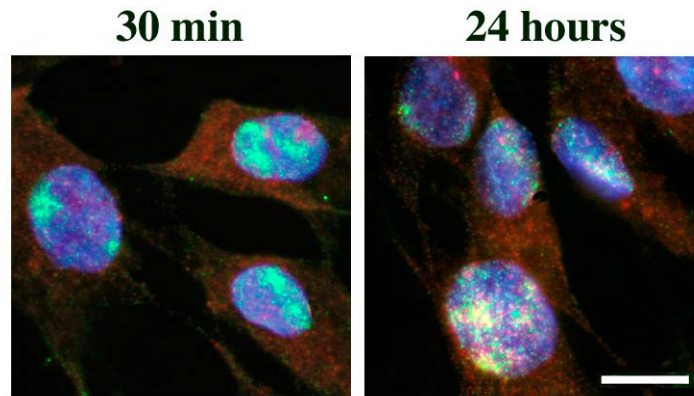


Fig. S3. Localisation of UV-induced CPDs and p21 protein, in locally irradiated XPA cells. After exposure to UV-C (15 J/m^2) through filters with 3 mm-pores, cells were lysed in situ and fixed. Immunostaining with anti-CPDs monoclonal antibody (green fluorescence), and anti-p21 polyclonal antibody (red fluorescence) was performed after mild DNA denaturation with DNase I, to expose UV-lesions. Green spots indicate the presence of CPDs, while yellow spots indicate the presence of both UV-lesions and p21, at irradiated areas. Bar, 10 μm .

2.4. XRCC1 and PCNA are loading platforms with distinct kinetic properties and different capacities to respond to multiple DNA lesions.

Research article

Open Access

XRCCI and PCNA are loading platforms with distinct kinetic properties and different capacities to respond to multiple DNA lesions

Oliver Mortusewicz and Heinrich Leonhardt*

Address: Ludwig Maximilians University Munich, Department of Biology II, 82152 Planegg-Martinsried, Germany

Email: Oliver Mortusewicz - o.mortusewicz@lmu.de; Heinrich Leonhardt* - H.Leonhardt@lmu.de

* Corresponding author

Published: 19 September 2007

Received: 1 June 2007

BMC Molecular Biology 2007, 8:81 doi:10.1186/1471-2199-8-81

Accepted: 19 September 2007

This article is available from: <http://www.biomedcentral.com/1471-2199/8/81>

© 2007 Mortusewicz and Leonhardt; licensee BioMed Central Ltd.

This is an Open Access article distributed under the terms of the Creative Commons Attribution License (<http://creativecommons.org/licenses/by/2.0>), which permits unrestricted use, distribution, and reproduction in any medium, provided the original work is properly cited.

Abstract

Background: Genome integrity is constantly challenged and requires the coordinated recruitment of multiple enzyme activities to ensure efficient repair of DNA lesions. We investigated the dynamics of XRCCI and PCNA that act as molecular loading platforms and play a central role in this coordination.

Results: Local DNA damage was introduced by laser microirradiation and the recruitment of fluorescent XRCCI and PCNA fusion proteins was monitored by live cell microscopy. We found an immediate and fast recruitment of XRCCI preceding the slow and continuous recruitment of PCNA. Fluorescence bleaching experiments (FRAP and FLIP) revealed a stable association of PCNA with DNA repair sites, contrasting the high turnover of XRCCI. When cells were repeatedly challenged with multiple DNA lesions we observed a gradual depletion of the nuclear pool of PCNA, while XRCCI dynamically redistributed even to lesions inflicted last.

Conclusion: These results show that PCNA and XRCCI have distinct kinetic properties with functional consequences for their capacity to respond to successive DNA damage events.

Background

Mammalian cells have to deal with a wide variety of different DNA lesions caused by cellular metabolites, replication errors, spontaneous disintegration and environmental influences. These lesions can occur at successive times and in distant parts of the genome constituting a permanent threat to the genetic integrity. Numerous repair pathways have evolved to reestablish and maintain the genetic information [1,2]. The recent identification of DNA methyltransferase I at repair sites indicated that not only the genetic but also the epigenetic information is restored [3].

The repair of DNA lesions involves multiple steps including initial damage recognition, intracellular signaling and the recruitment of repair factors. For the latter step so called loading platforms are considered to play a central role by locally concentrating and coordinating repair factors at sites of DNA damage. These loading platforms have no enzymatic activity of their own but interact with numerous proteins through highly conserved binding motifs. XRCCI (X-ray cross complementing factor 1) and PCNA (proliferating cell nuclear antigen) both fulfill these criteria and are therefore considered to act as central loading platforms in DNA replication and repair (reviewed in [4-6]).

XRCC1 was first identified in the Chinese Hamster ovary (CHO) mutant cell line EM9 [7]. This cell line shows a defect in single strand break repair (SSBR) and increased sensitivity to alkylating agents and ionizing irradiation resulting in elevated frequency of spontaneous chromosome aberrations and deletions. The importance of XRCC1 is further underlined by the embryonic lethality of XRCC1^{-/-} mice [8]. The fact that XRCC1 interacts with various proteins involved in SSBR and base excision repair (BER), including PARP-1, PARP-2 [9-11] Polymerase- β [12,13] and DNA Ligase III [9,14] suggests that XRCC1 acts as a loading platform in these pathways. Interestingly, XRCC1 also interacts with PCNA and it was proposed that this interaction facilitates efficient SSBR during DNA replication [15].

PCNA forms a homotrimeric ring around the DNA allowing both stable association with and sliding along the DNA double helix. Therefore PCNA is often referred to as a "sliding clamp" mediating interaction of various proteins with DNA in a sequence-independent manner. Photobleaching experiments have shown that in DNA replication PCNA acts as stationary loading platform for transiently interacting Okazaki fragment maturation proteins [16,17]. In the last few years it has become evident that PCNA is not only essential for DNA replication but also for various DNA repair pathways including nucleotide excision repair (NER) [18], base excision repair (BER) [19,20], mismatch repair (MMR) [21-23] and repair of double strand breaks (DSBs) [24,25]. Recently it has been shown, that accumulation of PCNA at DNA repair sites is independent of the RFC complex, which loads PCNA onto DNA during DNA replication [26]. Furthermore PCNA plays also an important role in postreplicative processes such as cytosine methylation and chromatin assembly [27,28]. In most cases, proteins involved in these processes directly bind to PCNA through a conserved PCNA-binding domain (PBD). This raises the question of how binding is coordinated and sterical hindrance avoided in DNA replication and repair. Recent studies have shown that posttranslational modifications of PCNA such as ubiquitinylation and sumoylation [29-34] mediate a switch between DNA replication and different repair pathways.

To study the dynamics of the two loading platforms XRCC1 and PCNA at DNA repair sites in HeLa cells we used a combination of microirradiation, live cell microscopy and photobleaching techniques. We found that XRCC1 and PCNA exhibit distinct recruitment and binding kinetics at repair sites resulting in different capacities to respond to successive DNA damage events.

Results and discussion

XRCC1 is less tightly associated with repair sites than PCNA

XRCC1 and PCNA have no known enzymatic function, are present at repair sites and interact with a high number of different proteins suggesting that they act as loading platforms in DNA repair. To investigate the role of XRCC1 and PCNA in DNA repair we performed immunostainings of microirradiated HeLa cells. We employed a confocal laser scanning microscope to generate DNA damage at preselected subnuclear sites with a long wavelength UV diode laser in BrdU-sensitized cells as described before [3,35]. Microirradiated sites stained positive for phosphorylated histone variant H2AX (γ H2AX), a marker for double strand breaks (DSBs), and poly(ADP-Ribose) which is generated by PARP at single strand breaks (SSBs) (Additional file 1). This indicates that microirradiation with a 405 nm laser generates a mixture of different types of DNA damage that are substrates for distinct DNA repair pathways involving XRCC1 and/or PCNA. Immunofluorescence stainings with specific antibodies revealed that endogenous PCNA and XRCC1 are both present at DNA damage sites as early as 2–4 min after irradiation (Figure 1A). To investigate the binding properties of XRCC1 and PCNA at DNA repair sites we performed salt extraction experiments. Microirradiated cells were permeabilized for 30 s followed by extraction with phosphate buffer containing 500 mM NaCl for 1 min. Immediately after salt

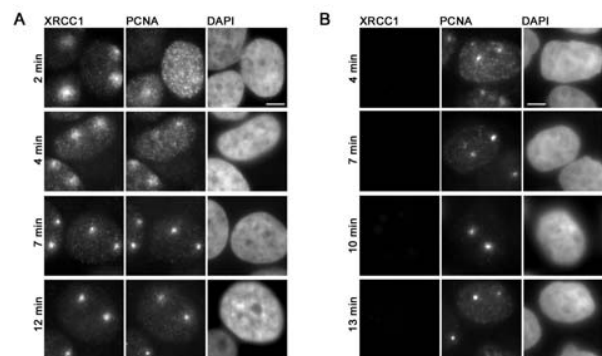


Figure 1

Immunochemical detection of endogenous XRCC1 and PCNA at DNA repair sites. Widefield fluorescence images of HeLa cells are shown. Cells were fixed at indicated time points after laser microirradiation. (A) Both, XRCC1 and PCNA, accumulate at laser-induced DNA damage sites. (B) Microirradiated HeLa cells were extracted with 0.5% Triton-X100 and 500 mM NaCl prior to fixation. After in situ extraction no endogenous XRCC1 can be detected at microirradiated sites while PCNA accumulations can still be observed. Scale bars, 5 μ m.

extraction, the cells were fixed and stained for endogenous proteins showing that XRCC1 and PCNA were both extracted in non-S phase cells that were not microirradiated. In microirradiated non-S phase cells only XRCC1 was extracted while PCNA could still be detected at DNA damage sites (Figure 1B), which is in good agreement with an earlier study, where detergent resistant foci of PCNA could be observed after local UV irradiation [36]. As previously reported [15] we also detected a partial colocalization of XRCC1 with PCNA at replication sites, but noticed dramatically different binding properties. Thus XRCC1 was readily extracted, whereas PCNA was still stably associated with sites of DNA replication (Figure 1B). Taken together these results show that endogenous XRCC1 and PCNA are both present at DNA replication and repair sites but exhibit different binding properties.

Recruitment and mobility of XRCC1 and PCNA at DNA repair sites

To further investigate the dynamics detected with salt extraction experiments we combined the microirradiation technique with live cell microscopy and photobleaching analysis (FRAP). We first determined the recruitment kinetics of XRCC1 and PCNA in living cells by quantifying the amount of GFP- and RFP-tagged XRCC1 and PCNA accumulated at microirradiated sites. The intensity values were corrected for background and for total nuclear loss of fluorescence over the time course and normalized to the pre-irradiation value.

A direct comparison of GFP- and RFP-tagged XRCC1 and PCNA showed a significantly slower recruitment of PCNA in contrast to the very fast accumulation of XRCC1 at microirradiated sites (Figure 2A). The fluorescence intensity of PCNA at the irradiated site increased during the observation period of 5 min, while XRCC1 accumulation reached a maximum about 1–2 min after irradiation (Figure 2B). These kinetic differences are in good agreement with earlier studies comparing the recruitment of XRCC1 and PCNA to laser-induced DNA damage sites [37].

Having shown that XRCC1 and PCNA are recruited with distinct kinetics we performed FRAP analysis to determine their dynamics at laser-induced DNA damage sites. Two separate spots were microirradiated in living cells coexpressing GFP-XRCC1 and RFP-PCNA. After 5 min one region was bleached with a high energy laser pulse for 300 ms and the fluorescence recovery was determined. After bleaching of the repair foci we observed complete recovery of the XRCC1 signal within 24 s (Figure 3). Since fluorescence intensity at repair sites had already peaked and did not increase any further, the measured recovery has to be attributed to a rapid turnover of XRCC1.

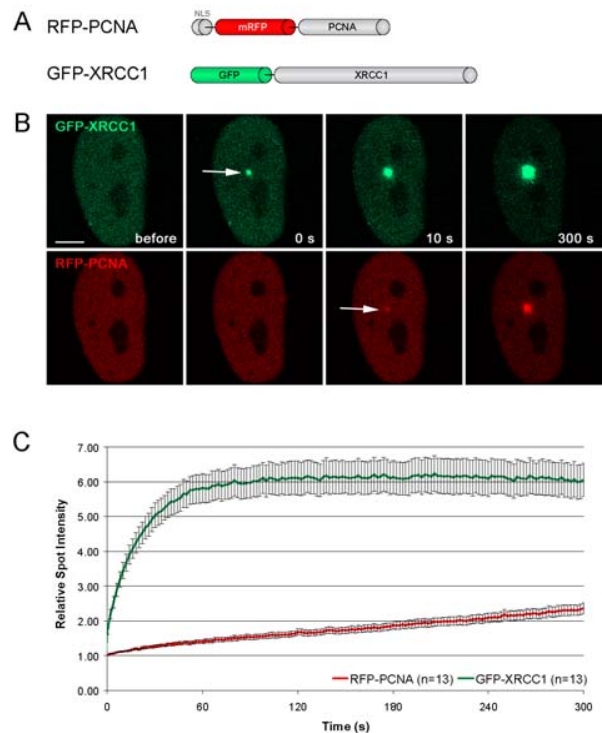


Figure 2

Recruitment of XRCC1 and PCNA at DNA damage sites in living cells. (A) Schematic representation of the fluorescent fusion proteins. (B) Live cell imaging of a microirradiated HeLa cell coexpressing GFP-XRCC1 and RFP-PCNA. Accumulation of GFP-XRCC1 can be observed immediately after microirradiation, while RFP-PCNA accumulates with a short delay of about 2–10 s (indicated by arrows). (C) Quantitative evaluation of recruitment kinetics showing mean curves. Error bars represent the standard error of the mean. Immediate and fast recruitment of GFP-XRCC1 precedes slow and constant recruitment of RFP-PCNA at DNA damage sites. Scale bar, 5 μm.

In contrast, no recovery of PCNA at DNA repair sites could be observed within the observation period, which is in good agreement with previous studies where DNA damage was induced by chemical agents or irradiation with a UV lamp [30,38].

To determine the dissociation kinetics of XRCC1 and PCNA from DNA damage sites we performed FLIP experiments in HeLa cells expressing GFP-XRCC1 and RFP-PCNA. 5 min after microirradiation half of the nucleus was repeatedly bleached with a high energy laser pulse over a time period of 150 s and the loss of fluorescence at the microirradiated site located outside the bleaching area was determined (Figure 4, inset). The intensity values

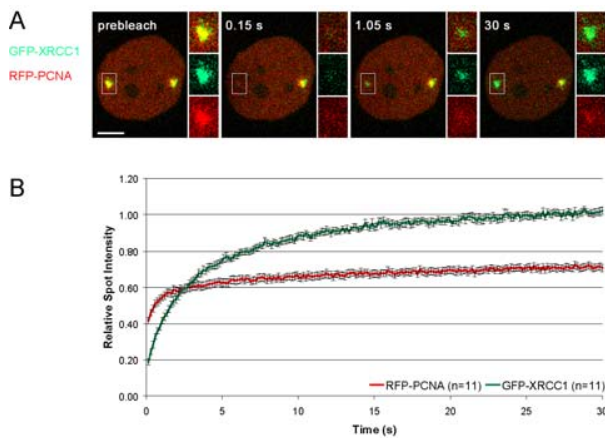


Figure 3

Mobility of XRCC1 and PCNA at DNA damage sites. (A) Two separate subnuclear spots of a transiently transfected HeLa cell were microirradiated. The mobility of accumulated fluorescent fusion proteins was determined by bleaching one of the two spots 5 min after microirradiation and subsequent recovery measurements. Inset shows the bleached microirradiated site. Scale bar, 5 μ m. **(B)** FRAP data from 11 individual experiments are shown as mean curves. Error bars represent the standard error of the mean.

were corrected for background fluorescence and normalized to the pre-bleach value.

Within the first 10–15 s both fusion proteins showed a rapid loss of fluorescence due to depletion of highly mobile, unbound fluorescent molecules within the region of interest. After this initial phase XRCC1 and PCNA exhibited dramatically different dissociation kinetics. We could observe a rapid decrease of XRCC1 fluorescence to 10% of the initial intensity within the observation period while the intensity of PCNA was only reduced to 34% (Figure 4). This argues for a constant exchange of fluorescent XRCC1 molecules between the damage site and the bleached half of the nucleus, while most RFP-PCNA molecules remained bound at DNA repair sites.

These results show that the two loading platforms XRCC1 and PCNA exhibit distinct recruitment kinetics and mobility (association and dissociation rates) at DNA repair sites, which is consistent with an involvement of XRCC1 and PCNA in distinct repair pathways. On the one hand, PCNA is involved in repair pathways where the synthesis of long stretches of DNA requires a stable and processive repair machinery. On the other hand, XRCC1 is part of the short patch BER pathway where only a single

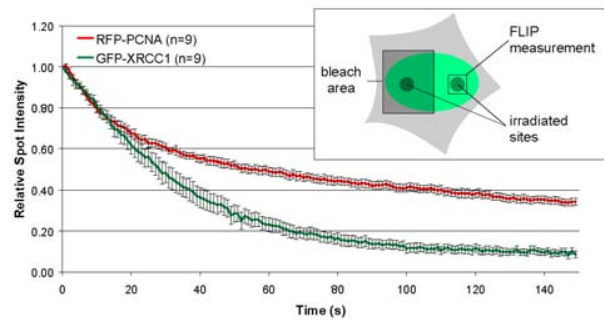


Figure 4

Different binding kinetics of XRCC1 and PCNA at DNA repair sites. FLIP data from 9 individual experiments are shown as mean curves. The scheme of the experiment is outlined in the inset. Two separate subnuclear spots of transiently transfected HeLa cells were microirradiated. Half of the nucleus containing one irradiated site was repeatedly bleached for 1 s over a total time period of 150 s, starting 5 min after microirradiation. The decay of the fluorescence intensity at the microirradiated site within the non-bleached half of the nucleus was measured and plotted over time. Error bars represent the standard error of the mean.

nucleotide needs to be replaced and no processive and stable machinery is required.

To further investigate the role of XRCC1 and PCNA as central loading platforms in DNA repair we extended our photobleaching analysis to their respective interaction partners DNA Ligase III and I. In a previous study we compared the recruitment kinetics of these highly conserved DNA Ligases and found that they are recruited to DNA repair sites with distinct kinetics. Using mutational analysis and binding studies we could show, that DNA Ligase I is recruited to repair sites through interaction with PCNA, while DNA Ligase III is recruited via its BRCT domain interacting with XRCC1 [35]. FRAP analysis revealed that both DNA Ligases show a high turnover at repair sites, with DNA Ligase I recovering faster than DNA Ligase III (Additional file 2). Interestingly, DNA Ligase III showed the same recovery rate as its loading platform XRCC1, while the mobility of DNA Ligase I and PCNA at repair sites differed dramatically (Additional file 2).

These results demonstrate that these loading platforms and their interacting repair factors have independent binding properties at repair sites. We speculate that even transient interaction of repair factors with their respective loading platform enhances the efficiency of DNA repair by local concentration of enzyme activities at repair sites,

allowing faster recognition and binding of repair substrates.

Flexible response of XRCC1 and PCNA to multiple DNA damage events

To investigate whether the different binding properties of XRCC1 and PCNA have functional consequences we tested their ability to respond to multiple DNA lesions. Successive DNA lesions were introduced with a time interval of 2.5 min at separate spots and the recruitment kinetics were determined for each individual spot. We observed a constant decrease of PCNA accumulation at sites irradiated at later time points (Figure 5). In contrast, XRCC1 accumulation at early and late irradiated sites was similar.

These differences can be explained by the tight binding of PCNA at repair sites leading to a depletion of the cellular pool of PCNA molecules available for repair of subsequent damages.

In contrast, the dynamic binding of XRCC1 enables fast exchange between multiple DNA damages sites separated in time and space. Taken together these findings argue for a role of PCNA as a stationary loading platform in DNA repair allowing efficient and accurate repair, whereas the fast recruitment and high turnover of XRCC1 enables a

flexible response to multiple DNA damage events occurring at distant sites and successive times in the genome.

Conclusion

In summary, we found that XRCC1 and PCNA exhibit distinct recruitment and binding kinetics at repair sites, which goes beyond earlier studies comparing only the accumulation of XRCC1 and PCNA at repair sites [37]. Efficient repair of DNA lesions requires avid recognition of the damage and coordinated recruitment of a multitude of repair factors. The principle dilemma faced by the repair machinery is that the stable complex formation required for processivity and completion of multi-step processes is incompatible with a flexible response to later changes like subsequent DNA damages. Our live cell recruitment and photobleaching analyses showed that XRCC1 and PCNA represent opposite strategies. We clearly demonstrate that the stable binding of the processivity factor PCNA limits its capacity to respond to successive damage events. While the avid and transient binding of XRCC1 might be sufficient for single nucleotide replacement but allows a flexible response to multiple consecutive DNA lesions. This type of live cell analysis should also help to explore the flexibility of other repair factors and complex cellular machineries in response to changing requirements.

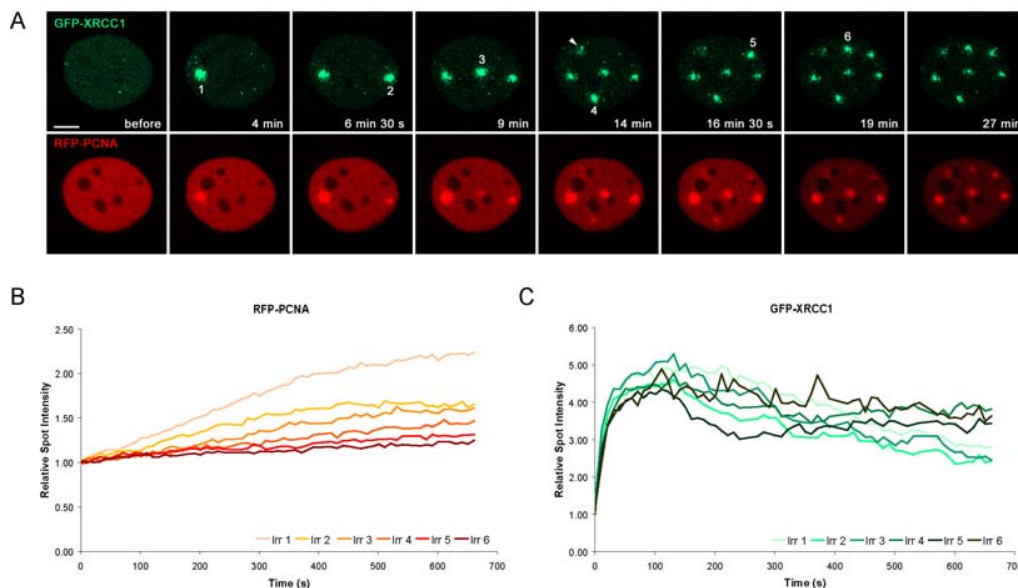


Figure 5

Flexible response of XRCC1 to multiple DNA damage events. (A) Consecutive/Successive DNA lesions were introduced with a time interval of 2.5 min, starting 4 min after microirradiation of the first spot. One spot irradiated in close proximity to the nucleoli was not evaluated (arrowhead) (B) The recruitment kinetics of XRCC1 and PCNA at consecutively microirradiated sites were evaluated and plotted over time. Representative curves of one HeLa cell are shown.

Methods

Cell culture and transfection

HeLa cells were cultured in DMEM containing 50 µg/ml gentamicin supplemented with 10% FCS. Cells grown on µ-slides (Ibidi) or on gridded coverslips were cotransfected with jetPEI (PolyPlus Transfection) or TransFectin transfection reagent (Bio-Rad) according to the manufacturers instructions. For microirradiation experiments cells were sensitized by incubation in medium containing BrdU (10 µg/ml) for 24–48 h.

Expression plasmids

Mammalian expression constructs encoding translational fusions of human PCNA with either green (GFP) or red (RFP) fluorescent protein were previously described [17]. Red variants of the previously described GFP-Ligase III [3] and GFP-XRCC1 [39] were generated by replacing GFP with RFP [40] and termed RFP-Ligase III and RFP-XRCC1, respectively. In all cases expression was under the control of the CMV promoter. We tested all fusion proteins by expression in 293T cells followed by western blot analysis.

Immunofluorescence and Detergent Extraction

Cells were fixed in 3,7% formaldehyde for 10 min and permeabilized with ice-cold methanol for 5 min. The following primary antibodies (diluted in PBS containing 2% BSA) were used: anti-γ H2AX (Ser139) rabbit antibody (Upstate), anti-PAR mouse monoclonal antibody (Trevigen), anti-XRCC1 mouse monoclonal antibody (Abcam) and anti-PCNA rat monoclonal antibody [41]. Secondary antibodies (diluted 1:400 in PBS containing 2% BSA) conjugated to Alexa Fluor 488, 555 or 647 (Molecular Probes) were used. Cells were counterstained with DAPI and mounted in Vectashield (Vector Laboratories). For in situ detergent extraction, cells were permeabilized for 30 s with 0,5% Triton X-100 in PBS and extracted for 1 min with 500 mM NaCl in PBS before fixation.

Live-cell Microscopy, microirradiation and photobleaching experiments

Live cell imaging, microirradiation and photobleaching experiments were carried out with a Leica TCS SP2/AOBS confocal laser scanning microscope equipped with a UV-transmitting HCX PL 63×/1.4 oil objective. Fluorophores were excited using a 488 nm Ar laser line and a 561 nm diode laser line. The microscope was equipped with a heated environmental chamber set to 37°C. Confocal image series were typically recorded with a frame size of 256 × 256 pixels and a pixel size of 90 nm.

Microirradiation was carried out with a 405 nm diode laser set to maximum power at 100% transmission. Preselected spots of ~1 µm in diameter within the nucleus were microirradiated for 1 s. Before and after microirradiation confocal image series of one mid z-section were recorded

at 2 s time interval (typically 6 pre-irradiation and 150 post-irradiation frames). For evaluation of recruitment kinetics, fluorescence intensities at the irradiated region were corrected for background and for total nuclear loss of fluorescence over the time course and normalized to the pre-irradiation value.

For FRAP analysis, a region of interest was selected and photobleached for 300 ms with all laser lines of the Ar-laser and the 561 nm DPSS laser set to maximum power at 100% transmission. Before and after bleaching, confocal image series were recorded at 150 ms time intervals (typically 10 prebleach and 200 postbleach frames). Mean fluorescence intensities of the bleached region were corrected for background and for total nuclear loss of fluorescence over the time course and normalized to the mean of the last 4 prebleach values.

For FLIP analysis, one half of the nucleus was repeatedly photobleached (typically 150 frames) with all laser lines of the Ar-laser and the 561 nm DPSS laser set to maximum power at 100% transmission for 1 s. Mean fluorescence intensities of the bleached region were corrected for background and normalized to the initial value.

For quantitative evaluation of microirradiation and photobleaching experiments, data of at least 9 nuclei were averaged and the mean curve as well as the standard error of the mean calculated and plotted using Microsoft Excel software.

Images of fixed cells were taken with a Zeiss Axiophot 2 widefield epifluorescence microscope using a Zeiss Plan-Apochromat 63×/1.40 oil objective and a cooled CCD camera (Visitron Systems).

Abbreviations

BER: base excision repair

DSBs: double strand breaks

FLIP: fluorescence loss in photobleaching

FRAP: fluorescence recovery after photobleaching

PCNA: proliferating cell nuclear antigen

SSBR: single strand break repair

SSBs: single strand breaks

XRCC1: X-ray cross complementing factor 1

Competing interests

The author(s) declares that there are no competing interests.

Authors' contributions

OM designed and performed the experiments, analyzed the data and participated in writing the manuscript. HL participated in experimental design and writing the manuscript. All authors read and approved the final manuscript.

Additional material

Additional file 1

Laser microirradiation generates different types of DNA damage. Description: The data provided shows that laser microirradiation with a 405 nm laser generates different types of DNA damage, including SSBs and DSBs. Click here for file

[<http://www.biomedcentral.com/content/supplementary/1471-2199-8-81-S1.doc>]

Additional file 2

Mobility of XRCC1 and PCNA and their respective binding partners DNA Ligase III and I at DNA damage sites. Description: The data provided indicates that XRCC1 and its binding partner DNA Ligase III show similar turnover rates at DNA damage sites, while the mobility of PCNA and its binding partner DNA Ligase I differ dramatically. Click here for file

[<http://www.biomedcentral.com/content/supplementary/1471-2199-8-81-S2.doc>]

Acknowledgements

We are indebted to Dr R. Tsien for providing the mRFP1 expression vector and to Dr. G. de Murcia for providing the GFP-XRCC1 expression vector. We are grateful to Drs. M. Cristina Cardoso, Fabio Spada and Gilbert de Murcia for their help and comments on the manuscript. This work was supported by grants from the Deutsche Forschungsgemeinschaft and the Volkswagenstiftung to H.L.

References

- Hoeijmakers JH: **Genome maintenance mechanisms for preventing cancer.** *Nature* 2001, **411**:366-374.
- Friedberg EC: **DNA damage and repair.** *Nature* 2003, **421**:436-440.
- Mortusewicz O, Schermelleh L, Walter J, Cardoso MC, Leonhardt H: **Recruitment of DNA methyltransferase I to DNA repair sites.** *Proc Natl Acad Sci U S A* 2005.
- Warbrick E: **The puzzle of PCNA's many partners.** *Bioessays* 2000, **22**:997-1006.
- Caldecott KW: **XRCC1 and DNA strand break repair.** *DNA Repair (Amst)* 2003, **2**:955-969.
- Maga G, Hubscher U: **Proliferating cell nuclear antigen (PCNA): a dancer with many partners.** *J Cell Sci* 2003, **116**:3051-3060.
- Thompson LH, Brookman KW, Dillehay LE, Carrano AV, Mazrimas JA, Mooney CL, Minkler JL: **A CHO-cell strain having hypersensitivity to mutagens, a defect in DNA strand-break repair, and an extraordinary baseline frequency of sister-chromatid exchange.** *Mutat Res* 1982, **95**:427-440.
- Tebbs RS, Flannery ML, Meneses JJ, Hartmann A, Tucker JD, Thompson LH, Cleaver JE, Pedersen RA: **Requirement for the Xrcc1 DNA base excision repair gene during early mouse development.** *Dev Biol* 1999, **208**:513-529.
- Caldecott KW, McKeown CK, Tucker JD, Ljungquist S, Thompson LH: **An interaction between the mammalian DNA repair protein XRCC1 and DNA ligase III.** *Mol Cell Biol* 1994, **14**:68-76.
- Masson M, Niedergang C, Schreiber V, Muller S, Menissier-de Murcia J, de Murcia G: **XRCC1 is specifically associated with poly(ADP-ribose) polymerase and negatively regulates its activity following DNA damage.** *Mol Cell Biol* 1998, **18**:3563-3571.
- Schreiber V, Ame JC, Dolle P, Schultz I, Rinaldi B, Fraulob V, Menissier-de Murcia J, de Murcia G: **Poly(ADP-ribose) polymerase-2 (PARP-2) is required for efficient base excision DNA repair in association with PARP-1 and XRCC1.** *J Biol Chem* 2002, **277**:23028-23036.
- Kubota Y, Nash RA, Klungland A, Schar P, Barnes DE, Lindahl T: **Reconstitution of DNA base excision-repair with purified human proteins: interaction between DNA polymerase beta and the XRCC1 protein.** *Embo J* 1996, **15**:6662-6670.
- Caldecott KW, Aoufouchi S, Johnson P, Shall S: **XRCC1 polypeptide interacts with DNA polymerase beta and possibly poly(ADP-ribose) polymerase, and DNA ligase III is a novel molecular 'nick-sensor' in vitro.** *Nucleic Acids Res* 1996, **24**:4387-4394.
- Wei YF, Robins P, Carter K, Caldecott K, Pappin DJ, Yu GL, Wang RP, Shell BK, Nash RA, Schar P, et al.: **Molecular cloning and expression of human cDNAs encoding a novel DNA ligase IV and DNA ligase III, an enzyme active in DNA repair and recombination.** *Mol Cell Biol* 1995, **15**:3206-3216.
- Fan J, Otterlei M, Wong HK, Tomkinson AE, Wilson DM 3rd: **XRCC1 co-localizes and physically interacts with PCNA.** *Nucleic Acids Res* 2004, **32**:2193-2201.
- Sporbert A, Gahl A, Ankerhold R, Leonhardt H, Cardoso MC: **DNA polymerase clamp shows little turnover at established replication sites but sequential de novo assembly at adjacent origin clusters.** *Mol Cell* 2002, **10**:1355-1365.
- Sporbert A, Domaing P, Leonhardt H, Cardoso MC: **PCNA acts as a stationary loading platform for transiently interacting Okazaki fragment maturation proteins.** *Nucleic Acids Res* 2005, **33**:3521-3528.
- Shivji KK, Kenny MK, Wood RD: **Proliferating cell nuclear antigen is required for DNA excision repair.** *Cell* 1992, **69**:367-374.
- Gary R, Kim K, Cornelius HL, Park MS, Matsumoto Y: **Proliferating cell nuclear antigen facilitates excision in long-patch base excision repair.** *J Biol Chem* 1999, **274**:4354-4363.
- Levin DS, McKenna AE, Motycka TA, Matsumoto Y, Tomkinson AE: **Interaction between PCNA and DNA ligase I is critical for joining of Okazaki fragments and long-patch base-excision repair.** *Curr Biol* 2000, **10**:919-922.
- Umar A, Buermeyer AB, Simon JA, Thomas DC, Clark AB, Liskay RM, Kunkel TA: **Requirement for PCNA in DNA mismatch repair at a step preceding DNA resynthesis.** *Cell* 1996, **87**:65-73.
- Johnson RE, Kovvali GK, Guzder SN, Amin NS, Holm C, Habraken Y, Sung P, Prakash L, Prakash S: **Evidence for involvement of yeast proliferating cell nuclear antigen in DNA mismatch repair.** *J Biol Chem* 1996, **271**:27987-27990.
- Jiricny J: **The multifaceted mismatch-repair system.** *Nat Rev Mol Cell Biol* 2006, **7**:335-346.
- Holmes AM, Haber JE: **Double-strand break repair in yeast requires both leading and lagging strand DNA polymerases.** *Cell* 1999, **96**:415-424.
- Dorazi R, Parker JL, White MF: **PCNA activates the Holliday junction endonuclease Hjc.** *J Mol Biol* 2006, **364**:243-247.
- Hashiguchi K, Matsumoto Y, Yasui A: **Recruitment of DNA repair synthesis machinery to sites of DNA damage/repair in living human cells.** *Nucleic Acids Res* 2007.
- Moggs JG, Grandi P, Quivy JP, Jonsson ZO, Hubscher U, Becker PB, Almouzni G: **A CAF-1-PCNA-mediated chromatin assembly pathway triggered by sensing DNA damage.** *Mol Cell Biol* 2000, **20**:1206-1218.
- Chuang LS, Ian HI, Koh TW, Ng HH, Xu G, Li BF: **Human DNA-(cytosine-5) methyltransferase-PCNA complex as a target for p21WAF1.** *Science* 1997, **277**:1996-2000.
- Pfander B, Moldovan GL, Sacher M, Hoege C, Jentsch S: **SUMO-modified PCNA recruits Srs2 to prevent recombination during S phase.** *Nature* 2005, **436**:428-433.

30. Solomon DA, Cardoso MC, Knudsen ES: **Dynamic targeting of the replication machinery to sites of DNA damage.** *J Cell Biol* 2004, **166**:455-463.
31. Hoegge C, Pfander B, Moldovan GL, Pyrowolakis G, Jentsch S: **RAD6-dependent DNA repair is linked to modification of PCNA by ubiquitin and SUMO.** *Nature* 2002, **419**:135-141.
32. Matunis MJ: **On the road to repair: PCNA encounters SUMO and ubiquitin modifications.** *Mol Cell* 2002, **10**:441-442.
33. Stelter P, Ulrich HD: **Control of spontaneous and damage-induced mutagenesis by SUMO and ubiquitin conjugation.** *Nature* 2003, **425**:188-191.
34. Papouli E, Chen S, Davies AA, Huttner D, Krejci L, Sung P, Ulrich HD: **Crosstalk between SUMO and ubiquitin on PCNA is mediated by recruitment of the helicase Srs2p.** *Mol Cell* 2005, **19**:123-133.
35. Mortusewicz O, Rothbauer U, Cardoso MC, Leonhardt H: **Differential recruitment of DNA Ligase I and III to DNA repair sites.** *Nucleic Acids Res* 2006, **34**:3523-3532.
36. Okano S, Lan L, Caldecott KW, Mori T, Yasui A: **Spatial and temporal cellular responses to single-strand breaks in human cells.** *Mol Cell Biol* 2003, **23**:3974-3981.
37. Lan L, Nakajima S, Oohata Y, Takao M, Okano S, Masutani M, Wilson SH, Yasui A: **In situ analysis of repair processes for oxidative DNA damage in mammalian cells.** *Proc Natl Acad Sci U S A* 2004, **101**:13738-13743.
38. Essers J, Theil AF, Baldeyron C, van Cappellen WA, Houtsmuller AB, Kanaar R, Vermeulen W: **Nuclear dynamics of PCNA in DNA replication and repair.** *Mol Cell Biol* 2005, **25**:9350-9359.
39. Levy N, Martz A, Bresson A, Spenlehauer C, de Murcia G, Menissier-de Murcia J: **XRCC1 is phosphorylated by DNA-dependent protein kinase in response to DNA damage.** *Nucleic Acids Res* 2006, **34**:32-41.
40. Campbell RE, Tour O, Palmer AE, Steinbach PA, Baird GS, Zacharias DA, Tsien RY: **A monomeric red fluorescent protein.** *Proc Natl Acad Sci U S A* 2002, **99**:7877-7882.
41. Spada F, Haemmer A, Kuch D, Rothbauer U, Schermelleh L, Kremmer E, Carell T, Langst G, Leonhardt H: **DNMT1 but not its interaction with the replication machinery is required for maintenance of DNA methylation in human cells.** *J Cell Biol* 2007, **176**:565-571.

Publish with **BioMed Central** and every scientist can read your work free of charge

"BioMed Central will be the most significant development for disseminating the results of biomedical research in our lifetime."

Sir Paul Nurse, Cancer Research UK

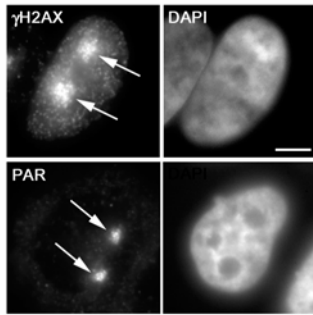
Your research papers will be:

- available free of charge to the entire biomedical community
- peer reviewed and published immediately upon acceptance
- cited in PubMed and archived on PubMed Central
- yours — you keep the copyright

Submit your manuscript here:
http://www.biomedcentral.com/info/publishing_adv.asp

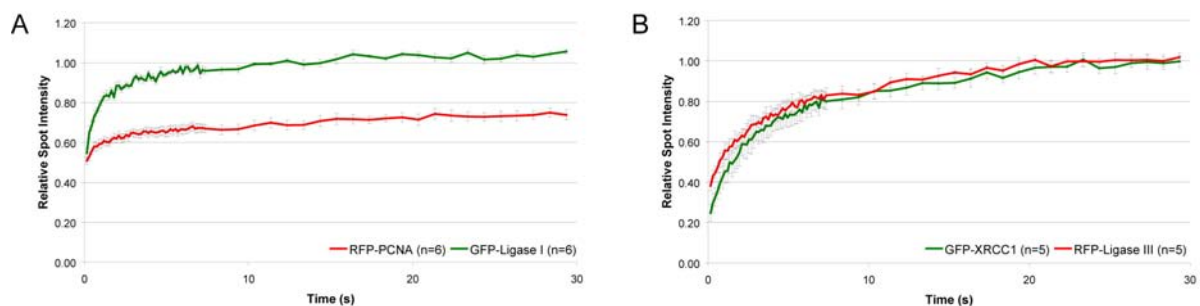


Supplementary Information



Supplementary Figure 1

Laser microirradiation generates different types of DNA damage. Widefield fluorescence images of HeLa cells are shown. Fixation and immunostaining was performed ~5 min after laser microirradiation. Arrows mark sites of irradiation. Laser microirradiation results in local generation of DSBs (A) and SSBs (B) detected by antibodies against γ -H2AX and PAR, respectively. Scale bar, 5 μ m.



Supplementary Figure 2

Mobility of XRCC1 and PCNA and their respective binding partners DNA Ligase III and I at DNA damage sites. Two separate subnuclear spots of transiently transfected HeLa cells were microirradiated and the mobility of accumulated fluorescent fusion proteins was determined as described in Figure 3. FRAP data from at least 5 different experiments are shown as mean curves. Error bars represent the standard error of the mean.

**2.5. Differential recruitment of DNA Ligase I and III to
DNA repair sites.**

Differential recruitment of DNA Ligase I and III to DNA repair sites

Oliver Mortusewicz, Ulrich Rothbauer, M. Cristina Cardoso¹ and Heinrich Leonhardt*

Department of Biology II, Ludwig Maximilians University Munich, 82152 Planegg-Martinsried, Germany and ¹Max Delbrück Center for Molecular Medicine, 13125 Berlin, Germany

Received May 9, 2006; Revised June 22, 2006; Accepted June 27, 2006

ABSTRACT

DNA ligation is an essential step in DNA replication, repair and recombination. Mammalian cells contain three DNA Ligases that are not interchangeable although they use the same catalytic reaction mechanism. To compare the recruitment of the three eukaryotic DNA Ligases to repair sites *in vivo* we introduced DNA lesions in human cells by laser microirradiation. Time lapse microscopy of fluorescently tagged proteins showed that DNA Ligase III accumulated at microirradiated sites before DNA Ligase I, whereas we could detect only a faint accumulation of DNA Ligase IV. Recruitment of DNA Ligase I and III to repair sites was cell cycle independent. Mutational analysis and binding studies revealed that DNA Ligase I was recruited to DNA repair sites by interaction with PCNA while DNA Ligase III was recruited via its BRCT domain mediated interaction with XRCC1. Selective recruitment of specialized DNA Ligases may have evolved to accommodate the particular requirements of different repair pathways and may thus enhance efficiency of DNA repair.

INTRODUCTION

Higher eukaryotes are challenged with various types of DNA damage caused by replication errors, radiation, environmental agents and by-products of cellular metabolism. Numerous repair pathways re-establishing the genetic information are known (1,2). An increasing number of proteins have been identified and assigned to these repair pathways, but the recruitment mechanisms and the spatio-temporal coordination of these repair factors at DNA damage sites remains largely unknown. One of the late steps in DNA repair is the joining of breaks in the phosphodiester backbone of duplex DNA, which is catalyzed by members of the DNA Ligase family. The ATP-dependent DNA Ligase family comprises three

enzymes termed DNA Ligase I, III and IV, which all contain a highly conserved catalytic domain responsible for the ligation reaction. Although all three DNA Ligases use the same basic reaction mechanism, they have distinct functions and are not interchangeable (3,4).

DNA Ligase I is required for the joining of Okazaki fragments during lagging strand synthesis and is implicated in long-patch or replicative base-excision repair (BER) and nucleotide excision repair (NER). The end-joining activity of DNA Ligase I is directed to DNA replication sites by its interaction with PCNA, a central component of the replication machinery. This interaction and localization is mediated by the N-terminal PCNA-binding domain (PBD) of DNA Ligase I (5,6). It has been shown that loss of DNA Ligase I function, leads to abnormal joining of Okazaki fragments during S-phase (7), defective long-patch BER (8) and reduced repair of double strand breaks (DSBs) by homologous recombination (9).

DNA Ligase III is implicated in short-patch BER and single strand break (SSB) repair (SSBR) and forms a complex with XRCC1 (10–12). XRCC1 and DNA Ligase III normally exist as a preformed complex *in vivo* interacting via the C-terminal BRCT (BRCA1 C-terminal) domain of DNA Ligase III (10,13–15). XRCC1 also interacts with PARP-1, PARP-2, DNA polymerase β and PCNA (16) and appears to act as a scaffold protein during BER. The unique zinc finger near the N-terminus of DNA Ligase III was shown to bind DNA SSBs (17). Interestingly, this DNA Ligase III zinc finger shows homology with the two zinc finger motifs of poly(ADP-ribose) polymerase (PARP) which also bind DNA strand breaks (11). Therefore, it was suggested that binding of DNA Ligase III via its zinc finger may displace PARP from the DNA break allowing access of DNA Ligase III and other repair proteins to the DNA lesion (17). Recently DNA Ligase III was also identified as a candidate component of the non-homologous end joining (NHEJ) backup pathway (B-NHEJ) (18) and might thus be implicated in double strand break repair.

DNA Ligase IV is implicated in the NHEJ pathway and forms a complex with XRCC4 (19,20). Cultured cells that lack DNA Ligase IV are defective in V(D)J recombination

*To whom correspondence should be addressed. Tel: +49 89 2180 74232; Fax: +49 89 2180 74236; E-mail: h.leonhardt@lmu.de

© 2006 The Author(s).

This is an Open Access article distributed under the terms of the Creative Commons Attribution Non-Commercial License (<http://creativecommons.org/licenses/by-nc/2.0/uk/>) which permits unrestricted non-commercial use, distribution, and reproduction in any medium, provided the original work is properly cited.

and show increased sensitivity to ionizing radiation (21). Inactivation of DNA Ligase IV in mice leads to embryonic lethality, implying that DNA Ligase IV may have essential functions during early mammalian development (21,22).

We investigated the recruitment of DNA Ligases to repair sites in HeLa cells using a combination of microirradiation, live cell microscopy and binding studies. We could detect only a faint accumulation of DNA Ligase IV at laser-induced DNA damage sites. Kinetic studies and deletion analysis indicated that selective recruitment of DNA Ligase I and III to specific repair pathways is mediated through interaction with PCNA and XRCC1, respectively. These results suggest that PCNA and XRCC1 play a central role in the spatio-temporal coordination of repair factors and thereby enhance the specificity and efficiency of DNA repair in eukaryotic cells.

MATERIALS AND METHODS

Cell culture and transfection

Human HeLa or HEK 293T cells and mouse C2C12 myoblasts were cultured in DMEM containing 50 µg/ml gentamicin supplemented with 10 and 20% FCS, respectively. For transfection, cells grown on µ-slides (Ibidi) or on gridded coverslips were cotransfected with jetPEI (PolyPlus Transfection) or TransFectin transfection reagent (Bio-Rad) according to the manufacturer's instructions. Cells were subsequently incubated for 24–48 h before performing microirradiation and live cell analyses or immunostainings. 293T cells were transfected with plasmid DNA using TransFectin reagent (Bio-Rad) and incubated for 48 h before immunoprecipitations.

Expression plasmids

Mammalian expression constructs encoding translational fusions of human DNA Ligase I, human FEN1 and human PCNA with either green (GFP) or red (RFP) fluorescent protein were previously described (23). Red variants of the previously described GFP-Ligase III (24) and GFP-XRCC1 (25) were generated by replacing GFP with RFP (26) and termed RFP-Ligase III and RFP-XRCC1, respectively. Deletion expression constructs were amplified by PCR with primers containing a SalI and BamHI restriction site and subcloned into the SalI and BamHI site of the peGFP-C1 vector (Clontech) downstream of GFP. The Ligase I PBD-GFP construct was made by subcloning oligonucleotides corresponding to the first 20 amino acids of DNA Ligase I into the EcoRI and XmaI site of peGFP-N2 (Clontech). The GFP-Ligase IV construct was generated by cloning the human DNA Ligase IV cDNA (11) into the peGFP-C1 (Clontech) vector. DNA Ligase IV was amplified using the following oligonucleotides as primers for the PCR: forward 5'-gggg **gtc gac** gct gcc tca caa ac-3'; reverse 5'-cccc **gga tcc** aat caa ata ctg gtt ttc-3'. The residues in bold indicate a SalI and a BamHI site encoded in the forward and reverse primer, respectively, for subcloning the PCR fragment into the SalI and BamHI sites of the peGFP-C1 vector downstream of GFP. PCR amplified sequences were verified by DNA sequencing. The Ku70-GFP construct (27) was provided by

William Rodgers. In all cases expression was under the control of the CMV promoter. All fusion proteins were tested by expression in HEK 293T cells followed by western blot analysis.

Immunofluorescence and chemicals

Cells were fixed in 3.7% formaldehyde for 10 min and permeabilized with ice-cold methanol for 5 min. The following primary antibodies (diluted in PBS containing 2% BSA) were used: anti-γ H2AX (Ser139) rabbit antibodies (Upstate), anti-PAR mouse monoclonal antibody (Trevigen), anti-DNA Ligase III mouse monoclonal antibody (Gene-Tex), rabbit affinity purified DNA Ligase I antibodies (5), anti-XRCC1 mouse monoclonal antibody (Abcam) and anti-PCNA rat monoclonal antibody. Primary antibodies were detected using secondary antibodies (diluted 1:400 in PBS containing 2% BSA) conjugated to Alexa Fluor 488, 555 or 647 (Molecular Probes). Cells were counterstained with DAPI and mounted in Vectashield (Vector Laboratories).

Microscopy

Time series were taken with a Leica TCS SP2/AOBS confocal laser scanning microscope equipped with a HCX PL 63x/1.4 oil objective using a 488 nm Ar laser line and a 561 nm DPSS laser line. Before and after microirradiation confocal image series of one mid z-section were recorded at 2 s time intervals (typically 6 pre-irradiation and 150 post-irradiation frames) with a pixel size of 90 nm.

Images of fixed cells were taken with a Zeiss Axiophot 2 widefield epifluorescence microscope using a Zeiss Plan-Apochromat 63x/1.40 oil objective and a cooled CCD camera (Visitron Systems).

UVA laser microirradiation

Cells were either seeded on µ-slides (ibidi) or on 40 mm round coverslips and sensitized for microirradiation by incubation in a medium containing BrdU (10 µg/ml) for 24–48 h. For live cell microscopy and irradiation round coverslips were mounted in a POC live-cell chamber (Visitron Systems). Microirradiation was carried out with a 405 nm diode laser coupled into a Leica TCS SP2/AOBS confocal laser scanning microscope. The 405 nm laser was set to maximum power at 100% transmission and was focused through a UV transmitting Leica HCX PL APO 63x/1.40–0.60 oil objective to locally irradiate preselected spots of ~1 µm in diameter within the nucleus for 1 s. For evaluation of the recruitment kinetics, fluorescence intensities of the irradiated region were corrected for background and for total nuclear loss of fluorescence over the time course and normalized to the pre-irradiation value.

Immunoprecipitations

HEK 293T cells were transiently cotransfected with expression plasmids as described. After 48 h the transfection rate was checked by fluorescence microscopy. About 70–90% of the cells were coexpressing the GFP and RFP fusion constructs. For immunoprecipitations ~2 × 10⁷ cells were harvested in ice cold 1× PBS, washed twice and subsequently homogenized in 200 µl lysis buffer (20 mM Tris-HCl, pH 7.5, 150 mM NaCl, 0.5 mM EDTA, 2 mM PMSF and

0.5% NP40). After a centrifugation step (10 min, 20 000× g, 4°C) the supernatant was adjusted with dilution buffer (20 mM Tris-HCl, pH 7.5, 150 mM NaCl, 0.5 mM EDTA, 2 mM PMSF) to 500 µl. Totally 50 µl were added to SDS-containing sample buffer (referred to as input). For immunoprecipitation 1 µg of a purified α -GFP antibody was added and incubated for 2 h rotating at 4°C. For pull down of immunocomplexes 25 µl of equilibrated protein A agarose beads (Amersham Pharmacia, NJ, USA) were added and incubated for 1 h. After centrifugation (2 min, 5000× g, 4°C) the supernatant was removed and 50 µl were collected (referred to as non-bound). The beads were washed two times with 1 ml dilution buffer containing 300 mM NaCl. After the last washing step 100 µl of the supernatant was collected (referred to as wash) and the beads were resuspended in 2× SDS-containing sample buffer and boiled for 10 min at 95°C.

Western blot analysis.

For immunoblot analysis 1% of the input, the non-bound and the wash fractions as well as 20% of the soluble supernatants were separated on 12 or 10% SDS-PAGE and then electrophoretically transferred to a nitrocellulose membrane (Bio-Rad Laboratories, CA, USA). The membrane was blocked with 3% milk in PBS and incubated overnight at 4°C with either a mouse monoclonal α -GFP antibody or an α -mRFP rabbit polyclonal antibody. After washing with PBS containing 0.1% Tween-20, the blots were incubated with the appropriate secondary antibody conjugated with horseradish peroxidase. Immunoreactive bands were visualized with ECL plus Western Blot Detection Kit (Amersham Biosciences, NJ, USA).

RESULTS

DNA Ligase I and III accumulate at DNA repair sites

Ligation of DNA is the ultimate step in DNA repair to restore genome integrity. To investigate the involvement of DNA Ligase I and III in DNA repair we performed immunostainings of microirradiated HeLa cells. We employed a confocal laser scanning microscope to locally generate DNA damage at preselected subnuclear sites in BrdU-sensitized cells. In contrast to previous studies we used a long wavelength ultraviolet 405 nm diode laser for microirradiation. Using specific antibodies for different types of DNA damage we could detect phosphorylated histone variant H2AX (γ -H2AX), a marker for DSBs, at microirradiated sites. In addition, we detected poly(ADP-Ribose) which is generated by PARP at SSBs (Figure 1A). These results show that microirradiation with a 405 nm laser generates a mixture of different types of DNA damage that are substrates for different DNA repair pathways involving either DNA Ligase I or III. Immunofluorescence stainings with specific antibodies revealed that endogenous DNA Ligase I and III as well as their binding partners PCNA and XRCC1 are present at DNA damage sites as early as 5 min after irradiation (Figure 1B and C). These results demonstrate that this microirradiation technique allows the direct comparison of factors from different repair pathways within the same cell.

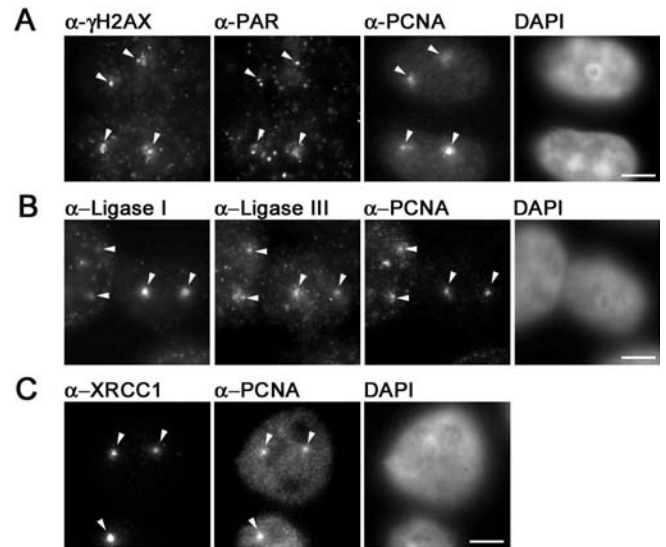


Figure 1. Immunofluorescence detection of DNA repair intermediates after laser microirradiation. Widefield fluorescence images of HeLa cells are shown. Cells were fixed ~5 min after laser microirradiation. Arrows mark sites of irradiation. (A) Laser microirradiation with 405 nm results in local generation of DSBs and SSBs detected by antibodies against γ -H2AX and PAR, respectively. Accumulation of endogenous PCNA can be observed at these sites. (B) Both, DNA Ligase I and III accumulate at sites of DNA damage and colocalize with PCNA. (C) XRCC1 and PCNA accumulate at laser-induced DNA damage sites. Scale bars, 5 µm.

Recruitment kinetics of DNA Ligases at repair sites

The fact that DNA Ligase I and III although being involved in different repair pathways are both present at microirradiated sites raised the question whether they are recruited by similar mechanisms. First hints for kinetic differences in the recruitment of repair factors involved in SSB repair and BER came from single measurements with GFP-fusion proteins (28). To directly compare the recruitment kinetics of DNA Ligase I and III we microirradiated BrdU-sensitized cells and quantified the accumulation of different GFP- and RFP-tagged proteins at DNA damage site (Figure 2). The intensity values were corrected for background and for total nuclear loss of fluorescence over the time course and normalized to the pre-irradiation value. Mean values of at least eight different cells are shown. A direct comparison of GFP- and RFP-tagged Ligases showed a significantly slower recruitment of DNA Ligase I in contrast to the very fast accumulation of DNA Ligase III at microirradiated sites (Figure 3A and B and Supplementary Fig3video1). Recruitment kinetics of DNA Ligase I and III were independent of the fluorescence tag as swapping of GFP and RFP gave similar results (Supplementary Figure 1). To gain further insights into the mechanisms underlying the different recruitment kinetics of DNA Ligases to repair sites we extended our analysis to their reported interaction partners. Since DNA Ligase I is targeted to replication sites by PCNA in S phase we compared the accumulation of DNA Ligase I with that of PCNA and found similar recruitment kinetics (Figure 3C and D and Supplementary Fig3video2). Both proteins showed a slow but constant accumulation at DNA repair sites and fluorescence intensities reached a maximum after ~5 min. This suggests

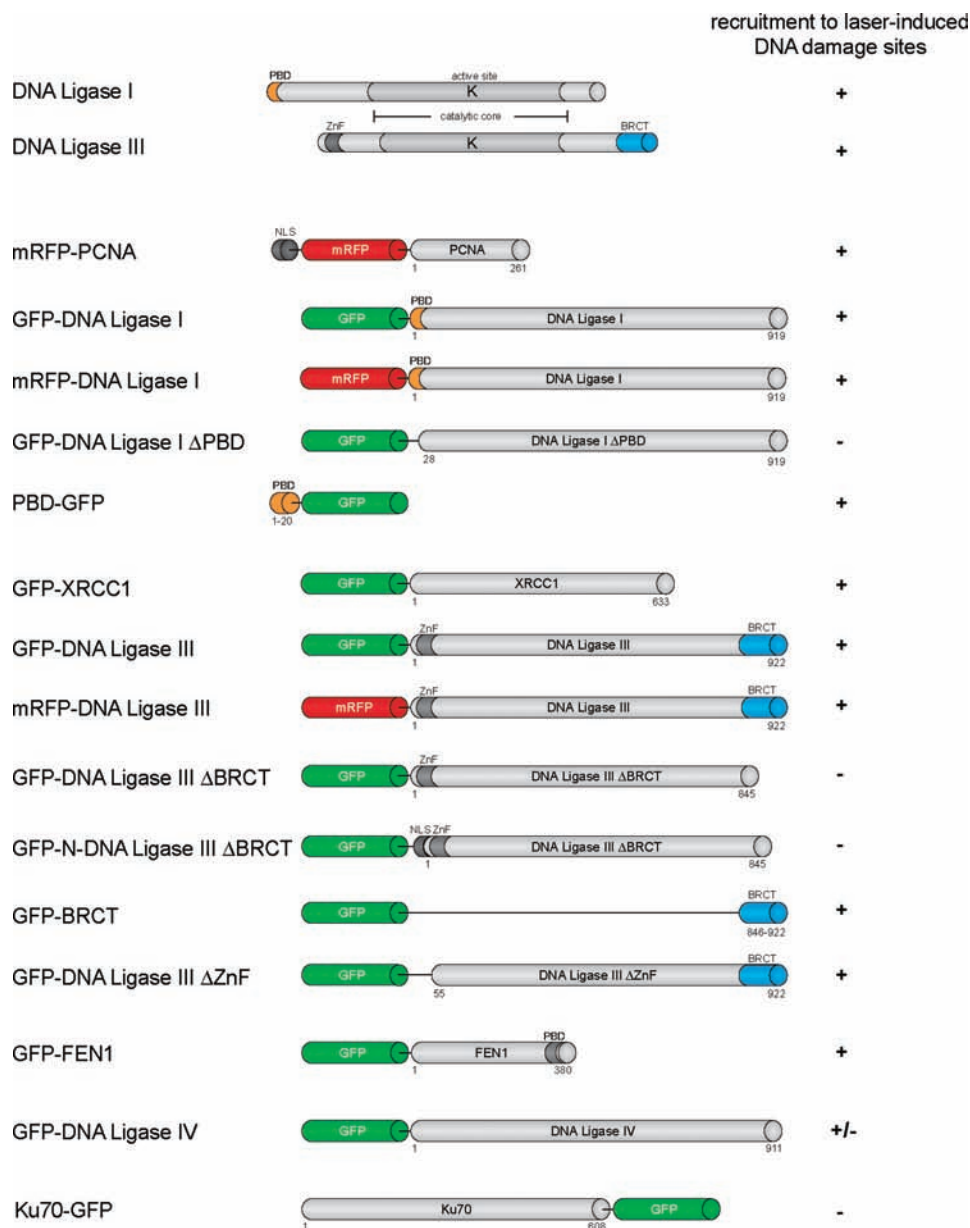


Figure 2. Schematic outline of the structure of DNA Ligase I and III and of fusion proteins used in this study. The catalytic core (highlighted in grey shading) is highly similar in both Ligases. The relative position of the conserved lysine residue (K) in the catalytic center is indicated.

that PCNA might be responsible for recruitment of DNA Ligase I to sites of DNA repair.

Since biochemical studies had suggested an interaction of DNA Ligase III with XRCC1 during short-patch BER (10,13–15) we directly compared their recruitment to micro-irradiated sites. Remarkably, we found that DNA Ligase III and XRCC1 redistributed to sites of DNA damage with similar kinetics. After a very fast initial accumulation, intensities of both proteins reached a maximum within 100–120 s after irradiation and then began to decline. These observations support the idea that DNA Ligase III is targeted to DNA repair sites through interaction with XRCC1.

To test whether DNA Ligase I and III not only differ in their recruitment but also in their release kinetics we

performed long-term observations of irradiated HeLa cells with 5 min time intervals to compare their release from repair sites. After reaching a maximum the mean fluorescence intensities of PCNA, XRCC1, DNA Ligase I and III decreased gradually at the irradiated sites (Figure 4 and data not shown). Both, DNA Ligase I and III reached basal levels ~120 min after irradiation (Figure 4). We found similar release kinetics for their respective binding partners PCNA and XRCC1 (data not shown). This indicates that although DNA Ligase I and III differ in their recruitment to repair sites they show similar release kinetics.

Next we tested whether the recruitment of GFP-Ligase I and GFP-Ligase III is cell cycle dependent. The characteristic focal distribution of RFP-PCNA and GFP-Ligase I allowed

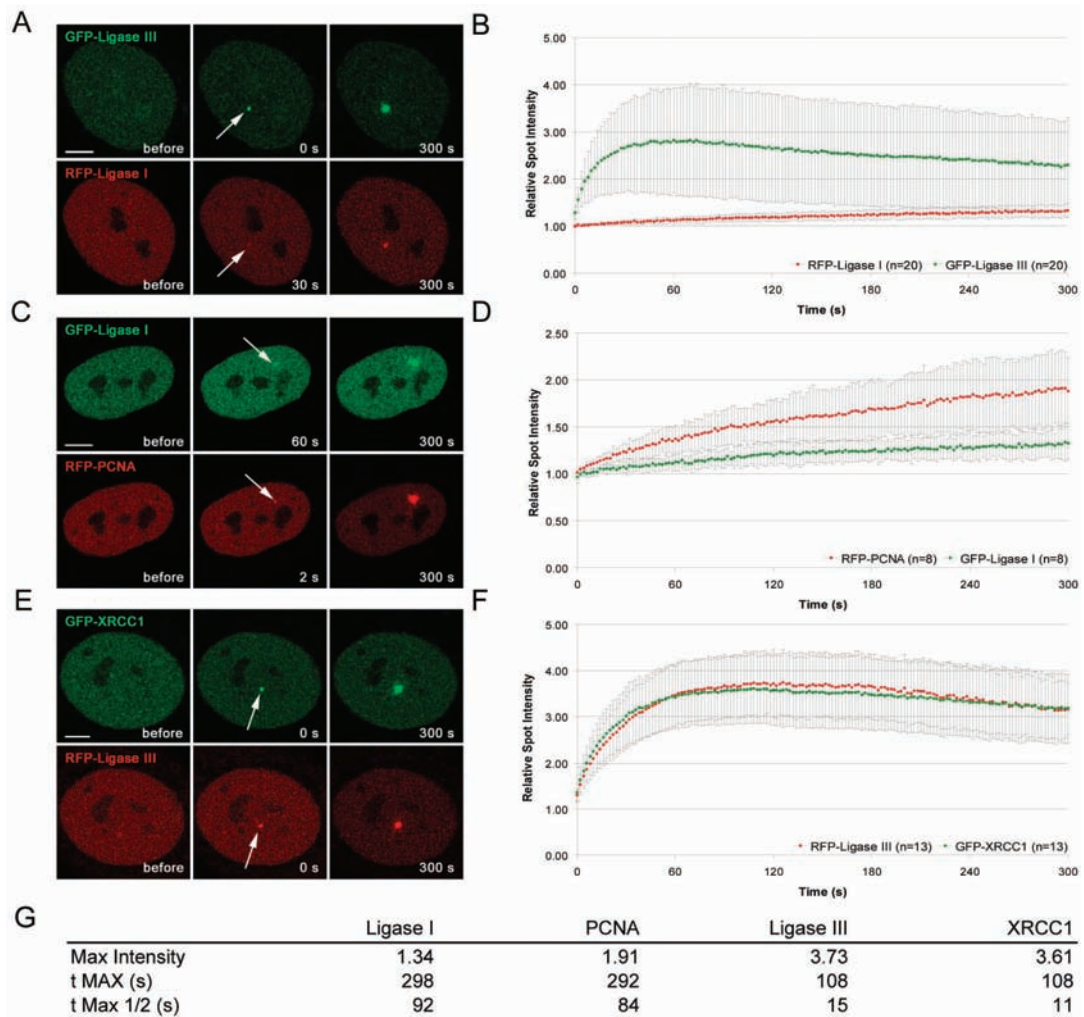


Figure 3. Recruitment kinetics of DNA Ligase I and III at DNA damage sites in living cells. Live cell imaging of microirradiated HeLa cells coexpressing various combinations of GFP- and RFP-tagged DNA Ligase I, DNA Ligase III, PCNA and XRCC1. For determination of the recruitment kinetics the relative fluorescence intensity at the irradiated spot was calculated and plotted as a function of time. The displayed curves were generated after integrating data from at least eight independent experiments. Error bars represent the SD. (A and B) Accumulation of DNA Ligase III at DNA repair sites precedes accumulation of DNA Ligase I (Supplementary Fig3video1). (C and D) Accumulation of RFP-PCNA can be observed as early as 2 s after irradiation, while DNA Ligase I accumulates with a delay of ~30–60 s (Supplementary Fig3video2). (E and F) Immediate and fast recruitment of GFP-XRCC1 and DNA Ligase III to DNA damage sites (Supplementary Fig3video3). Scale bars, 5 μ m. The table in (G) summarizes the kinetic parameters of PCNA, DNA Ligase I, XRCC1 and DNA Ligase III recruitment. Mean values of at least eight different cells are shown.

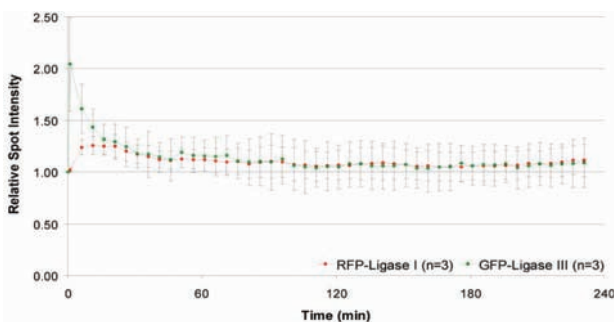


Figure 4. Release kinetics of DNA Ligase I and III at DNA repair sites. Microirradiated HeLa cells were followed up several hours with a time interval of 5 min. Maximum projections of 10–12 z-Stacks were collected and the fluorescence intensities at the irradiated sites calculated and plotted as a function of time.

identification of S phase in living cells (29,30). Accumulations of GFP-Ligase I and RFP-PCNA at DNA damage sites could be observed in all S phase stages (Supplementary Figure 2). We could also detect recruitment of RFP-PCNA and GFP-DNA Ligase I to sites of DNA damage in mouse C2C12 cells in S and non-S phase (Supplementary Figure 3). These results indicate that DNA Ligase I and PCNA are recruited with similar kinetics in both human and mouse cells. We also observed accumulation of DNA Ligase III in S phase cells (Supplementary Figure 4).

As laser microirradiation generates DSBs (Figure 1), we tested whether DNA Ligase IV, which is involved in NHEJ, gets recruited to laser-induced DNA damage sites.

We found only a very faint accumulation at repair sites that was barely detectable and in some cases not distinguishable from the nuclear background of unbound GFP-DNA

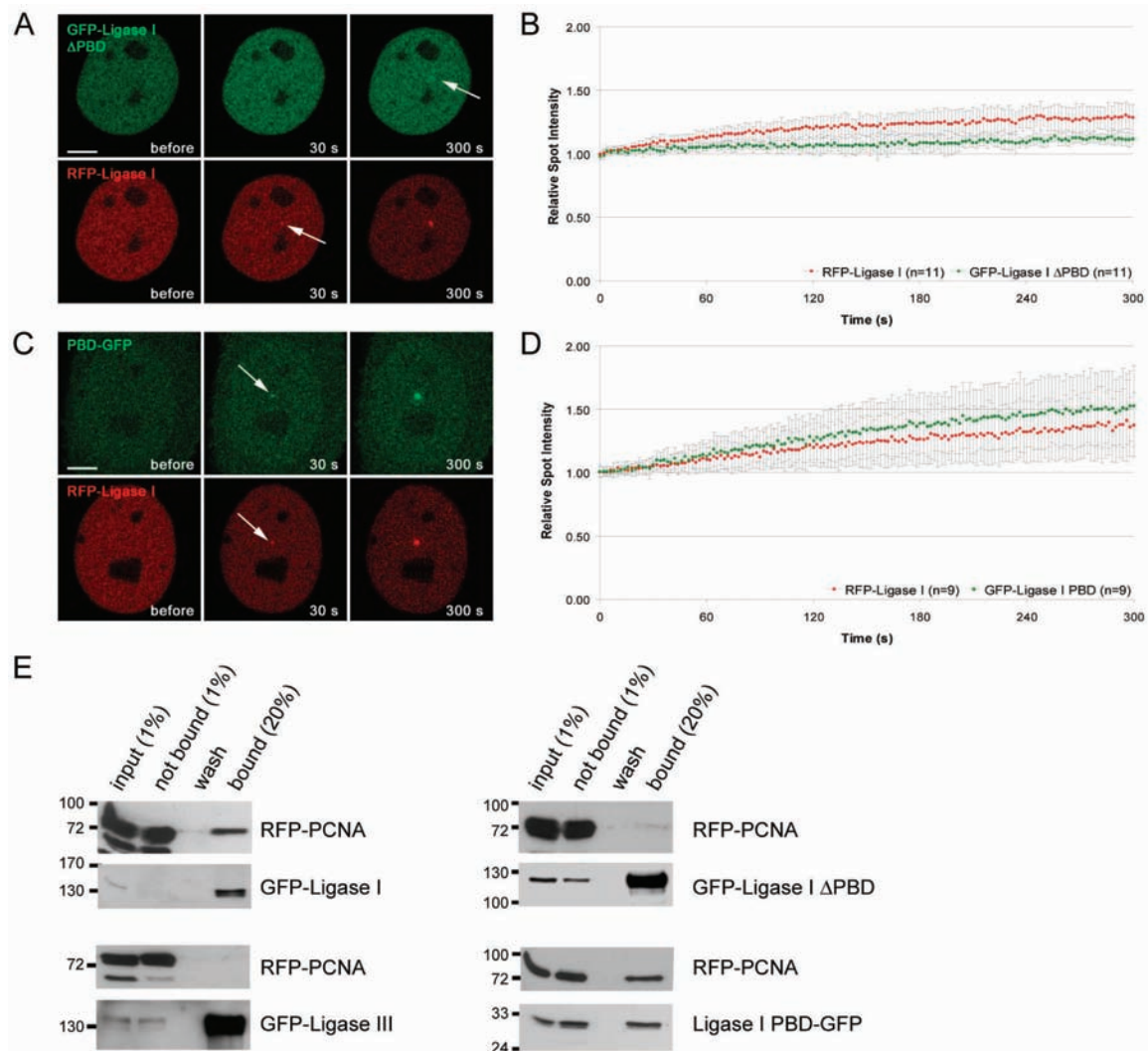


Figure 5. Recruitment of DNA Ligase I to DNA damage sites is mediated by PCNA. Recruitment kinetics were determined as described in Figure 3. (A) Live cell imaging of a microirradiated HeLa cell coexpressing GFP-DNA Ligase I Δ PBD and RFP-Ligase I. Deletion of the PBD in GFP-DNA Ligase I Δ PBD almost completely abolishes recruitment to sites of DNA damage, whereas RFP-Ligase I accumulates at these sites as seen in Figure 3 (arrow). (C) A HeLa cell coexpressing DNA Ligase I PBD-GFP and RFP-Ligase I shows accumulation of both, RFP-Ligase I and DNA Ligase I PBD-GFP, at sites of microirradiation (arrows). Times after microirradiation are indicated. Scale bars, 5 μ m. (B and D) Recruitment kinetics of fluorescence-tagged proteins at microirradiated sites. (E) Coimmunoprecipitations were performed in 293T cells coexpressing different combinations of RFP and GFP fusion constructs. For interaction mapping the same deletion constructs as in A–D were used. Immunoprecipitations were performed with an antibody against GFP. Precipitated fusion proteins were then detected with specific antibodies against RFP and GFP on western blots. RFP-PCNA coprecipitated with GFP-Ligase I but not with GFP-Ligase III (left panel). RFP-PCNA was also coprecipitated with Ligase I PBD-GFP but not with GFP-Ligase I Δ PBD (right panel).

Ligase IV (Supplementary Figure 5A). This is consistent with earlier reports failing to detect recruitment of factors involved in DSB repair like Ku70, DNA-PK and Smc (31). In agreement with this report, we found that Ku70-GFP was not recruited to DNA damage sites after 405 nm irradiation (Supplementary Figure 5B). These results suggest that the number of DSBs generated by microirradiation and the stoichiometry of the repair complex yield only faint signals that are barely above background and hard to analyse with this experimental system.

Taken together, these results show that DNA Ligase I and III are recruited to microirradiated sites with distinct kinetics which match similar differences of their respective binding partners. The recruitment of both DNA Ligases

occurred independently of the cell cycle stage in S and in non-S phase cells.

Recruitment of DNA Ligase I to sites of DNA damage depends on its interaction with PCNA

During S phase, DNA Ligase I is targeted to sites of DNA replication via its PCNA-binding domain (PBD) (5,6). To test whether PCNA also mediates recruitment of DNA Ligase I during DNA repair, we deleted the PBD of DNA Ligase I (GFP-Ligase I Δ PBD) and expressed the deletion construct in HeLa cells together with full-length RFP-Ligase I. After laser microirradiation GFP-Ligase I Δ PBD showed only minor accumulation at irradiated sites compared to the wild

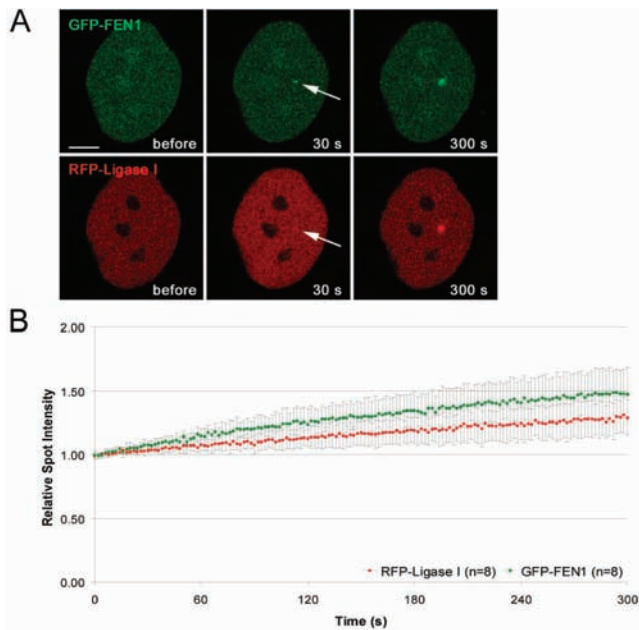


Figure 6. Recruitment kinetics of the PCNA interacting proteins DNA Ligase I and FEN-1 are similar. The structure of the fusion proteins is depicted in Figure 2. (A) Live cell imaging of a microirradiated HeLa cell coexpressing GFP-FEN-1 and RFP-Ligase I. Both FEN-1 and DNA Ligase I accumulate at DNA repair sites (arrow) with similar kinetics. Times after microirradiation are indicated. Scale bars, 5 μ m. (B) Recruitment kinetics of fluorescence-tagged proteins at microirradiated sites.

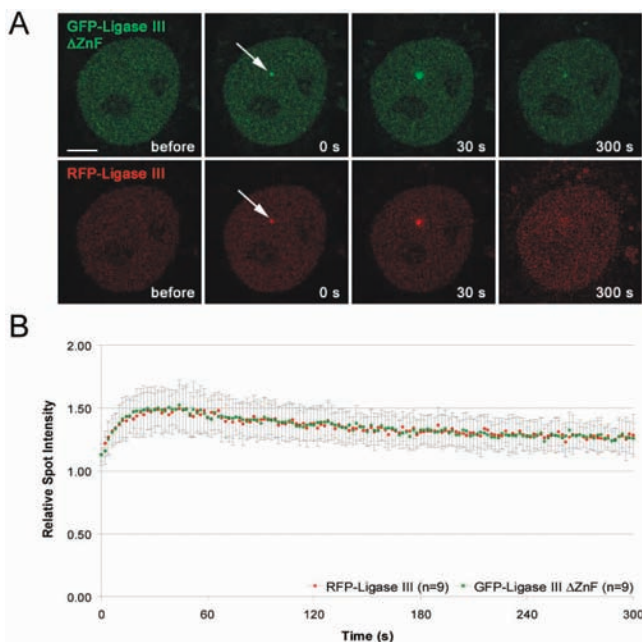


Figure 7. Deletion of the ZnF motif does not abolish recruitment of DNA Ligase III. Recruitment kinetics were determined as described in Figure 3. (A) Live cell imaging of a microirradiated HeLa cell coexpressing GFP-DNA Ligase III Δ ZnF and RFP-Ligase III which accumulate at DNA repair sites (arrow). Times after microirradiation are indicated. Scale bars, 5 μ m. (B) Recruitment kinetics of GFP-DNA Ligase III Δ ZnF and RFP-Ligase III at microirradiated sites.

type fusion construct (Figure 5A and B). This suggests that the PBD plays a critical role in the recruitment of DNA Ligase I to repair sites. The observed residual accumulation of the deletion construct is likely owing to recruitment via trimerization (32) with the endogenous or the full length DNA Ligase I construct. To directly study the function of the PBD we fused the PBD alone with GFP (PBD-GFP). Besides association with replication sites, the PBD fusion protein was recruited to sites of DNA damage with kinetics similar to the full-length DNA Ligase I construct (Figure 5C and D and Supplementary Figure 6).

These kinetic measurements of deletion constructs indicated that recruitment to repair sites is mediated by an interaction of the PBD of DNA Ligase I with PCNA. To test this interaction we performed coimmunoprecipitation assays with the same constructs as used for live cell microscopy. We found that deletion of the PBD abolished the interaction of DNA Ligase I with PCNA, while the PBD alone was sufficient to coprecipitate PCNA (Figure 5E). These lines of evidence strongly suggest that the PBD-mediated interaction of DNA Ligase I with PCNA is necessary and sufficient for targeting of DNA Ligase I to repair sites.

To test whether this mechanism applies also to other PCNA binding proteins we compared the recruitment kinetics of DNA Ligase I with FEN-1, another PBD-containing protein involved in DNA replication and repair. After microirradiation FEN-1 accumulated at DNA repair sites with similar recruitment kinetics as DNA Ligase I (Figure 6). These results point to a common mechanism for the recruitment of PBD containing enzymes like DNA Ligase I and FEN-1 in DNA replication and repair.

Recruitment of DNA Ligase III to sites of DNA damage depends on its interaction with XRCC1

The unique Zn-Finger motif at the N-terminus of DNA Ligase III binds to unusual DNA secondary structures and it was suggested that this domain could recruit DNA Ligase III to damaged DNA (17,33,34). We generated a deletion construct of DNA Ligase III lacking the N-terminal ZnF motif (GFP-Ligase III Δ ZnF) and expressed this construct together with the full length RFP-Ligase III in HeLa cells. After microirradiation, no difference could be observed and both fusion proteins showed similar recruitment kinetics (Figure 7). We then tested whether the BRCT domain of DNA Ligase III, which was described to be essential for the interaction with XRCC1 (10,13–15) is required for recruitment to repair sites *in vivo*. We generated a deletion construct lacking the C-terminal BRCT domain of DNA Ligase III (GFP-Ligase III Δ BRCT). This fusion protein did not enter the nucleus but remained in the cytoplasm indicating that the BRCT domain is responsible for nuclear localization of DNA Ligase III (Figure 8E). After addition of an SV40-NLS (GFP-N-Ligase III Δ BRCT) the fusion protein entered the nucleus but showed, in comparison with the full-length construct, only a minor accumulation at DNA repair sites (Figure 8A and C). Having shown that deletion of the BRCT domain abolishes recruitment of DNA Ligase III, we next fused the BRCT domain alone to GFP (GFP-BRCT). The BRCT fusion protein redistributed to

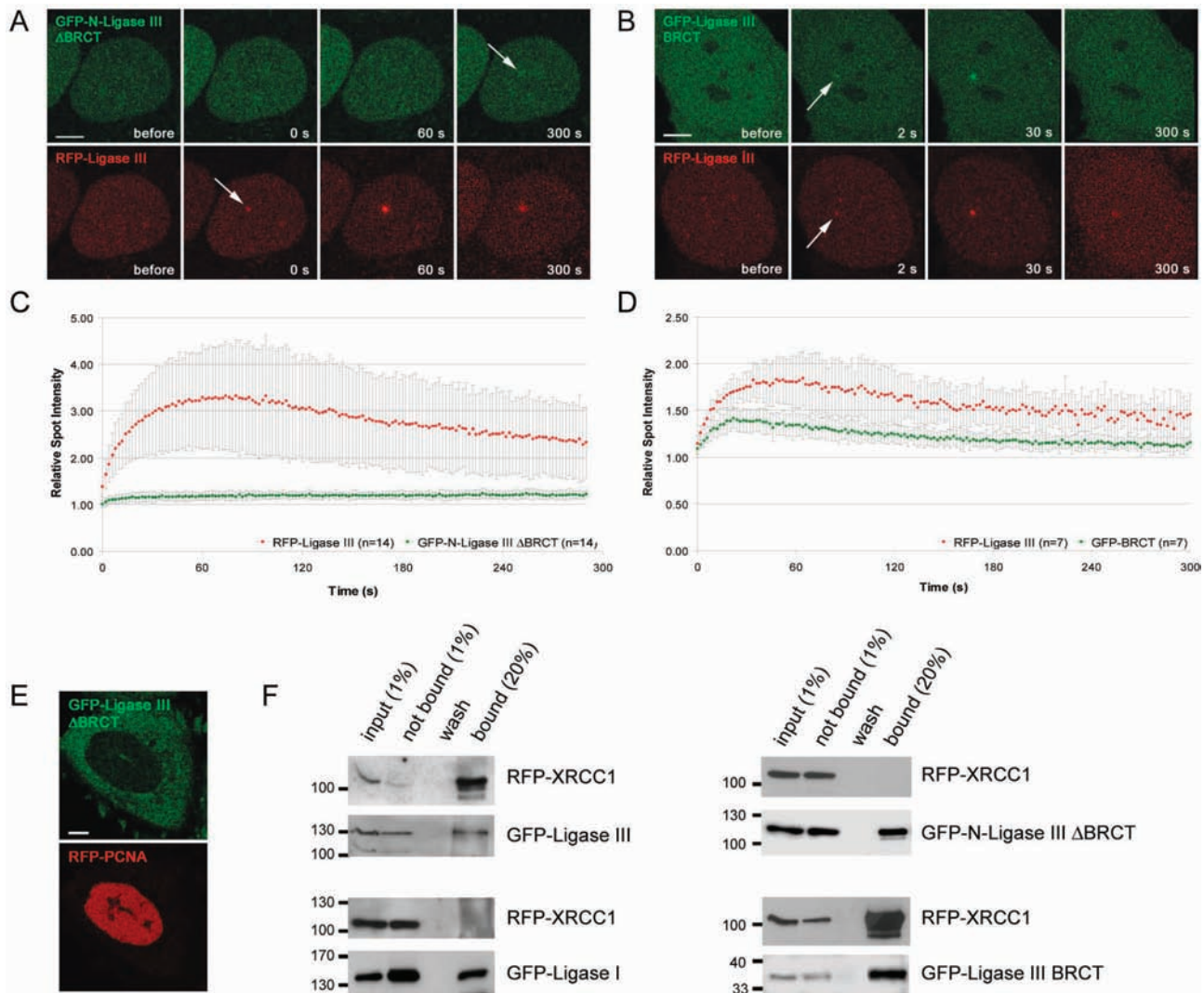


Figure 8. Recruitment of DNA Ligase III to DNA damage sites is mediated by XRCC1. Recruitment kinetics were determined as described in Figure 3. (A) Live cell imaging of a microirradiated HeLa cell coexpressing GFP-N-DNA Ligase III Δ BRCT, containing an additional SV40 NLS and RFP-Ligase III. Deletion of the BRCT domain in GFP-N-DNA Ligase III Δ BRCT abolishes recruitment to sites of DNA damage, whereas RFP-Ligase III accumulates at these sites as seen in Figure 3 (arrow). (B) A HeLa cell coexpressing GFP-Ligase III BRCT and RFP-Ligase III which both accumulate at sites of microirradiation (arrows). Times after microirradiation are indicated. Scale bars, 5 μ m. (C and D) Recruitment kinetics of fluorescence-tagged proteins at microirradiated sites. (E) Deletion of the BRCT domain results in cytoplasmic localization of the fusion protein. (F) Coimmunoprecipitations were performed with 293T cells coexpressing RFP-XRCC1 and GFP-Ligase I or GFP-Ligase III, respectively. For interaction mapping the same deletion constructs as in A–D were used. Immunoprecipitations were performed with an antibody against GFP. Precipitated fusion proteins were then detected with specific antibodies against RFP and GFP on western blots. RFP-XRCC1 was coprecipitated with GFP-Ligase III but not with GFP-Ligase I (left panel). RFP-XRCC1 was also coprecipitated with GFP-Ligase III Δ BRCT but not with GFP-N-Ligase III Δ BRCT (right panel).

DNA repair sites and showed a similar although weaker accumulation at these sites as the full-length DNA Ligase III (Figure 8C and D). The slightly reduced accumulation of the isolated BRCT domain could be explained by additional protein sequences of DNA Ligase III enhancing recruitment or proper protein folding.

To investigate the role of the BRCT domain in the interaction of DNA Ligase III with XRCC1 we performed coimmunoprecipitation assays. We found that deletion of the BRCT domain abolished binding of DNA Ligase III to XRCC1, while the BRCT domain alone was sufficient for interaction (Figure 8F). These data fit well with the results

obtained from kinetic measurements which altogether indicate that the BRCT domain is necessary and sufficient for recruitment of DNA Ligase III to repair sites while the ZnF domain does not seem to be involved.

DISCUSSION

Different DNA repair pathways have evolved to deal with various types of DNA damage caused by normal cellular metabolism or exogenous factors. The common essential step in all these different repair pathways is the joining of

DNA ends by members of the DNA Ligase family. Although the catalytic core of DNA Ligase I and III is highly conserved they have no or only poorly overlapping functions and are not interchangeable (7–10,18,35). Extracts from the cell line EM9 which is deficient in DNA Ligase III (10) are defective in short-patch BER (12) while extracts from the DNA Ligase I deficient cell line 46BR.1G1 (36) are defective in long-patch BER (8). Furthermore, generation of partially DNA Ligase I defective mouse embryonic stem cells revealed that DNA Ligase III could not compensate for loss of DNA Ligase I function in cell proliferation (35).

To explore possible differences that could explain the non-redundant functions of these highly homologous enzymes we compared the recruitment kinetics of DNA Ligase I and III at local DNA lesions generated by laser microirradiation. We found that DNA Ligases I and III accumulated at DNA damage sites with distinct kinetics suggesting that they catalyze the same reaction but use different mechanisms for recruitment. With deletion and binding studies we could demonstrate that the PCNA binding domain (PBD) of DNA Ligase I mediates targeting DNA repair sites. Interestingly, the PBD is not required for enzyme activity *in vitro* but rescue experiments with DNA Ligase I deficient cells demonstrated that the PBD is essential *in vivo* (8,9,35). These results suggest that PCNA mediated recruitment of DNA Ligase I could enhance the efficiency of the ligation reaction *in vivo* by locally concentrating DNA Ligase I at sites of replication and repair.

In further studies, we also observed recruitment of FEN-1 to DNA repair sites, which like DNA Ligase I interacts with PCNA during DNA replication (37,38) and is implicated in long-patch BER (39,40). Remarkably, FEN-1 showed the same recruitment kinetics as DNA Ligase I although it has a completely different function in replication and repair. Likewise, the PBD of DNA methyltransferase 1 (Dnmt1) is also necessary and sufficient for accumulation of Dnmt1 at repair sites (24). Taken together our results show that various PBD-containing proteins involved in the restoration of genetic and epigenetic information are recruited to replication as well as repair sites by PCNA.

On one hand, it has been proposed that the ZnF motif of DNA Ligase III could act as a nick sensor, recruiting DNA Ligase III to DNA nicks and altered DNA structures (17,33,34). We found, however, that deletion of the ZnF did not influence the recruitment kinetics of DNA Ligase III. On the other hand, biochemical studies have suggested that the BRCT domain of DNA Ligase III is essential for its interaction with XRCC1 (10,13–15). Here, we demonstrate that the deletion of the BRCT domain of DNA Ligase III abolishes recruitment of DNA Ligase III to repair sites *in vivo*. Moreover, the BRCT domain alone was sufficient to mediate recruitment of the fusion protein to DNA repair sites and is essential for nuclear localization of DNA Ligase III.

These different mechanisms for the localization of DNA Ligases at repair sites are consistent with specific characteristics of the respective repair pathways. The continuous synthesis of long stretches of DNA during long patch BER resembles the process of DNA replication. Consequently, also similar recruitment mechanisms seem to be used. In both processes DNA Ligase I is recruited through interaction

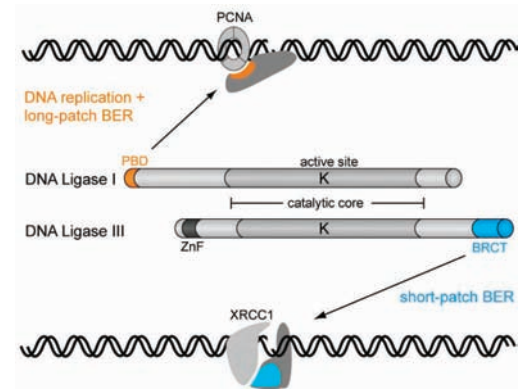


Figure 9. Model for selective targeting of DNA Ligase I and III to DNA replication and different repair pathways. All DNA Ligases use the same catalytic mechanism and show high sequence similarity in the catalytic core (grey shading). The active site lysine residue (K) in the center of the catalytic domain is directly involved in the ligation reaction. However, DNA Ligases have non-overlapping functions in DNA repair and replication and are not interchangeable. We could show that DNA Ligase I and III are targeted to different repair pathways through their regulatory PBD and BRCT domains which mediate interaction with PCNA and XRCC1, respectively. This selective recruitment of specialized DNA Ligases may accommodate the specific requirements of different repair pathways and thereby enhance repair efficiency.

with the sliding clamp and processivity factor PCNA. In contrast, replacement of just a single nucleotide during short patch BER does not require a processive repair machinery sliding along the DNA but rather a stationary repair complex recruiting DNA Ligase III.

In summary, although DNA Ligase I and III share a highly similar catalytic core, they have distinct functions in DNA replication and repair and are not interchangeable. Here we identified differences in the adjacent regulatory domains of DNA Ligases which may explain their non-redundant functions in eukaryotic cells. Thus, the PBD domain of DNA Ligase I and the BRCT domain of DNA Ligase III mediate interaction with PCNA and XRCC1, respectively, and target them to different repair pathways (Figure 9). This selective recruitment may contribute to the spatio-temporal coordination of different repair factors and could thus enhance accuracy and efficiency of DNA repair in eukaryotic cells.

SUPPLEMENTARY DATA

Supplementary Data are available at NAR Online.

ACKNOWLEDGEMENTS

The authors are indebted to Dr R. Tsien for providing the mRFP1 expression vector, Dr G. de Murcia for providing the GFP-XRCC1 expression vector, Dr W. Rodgers for providing the Ku70-GFP expression vector and Dr T. Lindahl for providing cDNAs of DNA Ligases. The authors are grateful to A. Gahl, I. Grunewald and K. Zolghadr for their help and to Lothar Schermelleh and Fabio Spada for helpful comments on the manuscript. This work was supported by grants from the Deutsche Forschungsgemeinschaft and the

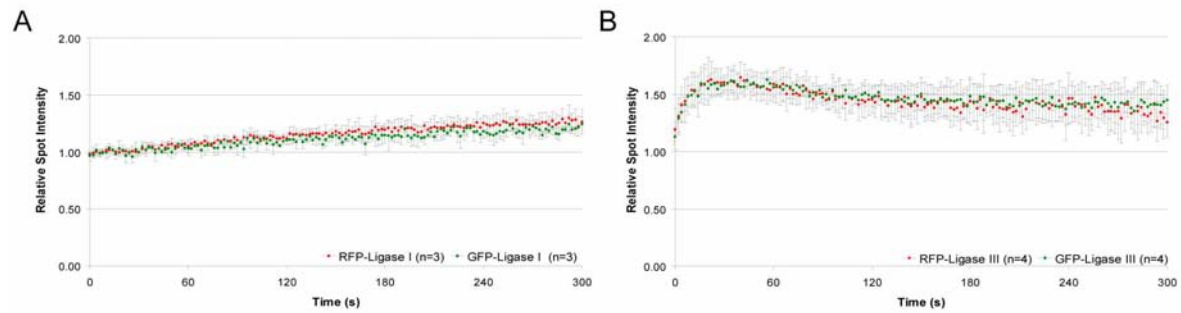
Volkswagenstiftung to H.L. and M.C.C. Funding to pay the Open Access publication charges for this article was provided by Deutsche Forschungsgemeinschaft (DFG).

Conflict of interest statement. None declared.

REFERENCES

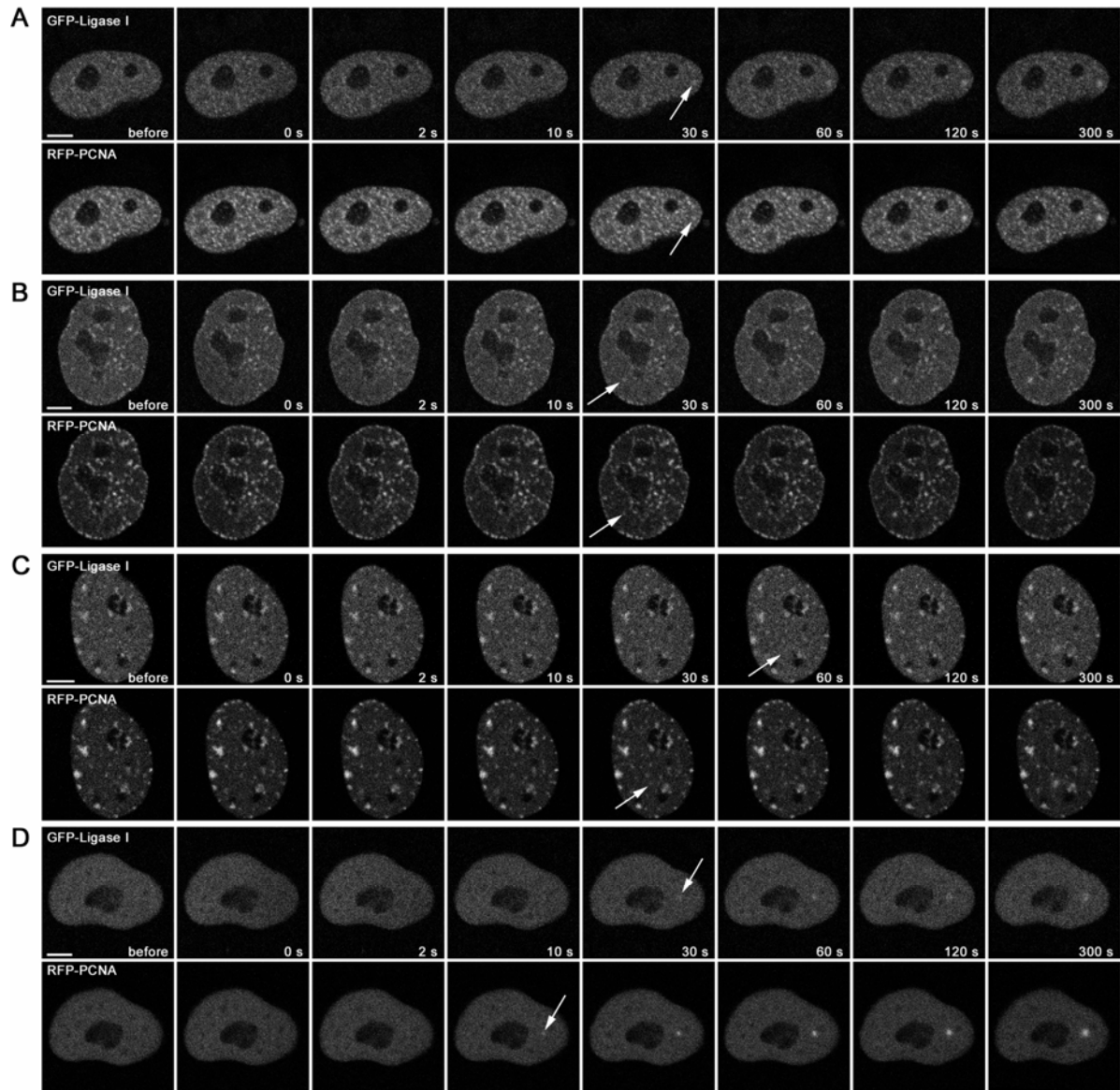
- Friedberg,E.C. (2003) DNA damage and repair. *Nature*, **421**, 436–440.
- Hoeijmakers,J.H. (2001) Genome maintenance mechanisms for preventing cancer. *Nature*, **411**, 366–374.
- Timson,D.J., Singleton,M.R. and Wigley,D.B. (2000) DNA ligases in the repair and replication of DNA. *Mutat. Res.*, **460**, 301–318.
- Martin,I.V. and MacNeill,S.A. (2002) ATP-dependent DNA ligases. *Genome Biol.*, **3**, REVIEWS3005.
- Cardoso,M.C., Joseph,C., Rahn,H.P., Reusch,R., Nadal-Ginard,B. and Leonhardt,H. (1997) Mapping and use of a sequence that targets DNA ligase I to sites of DNA replication. *J. Cell. Biol.*, **139**, 579–587.
- Montecucco,A., Savini,E., Weighardt,F., Rossi,R., Ciarrocchi,G., Villa,A. and Biamonti,G. (1995) The N-terminal domain of human DNA ligase I contains the nuclear localization signal and directs the enzyme to sites of DNA replication. *Embo J.*, **14**, 5379–5386.
- Mackenney,V.J., Barnes,D.E. and Lindahl,T. (1997) Specific function of DNA ligase I in simian virus 40 DNA replication by human cell-free extracts is mediated by the amino-terminal non-catalytic domain. *J. Biol. Chem.*, **272**, 11550–11556.
- Levin,D.S., McKenna,A.E., Motycka,T.A., Matsumoto,Y. and Tomkinson,A.E. (2000) Interaction between PCNA and DNA ligase I is critical for joining of Okazaki fragments and long-patch base-excision repair. *Curr. Biol.*, **10**, 919–922.
- Goetz,J.D., Motycka,T.A., Han,M., Jasin,M. and Tomkinson,A.E. (2005) Reduced repair of DNA double-strand breaks by homologous recombination in a DNA ligase I-deficient human cell line. *DNA Repair (Amst)*, **4**, 649–654.
- Caldecott,K.W., McKeown,C.K., Tucker,J.D., Ljungquist,S. and Thompson,L.H. (1994) An interaction between the mammalian DNA repair protein XRCC1 and DNA ligase III. *Mol. Cell. Biol.*, **14**, 68–76.
- Wei,Y.F., Robins,P., Carter,K., Caldecott,K., Pappin,D.J., Yu,G.L., Wang,R.P., Shell,B.K., Nash,R.A., Schar,P. *et al.* (1995) Molecular cloning and expression of human cDNAs encoding a novel DNA ligase IV and DNA ligase III, an enzyme active in DNA repair and recombination. *Mol. Cell Biol.*, **15**, 3206–3216.
- Cappelli,E., Taylor,R., Cevasco,M., Abbondandolo,A., Caldecott,K. and Frosina,G. (1997) Involvement of XRCC1 and DNA ligase III gene products in DNA base excision repair. *J. Biol. Chem.*, **272**, 23970–23975.
- Taylor,R.M., Wickstead,B., Cronin,S. and Caldecott,K.W. (1998) Role of a BRCT domain in the interaction of DNA ligase III- α with the DNA repair protein XRCC1. *Curr. Biol.*, **8**, 877–880.
- Beernink,P.T., Hwang,M., Ramirez,M., Murphy,M.B., Doyle,S.A. and Thelen,M.P. (2005) Specificity of protein interactions mediated by BRCT domains of the XRCC1 DNA repair protein. *J. Biol. Chem.*, **280**, 30206–30213.
- Dulic,A., Bates,P.A., Zhang,X., Martin,S.R., Freemont,P.S., Lindahl,T. and Barnes,D.E. (2001) BRCT domain interactions in the heterodimeric DNA repair protein XRCC1-DNA ligase III. *Biochemistry*, **40**, 5906–5913.
- Fan,J., Otterlei,M., Wong,H.K., Tomkinson,A.E. and Wilson,D.M.,III (2004) XRCC1 co-localizes and physically interacts with PCNA. *Nucleic Acids Res.*, **32**, 2193–2201.
- Mackey,Z.B., Niedergang,C., Murcia,J.M., Leppard,J., Au,K., Chen,J., de Murcia,G. and Tomkinson,A.E. (1999) DNA ligase III is recruited to DNA strand breaks by a zinc finger motif homologous to that of poly(ADP-ribose) polymerase. Identification of two functionally distinct DNA binding regions within DNA ligase III. *J. Biol. Chem.*, **274**, 21679–21687.
- Wang,H., Rosidi,B., Perrault,R., Wang,M., Zhang,L., Windhofer,F. and Iliakis,G. (2005) DNA ligase III as a candidate component of backup pathways of nonhomologous end joining. *Cancer Res.*, **65**, 4020–4030.
- Critchlow,S.E., Bowater,R.P. and Jackson,S.P. (1997) Mammalian DNA double-strand break repair protein XRCC4 interacts with DNA ligase IV. *Curr. Biol.*, **7**, 588–598.
- Grawunder,U., Wilm,M., Wu,X., Kulesza,P., Wilson,T.E., Mann,M. and Lieber,M.R. (1997) Activity of DNA ligase IV stimulated by complex formation with XRCC4 protein in mammalian cells. *Nature*, **388**, 492–495.
- Frank,K.M., Sekiguchi,J.M., Seidl,K.J., Swat,W., Rathbun,G.A., Cheng,H.L., Davidson,L., Kangaloo,L. and Alt,F.W. (1998) Late embryonic lethality and impaired V(D)J recombination in mice lacking DNA ligase IV. *Nature*, **396**, 173–177.
- Barnes,D.E., Stamp,G., Rosewell,I., Denzel,A. and Lindahl,T. (1998) Targeted disruption of the gene encoding DNA ligase IV leads to lethality in embryonic mice. *Curr. Biol.*, **8**, 1395–1398.
- Sporbert,A., Domaing,P., Leonhardt,H. and Cardoso,M.C. (2005) PCNA acts as a stationary loading platform for transiently interacting Okazaki fragment maturation proteins. *Nucleic Acids Res.*, **33**, 3521–3528.
- Mortusewicz,O., Schermelleh,L., Walter,J., Cardoso,M.C. and Leonhardt,H. (2005) Recruitment of DNA methyltransferase I to DNA repair sites. *Proc. Natl Acad. Sci. USA*, **102**, 8905–8909.
- Levy,N., Martz,A., Bresson,A., Spelshauer,C., de Murcia,G. and Menissier-de Murcia,J. (2006) XRCC1 is phosphorylated by DNA-dependent protein kinase in response to DNA damage. *Nucleic Acids Res.*, **34**, 32–41.
- Campbell,R.E., Tour,O., Palmer,A.E., Steinbach,P.A., Baird,G.S., Zacharias,D.A. and Tsien,R.Y. (2002) A monomeric red fluorescent protein. *Proc. Natl Acad. Sci. USA*, **99**, 7877–7882.
- Rodgers,W., Jordan,S.J. and Capra,J.D. (2002) Transient association of Ku with nuclear substrates characterized using fluorescence photobleaching. *J. Immunol.*, **168**, 2348–2355.
- Lan,L., Nakajima,S., Oohata,Y., Takao,M., Okano,S., Masutani,M., Wilson,S.H. and Yasui,A. (2004) *In situ* analysis of repair processes for oxidative DNA damage in mammalian cells. *Proc. Natl Acad. Sci. USA*, **101**, 13738–13743.
- Leonhardt,H., Rahn,H.P., Weinzierl,P., Sporbert,A., Cremer,T., Zink,D. and Cardoso,M.C. (2000) Dynamics of DNA replication factories in living cells. *J. Cell. Biol.*, **149**, 271–280.
- Sporbert,A., Gahl,A., Ankerhold,R., Leonhardt,H. and Cardoso,M.C. (2002) DNA polymerase clamp shows little turnover at established replication sites but sequential *de novo* assembly at adjacent origin clusters. *Mol. Cell*, **10**, 1355–1365.
- Bekker-Jensen,S., Lukas,C., Kitagawa,R., Melander,F., Kastan,M.B., Bartek,J. and Lukas,J. (2006) Spatial organization of the mammalian genome surveillance machinery in response to DNA strand breaks. *J. Cell. Biol.*, **173**, 195–206.
- Dimitriadis,E.K., Prasad,R., Vaske,M.K., Chen,L., Tomkinson,A.E., Lewis,M.S. and Wilson,S.H. (1998) Thermodynamics of human DNA ligase I trimerization and association with DNA polymerase beta. *J. Biol. Chem.*, **273**, 20540–20550.
- Kulczyk,A.W., Yang,J.C. and Neuhaus,D. (2004) Solution structure and DNA binding of the zinc-finger domain from DNA ligase III α . *J. Mol. Biol.*, **341**, 723–738.
- Taylor,R.M., Whitehouse,J., Cappelli,E., Frosina,G. and Caldecott,K.W. (1998) Role of the DNA ligase III zinc finger in polynucleotide binding and ligation. *Nucleic Acids Res.*, **26**, 4804–4810.
- Petrini,J.H., Xiao,Y. and Weaver,D.T. (1995) DNA ligase I mediates essential functions in mammalian cells. *Mol. Cell Biol.*, **15**, 4303–4308.
- Prigent,C., Satoh,M.S., Daly,G., Barnes,D.E. and Lindahl,T. (1994) Aberrant DNA repair and DNA replication due to an inherited enzymatic defect in human DNA ligase I. *Mol. Cell Biol.*, **14**, 310–317.
- Tom,S., Henriksen,L.A. and Bambara,R.A. (2000) Mechanism whereby proliferating cell nuclear antigen stimulates flap endonuclease I. *J. Biol. Chem.*, **275**, 10498–10505.
- Frank,G., Qiu,J., Zheng,L. and Shen,B. (2001) Stimulation of eukaryotic flap endonuclease-I activities by proliferating cell nuclear antigen (PCNA) is independent of its *in vitro* interaction via a consensus PCNA binding region. *J. Biol. Chem.*, **276**, 36295–36302.
- Matsumoto,Y., Kim,K., Hurwitz,J., Gary,R., Levin,D.S., Tomkinson,A.E. and Park,M.S. (1999) Reconstitution of proliferating cell nuclear antigen-dependent repair of apurinic/aprimidinic sites with purified human proteins. *J. Biol. Chem.*, **274**, 33703–33708.
- Gary,R., Kim,K., Cornelius,H.L., Park,M.S. and Matsumoto,Y. (1999) Proliferating cell nuclear antigen facilitates excision in long-patch base excision repair. *J. Biol. Chem.*, **274**, 4354–4363.

Supplementary Information



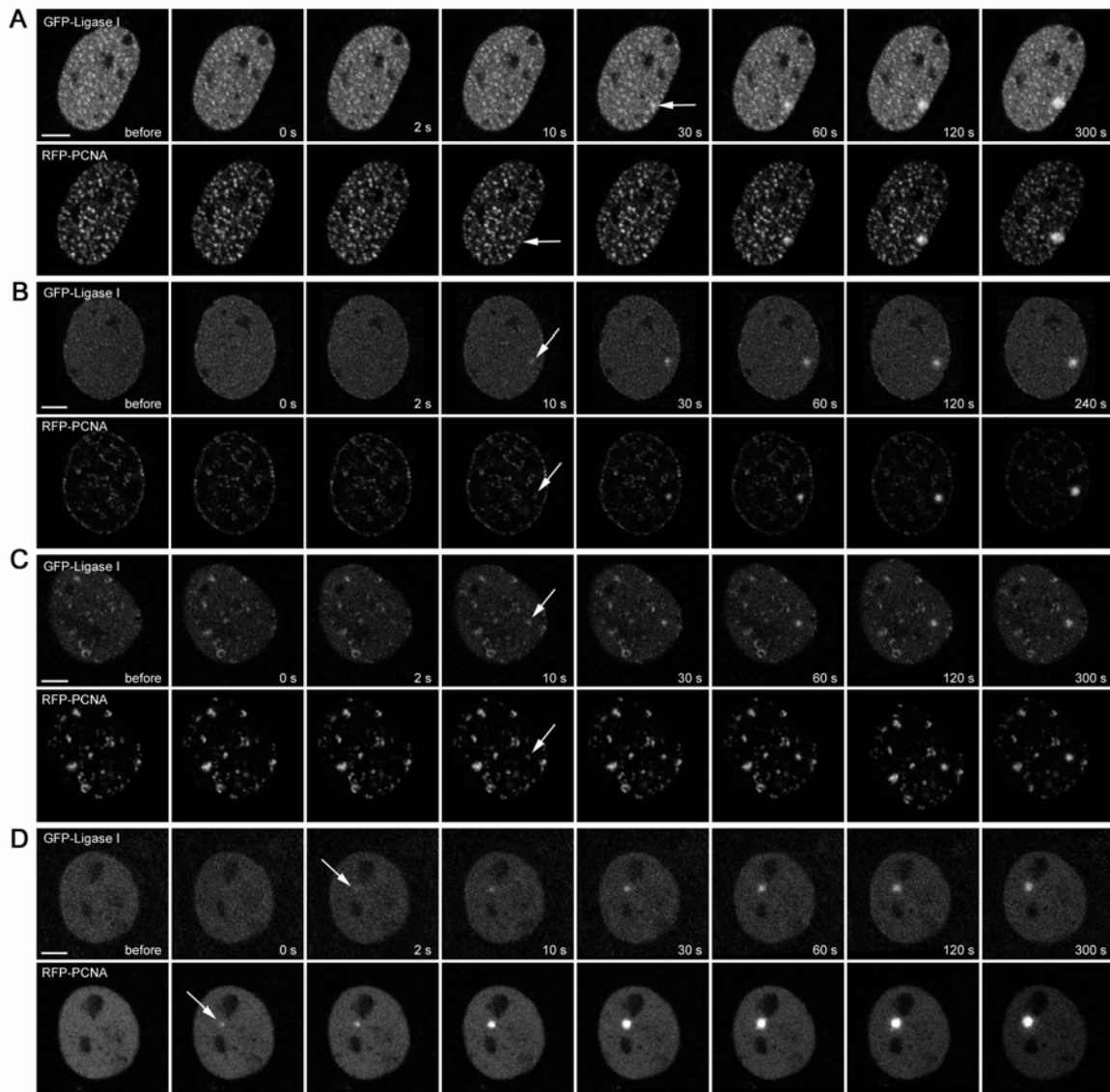
Supplementary Figure 1

Recruitment of DNA Ligase I and III to DNA repair sites is fluorescent-tag independent. Recruitment kinetics of DNA Ligase I (A) and DNA Ligase III (B) tagged with either GFP or RFP are very similar.



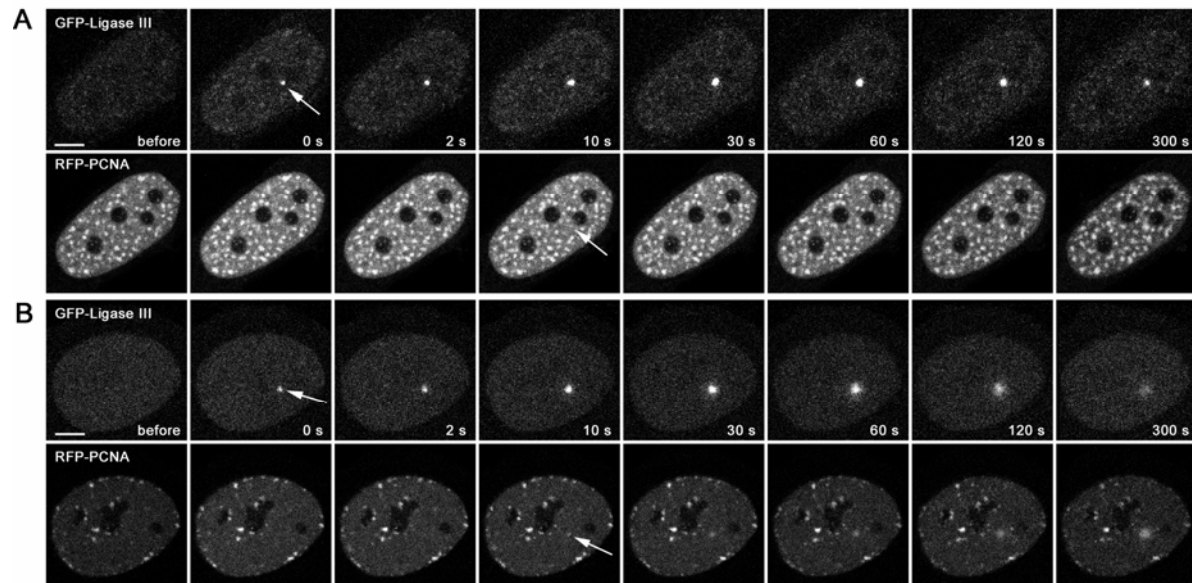
Supplementary Figure 2

Recruitment of GFP-DNA Ligase I and RFP-PCNA to repair sites in S and non S phase HeLa cells. The structure of the fusion proteins is depicted in Figure 2. Live cell imaging of microirradiated HeLa cells shows accumulation of RFP-PCNA and GFP-DNA Ligase I at sites of DNA damage (arrows) in early S (A), mid S (B), late S (C) and non S phase (D). Times after microirradiation are indicated. Scale bars, 5 μm.



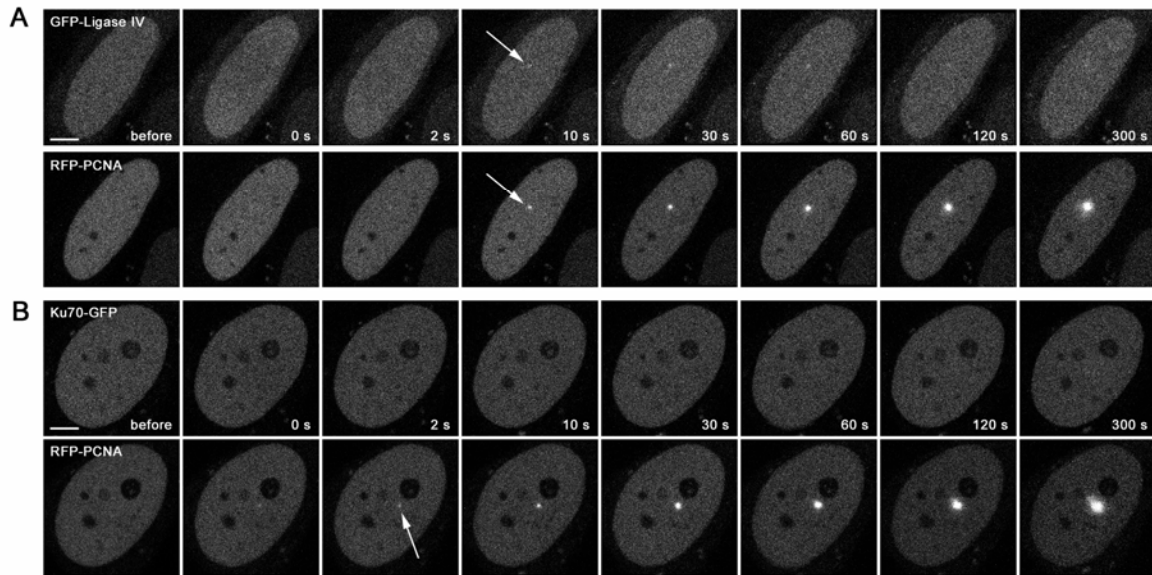
Supplementary Figure 3

Recruitment of GFP-DNA Ligase I and RFP-PCNA to repair sites in S and non S phase mouse C2C12 cells. The structure of the fusion proteins is depicted in Figure 2. Live cell imaging of microirradiated C2C12 cells in early S (A), mid S (B) late S (C) and non S phase (D) coexpressing GFP-DNA Ligase I and RFP-PCNA shows accumulation of RFP-PCNA and GFP-DNA Ligase I at sites of DNA damage (arrows). Times after microirradiation are indicated. Scale bars, 5 μ m.



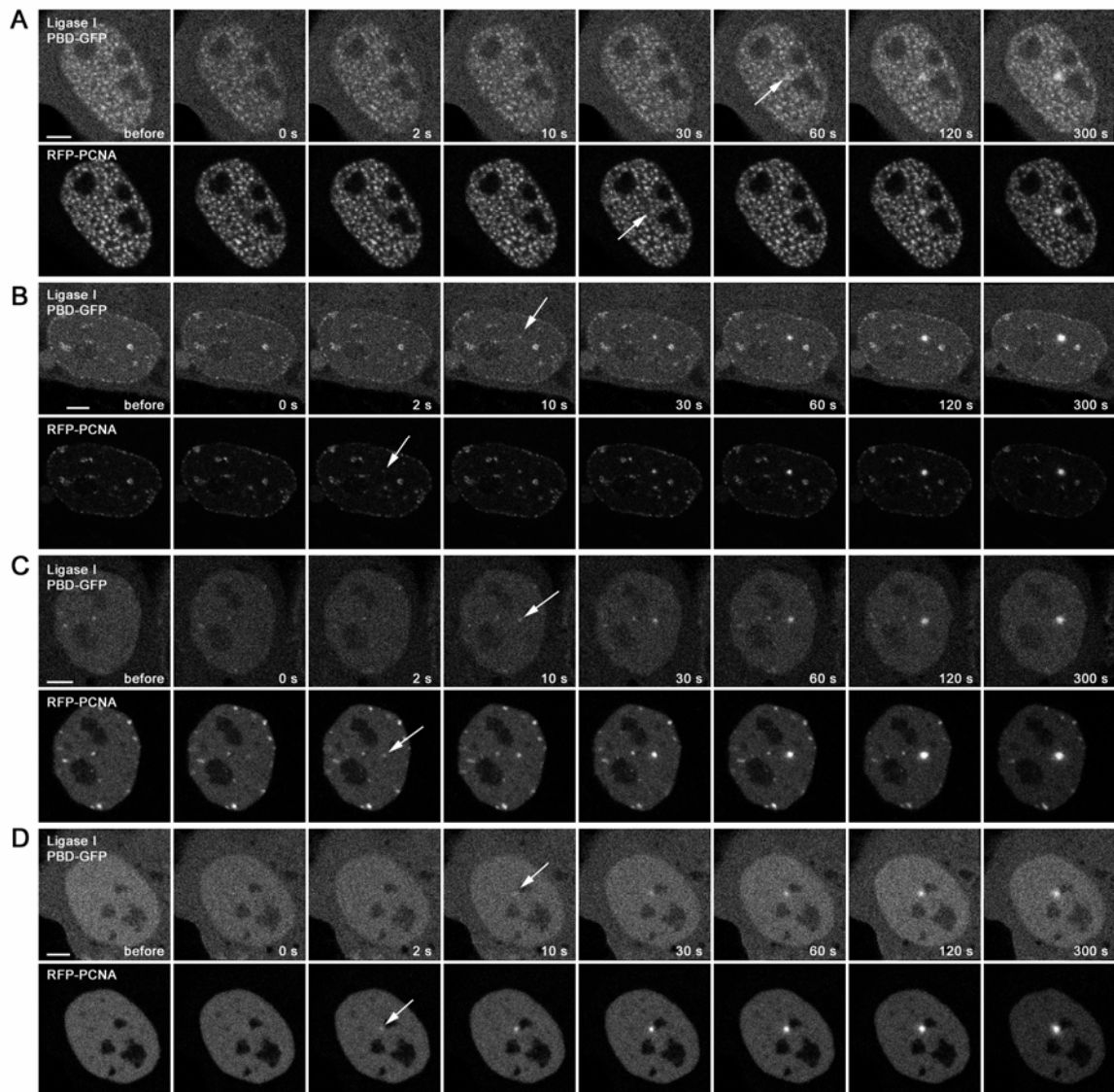
Supplementary Figure 4

Recruitment of GFP-DNA Ligase III and RFP-PCNA to repair sites in S phase HeLa cells. The structure of the fusion proteins is depicted in Figure 2. Live cell imaging of microirradiated HeLa cells in early (A) and late S phase (B) coexpressing GFP-DNA Ligase III and RFP-PCNA shows accumulation of RFP-PCNA and GFP-DNA Ligase III at sites of DNA damage (arrows). Times after microirradiation are indicated. Scale bars, 5 μm .



Supplementary Figure 5

The NHEJ-factor GFP-DNA Ligase IV shows only a minor accumulation at laser-induced DNA damage sites, while no accumulation of Ku70-GFP could be detected. The structure of the fusion proteins is depicted in Figure 2. Live cell imaging of microirradiated HeLa cells shows only a minor accumulation of GFP-DNA Ligase IV (A) and no accumulation of Ku70-GFP (B) at sites of DNA damage while RFP-PCNA accumulates at these sites as seen before (arrows). Scale bars, 5 μm .



Supplementary Figure 6

Recruitment of DNA Ligase I PBD-GFP and RFP-PCNA to repair sites in S and non S phase HeLa cells. The structure of the fusion proteins is depicted in Figure 2. Live cell imaging of microirradiated HeLa cells in early S (A), mid S (B), late S (C) and non S phase (D) coexpressing DNA Ligase I PBD-GFP and RFP-PCNA shows accumulation of RFP-PCNA and DNA Ligase I PBD-GFP at sites of DNA damage (arrows). Times after microirradiation are indicated. Scale bars, 5 μ m.

2.6. Recruitment of DNA methyltransferase 1 to DNA repair sites.

Recruitment of DNA methyltransferase I to DNA repair sites

Oliver Mortusewicz*, Lothar Schermelleh*, Joachim Walter*[†], M. Cristina Cardoso[‡], and Heinrich Leonhardt*[§]

*Department of Biology II, Ludwig Maximilians University Munich, 82152 Planegg-Martinsried, Germany; and [‡]Max Delbrück Center for Molecular Medicine, 13125 Berlin, Germany

Edited by Arthur B. Pardee, Dana-Farber Cancer Institute, Boston, MA, and approved May 11, 2005 (received for review February 7, 2005)

In mammalian cells, the replication of genetic and epigenetic information is directly coupled; however, little is known about the maintenance of epigenetic information in DNA repair. Using a laser microirradiation system to introduce DNA lesions at defined subnuclear sites, we tested whether the major DNA methyltransferase (Dnmt1) or one of the two *de novo* methyltransferases (Dnmt3a, Dnmt3b) are recruited to sites of DNA repair *in vivo*. Time lapse microscopy of microirradiated mammalian cells expressing GFP-tagged Dnmt1, Dnmt3a, or Dnmt3b1 together with red fluorescent protein-tagged proliferating cell nuclear antigen (PCNA) revealed that Dnmt1 and PCNA accumulate at DNA damage sites as early as 1 min after irradiation in S and non-S phase cells, whereas recruitment of Dnmt3a and Dnmt3b was not observed. Deletion analysis showed that Dnmt1 recruitment was mediated by the PCNA-binding domain. These data point to a direct role of Dnmt1 in the restoration of epigenetic information during DNA repair.

DNA methylation | Dnmt1 | microirradiation | proliferating cell nuclear antigen

In higher eukaryotes, maintenance and propagation of genetic and epigenetic information is essential for cellular identity and survival. By-products of normal cellular metabolism, spontaneous mutations, and environmental agents can lead to various types of DNA damage. Numerous DNA repair pathways reestablishing the genetic information are known and have been intensively described (1, 2). However, very little is known about enzymes and mechanisms involved in the restoration of the epigenetic information. There are two main epigenetic marks, DNA methylation and histone modifications, which are essential for cell type-specific gene expression and maintained over multiple cell divisions (3–7). Recently, chromatin assembly and remodeling have been linked to DNA repair (8–10).

DNA methylation is a postreplicative modification occurring mostly at cytosine residues of CpG dinucleotides and is essential for mammalian development (11), parental imprinting (12), X inactivation (13), and genome stability (14, 15). In mammalian cells, DNA methylation is catalyzed by two types of enzymes, maintenance (Dnmt1) and *de novo* methyltransferases (Dnmt3a, Dnmt3b) (16). The maintenance methyltransferase Dnmt1 has a preference for hemimethylated CpG sites generated during DNA replication and is ubiquitously expressed (16). Dnmt1 associates with replication sites by directly binding to proliferating cell nuclear antigen (PCNA) and thus maintains DNA methylation patterns in the newly synthesized strand after DNA replication (17, 18). In contrast to the maintenance methyltransferase Dnmt1, the *de novo* methyltransferases Dnmt3a and Dnmt3b are responsible for establishing new DNA methylation patterns during development and show a low and tissue-specific expression (19–21).

The importance of maintaining the epigenetic information was recently underscored by knockdown experiments. Lowering Dnmt1 to rate-limiting amounts in transgenic mice lead to a loss of DNA methylation, affecting gene expression and development, and even caused cancer (14, 15, 22).

These results clearly demonstrate the importance of DNA methylation, and raise the question whether and how this epigenetic information is maintained during DNA repair. Therefore, we investigated whether and which DNA methyltransferases are present at DNA repair sites. As an experimental system, we choose local DNA damage induction at preselected subnuclear sites by UVA laser microirradiation (23), which allows the study of protein dynamics involved in the repair process in living cells.

We showed that Dnmt1 and PCNA are recruited to microirradiated sites in S and non-S phase cells immediately after irradiation, whereas Dnmt3a and Dnmt3b are not accumulated. Recruitment of Dnmt1 to DNA repair sites is mediated by the PCNA-binding domain (PBD) of Dnmt1. These results suggest that PCNA recruits enzymes involved in DNA synthesis, DNA methylation, and chromatin assembly and that Dnmt1 contributes to the restoration of epigenetic information in DNA repair.

Materials and Methods

Cell Culture and Transfection. Mouse C2C12 myoblasts and human HeLa cells were cultured in DMEM containing 50 μ g/ml gentamicin supplemented with 20% and 10% FCS, respectively. For transfection, cells grown on gridded coverslips or on Lab-Tek chamber slides (Nunc) were either microinjected with plasmid DNA by using an automated microinjection system (Eppendorf) or cotransfected with TransFectin transfection reagent (Bio-Rad) according to the manufacturer's instructions. Cells were subsequently incubated overnight before performing microirradiation and live cell analyses or immunostainings.

Expression Plasmids. Mammalian expression constructs encoding translational fusions of mouse Dnmt1, Dnmt1 Δ PBD, and the PBD alone with enhanced GFP were described (24). Red variants of the previously described GFP-PCNA (25) and GFP-Dnmt1 were generated by replacing GFP with monomeric red fluorescent protein (mRFP1) (26) and termed RFP-PCNA and RFP-Dnmt1. GFP-Dnmt3a and GFP-Dnmt3b1 expression constructs were as described (27). The GFP-Ligase 3 construct was generated by cloning the human DNA Ligase 3 cDNA (28) into the pEGFP-C1 (Clontech) vector. DNA Ligase 3 was amplified by using the following oligonucleotides as primers for the PCR: forward, 5'-GGGG **GTCGAC** GCT GAG CAA CGG TTC-3'; reverse, 5'-CCCC **GGATCC** GCA GGG AGC TAC CAG-3'. The residues in bold indicate a SalI and a BamHI site encoded in the forward and reverse primer, respectively, for subcloning the PCR fragment into the SalI and BamHI sites of the pEGFP-C1 vector downstream of GFP.

In all cases, expression was under the control of the CMV

This paper was submitted directly (Track II) to the PNAS office.

Abbreviations: PCNA, proliferating cell nuclear antigen; PBD, PCNA-binding domain; RFP, red fluorescent protein.

[†]Present address: Till I.D. GmbH, 82152 Planegg-Martinsried, Germany.

[§]To whom correspondence should be addressed. E-mail: h.leonhardt@lmu.de.

© 2005 by The National Academy of Sciences of the USA

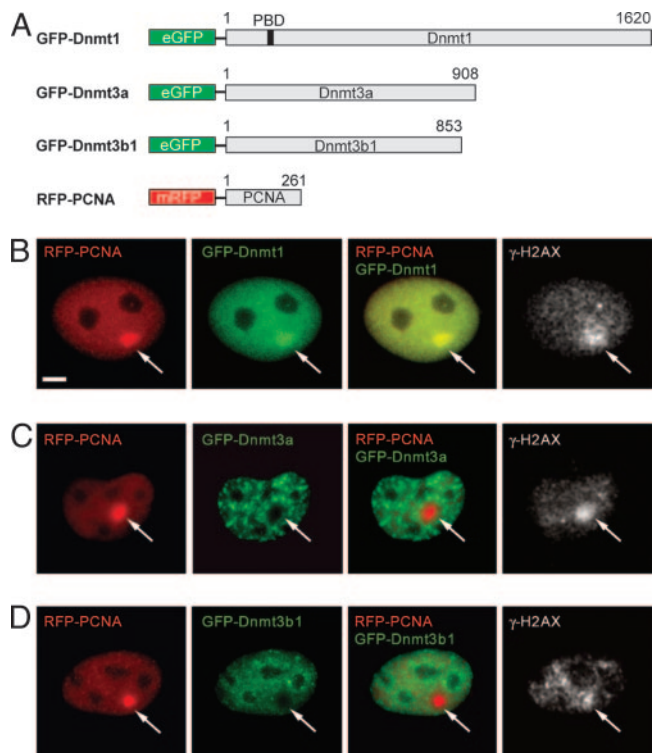


Fig. 1. GFP-Dnmt1 and RFP-PCNA but not GFP-Dnmt3a and GFP-Dnmt3b1 colocalize with γ -H2AX at microirradiated sites. Wide-field fluorescence images of cotransfected C2C12 cells formaldehyde fixed 25–30 min after UVA laser microirradiation. Double strand breaks were detected with rabbit polyclonal antibodies against γ -H2AX. Arrows mark sites of irradiation. (A) Schematic representation of the fusion proteins. (B) GFP-Dnmt1 and RFP-PCNA accumulate at sites of DNA damage and colocalize with γ -H2AX. (C and D) GFP-Dnmt3a and GFP-Dnmt3b1 are bleached at irradiated sites and do not redistribute to sites of DNA damage after microirradiation. (Scale bar, 5 μ m.)

promoter. We tested all fusion proteins by expression in COS7 or 293T cells followed by Western blot analysis (29).

Immunofluorescence. Cells were fixed with 3.7% formaldehyde in PBS and permeabilized with ice-cold methanol for 5 min or with 0.2% Triton-X-100 for 3 min. The following primary antibodies (diluted 1:200 in PBS containing 2% BSA) were used: anti- γ H2AX (Ser-139) rabbit antibodies (Upstate Biotechnology), anti-Dnmt1 rabbit antibodies raised against the N-terminal domain (18), and anti-PCNA (clone PC10) mouse monoclonal antibodies (Santa Cruz Biotechnology). Primary antibodies were detected by using secondary antibodies (diluted 1:400 in PBS containing 2% BSA) conjugated to Alexa Fluor 488, 635 (Molecular Probes) and Cy3 (Amersham Pharmacia), respectively. Cells were counterstained with DAPI and mounted in Vectashield (Vector Laboratories).

Microscopy. Stained cells were analyzed by using a Zeiss Axiovert 135 TV epifluorescence microscope equipped with a $\times 63/1.4$ numerical aperture Plan-Apochromat oil immersion objective. Images were recorded with a cooled charge-coupled device camera using METAMORPH software and appropriate filter sets.

For time lapse analysis, light optical sections were acquired with a Zeiss LSM410 confocal laser scanning microscope using the 488-nm Ar laser line and the 543-nm HeNe laser line, respectively. Six mid z sections at 0.5- μ m intervals were taken every 3–10 min, and cells were followed up to several hours. Focus drift over time was compensated with a macro that uses the reflection at the coverslip to medium interface as reference.

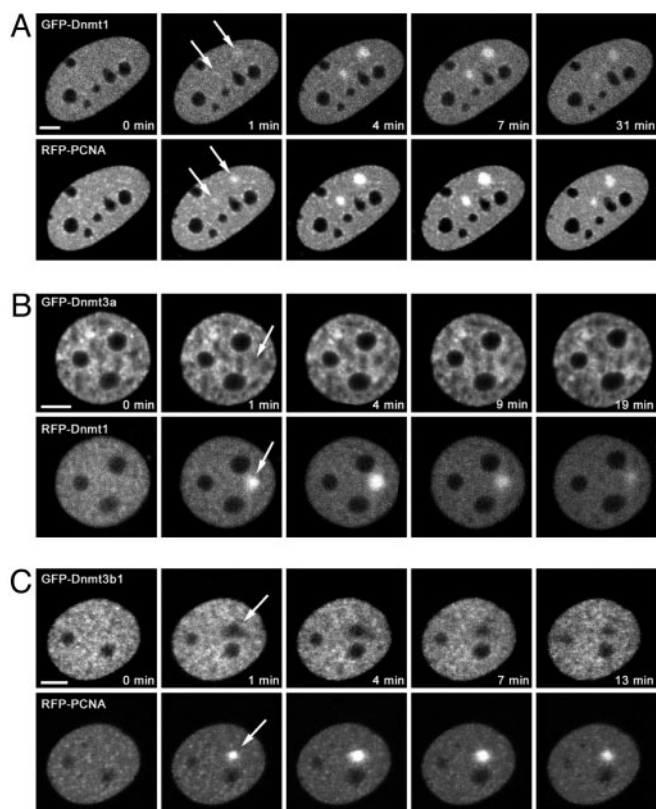


Fig. 2. Dynamics of DNA methyltransferase recruitment to repair sites in living cells. Live cell imaging of microirradiated C2C12 cells in S phase coexpressing fluorescent fusion constructs of DNA methyltransferases and PCNA is shown. The constructs used were the same as depicted in Fig. 1A except for the RFP-Dnmt1 construct where the GFP was replaced by monomeric RFP. Maximum projections of confocal midsections are shown and times after microirradiation are indicated. (A) A C2C12 cell in early to mid S phase coexpressing GFP-Dnmt1 and RFP-PCNA shows accumulation of RFP-PCNA and GFP-Dnmt1 at sites of DNA damage (arrows) as early as 1 min after irradiation. (B) An early S phase cell coexpressing GFP-Dnmt3a and RFP-Dnmt1 shows accumulation of RFP-Dnmt1 at the irradiated site (arrow), whereas GFP-Dnmt3a is bleached (arrow) and does not recover during the entire observation period. (C) An early S phase cell coexpressing GFP-Dnmt3b1 and RFP-PCNA shows bleaching of GFP-Dnmt3b1 (arrow) at the irradiation spot, whereas RFP-PCNA accumulates at this site (arrow). (Scale bars, 5 μ m.)

After image acquisition, a projection of all six z sections was performed from each time point by using IMAGEJ 1.34.

Alternatively, time series were taken with a Leica TCS SP2/AOBS confocal laser scanning microscope using the 488-nm Ar laser line and the 561-nm DPSS laser line. Before and after microirradiation, confocal image series of one mid z section were recorded at 2-s time interval (typically 1 preirradiation and 60–120 postirradiation frames) followed by an image series with 5-min time intervals.

UVA Laser Microirradiation. Cells were seeded on 40-mm-i.d. round coverslips and sensitized for microirradiation by incubation in medium containing BrdUrd (10 μ g/ml) for 20 h. For live cell microscopy and irradiation, coverslips were mounted in a FCS2 live-cell chamber (Bioptechs) and maintained at 37°C. Microirradiation was carried out with a laser microdissection system (PALM) coupled into a Zeiss LSM410 confocal laser scanning microscope. A pulsed N₂ laser (337 nm) coupled into the epifluorescence path of the microscope was focused through a UV transmitting Plan-Neofluar $\times 63/1.25$ numerical aperture objective to locally irradiate preselected spots of ≈ 1 μ m i.d.

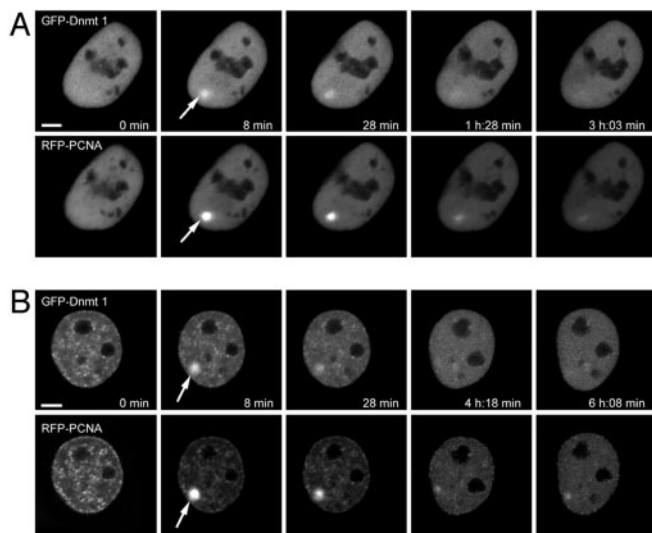


Fig. 3. Recruitment of GFP-Dnmt1 and RFP-PCNA to repair sites in S and non-S phase C2C12 cells. The structure of the fusion proteins is depicted in Fig. 1A. Live cell imaging of microirradiated C2C12 cells in G₁ (A) and late S phase (B) coexpressing GFP-Dnmt1 and RFP-PCNA shows accumulation of RFP-PCNA and GFP-Dnmt1 at sites of DNA damage (arrows). Maximum projections of confocal midsections are shown and times after microirradiation are indicated. (Scale bars, 5 μ m.)

within the nucleus. The pulse energy could be tuned with a rotatable absorption filter and was measured before passing through the objective with a power meter. Taking into account the 10% transmission of the objective at 337 nm, the energy

delivered to the target was estimated to be 8 nJ per pulse. BrdUrd-sensitized cells were usually irradiated with 30 pulses that corresponded to an estimated energy of 240 nJ per irradiated site. For the acquisition of time series, the objective was changed in some cases to a Plan-Apochromat $\times 63/1.4$ numerical aperture objective after irradiation.

Alternatively, BrdUrd-sensitized cells grown on Lab-Tek chamber slides (Nunc) were microirradiated with a 405-nm diode laser coupled into a Leica TCS SP2/AOBS confocal laser scanning microscope. The 405-nm laser was focused through a UV transmitting Leica HCX PL APO $\times 63/1.40$ numerical aperture oil objective to locally irradiate preselected spots of ≈ 1 μ m i.d. within the nucleus. For microirradiation, a region of interest was selected and irradiated with an intense 405-nm diode laser beam (laser set to maximum power, 50 mW, at 100% transmission) for 1 s. Under these conditions, thymine dimers and double strand breaks are generated as demonstrated by staining with specific antibodies (data not shown).

Results

Dnmt1 and PCNA Localize at DNA Repair Sites. To study whether and which DNA methyltransferases are recruited to sites of DNA repair, we used a UVA laser microirradiation system with a pulsed 337-nm N₂ laser to introduce DNA lesions. Local irradiation with this system causes a variety of different types of DNA damage at defined nuclear sites. Replicative incorporation of BrdUrd into DNA sensitizes cells and enhances the double strand break (DSB) formation upon irradiation (23, 30, 31). We microirradiated BrdUrd-sensitized mouse C2C12 myoblasts or human HeLa cells and determined DNA damage induction by immunostaining for γ -H2AX. The histone variant H2AX becomes phosphorylated (γ -H2AX) upon induction of DSBs within a few minutes and therefore serves as a DSB marker (31).

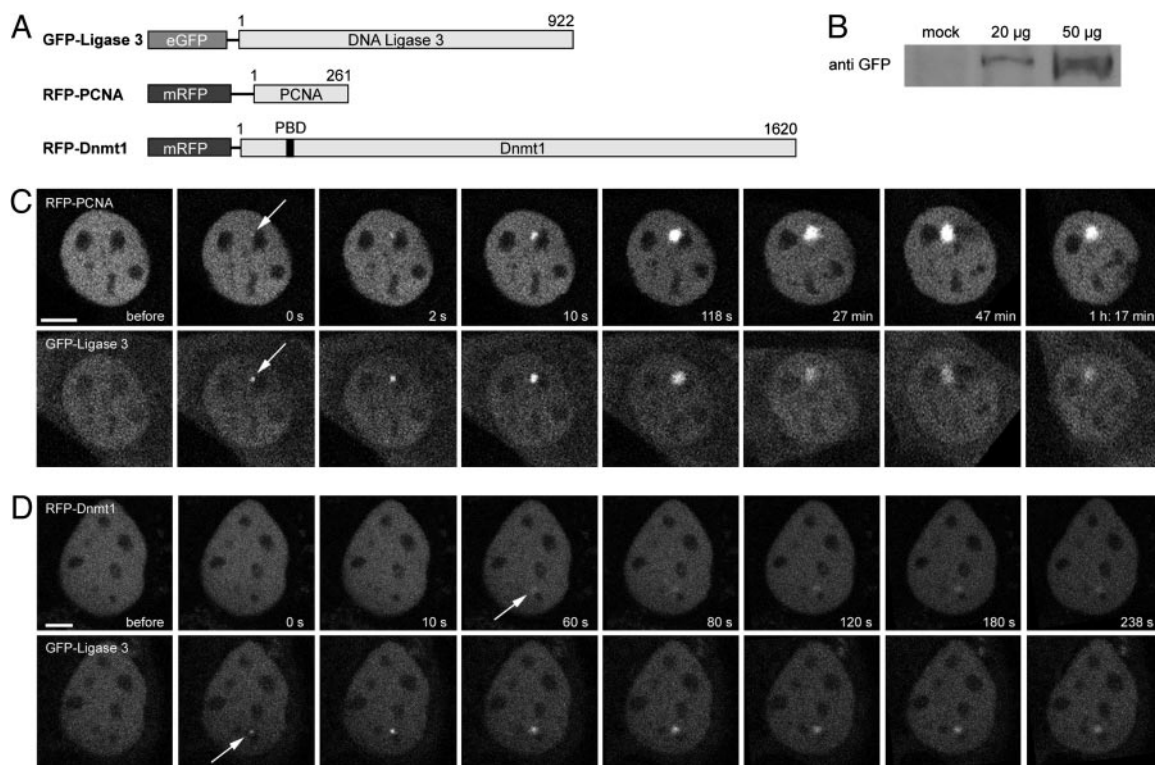


Fig. 4. Recruitment of human Ligase 3 fused to GFP (GFP-Ligase 3) and RFP-PCNA or RFP-Dnmt1 to DNA repair sites after microirradiation. (A) Schematic representation of the fusion proteins. (B) Correct expression of the GFP-Ligase 3 construct was determined by Western blot analysis. (C and D) Live cell imaging of C2C12 cells coexpressing GFP-Ligase 3 and either RFP-PCNA (C) or RFP-Dnmt1 (D). After microirradiation with a 405-nm diode laser, GFP-Ligase 3, RFP-PCNA, and RFP-Dnmt1 accumulate at sites of DNA damage (arrows). One confocal midsection is shown and times after microirradiation are indicated. (Scale bars, 5 μ m.)

Cells coexpressing GFP-Dnmt and RFP-PCNA fusion constructs were microirradiated and incubated for 25–30 min before fixation and immunodetection of γ -H2AX. At irradiated sites, an accumulation of RFP-PCNA and GFP-Dnmt1 colocalizing with γ -H2AX was observed (Fig. 1). In contrast, GFP-tagged Dnmt3a and Dnmt3b1 were found bleached at the irradiated region, indicating that *de novo* methyltransferases were not recruited to sites of induced DNA damage. Recruitment of endogenous Dnmt1 and PCNA at irradiated sites was confirmed by immunostaining of cells fixed \approx 20 min after irradiation (Fig. 6, which is published as supporting information on the PNAS web site). Accumulation of PCNA and Dnmt1 depended on BrdUrd treatment and the energy of the UVA laser beam (data not shown). These results clearly show that PCNA and Dnmt1 are recruited to UVA-induced nuclear DNA repair sites.

Kinetics of Dnmt1 and PCNA Recruitment. To study the kinetics of DNA methyltransferase and PCNA recruitment *in vivo*, we performed time lapse microscopy of microirradiated C2C12 cells expressing various combinations of fusion constructs for GFP- or RFP-tagged Dnmt1, Dnmt3a, Dnmt3b1, and PCNA. Short-term confocal live cell series of irradiated cells were recorded with time intervals of 3 min. Recruitment of RFP-PCNA and GFP-Dnmt1 to microirradiation sites could be observed as early as 1 min after irradiation, reached a maximum \approx 5–10 min after irradiation, and persisted throughout the observation period of \approx 30 min. As was observed before, neither GFP-Dnmt3a nor GFP-Dnmt3b1 accumulated at sites of DNA repair after microirradiation (Fig. 2). Instead, GFP fluorescence at the irradiated spot was bleached and did not recover over the total observation period, indicating that both Dnmt3a and Dnmt3b1 were rather immobile. These results were confirmed with further FRAP analyses of cells expressing RFP-Dnmt1 and GFP-Dnmt3a or GFP-Dnmt3b1 using a 488-nm Ar laser (data not shown).

Next we tested whether the recruitment of RFP-PCNA and GFP-Dnmt1 occurs in S phase and non-S phase cells. The characteristic focal distribution of RFP-PCNA allowed identification of S phase in living cells (25, 32). After irradiation, we followed cotransfected S and non-S phase cells over several hours, recording confocal z stacks every 5–10 min. Accumulations of GFP-Dnmt1 and RFP-PCNA at DNA damage sites could still be detected at the irradiated sites as late as several hours after irradiation (Fig. 3). Relative fluorescence intensities at the irradiated sites decreased with a half time of \approx 50 min.

Recruitment of RFP-PCNA and GFP-Dnmt1 to sites of DNA damage could also be observed in human HeLa cells in S and non-S phase (Fig. 7, which is published as supporting information on the PNAS web site). These results show that PCNA and Dnmt1 are recruited with similar kinetics in both human and mouse cells.

To compare the recruitment kinetics of PCNA and Dnmt1 with a known repair protein, we microirradiated C2C12 cells cotransfected with human DNA Ligase 3 fused to GFP (GFP-Ligase 3) and RFP-PCNA or RFP-Dnmt1 expression vectors. DNA Ligase 3 is known to be involved in base excision repair, single strand break repair, and error-prone nonhomologous end joining (33–35). Immediately after laser microirradiation, recruitment of GFP-Ligase 3 and RFP-PCNA could be observed, whereas Dnmt1 became visible with a delay of \approx 1 min (Fig. 4). The distinct recruitment kinetics at repair sites probably reflects their different functions in repair. Thus, the slightly delayed accumulation of Dnmt1 at repair sites fits well with a role in post synthetic maintenance of DNA methylation.

Dnmt1-Recruitment to Sites of DNA Damage via PCNA. During S phase, Dnmt1 is targeted to sites of DNA replication via its PBD (17, 24). To test whether PCNA is also responsible for the

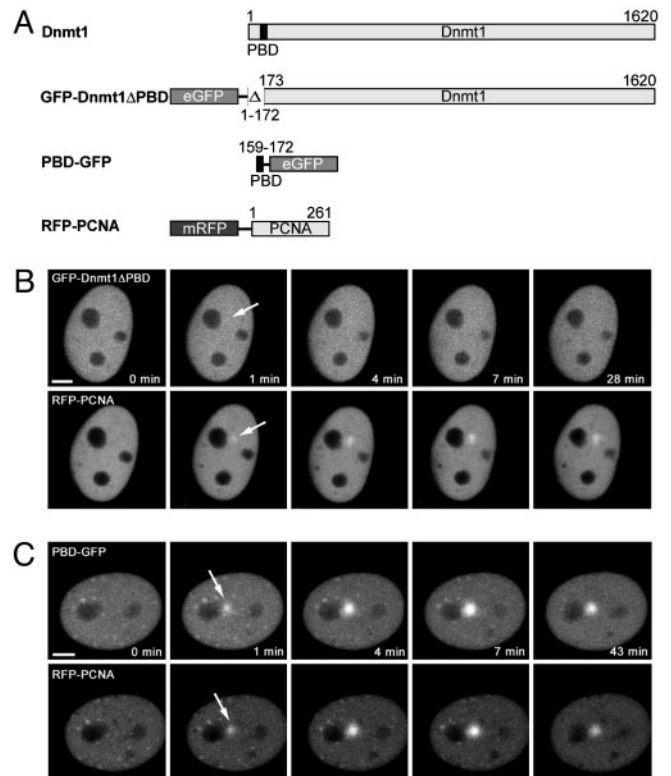


Fig. 5. Recruitment of Dnmt1 to DNA damage sites is mediated by PCNA. (A) Schematic representation of the fusion proteins. (B) Live cell imaging of a microirradiated C2C12 cell coexpressing GFP-Dnmt1 Δ PBD and RFP-PCNA. Deletion of the PBD in GFP-Dnmt1 Δ PBD abolishes recruitment to sites of DNA damage, whereas RFP-PCNA accumulates at these sites as seen before (arrow). (C) A late S phase cell coexpressing PBD-GFP and RFP-PCNA shows accumulation of both RFP-PCNA and PBD-GFP at sites of microirradiation (arrows). Maximum projections of confocal midsections are shown and times after microirradiation are indicated. (Scale bars, 5 μ m.)

recruitment of Dnmt1 during DNA repair, we deleted the PBD of Dnmt1 (GFP-Dnmt1 Δ PBD) and expressed this deletion construct in C2C12 cells together with RFP-PCNA. After UVA laser microirradiation, GFP-Dnmt1 Δ PBD, unlike RFP-PCNA, remained diffuse and showed no accumulation at irradiated sites (Fig. 5). This finding suggests that the PBD plays a critical role in the recruitment of Dnmt1. To directly study the function of the PBD, we fused the PBD alone with GFP (PBD-GFP). Besides association to replication sites, the PBD fusion protein was recruited to sites of DNA damage with kinetics similar to the full-length Dnmt1 fusion construct (Fig. 5). These results demonstrate that the PBD of Dnmt1 is necessary and sufficient for localization at repair sites.

Discussion

Higher eukaryotes have established a number of DNA repair pathways to deal with various types of DNA damage occurring during normal cellular metabolism. Whereas repair of the genetic information has been intensively studied, the mechanism by which the epigenetic information is reestablished during DNA repair is poorly understood.

The low and tissue-specific expression of Dnmt3a and -3b (19), as well as their binding to pericentromeric heterochromatin (36), makes these *de novo* methyltransferases rather unlikely candidates for an involvement in the genome-wide restoration of DNA methylation in DNA repair. In contrast, Dnmt1 is ubiquitously expressed at high levels and has a highly mobile fraction in the nucleus (unpublished data). Using a laser microirradiation sys-

tem to induce DNA lesions at defined nuclear sites, we observed recruitment of Dnmt1 but did not detect any accumulation of Dnmt3a or Dnmt3b at repair sites in living mammalian cells. These results fit well with the recent identification of Dnmt1 as a potential component of the mismatch repair (MMR) pathway in a genetic screen for MMR mutants using Bloom's syndrome protein (Blm)-deficient embryonic mouse stem cells (37). The accumulation of Dnmt1 at repair sites suggests that, like in DNA replication, Dnmt1 maintains the DNA methylation pattern in the DNA newly synthesized during the repair process. Thus, Dnmt1 likely prevents a loss of DNA methylation in repair, which otherwise could cause epigenetic deregulation (38) and genomic instability (14, 15). In addition, Dnmt1 has been reported to interact with histone deacetylases (39, 40) and could thus, together with chromatin assembly factor 1 (CAF-1) (8), contribute to the reestablishment of chromatin structures and respective histone modifications. Finally, Dnmt1 may also participate in the identification of the template strand in various repair pathways as was suggested for MMR (41, 42). Scope and details of Dnmt1 function(s) at DNA repair sites remain to be elucidated.

Key steps in DNA repair are recognition of the DNA damage and recruitment of the repair machinery. We could

follow the accumulation of PCNA at DNA damage sites in living cells, which fits well with earlier reports identifying PCNA at DNA lesions (8, 43–45). Here, we could demonstrate that Dnmt1 is recruited to DNA damage sites via PCNA and that the PBD of Dnmt1 is necessary and sufficient for this recruitment. Our results show that PCNA mediates recruitment of the maintenance methyltransferase Dnmt1 not only to replication sites but also to DNA repair sites. Interestingly, PCNA is controlled by ubiquitination and sumoylation leading to a switch between alternative repair pathways (45, 46). In summary, PCNA plays a central role in DNA replication and repair, thus serving as a versatile loading platform for enzymes involved in DNA synthesis, chromatin assembly, and maintenance of DNA methylation.

We thank Dr. E. Li (Novartis Institutes for Biomedical Research, Cambridge, MA) (GFP-Dnmt3a and GFP-Dnmt3b1), Dr. R. Tsien (Howard Hughes Medical Institute, University of California, San Francisco) (mRFP1), and Dr. T. Lindahl (Imperial Cancer Research Center, Clare Hall Laboratories, London) (hLigase 3) for providing cDNAs and expression vectors. We are grateful to I. Grunewald, A. Gahl, Dr. U. Rothbauer, and K. Zolghadr for help and advice. This work was supported by grants from the Deutsche Forschungsgemeinschaft and the Volkswagenstiftung (to H.L. and M.C.C.).

- Friedberg, E. C. (2003) *Nature* **421**, 436–440.
- Hoeijmakers, J. H. (2001) *Nature* **411**, 366–374.
- Jaenisch, R. & Bird, A. (2003) *Nat. Genet.* **33**, Suppl., 245–254.
- Robertson, K. D. (2002) *Oncogene* **21**, 5361–5379.
- Leonhardt, H. & Cardoso, M. C. (2000) *J. Cell Biochem.*, Suppl. 35, 78–83.
- Jenuwein, T. & Allis, C. D. (2001) *Science* **293**, 1074–1080.
- Felsenfeld, G. & Groudine, M. (2003) *Nature* **421**, 448–453.
- Green, C. M. & Almouzni, G. (2003) *EMBO J.* **22**, 5163–5174.
- Okano, S., Lan, L., Caldecott, K. W., Mori, T. & Yasui, A. (2003) *Mol. Cell Biol.* **23**, 3974–3981.
- van Attikum, H., Fritsch, O., Hohn, B. & Gasser, S. M. (2004) *Cell* **119**, 777–788.
- Li, E., Bestor, T. H. & Jaenisch, R. (1992) *Cell* **69**, 915–926.
- Li, E., Beard, C. & Jaenisch, R. (1993) *Nature* **366**, 362–365.
- Panning, B. & Jaenisch, R. (1996) *Genes Dev.* **10**, 1991–2002.
- Eden, A., Gaudet, F., Waghmare, A. & Jaenisch, R. (2003) *Science* **300**, 455.
- Gaudet, F., Hodgson, J. G., Eden, A., Jackson-Grusby, L., Dausman, J., Gray, J. W., Leonhardt, H. & Jaenisch, R. (2003) *Science* **300**, 489–492.
- Bestor, T. H. (2000) *Hum. Mol. Genet.* **9**, 2395–2402.
- Chuang, L. S., Ian, H. I., Koh, T. W., Ng, H. H., Xu, G. & Li, B. F. (1997) *Science* **277**, 1996–2000.
- Leonhardt, H., Page, A. W., Weier, H. U. & Bestor, T. H. (1992) *Cell* **71**, 865–873.
- Okano, M., Xie, S. & Li, E. (1998) *Nat. Genet.* **19**, 219–220.
- Okano, M., Bell, D. W., Haber, D. A. & Li, E. (1999) *Cell* **99**, 247–257.
- Xu, G. L., Bestor, T. H., Bourc'his, D., Hsieh, C. L., Tommerup, N., Bugge, M., Hulten, M., Qu, X., Russo, J. J. & Viegas-Pequignot, E. (1999) *Nature* **402**, 187–191.
- Gaudet, F., Rideout, W. M., III, Meissner, A., Dausman, J., Leonhardt, H. & Jaenisch, R. (2004) *Mol. Cell Biol.* **24**, 1640–1648.
- Tashiro, S., Walter, J., Shinohara, A., Kamada, N. & Cremer, T. (2000) *J. Cell Biol.* **150**, 283–291.
- Easwaran, H. P., Schermelleh, L., Leonhardt, H. & Cardoso, M. C. (2004) *EMBO Rep.* **5**, 1181–1186.
- Leonhardt, H., Rahn, H. P., Weinzierl, P., Sporbert, A., Cremer, T., Zink, D. & Cardoso, M. C. (2000) *J. Cell Biol.* **149**, 271–280.
- Campbell, R. E., Tour, O., Palmer, A. E., Steinbach, P. A., Baird, G. S., Zacharias, D. A. & Tsien, R. Y. (2002) *Proc. Natl. Acad. Sci. USA* **99**, 7877–7882.
- Hata, K., Okano, M., Lei, H. & Li, E. (2002) *Development (Cambridge, U.K.)* **129**, 1983–1993.
- Wei, Y. F., Robins, P., Carter, K., Caldecott, K., Pappin, D. J., Yu, G. L., Wang, R. P., Shell, B. K., Nash, R. A., Schar, P., et al. (1995) *Mol. Cell Biol.* **15**, 3206–3216.
- Easwaran, H. P., Leonhardt, H. & Cardoso, M. C. (2005) *Cell Cycle* **4**, e53–e55.
- Lukas, C., Falck, J., Bartkova, J., Bartek, J. & Lukas, J. (2003) *Nat. Cell Biol.* **5**, 255–260.
- Rogakou, E. P., Boon, C., Redon, C. & Bonner, W. M. (1999) *J. Cell Biol.* **146**, 905–916.
- Sporbert, A., Gahl, A., Ankerhold, R., Leonhardt, H. & Cardoso, M. C. (2002) *Mol. Cell* **10**, 1355–1365.
- Caldecott, K. W., McKeown, C. K., Tucker, J. D., Ljungquist, S. & Thompson, L. H. (1994) *Mol. Cell Biol.* **14**, 68–76.
- Mackey, Z. B., Niedergang, C., Murcia, J. M., Leppard, J., Au, K., Chen, J., de Murcia, G. & Tomkinson, A. E. (1999) *J. Biol. Chem.* **274**, 21679–21687.
- Gottlich, B., Reichenberger, S., Feldmann, E. & Pfeiffer, P. (1998) *Eur. J. Biochem.* **258**, 387–395.
- Bachman, K. E., Rountree, M. R. & Baylin, S. B. (2001) *J. Biol. Chem.* **276**, 32282–32287.
- Guo, G., Wang, W. & Bradley, A. (2004) *Nature* **429**, 891–895.
- Jackson-Grusby, L., Beard, C., Possemato, R., Tudor, M., Fambrough, D., Csankovszki, G., Dausman, J., Lee, P., Wilson, C., Lander, E. & Jaenisch, R. (2001) *Nat. Genet.* **27**, 31–39.
- Rountree, M. R., Bachman, K. E. & Baylin, S. B. (2000) *Nat. Genet.* **25**, 269–277.
- Fuks, F., Burgers, W. A., Brehm, A., Hughes-Davies, L. & Kouzarides, T. (2000) *Nat. Genet.* **24**, 88–91.
- Kim, M., Trinh, B. N., Long, T. I., Oghamian, S. & Laird, P. W. (2004) *Nucleic Acids Res.* **32**, 5742–5749.
- Wang, K. Y. & James Shen, C. K. (2004) *Oncogene* **23**, 7898–7902.
- Jakob, B., Scholz, M. & Taucher-Scholz, G. (2002) *Int. J. Radiat Biol.* **78**, 75–88.
- Balajee, A. S. & Geard, C. R. (2001) *Nucleic Acids Res.* **29**, 1341–1351.
- Solomon, D. A., Cardoso, M. C. & Knudsen, E. S. (2004) *J. Cell Biol.* **166**, 455–463.
- Hoegge, C., Pfander, B., Moldovan, G. L., Pyrowolakis, G. & Jentsch, S. (2002) *Nature* **419**, 135–141.

Supplementary Information

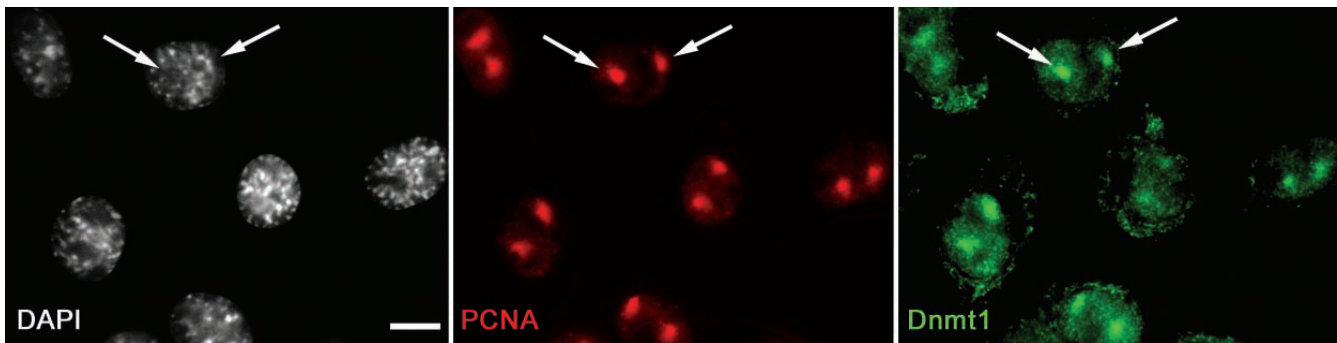


Fig. 6. Accumulation of endogenous proliferating cell nuclear antigen (PCNA) and Dnmt1 at microirradiated sites. Wide-field fluorescence images of C2C12 cells. Fixation and immunostaining was performed ~20 min after UVA laser irradiation using mouse monoclonal anti-PCNA antibodies and rabbit polyclonal antibodies against the N terminus of Dnmt1. Both, endogenous PCNA and Dnmt1 are recruited to induced DNA damage sites (arrows). Scale bar, 10 μ m.

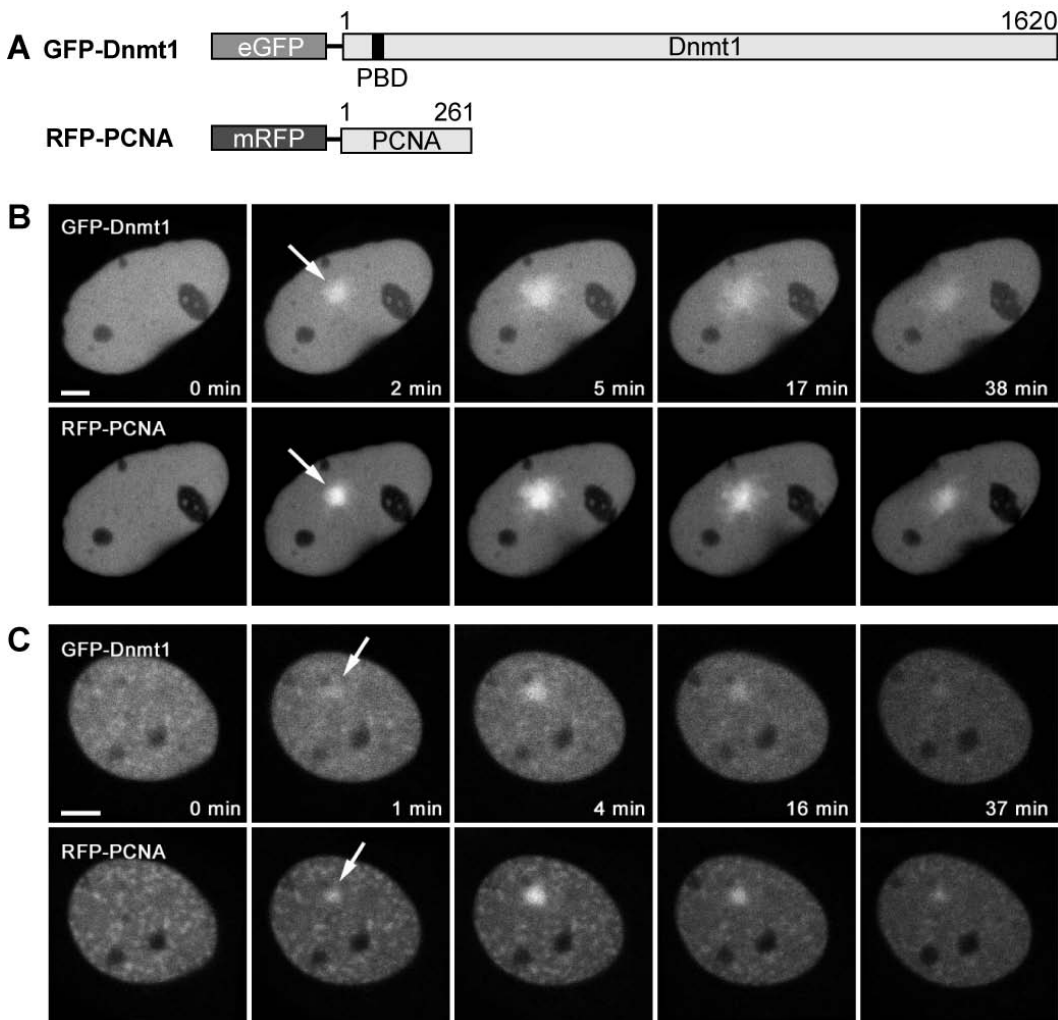


Fig. 7. Recruitment of GFP-Dnmt1 and red fluorescent protein-proliferating cell nuclear antigen (RFP-PCNA) to microirradiation sites in HeLa cells. (A) Schematic representation of the fusion constructs. Live cell imaging of microirradiated S phase (B) and non-S phase (C) HeLa cells coexpressing GFP-Dnmt1 and RFP-PCNA show accumulation of both fusion proteins at sites of DNA damage (arrows) as early as 1 min after irradiation. Scale bar, 5 μ m.

2.7. A fluorescent two-hybrid (F2H) assay for direct visualization of protein interactions in living cells.

A fluorescent two-hybrid (F2H) assay for direct visualization of protein interactions in living cells

Kourosh Zolghadr^{1,2}, Oliver Mortusewicz^{1,2}, Ulrich Rothbauer^{1,2},
Regina Kleinhans^{1,2}, Heike Goehler^{3,4}, Erich E. Wanker³,
M. Cristina Cardoso³ and Heinrich Leonhardt^{1,2}

¹Ludwig Maximilians University Munich, Department Biology II, 82152 Planegg-Martinsried, Germany

²Munich Center for Integrated Protein Science CiPS^M

³Max Delbrueck Center for Molecular Medicine, 13125 Berlin, Germany

⁴present address: Medizinisches Proteom Center, Ruhr University Bochum, Germany

Correspondence should be addressed to H.L. (E-mail: h.leonhardt@lmu.de)

Abstract

Genetic high-throughput screens have yielded large sets of potential protein-protein interactions now to be verified and further investigated. Here we present a simple assay to directly visualize protein-protein interactions in single living cells. Using a modified lac repressor system, we tethered a fluorescent bait at a chromosomal *lac* operator array and assayed for co-localization of fluorescent prey fusion proteins. With this fluorescent two-hybrid (F2H) assay we successfully investigated the interaction of proteins from different subcellular compartments including nucleus, cytoplasm and mitochondria. In combination with an S phase marker we also studied the cell cycle dependence of protein-protein interactions. These results indicate that the F2H assay is a powerful tool to investigate protein-protein interactions within their cellular environment and to monitor the response to external stimuli in real-time.

Introduction

After sequencing the human genome the next challenge is now to analyze the complex protein-networks underlying cellular functions. In the last decade a wide variety of methods to study protein-protein interactions ranging from biochemical to genetic or cell-based approaches have been developed. Biochemical methods like affinity purification or co-immunoprecipitation allow the detection of protein complexes *in vitro*. Genetic methods, such as the yeast two-hybrid (Y2H) system, enable efficient high-throughput screening of interactions within the cellular environment. The analysis of mammalian protein interactions in yeast may, however, suffer from the absence or insufficient conservation of cellular factors modulating protein-protein interactions, e.g. through posttranslational modifications ¹.

In recent years new fluorescence-based methods for in-cell visualization of protein-protein-interactions have been introduced. Two established techniques, fluorescence resonance energy transfer (FRET) ^{2,3} and bimolecular fluorescence complementation (BiFC) ⁴, are based on the expression of fluorescently labelled proteins or fragments thereof. However, FRET requires costly instrumentation and advanced technical expertise, while BiFC is based on the irreversible complementation and slow maturation of fluorophores which does not allow real-time detection of protein-protein interactions ⁴.

All these methods have inherent shortcomings and are typically combined to obtain more reliable results. We have now developed a novel fluorescent two-hybrid (F2H) assay for the direct visualization of protein-protein interactions in living mammalian cells. The simple optical readout of this F2H assay allows observation of protein-protein interactions in real time and should also be suitable for high-throughput screens.

Results

To visualize protein-protein interactions in living cells in real time we developed a fluorescence two-hybrid (F2H) assay. The rationale for the F2H assay is based on the fact that proteins are freely roaming the cell unless interactions with other cellular components immobilize them at specific structures⁵.

We used a previously described BHK and an U2OS cell line which both harbor a stable integration of about 200-1000 copies of a plasmid carrying 256 copies of the *lac* operator sequence^{6,7}. We generated an expression construct encoding a fluorescent bait protein consisting of a fluorescent protein (FP), the *lac* repressor (LacI) and the protein X to be tested for interactions (bait) resulting in the triple fusion protein *FP-LacI-X* (**Fig. 1a**) or *X-LacI-FP*. This fusion protein binds to the operator array, which then becomes visible due to the focal enrichment of the FP signal. A second, differently labelled fusion protein (FP-Y, prey) may either interact with the bait protein X leading to co-localization of the FP signals (**Fig. 1b**) or may not interact, resulting in a dispersed distribution of the prey fluorescence (**Fig. 1c**).

Visualization of interactions between DNA repair proteins

To test the F2H assay, the previously described interaction between the two DNA repair proteins DNA Ligase III and XRCC1^{8,9} was analyzed and the results were compared with data obtained from pull down assays. We have previously shown that this interaction is mediated by the BRCT domain of DNA Ligase III which targets it to DNA repair sites¹⁰. We generated a bait fusion protein consisting of XRCC1 followed by the LacI and the monomeric red fluorescent protein RFP (mRFP). As expected this fusion protein localized at the *lac* operator array in transiently transfected BHK cells (**Fig. 2a**). Both, the full length GFP-tagged DNA Ligase III as well as the isolated GFP-labelled BRCT domain co-localize with XRCC1 at the *lac* operator array, while a fusion protein missing the BRCT domain shows a dispersed distribution. Notably, the highly homologous DNA Ligase I, which catalyzes the same reaction as DNA Ligase III, does not bind to XRCC1 (**Fig. 2a** and **supplementary Figure 1**). A direct comparison of the F2H data with data obtained from Co-IP experiments reveals that these two methods gave similar results (**Fig. 2b**). In addition, we could also observe the recently described interaction of XRCC1 with PCNA¹¹ and the two DNA-damage dependent PARPs, PARP-1 and PARP-2^{12,13} (**supplementary Figure 2**). These results demonstrate that the F2H assay is well suited to study protein-protein interactions in living cells.

Analysis of cell cycle dependence of protein-protein interactions

A challenge in the analysis of protein-protein interactions is to monitor transient changes caused by for example cell cycle progression or other external stimuli. We analyzed the previously described interaction between DNA methyltransferase 1 (Dnmt1) and PCNA which is mediated by the PCNA binding domain (PBD) and targets Dnmt1 to sites of DNA replication in S phase^{14,15}. These findings raised the question whether this interaction occurs only in S phase at replication foci or throughout the cell cycle. We generated two bait-proteins comprising parts of Dnmt1 fused to the LacI and YFP. One bait (PBD-LacI-YFP) comprises aa 118-427 of Dnmt1 including the PBD, while the second bait (Δ PBD-LacI-YFP) lacks the PBD and comprises aa 629-1089 of Dnmt1 (**Fig. 3a**). As a prey-protein we used RFP-PCNA which in addition marks sites of DNA replication allowing the identification of cells in S phase^{16,17}. The binding possibilities of these fusion proteins at the *lac* operator array and the replication fork are summarized in **Fig. 3b**.

In non S phase the LacI part of the bait proteins only binds to the chromosomally integrated *lac* operator array, which – dependent on the ploidy of the cell – becomes visible as one or two fluorescent spots in the nucleus. Interaction of RFP-PCNA with the PBD part of the bait protein results in co-localization of the fluorescent signals at the *lac* operator array (**Fig. 3c upper panel**), while deletion of the PBD in the bait protein leads to a dispersed distribution of RFP-PCNA in non S phase cells (**Fig. 3d upper panel**). This clearly illustrates that the PBD-dependent interaction of Dnmt1 with PCNA also occurs outside of S phase.

In S phase cells, RFP-PCNA localizes at sites of ongoing DNA replication and in addition is recruited to the *lac* operator array by the PBD-LacI-YFP bait protein (**Fig. 3c lower panel**). In contrast, when RFP-PCNA is coexpressed together with a bait protein lacking a functional PBD (Δ PBD-LacI-YFP), RFP-PCNA is exclusively enriched at DNA replication sites and not at the *lac* operator array highlighted by Δ PBD-LacI-YFP (**Fig. 3d lower panel**).

These results clearly show that the localization of RFP-PCNA (prey) at the *lac* operator array depends on the presence of the PBD in the bait construct and that this interaction is not restricted to S phase.

Next we analyzed the interaction of other PBD-containing proteins with PCNA. We generated a bait fusion protein comprising PCNA fused to an additional NLS followed by LacI and RFP (NLS-PCNA-LacI-RFP). When co-expressed with GFP-Ligase I, both fusion proteins localized to the *lac* operator array indicating interaction between PCNA and DNA Ligase I. Deletion of the PBD lead to a disperse distribution of DNA Ligase I, while the PBD of DNA Ligase I alone was sufficient for binding to PCNA at the *lac* operator array (**supplementary Figure 3**). This is in agreement with previous studies showing that the PBD of DNA Ligase I is necessary and sufficient for its targeting to DNA replication and repair sites^{10,18,19}. Notably, using the F2H assay we could demonstrate that DNA Ligase I, as well as the isolated PBD are capable of binding to PCNA also outside of S-phase. Likewise we could show binding of various additional replication and repair proteins like FEN1, p21 and the Polymerase δ subunit p66 to PCNA in non S-phase cells (**supplementary Figure 4**). Taken together we could show that the interaction between replication proteins and PCNA is not limited to S phase but also occurs in non S phase cells and outside the replication machinery. This illustrates that the F2H assay offers the unique potential to analyze cell cycle specific changes in protein-protein interactions in living cells.

Detection of interactions between proteins related to Huntington's disease

To investigate whether the F2H assay can also detect protein-protein interactions taking place in other cellular compartments, we tested the F2H assay with protein interactions identified in the context of Huntington's disease by yeast two-hybrid (Y2H) assays²⁰. We analyzed the interaction of one cytoplasmic (Vimentin) and two nuclear (HZFH and SUMO3) proteins. Vimentin has been described to be a cytoskeleton component and participates in transport processes, whereas HZFH and SUMO3 are involved in transcriptional regulation and DNA maintenance²⁰. These proteins were either fused with a red fluorescent mCherry-LacI-NLS or with NLS-GFP to generate sets of bait and prey proteins. BHK cells carrying a *lac* operator array were transfected with all possible combinations of expression constructs and subjected to microscopic analysis. We could detect an interaction between Vimentin and HZFH independent of whether these two proteins were used as bait or prey (**Fig.4** and data not shown). We could also detect the reported interaction between SUMO3 and HZFH while Vimentin and SUMO3 did not interact, as previously described (**Fig. 4**)²⁰. These results show that interactions of nuclear and cytoplasmic proteins can be studied with the F2H assay.

Detection of interactions between mitochondrial proteins

Next, we investigated whether the F2H assay is also suitable to detect protein-protein interactions occurring in other cellular organelles. To this end, we analyzed the interaction between two mitochondrial proteins, DDP1 (deafness dystonia peptide 1) and TIMM13. Both proteins are nuclear encoded and imported into the mitochondrial intermembrane space (IMS) forming a hexameric complex (**Fig. 5a**). Within the IMS the DDP1-TIMM13 complex facilitates the import of hydrophobic proteins of the mitochondrial import machinery into the mitochondrial innermembrane²¹. A mutation of the *DDP1* gene was associated with the Mohr-Tranebjaerg-Syndrome, which is a progressive, neurodegenerative disorder²². This C66W missense mutation is known to cause a full blown phenotype and affects the highly conserved Cys(4) motif of DDP1. Previous studies have shown, that this amino acid exchange abolishes the interaction between DDP1 and TIMM13 in the IMS²³.

Using a red fluorescent bait fusion protein comprising LacI-NLS-TIMM13 and GFP-tagged wildtype (GFP-DDP1) or mutant DDP1 (GFP-DDP1^{C66W}) prey proteins we analyzed this specific mitochondrial protein interaction with the F2H assay. We found that GFP-DDP1 co-localizes with TIMM13 at the *lac* operator array (**Fig. 5b**), while GFP-DDP1^{C66W} was evenly distributed (**Fig. 5c**). These results demonstrate that the F2H assay is also suitable for the analysis of protein-protein interactions occurring outside the nucleus and the characterization of disease related point mutations disrupting these interactions.

Discussion

Here we describe a new method to detect and visualize protein-protein interactions in living cells, which we termed fluorescent two-hybrid assay (F2H). This method is based on the immobilization of a fluorescently labeled bait protein at a distinct subcellular structure enabling the detection of protein-protein interactions as co-localization of a differently labeled prey protein at this defined structure. The F2H assay described takes advantage of cell lines with a stable integration of a *lac* operator array to immobilize a *lac* repressor fused to fluorescently labeled proteins of interest (bait). Readily usable cell lines have already been described for human, mouse, hamster and *Drosophila*^{6,7,24-27}. To be independent of specific transgenic cell lines this assay could be modified by using various cellular structures like the lamina, the cytoskeleton or centrosomes as anchoring structures to locally immobilize bait proteins.

Like other genetic two-hybrid methods also the F2H assay may yield false positive or false negative results, which need to be controlled for. Prey proteins that bind to the *lac* operator array in the absence of a bait protein can be identified by an initial screen and then be only used as baits. We analyzed more than 20 protein-protein interactions from different subcellular compartments with the F2H assay and obtained identical results as previously described with other genetic or biochemical methods. Only one protein (SUMO3) was found to bind by itself to the *lac* operator array and could therefore only be used as a bait protein. These results show that the F2H assay is a reliable and broadly applicable method to study protein-protein interactions.

In some cases, proteins may accumulate at subnuclear foci and thus complicate the F2H analysis. To bypass this problem, the *lac* operator array could be visualized and identified with a third fluorescent fusion protein like CFP-Lacl.

In summary, this new F2H assay allows the direct visualization of protein-protein interactions and should be ideally suited to investigate cell cycle or differentiation dependent changes in real-time in living cells. A significant advantage of the F2H assay over other cell-based techniques is its simplicity that does neither require costly instrumentation nor advanced technical expertise. The simple optical read-out of the F2H assay additionally offers the possibility to use this assay in automated high-throughput screens to systematically analyze the protein interactome in living cells.

Methods

Expression constructs

The LacI encoding sequence was PCR amplified from the p3'SS EGFP-LacI expression vector²⁴ using the following primers: forward primer 5'-TCT AGA AAG CTT TCC ATG GTG AAA CCA GTA-3' and reverse primer 5'-CCA TGC CCG GGA CAG GCT GCT TCG GGA AAC-3' (restriction sites in italic). This PCR fragment was digested with HindIII and XmaI and cloned into the same sites of two Dnmt1-YFP expression vectors (MTNY.2 and PBHD-YFP)¹⁵ generating PBD-LacI-YFP and ΔPBD-LacI-YFP. The NLS-PCNA-LacI-RFP and XRCC1-LacI-RFP constructs were generated by PCR amplification of the PCNA and XRCC1 cDNA using the following primers (restriction sites in italic):

PCNA forward	5'-CCCCCTCGAGATGTTTCGAGGCGCGC-3'
PCNA reverse	5'-GGGGAAGCTTGGAGATCCTTCTTCATCCTC-3'
XRCC1 forward	5'-CCCCAGATCTATGCCGGAGATCCGC-3'
XRCC1 reverse	5'-GGGGGAATTCGGGGCTTGCGGCACCAC-3'

Subsequently the PCR fragments were cloned into a LacI-RFP expression vector using the XhoI/HindIII sites for the NLS-PCNA-LacI-RFP and the BglII/EcoRI sites for the XRCC1-LacI-RFP expression vector.

All other F2H constructs were generated by PCR amplification of coding cDNAs and subsequent ligation into the AsiSI and NotI sites of the bait and prey expression vectors described in Figure 1 a. The following primers were used with the restriction site indicated in italics:

DDP1 forward	5'-CCCCGCGATCGCGATTCTCCTCCTCTTCCTC-3'
DDP1 reverse	5'-CCCCGCGGCCGCTCAGTCAGAAAGGCTTTCTG-3'
TIMM13 forward	5'-CCCCGCGATCGCGAGGGCGGCTTCGGCTCC-3'
TIMM13 reverse	5'-CCCCGCGATCGCGAGGGCGGCTTCGGCTCC-3'
HZFH forward	5'-GGGGGCGATCGCCACGCCGCTTCC-3'
HZFH reverse	5'-CCCCGCGGCCGCTTAGTCGTCTATACAGATCACCTCC-3'
SUMO3 forward	5'-CCCCGCGATCGCGCCGACGAAAAGCCCAAG-3'
SUMO3 reverse	5'-CCCCGCGGCCGCTCAGTAGACACCTCCG-3'
Vim forward	5'-GGGGTGACAGCGATCGCATGTGACCCACGCGT-3'
Vim reverse	5'-CCCCGAATTCGCGGCCGCTTATTCAAGGTCATCGTGATGCT-3'

Mammalian expression constructs encoding translational fusions of human DNMT1, DNA-Ligase I, DNA-Ligase III, p21, FEN I, Polymerase δ p66 subunit, PARP-1, PARP-2 and PCNA were previously described^{16,28-32}. Deletion constructs and isolated domains of DNA-Ligase I and III were described in Mortusewicz et al¹⁰. Immunoprecipitations were performed with a GFP-nanotrap³³ as described before¹⁰. All fusions constructs were tested for correct expression and localization.

Cell culture and transfection

Transgenic BHK cells (clone #2) and U2OS cells (clone 2-6-3) containing *lac* operator repeats were cultured under selective conditions in DMEM supplemented with 10% fetal calf serum and 150 μ g/ml hygromycin B (PAA Laboratories) as described^{6,7}. For microscopy cells were grown to 50-70% confluence either on 18x18 glass coverslips or in μ -slides (ibidi, Munich, Germany) and then co-transfected with the indicated expression constructs using Polyplus transfection reagent jetPEITM (BIOMOL GmbH, Hamburg, Germany) according to the manufacturer's instructions. After 6-10 hours the transfection medium was changed to fresh culture medium and cells were then incubated for another 12-24 hours before live cell microscopy or fixation with 3.7 % formaldehyde in PBS for 10 min at room temperature. Fixed cells were permeabilized with 0.2 % Triton X-100 in PBS for 3 min, counterstained with DAPI and mounted in Vectashield (Vector Laboratories, CA, USA).

Microscopy

Live or fixed cells expressing fluorescent proteins were analyzed using a Leica TCS SP2 AOBS confocal microscope equipped with a 63x/1.4 NA Plan-Apochromat oil immersion objective. Fluorophores were excited with a 405 nm Diode laser, a 488 nm and a 514 nm Ar laser and a 561 nm Diode-Pumped Solid-State (DPSS) laser. Confocal image stacks of living or fixed cells were typically recorded with a frame size of 512x512 pixels, a pixel size of 50-100 nm, a z-step size of 250 nm and the pinhole opened to 1 Airy unit. A maximum intensity projection of several mid z-sections was generated with ImageJ (Version 1.38, <http://rsb.info.nih.gov/ij/>).

Acknowledgements

We thank D.L. Spector for providing BHK clone#2 and U2OS.2-6-3 cells containing a *lac* operator array, V. Schreiber for GFP-tagged PARP-1 and PARP-2 constructs and R.Y. Tsien for mRFP1 and mCherry cDNA. We thank L. Schermelleh and F. Spada for helpful comments and suggestions. We are grateful to G. Li for help in plasmid construction. This work was supported by grants from the Deutsche Forschungsgemeinschaft to M.C.C. and H.L.

References

1. J. R. Parrish, K. D. Gulyas, and R. L. Finley, Jr., *Curr Opin Biotechnol* **17** (4), 387 (2006).
2. R. B. Sekar and A. Periasamy, *J Cell Biol* **160** (5), 629 (2003).
3. A. Miyawaki, *Dev Cell* **4** (3), 295 (2003).
4. T. K. Kerppola, *Nat Rev Mol Cell Biol* **7** (6), 449 (2006).
5. R. D. Phair and T. Misteli, *Nature* **404** (6778), 604 (2000).
6. T. Tsukamoto, N. Hashiguchi, S. M. Janicki et al., *Nat Cell Biol* **2** (12), 871 (2000).
7. S. M. Janicki, T. Tsukamoto, S. E. Salghetti et al., *Cell* **116** (5), 683 (2004).
8. K. W. Caldecott, C. K. McKeown, J. D. Tucker et al., *Mol Cell Biol* **14** (1), 68 (1994).
9. Y. F. Wei, P. Robins, K. Carter et al., *Mol Cell Biol* **15** (6), 3206 (1995).
10. O. Mortusewicz, U. Rothbauer, M. C. Cardoso et al., *Nucleic Acids Res* **34** (12), 3523 (2006).
11. J. Fan, M. Otterlei, H. K. Wong et al., *Nucleic Acids Res* **32** (7), 2193 (2004).
12. V. Schreiber, J. C. Ame, P. Dolle et al., *J Biol Chem* **277** (25), 23028 (2002).
13. M. Masson, C. Niedergang, V. Schreiber et al., *Mol Cell Biol* **18** (6), 3563 (1998).
14. L. S. Chuang, H. I. Ian, T. W. Koh et al., *Science* **277** (5334), 1996 (1997).
15. H. P. Easwaran, L. Schermelleh, H. Leonhardt et al., *EMBO Rep* **5** (12), 1181 (2004).
16. A. Sporbert, P. Domaing, H. Leonhardt et al., *Nucleic Acids Res* **33** (11), 3521 (2005).
17. H. P. Easwaran, H. Leonhardt, and M. C. Cardoso, *Cell Cycle* **4** (3) (2005).
18. M. C. Cardoso, C. Joseph, H. P. Rahn et al., *J Cell Biol* **139** (3), 579 (1997).
19. A. Montecucco, E. Savini, F. Weighardt et al., *Embo J* **14** (21), 5379 (1995).
20. H. Goehler, M. Lalowski, U. Stelzl et al., *Mol Cell* **15** (6), 853 (2004).
21. U. Rothbauer, S. Hofmann, N. Muhlenbein et al., *J Biol Chem* **276** (40), 37327 (2001).
22. L. Tranebjaerg, C. Schwartz, H. Eriksen et al., *J Med Genet* **32** (4), 257 (1995).
23. S. Hofmann, U. Rothbauer, N. Muhlenbein et al., *J Biol Chem* **277** (26), 23287 (2002).

-
24. C. C. Robinett, A. Straight, G. Li et al., *J Cell Biol* **135** (6 Pt 2), 1685 (1996).
 25. T. Tumber, G. Sudlow, and A. S. Belmont, *J Cell Biol* **145** (7), 1341 (1999).
 26. S. Dietzel, K. Zolghadr, C. Hepperger et al., *J Cell Sci* **117** (Pt 19), 4603 (2004).
 27. J. Vazquez, A. S. Belmont, and J. W. Sedat, *Curr Biol* **11** (16), 1227 (2001).
 28. O. Mortusewicz, L. Schermelleh, J. Walter et al., *Proc Natl Acad Sci U S A* (2005).
 29. L. Schermelleh, F. Spada, H. P. Easwaran et al., *Nat Methods* **2** (10), 751 (2005).
 30. O. Cazzalini, P. Perucca, F. Riva et al., *Cell Cycle* **2** (6), 596 (2003).
 31. Y. Maeda, T. C. Hunter, D. E. Loudy et al., *J Biol Chem* **281** (14), 9600 (2006).
 32. V. S. Meder, M. Boeglin, G. de Murcia et al., *J Cell Sci* **118** (Pt 1), 211 (2005).
 33. U. Rothbauer, K. Zolghadr, S. Muyldermans et al., *Mol Cell Proteomics* (2007).

Figures

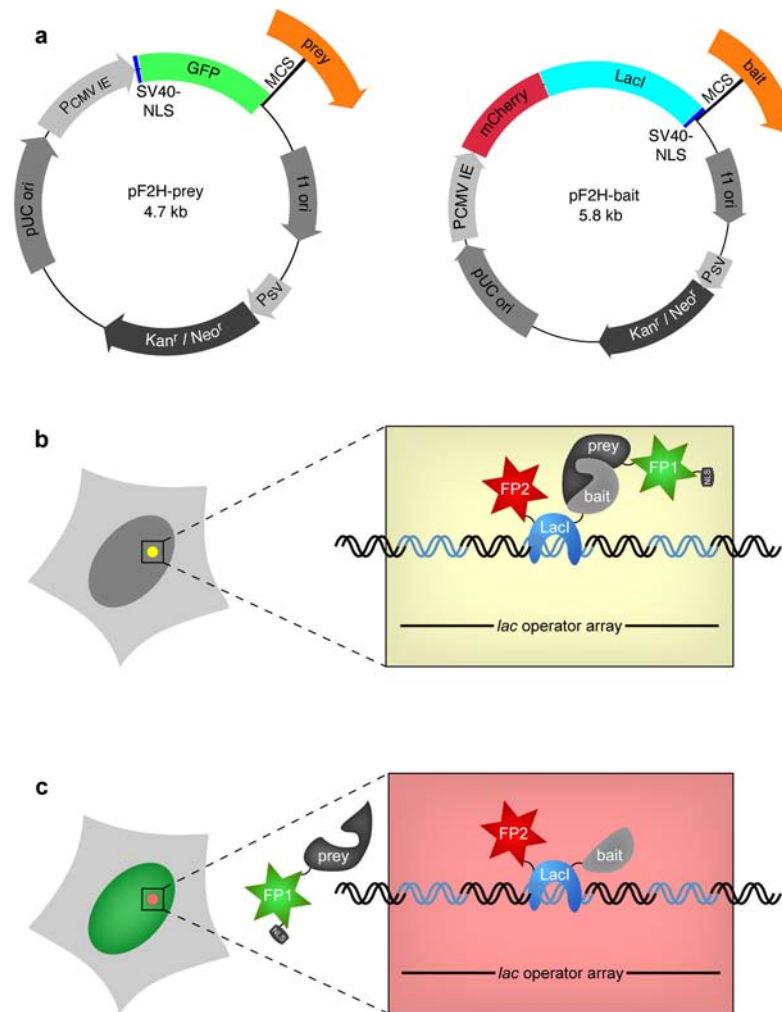
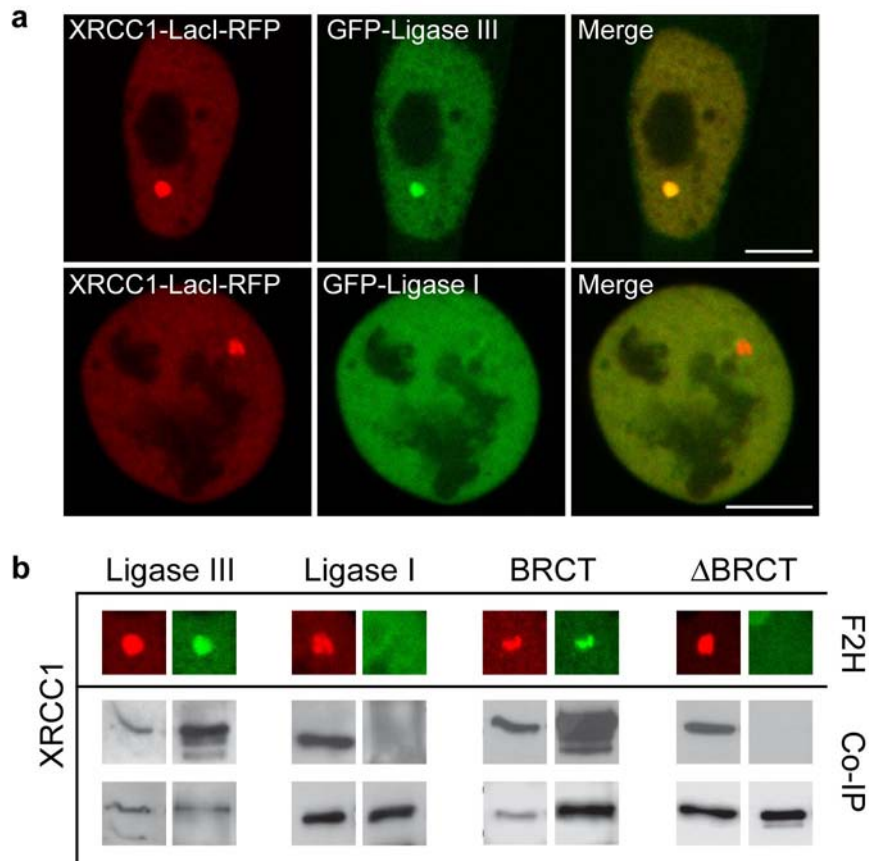


Figure 1

Schematic outline of the fluorescent two-hybrid (F2H) assay. (a) Outline of pF2H-prey and pF2H-bait expression vectors coding for fluorescently labeled prey- and bait- proteins used for the F2H assay (b) The LacI domain of the bait-protein mediates binding to the chromosomally integrated *lac* operator array, which is visible as a fluorescent spot in nuclei of transfected cells. If the differentially labeled prey interacts with the bait it becomes enriched at the same spot resulting in co-localization of fluorescent signals at the *lac* operator (visible as yellow spot in the overlay image). (c) If the prey does not interact with the bait protein it remains dispersed in the nucleus and the *lac* operator array is only visualized by the bait protein (red spot). FP1 and FP2 refer to two distinguishable fluorescent proteins, e.g. GFP or YFP and mCherry or mRFP.

**Figure 2**

Specific interaction of DNA Ligase III with XRCC1 revealed by F2H (a) Transgenic BHK cells containing a chromosomal *lac* operator array were co-transfected with XRCC1-LacI-RFP and GFP-tagged DNA Ligase III or DNA Ligase I constructs. The *lac* repressor part of the XRCC1-LacI-RFP fusion protein mediates binding to the *lac* operator array (visible by fluorescence microscopy as red spot). DNA Ligase III is recruited to the *lac* operator array through interaction with XRCC1. Note that the highly homologous DNA Ligase I does not accumulate at the *lac* operator array indicating that it does not interact with XRCC1. Scale bars 5 μ m. (b) Comparison of F2H results and co-immunoprecipitation (Co-IP) experiments. Co-IPs were performed with 293T cells co-expressing RFP-XRCC1 and GFP-Ligase III or GFP-Ligase I, respectively. For interaction mapping the GFP-tagged BRCT domain of DNA Ligase III and a deletion construct lacking the BRCT domain were used. Immunoprecipitations were performed with a GFP-nanotrap³³ (as shown before¹⁰). Precipitated fusion proteins were then detected with specific antibodies against RFP and GFP on western blots. RFP-XRCC1 was co-precipitated with GFP-Ligase III but not with GFP-Ligase I. RFP-XRCC1 was also co-precipitated with GFP-Ligase III BRCT but not with GFP-N-Ligase III Δ BRCT. For comparison of F2H

results the input (left) and bound (right) bands from Co-IPs were aligned with corresponding signals from the F2H assay. The LacI spot of the XRCC1-LacI-RFP bait construct shown in red and the bound fraction was aligned with the respective signal of the GFP-tagged prey constructs. Whole cell images of the respective F2H experiments are shown in (a) and **supplementary Figure 1**.

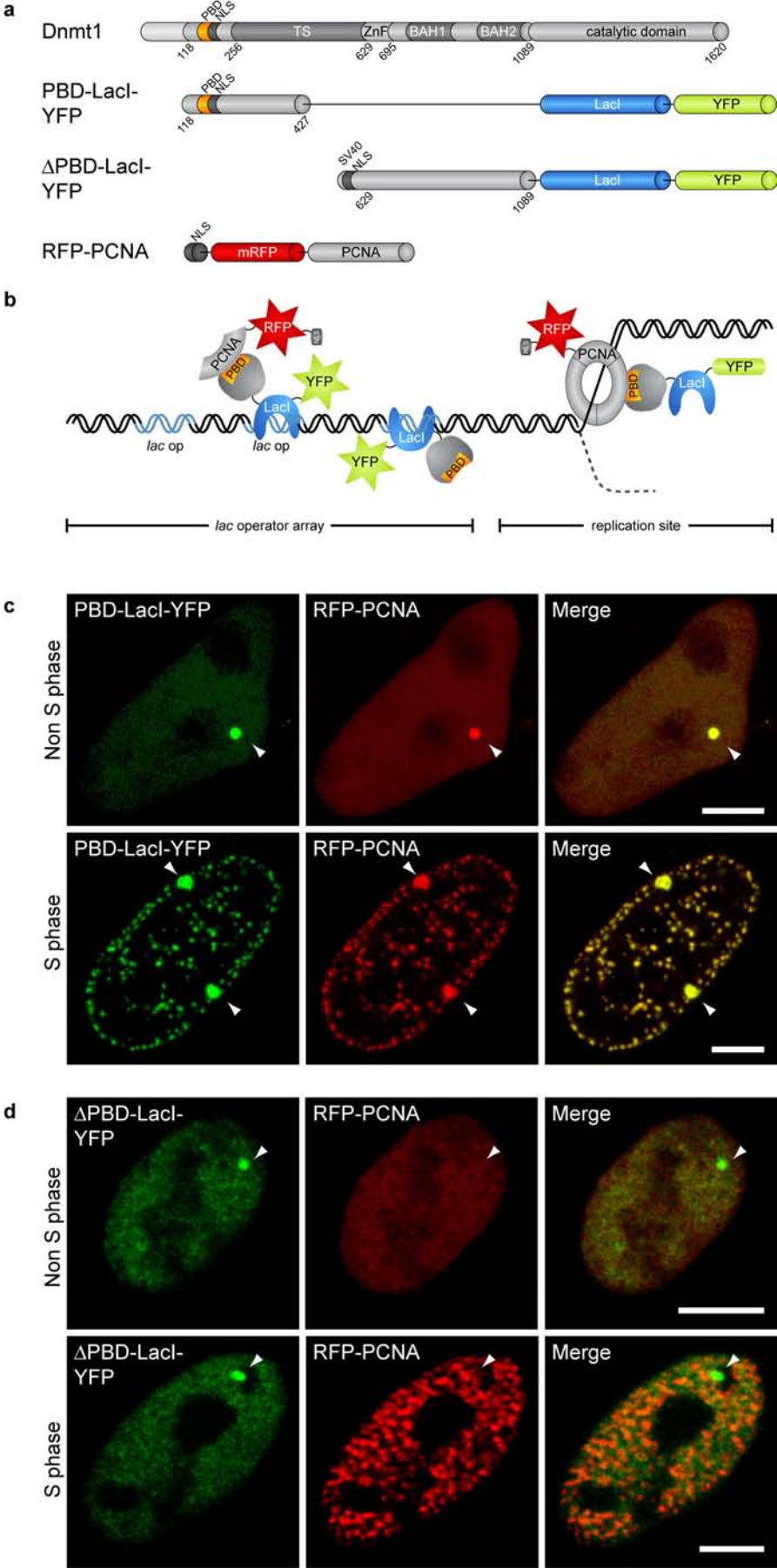
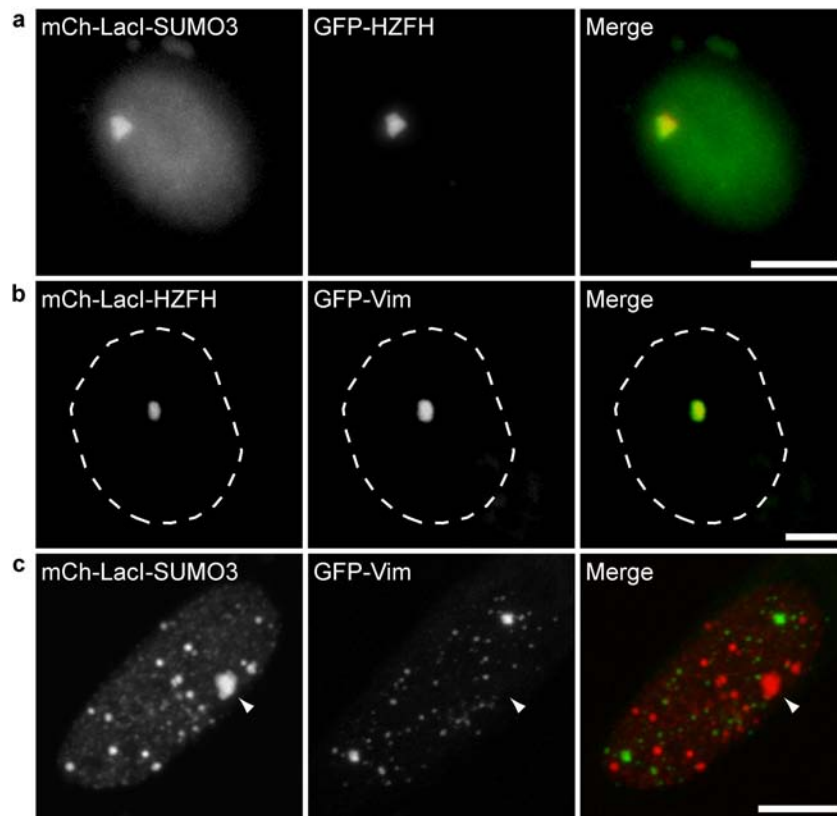


Figure 3

F2H analysis of cell cycle independent interaction of Dnmt1 with PCNA. (a) Schematic outline of full-length mouse Dnmt1 and fusion proteins. PBD, PCNA binding domain; NLS, nuclear localization sequence; TS, targeting sequence; ZnF, Zn²⁺-binding region; BAH 1 and 2, two Bromo Adjacent Homology domains. (b) Outline of binding possibilities of fusion proteins at the *lac* operator (*lac op*) array and at the replication fork. (c) Transgenic BHK cells containing a chromosomal *lac* operator array were co-transfected with PBD-LacI-YFP and RFP-PCNA constructs. RFP-PCNA shows the characteristic cell cycle dependent distribution (dispersed in non S phase cells (top row) and focal patterns in S phase (bottom row)). The *lac* repressor part of the PBD-LacI-YFP fusion protein mediates binding to the *lac* operator array (visible as green spot and highlighted by arrowheads) and the PBD mediates binding to PCNA at replication sites (focal pattern in S phase). Notice, RFP-PCNA is localized at the *lac* operator array in S and non S phase cells indicating an interaction of the PBD of Dnmt1 with PCNA throughout the cell cycle and independent of the replication machinery. (d) BHK cells were transfected with expression vectors for Δ PBD-LacI-YFP and RFP-PCNA. As above, RFP-PCNA shows a disperse distribution in non S phase (top row) and redistributes to replication sites in S phase (bottom row). The Δ PBD-LacI-YFP fusion protein binds to the *lac* operator array (green spot marked by arrowhead) but does not bind to replication sites in S phase since it lacks the PBD. Importantly, in these cells RFP-PCNA (prey) is not localized at the *lac* operator array (marked by arrowheads) indicating that binding depends on the presence of the PBD, which is absent in Δ PBD-LacI-YFP (bait). Scale bars 5 μ m

**Figure 4**

Analysis of Huntington's disease related interactions by F2H. (a) Reported interactions between (a) SUMO3 and HZFH and (b) HZFH and Vimentin revealed by F2H. (c) F2H analysis shows no interaction between SUMO3 and Vimentin as previously described²⁰. In (b) the nucleus is outlined by a dashed line and in (c) the *lac* operator array is indicated (arrowheads). Scale bars 5 μ m.

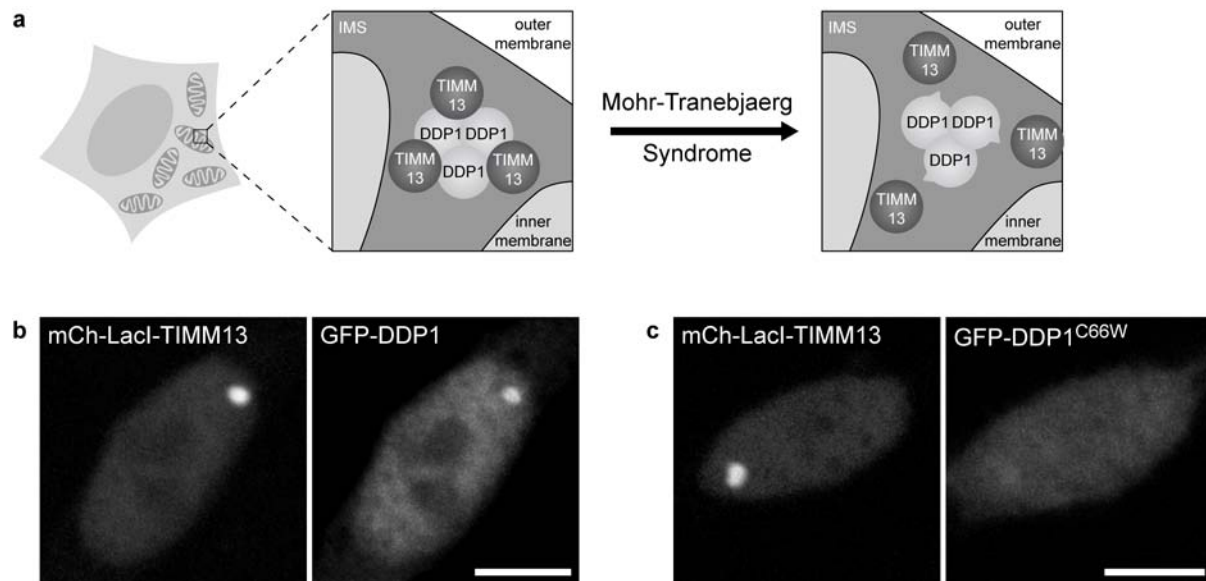
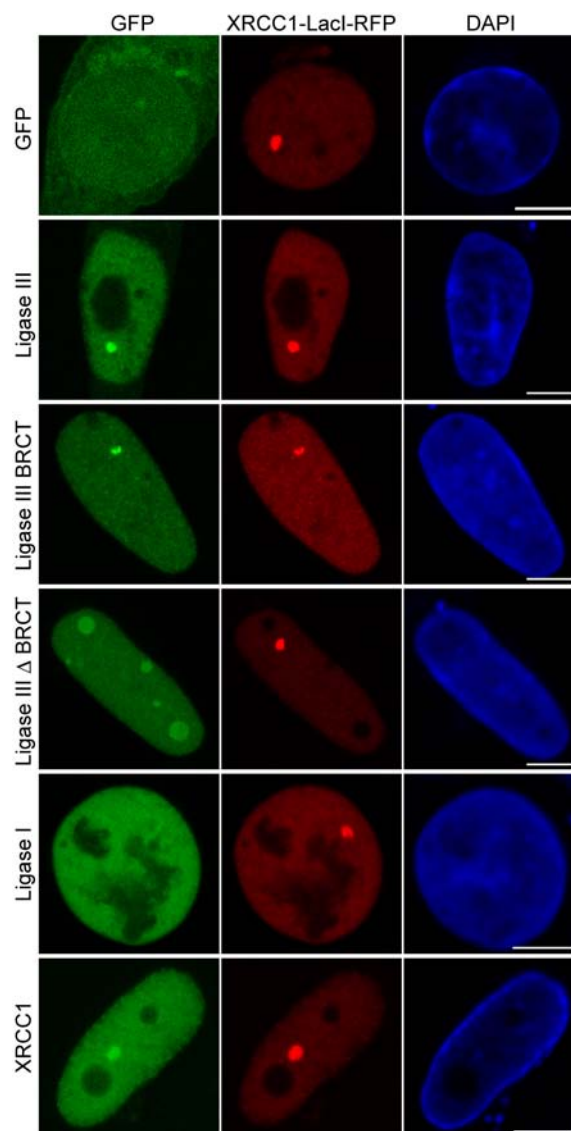
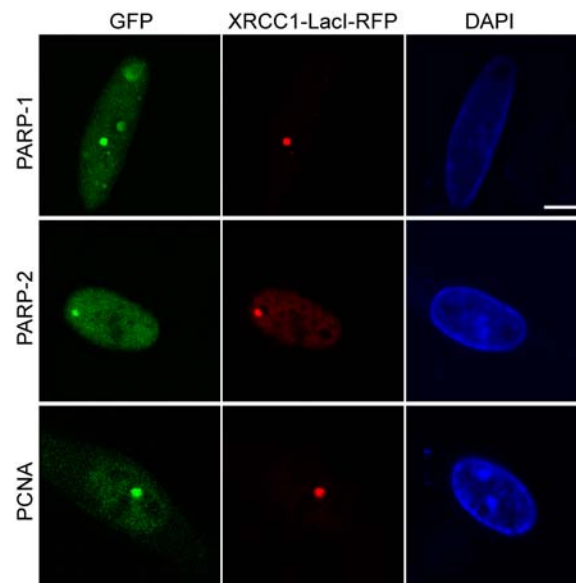


Figure 5

Analysis of mitochondrial protein-protein interactions and the effect of a mutation associated with the Mohr-Tranebjaerg Syndrome. (a) Schematic overview of the hexameric DDP1-TIMM13 complex in the intermembrane space (IMS) of mitochondria. (b + c) BHK cells expressing the bait-protein mCherry-LacI-TIMM13 together either with GFP-DDP1 (b) or the loss-of-function mutant GFP-DDP1^{C66W} (c). While the functional wt fusion GFP-DDP1 shows interaction with TIMM13 revealed by co-localization of fluorescent signals at the *lac* operator array (b), the GFP-DDP1^{C66W} mutant is dispersedly distributed throughout the nucleus indicating no interaction (c). Scale bars 5 μ m.

Supplementary Information**Supplementary Figure 1**

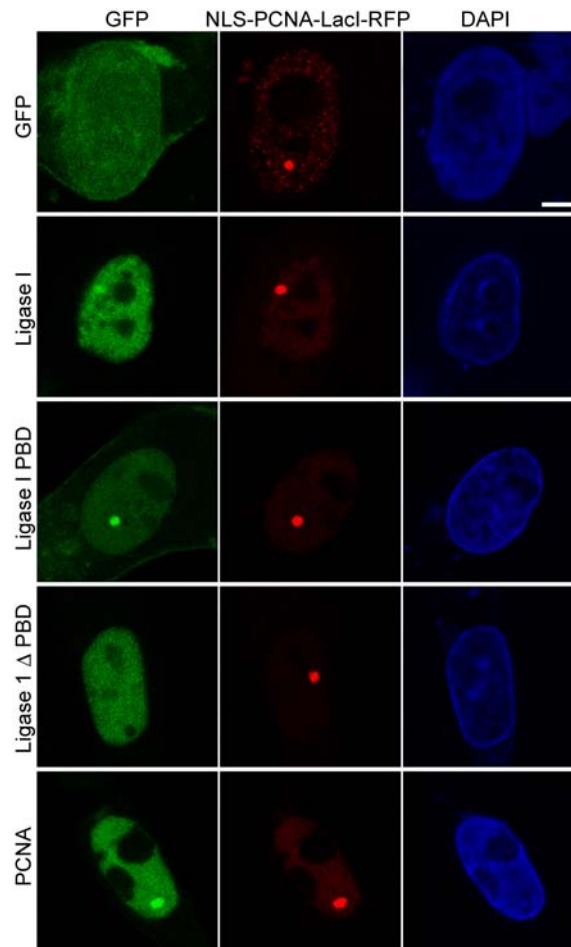
BRCT mediated interaction of DNA-Ligase III with XRCC1 revealed by the F2H assay. Transgenic BHK cells containing a *lac* operator array were co-transfected with XRCC1-LacI-RFP and various GFP-tagged DNA-Ligase III constructs. The *lac* repressor part of the XRCC1-LacI-RFP fusion protein mediates binding to the *lac* operator array (visible as red spot). The BRCT domain is necessary and sufficient for targeting of DNA Ligase III to the *lac* operator array through interaction with XRCC1. Note that the highly homologous DNA Ligase I does not accumulate at the *lac* operator array indicating that it does not interact with XRCC1. Scale bars 5 μ m.



Supplementary Figure 2

The F2H assay reveals the interaction of XRCC1 with PCNA, PARP-1 and PARP-2. BHK cells containing a *lac* operator array were transfected with expression vectors for XRCC1-LacI-RFP and either GFP-PARP-1, GFP-PARP-2 or GFP-PCNA. The *lac* repressor part of the XRCC1-LacI-RFP fusion protein mediates binding to the *lac* operator array (visible as red spot). GFP-PARP-1, GFP-PARP-2 and GFP-PCNA are targeted to the *lac* operator array indicating an interaction with XRCC1.

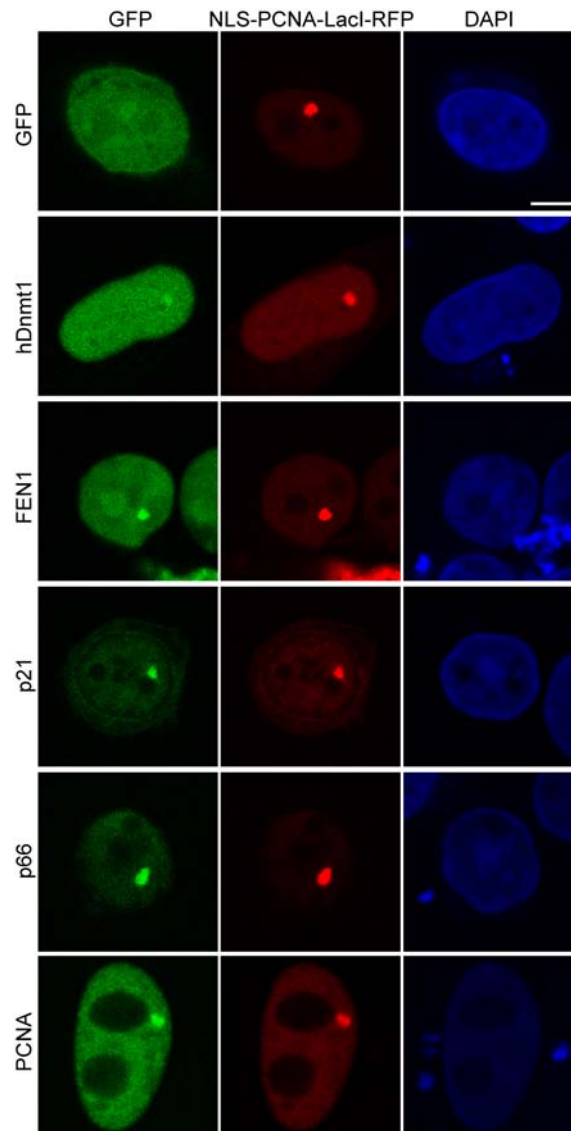
Scale bar 5 μ m.



Supplementary Figure 3

The F2H assay reveals the PBD-mediated interaction of DNA-Ligase I with PCNA. Transgenic U2OS cells containing a *lac* operator array were co-transfected with NLS-PCNA-LacI-RFP and various GFP-tagged DNA-Ligase I constructs. The *lac* repressor part of the NLS-PCNA-LacI-RFP fusion protein mediates binding to the *lac* operator array (visible as red spot). The PBD is necessary and sufficient for targeting of DNA Ligase I to the *lac* operator array through interaction with PCNA.

Scale bar 5 μ m.



Supplementary Figure 4

Interaction of various replication and repair proteins with PCNA revealed by the F2H assay. Transgenic BHK cells containing a *lac* operator array expressing NLS-PCNA-LacI-RFP and various GFP-tagged replication and repair proteins. All proteins tested interact with PCNA. Scale bar 5 μ m.

3. DISCUSSION

Pioneering work using mainly *in vitro* experiments gave detailed insights into the biochemical mechanisms and composition of the various DNA repair pathways. However, the identification of more and more proteins being involved in the various steps of DNA repair, as well as the emerging interconnection between different DNA repair pathways, requires studying the spatio-temporal coordination of DNA repair in living cells. In recent years, several methods have been introduced that allow DNA lesion induction and subsequent real-time analysis of the DNA damage response in living cells. Using laser microirradiation, live cell microscopy and photobleaching analysis in combination with specific inhibitors and mutants, we studied the recruitment kinetics and role of various DNA repair factors involved in processes ranging from DNA lesion detection to restoration of epigenetic information (**Figure 4**).

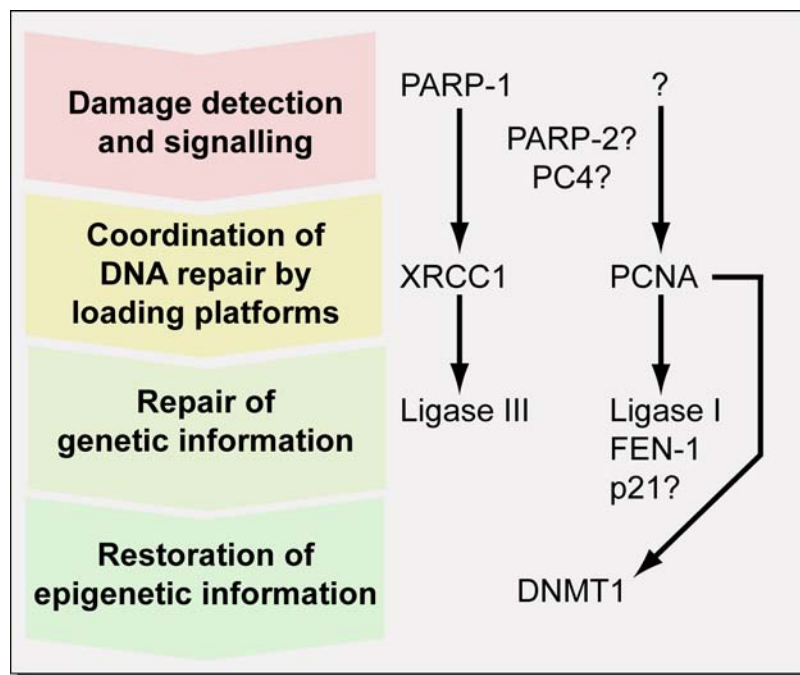


Figure 4 Summary of proteins analyzed in this study and their respective role in the four major steps of the DNA damage response. Question marks indicate that the precise function(s) of the respective protein is still unclear.

3.1. DNA lesion detection and signalling

Immediate and efficient sensing of DNA lesions is crucial for cellular survival. Several enzymes have been described to be involved in this first common step of all DNA repair pathways. However, it is still unclear how specific lesions are recognized within the context of chromatin. To gain insights into the mechanisms of lesion detection and signalling, we analyzed the recruitment kinetics of the two DNA-damage-dependent PARPs, PARP-1 and PARP-2, and of a recently identified potential component of the DNA damage response, the RNA Polymerase II cofactor PC4.

PARP-1 and PARP-2 are involved in the early steps of DNA repair

The requirement of the two DNA-damage dependent PARPs, PARP-1 and PARP-2, for DNA repair have been demonstrated by various genetic studies of knock-out mice and cells (de Murcia et al., 1997; Masutani et al., 1999; Menissier de Murcia et al., 2003; Schreiber et al., 2002; Trucco et al., 1998; Wang et al., 1997). Based on the interaction of PARP-1 and PARP-2 with common proteins involved in genome restoration on the one hand and their binding to different DNA lesions and substrates on the other hand, it was suggested that PARP-1 and PARP-2 have both overlapping and non-redundant functions (Menissier de Murcia et al., 2003; Schreiber et al., 2002; Werten et al., 1998). Yet, there have been reports questioning the importance of PARP-1 or PARP-2 for DNA repair (Fisher et al., 2007; Vodenicharov et al., 2000). We compared the spatio-temporal redistribution of PARP-1 and PARP-2 in response to DNA damage induced by laser microirradiation in living cells. Both DNA-damage dependent PARPs were recruited to laser-induced DNA damage sites, albeit with different kinetics. While PARP-1 showed a fast and transient accumulation consistent with its proposed role as a DNA damage sensor, PARP-2 exhibited a slow and constant accumulation at DNA damage sites. Together with earlier findings demonstrating that PARP-2 has a high affinity for gap and flap structures (Schreiber, 2004) this suggests, that PARP-2 is rather involved in the latter steps of DNA repair, like processing of repair intermediates.

Interestingly, we found that the recruitment efficiency of both, PARP-1 and PARP-2, depends on their enzymatic activity. Further analysis of PARP-1 recruitment mechanisms showed that PARP-1 recruitment is mainly mediated by its N-terminal DNA binding domain (DBD). PAR generated by PARP-1 at the damage site is then recognized by the BRCT domain of PARP-1 leading to a second wave of PARP-1

recruitment. In addition to being required for efficient recruitment of PARP-1, the catalytic activity of PARP-1 is also needed for its dissociation from repair sites. This observation could be explained with earlier findings, showing that automodification of PARP-1 abolishes DNA binding *in vitro* (Ferro and Olivera, 1982). Finally, using knock-out cells and rescue experiments we could show, that PARP-1 activity is essential for the rapid recruitment of the central loading platform XRCC1 by generating high affinity binding sites. Taken together, these data argue for three distinct roles of PARP-1 in response to DNA damage: the detection and labelling of the damaged site, the local relaxation of chromatin structure and the recruitment of repair factors.

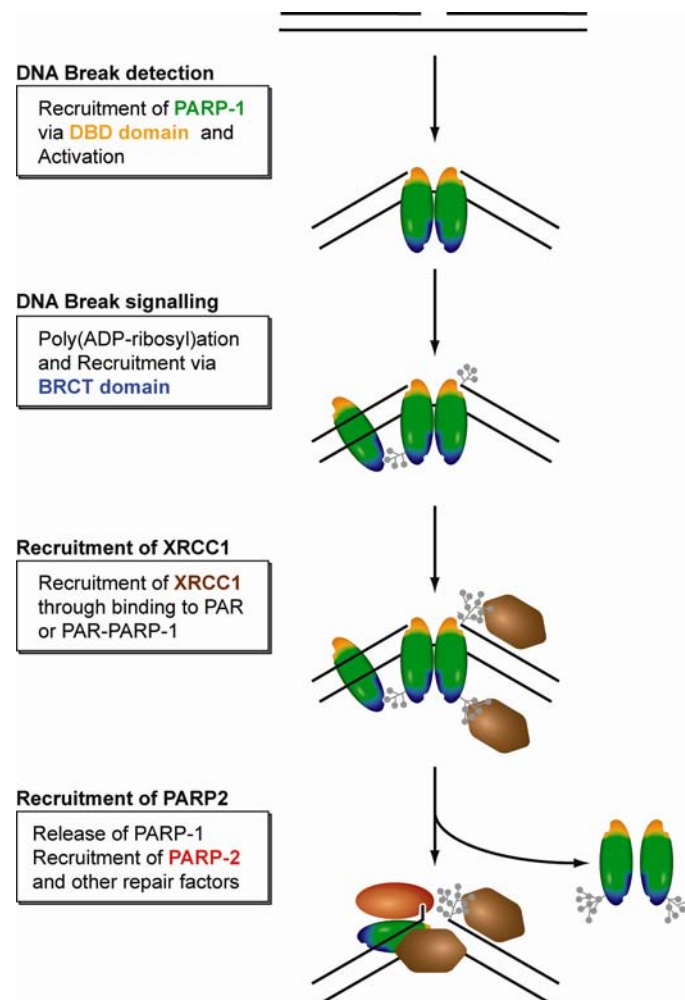


Figure 5 Simplified model for the recruitment of repair factors to SSB. For a detailed discussion of the role and regulation of PARPs see text.

In summary, we propose the following model for the spatio-temporal accumulation of SSB/BER factors at DNA strand breaks (**Figure 5**). Single strand breaks are detected by the DNA binding domain of PARP-1. Poly(ADP-ribosylation) by PARP-1

leads to chromatin relaxation and attracts additional PARP-1 molecules via its BRCT domain. Further poly(ADP-ribosyl)ation at DNA lesions then leads to the release of PARP-1 through charge repulsion enabling a switch to the next step in DNA repair initiated by the recruitment of the versatile loading platform XRCC1. Interestingly, PARP-2 which is required for DNA repair could not replace PARP-1 in the rapid recruitment of repair factors. However, we cannot exclude that PARP-2 could contribute to the slow recruitment of XRCC1 observed in *parp-1*^{-/-} MEFs.

We have identified a complex feedback network for the recruitment of the DNA damage sensor PARP-1. After lesion detection, PARP-1 activation and poly(ADP-ribosyl)ation leads to a positive feedback loop accumulating more PARP-1 and thus amplifying the signal for rapid recruitment of repair factors. Further accumulation is countered by a negative feedback resulting in the release of PARP-1 likely to protect against uncontrolled poly(ADP-ribosyl)ation which would disrupt cellular functions and lead to apoptosis. This feedback regulated recruitment of PARP-1 at DNA lesions thus allows a balance between signal amplification for rapid recruitment of repair factors and protection against extensive poly(ADP-ribosyl)ation.

Role of the RNA Polymerase II cofactor PC4 in DNA repair

Detection of DNA lesions induces various cellular responses including alterations in transcription. Recently, an interesting connection between transcriptional regulation and DNA repair has been drawn by the identification of the RNA Polymerase II cofactor PC4 as a potential DNA repair factor (Wang et al., 2004). We analyzed the role of PC4 in the mammalian DNA damage response using live cell microscopy in combination with microirradiation and FRAP analysis. We found a fast and transient accumulation of the transcriptional cofactor PC4 at DNA damage sites depending on its single strand binding capacity. This observation suggested that PC4 might fulfil similar roles in DNA repair as the single strand binding protein RPA. However, the different recruitment kinetics and turnover rates of PC4 and RPA at laser-induced DNA damage sites argue for distinct roles in DNA repair. PC4 might in fact inhibit the functions of RPA in S phase leading to a stop of DNA replication as a response to DNA damage (Pan et al., 1996). In addition, PC4 might also stop transcription as a response to DNA damage which is supported by the fact that PC4 is a potent repressor of transcription at specific DNA structures such as ssDNA, DNA ends and heteroduplex DNA which are generated during DNA repair (Werten et al., 1998).

Moreover, PC4 could have a helicase-like function (Werten and Moras, 2006; Werten et al., 1998), which through binding and multimerization along ssDNA is predicted to enable ATP-independent unwinding of duplex DNA.

The crystallization of PC4 in complex with ssDNA revealed that the subunits of the PC4 homodimer cooperate in the sequence-independent binding (Ballard et al., 1988) of two opposing DNA backbones, exposing the DNA bases to the surrounding environment (Werten and Moras, 2006). These observations together with the rapid recruitment of PC4 to DNA damage sites argue for a role of PC4 in the detection and/or exposure of DNA damages. During the subsequent repair process PC4 may be displaced, as suggested by the observed transient binding at damaged sites.

3.2. The role of p21 in DNA repair

The next important step in the DNA damage response after lesion detection is the activation of checkpoint controls leading to cell cycle arrest, which allows time for repair. A protein, which is believed to play a central role in checkpoint activation, is the cyclin dependent kinase inhibitor p21. However, the precise role of p21 in the DNA damage response is under heavy debate. While some data indicated that p21 inhibits DNA repair and thus has to be degraded to allow efficient repair of DNA lesions (Cooper et al., 1999; Pan et al., 1995; Podust et al., 1995), other experiments suggested that p21 has no negative or even a stimulating effect on DNA repair (Li et al., 1996; McDonald et al., 1996; Ruan et al., 1998; Sheikh et al., 1997; Shivji et al., 1998; Shivji et al., 1994). To shed light on the role of p21 in the DNA damage response, we analyzed the redistribution of p21 to laser-induced DNA damage sites in mouse and human cells. We could observe an immediate accumulation of both, p21-GFP and RFP-PCNA at microirradiated sites persisting for 1-2 h, which is in good agreement with estimated repair times under local irradiation conditions (Houtsmuller et al., 1999). Analysis of the recruitment kinetics revealed, that RFP-PCNA accumulated at DNA damage sites slightly faster than p21-GFP. Furthermore, the spatio-temporal accumulation of p21-GFP resembled that of other PCNA-binding proteins, like DNMT1, Ligase I and FEN-1 (Mortusewicz et al., 2006; Mortusewicz et al., 2005). This suggests that p21-GFP is recruited to DNA damage sites through its PBD-mediated interaction with PCNA. The precise function(s) of p21 at DNA damage sites and its potential role in modifying the DNA damage response and/or PCNA functions have to be elucidated in future studies.

3.3. Coordination of DNA repair by central loading platforms

Different capacities of the two loading platforms XRCC1 and PCNA to respond to successive DNA damage

Efficient repair of DNA lesions requires avid recognition of the damage and coordinated recruitment of a multitude of repair factors. The principle dilemma faced by the repair machinery is, that the stable complex formation required for processivity and completion of multi-step processes may limit the ability to respond to later changes like subsequent DNA damages. We compared the recruitment kinetics of the two loading platforms XRCC1 and PCNA and studied their capacity to respond to successive DNA damage events. Recruitment and photobleaching analyses showed that XRCC1 and PCNA represent opposite strategies. We clearly demonstrate that the stable binding of the processivity factor PCNA limits its capacity to respond to successive damage events. While the avid and transient binding of XRCC1 might be sufficient for single nucleotide replacement allowing a flexible response to multiple consecutive DNA lesions. This type of live cell analysis should also help to explore the flexibility of other repair factors and complex cellular machineries to respond to changing requirements.

The loading platforms XRCC1 and PCNA coordinate the recruitment of DNA repair factors

To further study the role of loading platforms in the coordination of DNA repair we extended our analysis to two well-characterized binding partners of PCNA and XRCC1, DNA Ligase I and III. DNA Ligases are essential for most DNA repair pathways as they are catalyzing the rejoining of DNA ends. Although the catalytic core of DNA Ligase I and III is highly conserved they have no or only poorly overlapping functions and are not interchangeable (Caldecott et al., 1994; Goetz et al., 2005; Levin et al., 2000; Mackenney et al., 1997; Petrini et al., 1995; Wang et al., 2005). To explore possible differences that could explain the non redundant functions of these highly homologous enzymes, we compared the recruitment kinetics of DNA Ligase I and III at local DNA lesions generated by laser microirradiation.

We found that DNA Ligases I and III both accumulated at DNA damage sites, albeit with distinct kinetics suggesting that although they catalyze the same reaction they use different mechanisms for recruitment. With deletion and binding studies we could demonstrate that the PBD of DNA Ligase I mediates targeting to DNA repair sites.

Interestingly, the PBD is not required for enzyme activity *in vitro* but rescue experiments with DNA Ligase I deficient cells demonstrated that the PBD is essential *in vivo* (Goetz et al., 2005; Levin et al., 2000; Petrini et al., 1995). These results suggest that PCNA mediated recruitment of DNA Ligase I could enhance the efficiency of the ligation reaction *in vivo* by locally concentrating DNA Ligase I at sites of replication and repair.

In further studies, we also observed recruitment of FEN-1 to DNA repair sites, which like DNA Ligase I interacts with PCNA during DNA replication (Frank et al., 2001; Tom et al., 2000) and is implicated in long-patch BER (Gary et al., 1999; Matsumoto et al., 1999). Remarkably, FEN-1 showed the same recruitment kinetics as DNA Ligase I although it has a completely different function in replication and repair. Likewise, the PBD of DNA methyltransferase 1 (DNMT1) is also necessary and sufficient for accumulation of DNMT1 at repair sites (Mortusewicz et al., 2005). In addition, the recruitment kinetics of another PBD containing protein, p21, resembled that of DNA Ligase I, FEN-1 and DNMT1 (Perucca et al., 2006). Taken together, our results show that various PBD-containing proteins involved in the restoration of genetic and epigenetic information are recruited to replication (Savio et al., 1996; Schermelleh et al., 2007; Sporbett et al., 2005; Sporbett et al., 2002) as well as repair sites by PCNA with similar kinetics. This suggests that PCNA fulfils an essential role as a central loading platform in both DNA replication and repair, coordinating the recruitment of various enzymatic activities.

On one hand, it has been proposed that the ZnF motif of DNA Ligase III could act as a nick sensor, recruiting DNA Ligase III to DNA nicks and altered DNA structures (Kulczyk et al., 2004; Mackey et al., 1999; Taylor et al., 1998a). We found, however, that deletion of the ZnF did not influence the recruitment kinetics of DNA Ligase III. On the other hand, biochemical studies have suggested that the BRCT domain of DNA Ligase III is essential for its interaction with XRCC1 (Beernink et al., 2005; Caldecott et al., 1994; Dulic et al., 2001; Taylor et al., 1998b). Here, we demonstrate that the deletion of the BRCT domain of DNA Ligase III abolishes recruitment of DNA Ligase III to repair sites *in vivo*. Moreover, the BRCT domain alone was sufficient to mediate recruitment of the fusion protein to DNA repair sites and is essential for nuclear localization of DNA Ligase III.

These different mechanisms for the localization of DNA Ligases at repair sites are consistent with specific characteristics of the respective repair pathways. The

continuous synthesis of long stretches of DNA during long patch BER resembles the process of DNA replication. Consequently, also similar recruitment mechanisms seem to be used. In both processes DNA Ligase I is recruited through interaction with the sliding clamp and processivity factor PCNA. In contrast, replacement of just a single nucleotide during short patch BER does not require a processive repair machinery sliding along the DNA but rather a stationary repair complex recruiting DNA Ligase III.

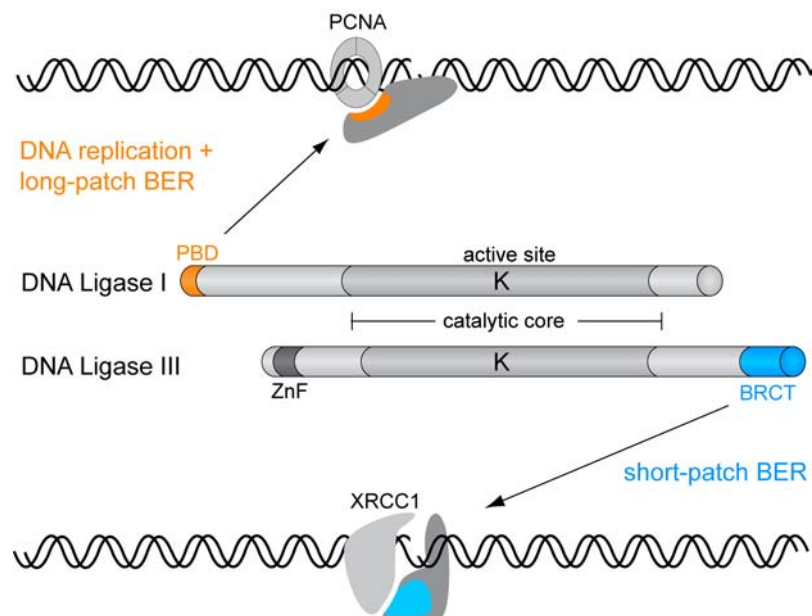


Figure 6 Model for selective targeting of DNA Ligase I and III to DNA replication and different repair pathways. All DNA Ligases use the same catalytic mechanism and show high sequence similarity in the catalytic core (grey shading). The active site lysine residue (K) in the center of the catalytic domain is directly involved in the ligation reaction. However, DNA Ligases have non-overlapping functions in DNA repair and replication and are not interchangeable. We could show that DNA Ligase I and III are targeted to different repair pathways through their regulatory PBD and BRCT domains which mediate interaction with PCNA and XRCC1, respectively. This selective recruitment of specialized DNA Ligases may accommodate the specific requirements of different repair pathways and thereby enhance repair efficiency.

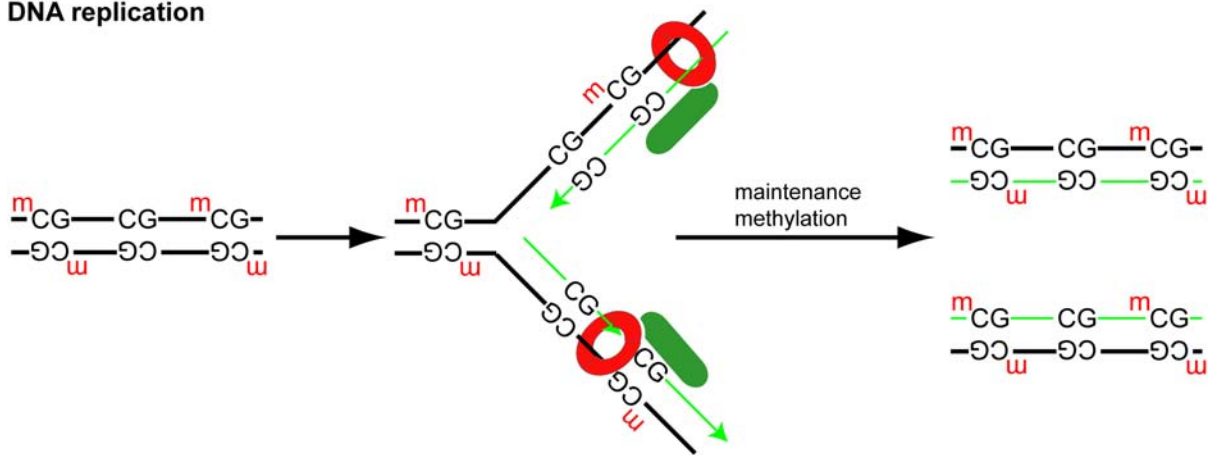
In summary, although DNA Ligase I and III share a highly similar catalytic core, they have distinct functions in DNA replication and repair and are not interchangeable. Here we identified differences in the regulatory domains of DNA Ligases which may explain their non-redundant functions in eukaryotic cells. Thus, the PBD of DNA Ligase I and the BRCT domain of DNA Ligase III mediate interaction with PCNA and XRCC1, respectively, and target them to different repair pathways (**Figure 6**). This selective recruitment may contribute to the spatio-temporal coordination of different repair factors and could thus enhance accuracy and efficiency of DNA repair in eukaryotic cells.

3.4. Maintenance of DNA methylation patterns in DNA repair

Repairing only the genetic information would not fully restore the genome integrity of a cell. In addition, chromatin states and methylation patterns have to be re-established to maintain a cell's identity. While various processes involved in chromatin rearrangement and maintenance have been described (reviewed in (Downs et al., 2007; Groth et al., 2007; van Attikum and Gasser, 2005)), the mechanisms ensuring the preservation of methylation patterns in DNA repair were largely unknown. We used laser microirradiation in combination with live cell microscopy to study the recruitment of DNA methyltransferases to DNA damage sites. While we could observe a clear recruitment of DNMT1, we could not detect any accumulation of the *de novo* methyltransferases DNMT3a and DNMT3b at repair sites in living mammalian cells. These results fit well with the recent identification of DNMT1 as a potential component of the mismatch repair (MMR) pathway in a genetic screen for MMR mutants using Bloom's syndrome protein (Blm)-deficient embryonic mouse stem cells (Guo et al., 2004). The accumulation of DNMT1 at DNA repair sites suggests that, like in DNA replication, DNMT1 maintains the DNA methylation pattern in the DNA newly synthesized during the repair process. Thus DNMT1 likely prevents a loss of DNA methylation in repair, which otherwise could cause epigenetic deregulation (Jackson-Grusby et al., 2001) and genomic instability (Brown and Robertson, 2007; Chen et al., 2007; Eden et al., 2003; Espada et al., 2007; Gaudet et al., 2003). In addition, DNMT1 has been reported to interact with histone deacetylases (HDACs) (Fuks et al., 2000; Rountree et al., 2000) and could thus, together with chromatin assembly factor 1 (CAF-1) (Green and Almouzni, 2003), contribute to the reestablishment of chromatin structures and respective histone modifications. Finally, DNMT1 may also participate in the identification of the template strand in various repair pathways as was suggested for MMR (Kim et al., 2004; Wang and James Shen, 2004). Scope and details of DNMT1 function(s) at DNA repair sites remain to be elucidated.

Key steps in DNA repair are recognition of the DNA damage and recruitment of the repair machinery. Here we could demonstrate that DNMT1 is recruited to DNA damage sites via PCNA and that the PBD of DNMT1 is necessary and sufficient for this recruitment. Our results show that PCNA not only mediates recruitment of the maintenance methyltransferase DNMT1 to replication sites but also to DNA repair sites (**Figure 7**).

DNA replication



DNA repair

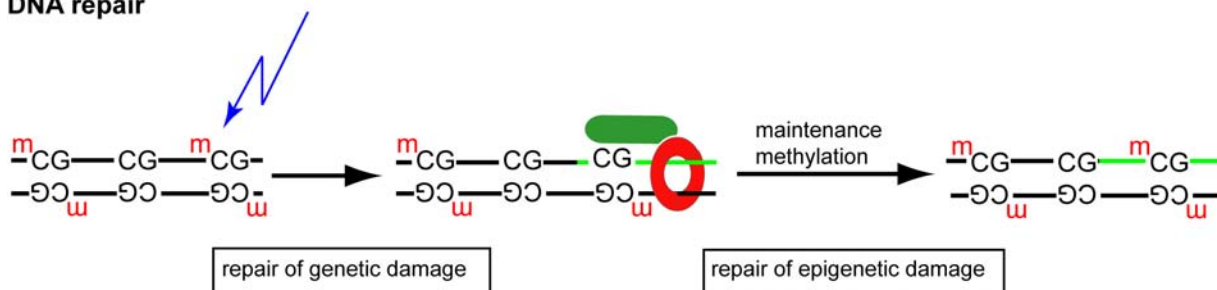


Figure 7 PCNA mediates recruitment of DNMT1 to replication and repair sites. During DNA replication, PCNA (shown as a trimer in red) targets DNMT1 (shown in green) to the newly synthesized strand. DNMT1 recognizes hemimethylated sites and catalyzes the methylation of unmethylated Cytosines, thus maintaining the methylation pattern during DNA replication. We propose that during DNA repair, PCNA likewise recruits DNMT1 to repaired stretches of DNA leading to the preservation of methylation patterns in DNA repair.

3.5. A new assay to visualize protein-protein interactions in living cells

More and more proteins involved in the various steps of DNA repair have been identified in recent years. To understand the complex regulation and coordination of DNA repair, the interaction and regulation of these proteins need to be studied in living cells. We developed a new simple method for the in-cell visualization of protein-protein interactions termed fluorescence two-hybrid (F2H) assay. This assay is based on the immobilization of a fluorescently labelled bait protein at distinct subcellular structures enabling the detection of protein-protein interactions as colocalization with a differently labelled prey protein. The F2H assay described takes advantage of cell lines with a stable integration of a *lac* operator array to immobilize fusion proteins consisting of a Lac repressor fused to fluorescently tagged proteins of interest (bait) (Figure 8).

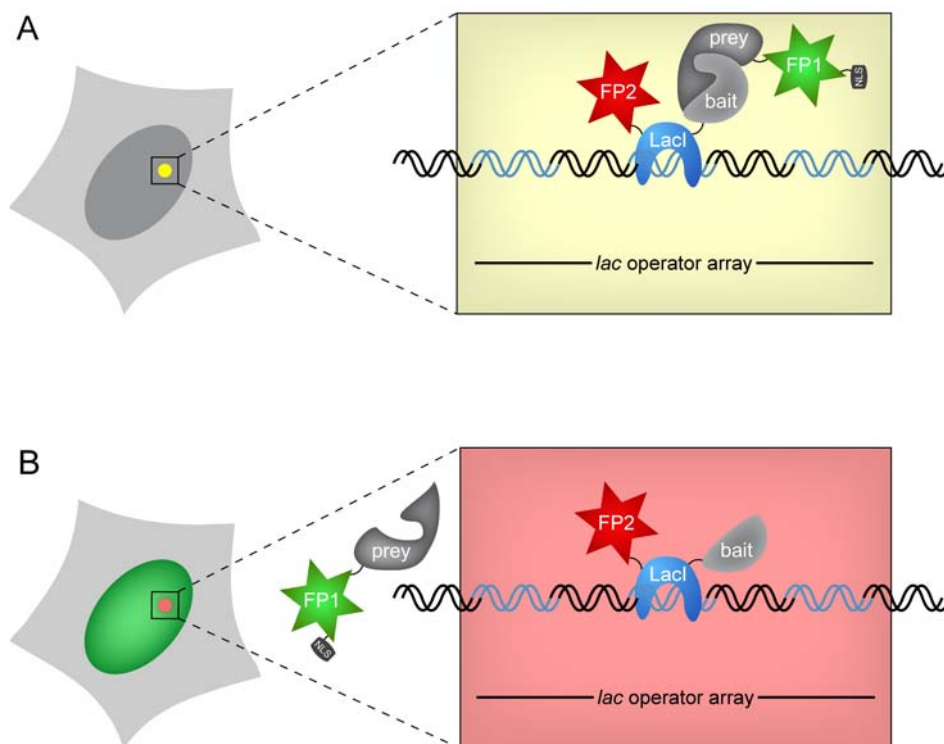


Figure 8 Schematic outline of the fluorescent two-hybrid (F2H) assay (kindly provided by K. Zolghadr). (A) The LacI domain of the bait protein mediates binding to the chromosomally integrated *lac* operator array, which is visible as a fluorescent spot in nuclei of transfected cells. If the differentially labelled prey interacts with the bait it becomes enriched at the same spot resulting in colocalization of fluorescent signals at the *lac* operator (visible as yellow spot in the overlay image). (B) If the prey does not interact with the bait protein it remains dispersed in the nucleus and the *lac* operator array is only visualized by the bait protein (red spot).

Readily usable cell lines have already been described for human, mouse, hamster and drosophila (Dietzel et al., 2004; Janicki et al., 2004; Robinett et al., 1996; Tsukamoto et al., 2000; Tumber et al., 1999; Vazquez et al., 2001). To be independent of specific transgenic cell lines, this assay could be modified by using various cellular structures like the lamina, the cytoskeleton or centrosomes as anchoring structures to locally immobilize bait proteins.

Like other methods also the F2H assay may yield false positive or false negative results, which need to be controlled for. Prey proteins that bind to the *lac* operator array in the absence of a bait protein can be identified by an initial screen and then be only used as baits.

In some cases, proteins may accumulate at subnuclear foci, which complicates the identification of the *lac* operator array in the F2H analysis. To bypass this problem, the *lac* operator array could be visualized with a third fluorescent fusion protein like, e.g. CFP-LacI.

In summary, the new F2H assay allows the direct visualization of protein-protein interactions and should be ideally suited to investigate cell cycle or differentiation dependent changes in real-time in living cells. A significant advantage of the F2H assay over other cell-based techniques is its simplicity that does neither require costly instrumentation nor advanced technical expertise. The simple optical read-out of the F2H assay additionally offers the possibility to use this assay in automated high-throughput screens to systematically analyze the protein interactome in living cells.

4. ANNEX

4.1. Abbreviations

ATM	ataxia telangiectasia mutated
BER	base excision repair
BiFC	bimolecular fluorescence complementation
B-NHEJ	nonhomologous end joining backup pathway
BRCT	BRCA1 carboxy terminal
BrdU	5-bromo-2'-deoxyuridine
CAF-1	chromatin assembly factor-1
CTD	C-terminal domain
DBD	DNA binding domain
DNMT1	DNA methyltransferase 1
DNMT3a	DNA methyltransferase 3a
DNMT3b1	DNA methyltransferase 3b1
DSBR	double strand break repair
DSBs	double strand breaks
dsDNA	double stranded DNA
F2H	fluorescence two-hybrid
FEN-1	flap structure-specific endonuclease-1
FLIP	fluorescence loss in photobleaching
FP	fluorescent protein
FRET	fluorescence resonance energy transfer
FRAP	fluorescence recovery after photobleaching
H ₂ O ₂	hydrogen peroxide
HDACs	histone deacetylases
IRIF	ionizing radiation-induced foci
LacI	Lac repressor
MMR	mismatch repair
NER	nucleotide excision repair
NHEJ	nonhomologous end joining
PAR	poly(ADP-ribose)
PARP	poly(ADP-ribose) polymerase
PARP-1	poly(ADP-ribose) polymerase-1
PARP-2	poly(ADP-ribose) polymerase-2

PBD	PCNA-binding domain
PCNA	proliferating cell nuclear antigen
PIC	preinitiation complex
PC4	positive cofactor 4
RPA	replication protein A
SSBR	single strand break repair
SSBs	single strand breaks
ssDNA	single stranded DNA
Y2H	Yeast two-hybrid
XRCC1	X-ray cross complementing factor 1
ZnF	Zinc finger

4.2. Contributions

Declaration of contributions to “Feedback regulated poly(ADP-ribosyl)ation by PARP-1 is required for rapid response to DNA damage in living cells.”

This project was initiated by Gilbert de Murcia and Valérie Schreiber at the CNRS in Strasbourg. I conceived the study together with Valérie Schreiber, Gilbert de Murcia and Heinrich Leonhardt. Valérie Schreiber and Jean-Christophe Amé provided the wildtype and knock-out cell lines and generated the GFP-tagged fusion proteins used in this study. I designed and performed all microirradiation and photobleaching experiments. I analyzed the data, prepared the figures and wrote the manuscript with help and advice from Heinrich Leonhardt and Valérie Schreiber.

Declaration of contributions to “Recruitment of RNA Polymerase II cofactor PC4 to DNA repair sites.”

This project was initiated by Wera Roth and Michael Meisterernst from the GSF in Munich. I conceived the study together with Wera Roth and Heinrich Leonhardt. Wera Roth generated all expression constructs except the fluorescently tagged RPA and PCNA fusion proteins which were provided by the laboratory of Cristina Cardoso. My contributions to this publication include: design and performance of all microirradiation and photobleaching experiments, data analysis, preparation of the figures and manuscript with help from Heinrich Leonhardt, Wera Roth and Michael Meisterernst.

Declaration of contributions to “Spatiotemporal dynamics of p21CDKN1A protein recruitment to DNA damage sites and interaction with proliferating cell nuclear antigen.”

The project was started as a collaboration with the laboratory of Ennio Prosperi. I contributed the microirradiation experiments and subsequent data analysis, revealing that the cyclin dependent kinase inhibitor p21 is recruited to DNA damage sites in living cells. In addition, I prepared Figure 3 of the manuscript and wrote the corresponding Figure legend and Material and Methods section. I discussed the data and the manuscript with Ennio Prosperi, Cristina Cardoso and Heinrich Leonhardt.

Declaration of contributions to “XRCC1 and PCNA are loading platforms with distinct kinetic properties and different capacities to respond to multiple DNA lesions.”

I laid out the project aims and conceived the study together with Heinrich Leonhardt. The GFP-XRCC1 fusion was provided by Valérié Schreiber, while the fluorescently labelled PCNA fusions were provided by the laboratory of Cristina Cardoso. My contributions to this publication include: design and performance of all microirradiation and photobleaching experiments, generation of RFP-tagged XRCC1, data analysis, preparation of the figures and manuscript with help from Heinrich Leonhardt.

Declaration of contributions to “Differential recruitment of DNA Ligase I and III to DNA repair sites.”

I laid out the project aims and conceived the study together with Heinrich Leonhardt. The GFP-XRCC1 fusion was provided by Valérié Schreiber, while the fluorescently labelled PCNA fusions were provided by the laboratory of Cristina Cardoso. The co-immunoprecipitation experiments and corresponding figures were prepared by Ulrich Rothbauer. My contributions to this publication include: design and performance of all microirradiation and photobleaching experiments, data analysis, preparation of the figures and manuscript with help from Heinrich Leonhardt and Ulrich Rothbauer.

Declaration of contributions to “Recruitment of DNA methyltransferase I to DNA repair sites.”

Heinrich Leonhardt, Lothar Schermelleh and I laid out the project aims and conceived the study. Joachim Walter introduced me to and helped me with the microirradiation experiments. I designed and performed all the experiments and analyzed the data together with Lothar Schermelleh. In addition, Lothar Schermelleh introduced me to and helped me with the microinjection of expression constructs, which were provided by the laboratory of Cristina Cardoso. I prepared the figures and the manuscript together with Heinrich Leonhardt and Lothar Schermelleh.

Declaration of contributions to “A fluorescent two-hybrid (F2H) assay for direct visualization of protein interactions in living cells.”

Most of the expression constructs and experiments were performed by Kourosh Zolghadr. The study was conceived by Heinrich Leonhardt and Kourosh Zolghadr. I generated the XRCC1-LacI-RFP and PCNA-LacI-RFP expression constructs and analyzed the respective data together with Regina Kleinhans. In addition, I prepared supplementary Figures 1-4 and Figure 1 and wrote part of the manuscript.

Declaration according to the "Promotionsordnung der LMU München für die Fakultät Biologie"

Betreuung: Hiermit erkläre ich, dass die vorgelegte Arbeit an der LMU von Herrn Prof. Dr. Leonhardt betreut wurde

Anfertigung: Hiermit versichere ich ehrenwörtlich, dass die Dissertation selbstständig und ohne unerlaubte Hilfsmittel angefertigt wurde. Über Beiträge, die im Rahmen der kumulativen Dissertation in Form von Manuskripten in der Dissertation enthalten sind, wurde im Kapitel 4.2 Rechenschaft abgelegt und die eigenen Leistungen wurden aufgelistet.

Prüfung: Hiermit erkläre ich, dass die Dissertation weder als ganzes noch in Teilen an einem anderen Ort einer Prüfungskommission vorgelegt wurde. Weiterhin habe ich weder an einem anderen Ort eine Promotion angestrebt oder angemeldet oder versucht eine Doktorprüfung abzulegen.

(Oliver Mortusewicz)

4.3. Acknowledgements

The projects described in this thesis could not have been done without the help from a lot of people. Most of them appear as co-authors on the publications listed above. Especially I would like to thank Heinrich Leonhardt who always encouraged me and with whom I had many fruitful discussions about ongoing projects and future plans. He gave me the unique opportunity to leave the DNA methylation field and spend time on the analysis of the DNA damage response in living cells. For a lot of interesting ideas, discussions and suggestions I would like to thank Cristina Cardoso, who also kindly provided me with a lot of reagents essential for a great part of my work. In this regard I also would like to thank the people in Cristina's lab for a great time during our "Illuminati" meetings, which I really enjoyed (and not only the scientific part!).

The great atmosphere in Heinrich's lab provided the ground for this study and I would like to thank all the people I got to know during the last 3 years. You helped me a lot in every aspect of daily laboratory life. It was a pleasure to share not only the working bench but also the ale-bench with you, not to forget the hiking and sledging. Particularly, I am indebted to Anja for always helping out when it comes to ordering reagents. Gently but firm, she always made sure that the labs are kept clean and safe, which made work a lot easier. As a lot of evaluation and data analysis was done on a PC, I have to express my gratitude to Kourosh. Without his help and support, my computer would probably float in the nice little lake below our office window by now. For expertise advice and help on biochemical experiments, microscopic analysis and manuscript preparations I owe thanks to Ulrich, Lothar and Fabio.

Finally, I would like to thank my family who paved the way for my studies and always supported me in every possible way. Most of all, I would like to thank my girlfriend Ines, who had to tolerate my bad moods and frustration when an experiment did not turn out as expected. She always managed to cheer me up, made me laugh again and believed in me in times when I was not confident about my scientific skills.

4.4. References

- Ame, J.C., V. Rolli, V. Schreiber, C. Niedergang, F. Apiou, P. Decker, S. Muller, T. Hoger, J. Menissier-de Murcia, and G. de Murcia. 1999. PARP-2, A novel mammalian DNA damage-dependent poly(ADP-ribose) polymerase. *J Biol Chem.* 274:17860-8.
- Aten, J.A., J. Stap, P.M. Krawczyk, C.H. van Oven, R.A. Hoebe, J. Essers, and R. Kanaar. 2004. Dynamics of DNA double-strand breaks revealed by clustering of damaged chromosome domains. *Science.* 303:92-5.
- Bakkenist, C.J., and M.B. Kastan. 2003. DNA damage activates ATM through intermolecular autophosphorylation and dimer dissociation. *Nature.* 421:499-506.
- Ballard, D.W., W.M. Philbrick, and A.L. Bothwell. 1988. Identification of a novel 9-kDa polypeptide from nuclear extracts. DNA binding properties, primary structure, and in vitro expression. *J Biol Chem.* 263:8450-7.
- Barnes, D.E., G. Stamp, I. Rosewell, A. Denzel, and T. Lindahl. 1998. Targeted disruption of the gene encoding DNA ligase IV leads to lethality in embryonic mice. *Curr Biol.* 8:1395-8.
- Bartek, J., C. Lukas, and J. Lukas. 2004. Checking on DNA damage in S phase. *Nat Rev Mol Cell Biol.* 5:792-804.
- Bartek, J., and J. Lukas. 2007. DNA damage checkpoints: from initiation to recovery or adaptation. *Curr Opin Cell Biol.* 19:238-45.
- Becker, P.B. 2006. Gene regulation: a finger on the mark. *Nature.* 442:31-2.
- Beernink, P.T., M. Hwang, M. Ramirez, M.B. Murphy, S.A. Doyle, and M.P. Thelen. 2005. Specificity of protein interactions mediated by BRCT domains of the XRCC1 DNA repair protein. *J Biol Chem.* 280:30206-13.
- Bekker-Jensen, S., C. Lukas, F. Melander, J. Bartek, and J. Lukas. 2005. Dynamic assembly and sustained retention of 53BP1 at the sites of DNA damage are controlled by Mdc1/NFBD1. *J Cell Biol.* 170:201-11.
- Berger, S.L. 2007. The complex language of chromatin regulation during transcription. *Nature.* 447:407-12.
- Bestor, T.H. 2000. The DNA methyltransferases of mammals. *Hum Mol Genet.* 9:2395-402.
- Bird, A. 2007. Perceptions of epigenetics. *Nature.* 447:396-8.
- Blazek, E., G. Mittler, and M. Meisterernst. 2005. The mediator of RNA polymerase II. *Chromosoma.* 113:399-408.
- Bochkarev, A., R.A. Pfuetzner, A.M. Edwards, and L. Frappier. 1997. Structure of the single-stranded-DNA-binding domain of replication protein A bound to DNA. *Nature.* 385:176-81.
- Bornstein, G., J. Bloom, D. Sitry-Shevah, K. Nakayama, M. Pagano, and A. Hershko. 2003. Role of the SCFSkp2 ubiquitin ligase in the degradation of p21Cip1 in S phase. *J Biol Chem.* 278:25752-7.
- Bradshaw, P.S., D.J. Stavropoulos, and M.S. Meyn. 2005. Human telomeric protein TRF2 associates with genomic double-strand breaks as an early response to DNA damage. *Nat Genet.* 37:193-7.
- Brandsen, J., S. Werten, P.C. van der Vliet, M. Meisterernst, J. Kroon, and P. Gros. 1997. C-terminal domain of transcription cofactor PC4 reveals dimeric ssDNA binding site. *Nat Struct Biol.* 4:900-3.
- Brown, K.D., and K.D. Robertson. 2007. DNMT1 knockout delivers a strong blow to genome stability and cell viability. *Nat Genet.* 39:289-90.

- Caldecott, K.W. 2003. XRCC1 and DNA strand break repair. *DNA Repair (Amst)*. 2:955-69.
- Caldecott, K.W., C.K. McKeown, J.D. Tucker, S. Ljungquist, and L.H. Thompson. 1994. An interaction between the mammalian DNA repair protein XRCC1 and DNA ligase III. *Mol Cell Biol*. 14:68-76.
- Calvo, O., and J.L. Manley. 2001. Evolutionarily conserved interaction between CstF-64 and PC4 links transcription, polyadenylation, and termination. *Mol Cell*. 7:1013-23.
- Cappelli, E., R. Taylor, M. Cevasco, A. Abbondandolo, K. Caldecott, and G. Frosina. 1997. Involvement of XRCC1 and DNA ligase III gene products in DNA base excision repair. *J Biol Chem*. 272:23970-5.
- Cardoso, M.C., C. Joseph, H.P. Rahn, R. Reusch, B. Nadal-Ginard, and H. Leonhardt. 1997. Mapping and use of a sequence that targets DNA ligase I to sites of DNA replication in vivo. *J Cell Biol*. 139:579-87.
- Celeste, A., O. Fernandez-Capetillo, M.J. Kruhlak, D.R. Pilch, D.W. Staudt, A. Lee, R.F. Bonner, W.M. Bonner, and A. Nussenzweig. 2003. Histone H2AX phosphorylation is dispensable for the initial recognition of DNA breaks. *Nat Cell Biol*. 5:675-9.
- Chen, T., S. Hevi, F. Gay, N. Tsujimoto, T. He, B. Zhang, Y. Ueda, and E. Li. 2007. Complete inactivation of DNMT1 leads to mitotic catastrophe in human cancer cells. *Nat Genet*. 39:391-6.
- Chuang, L.S., H.I. Ian, T.W. Koh, H.H. Ng, G. Xu, and B.F. Li. 1997. Human DNA-(cytosine-5) methyltransferase-PCNA complex as a target for p21WAF1. *Science*. 277:1996-2000.
- Cooper, M.P., A.S. Balajee, and V.A. Bohr. 1999. The C-terminal domain of p21 inhibits nucleotide excision repair In vitro and In vivo. *Mol Biol Cell*. 10:2119-29.
- Coqueret, O. 2003. New roles for p21 and p27 cell-cycle inhibitors: a function for each cell compartment? *Trends Cell Biol*. 13:65-70.
- Critchlow, S.E., R.P. Bowater, and S.P. Jackson. 1997. Mammalian DNA double-strand break repair protein XRCC4 interacts with DNA ligase IV. *Curr Biol*. 7:588-98.
- Das, C., K. Hizume, K. Batta, B.R. Kumar, S.S. Gadad, S. Ganguly, S. Lorain, A. Verreault, P.P. Sadhale, K. Takeyasu, and T.K. Kundu. 2006. Transcriptional coactivator PC4, a chromatin-associated protein, induces chromatin condensation. *Mol Cell Biol*. 26:8303-15.
- de Murcia, J.M., C. Niedergang, C. Trucco, M. Ricoul, B. Dutrillaux, M. Mark, F.J. Oliver, M. Masson, A. Dierich, M. LeMeur, C. Walztinger, P. Chambon, and G. de Murcia. 1997. Requirement of poly(ADP-ribose) polymerase in recovery from DNA damage in mice and in cells. *Proc Natl Acad Sci U S A*. 94:7303-7.
- Dietzel, S., K. Zolghadr, C. Hepperger, and A.S. Belmont. 2004. Differential large-scale chromatin compaction and intranuclear positioning of transcribed versus non-transcribed transgene arrays containing {beta}-globin regulatory sequences. *J Cell Sci*. 117:4603-4614.
- Dorazi, R., J.L. Parker, and M.F. White. 2006. PCNA activates the Holliday junction endonuclease Hjc. *J Mol Biol*. 364:243-7.
- Dotto, G.P. 2000. p21(WAF1/Cip1): more than a break to the cell cycle? *Biochim Biophys Acta*. 1471:M43-56.
- Downs, J.A., M.C. Nussenzweig, and A. Nussenzweig. 2007. Chromatin dynamics and the preservation of genetic information. *Nature*. 447:951-8.

- Dulic, A., P.A. Bates, X. Zhang, S.R. Martin, P.S. Freemont, T. Lindahl, and D.E. Barnes. 2001. BRCT domain interactions in the heterodimeric DNA repair protein XRCC1-DNA ligase III. *Biochemistry*. 40:5906-13.
- Eden, A., F. Gaudet, A. Waghmare, and R. Jaenisch. 2003. Chromosomal instability and tumors promoted by DNA hypomethylation. *Science*. 300:455.
- Espada, J., E. Ballestar, R. Santoro, M.F. Fraga, A. Villar-Garea, A. Nemeth, L. Lopez-Serra, S. Roperio, A. Aranda, H. Orozco, V. Moreno, A. Juarranz, J.C. Stockert, G. Langst, I. Grummt, W. Bickmore, and M. Esteller. 2007. Epigenetic disruption of ribosomal RNA genes and nucleolar architecture in DNA methyltransferase 1 (Dnmt1) deficient cells. *Nucleic Acids Res*. 35:2191-8.
- Essers, J., A.B. Houtsmuller, L. van Veelen, C. Paulusma, A.L. Nigg, A. Pastink, W. Vermeulen, J.H. Hoeijmakers, and R. Kanaar. 2002. Nuclear dynamics of RAD52 group homologous recombination proteins in response to DNA damage. *Embo J*. 21:2030-7.
- Fan, J., M. Otterlei, H.K. Wong, A.E. Tomkinson, and D.M. Wilson, 3rd. 2004. XRCC1 co-localizes and physically interacts with PCNA. *Nucleic Acids Res*. 32:2193-201.
- Fernandez-Capetillo, O., and A. Nussenzweig. 2004. Linking histone deacetylation with the repair of DNA breaks. *Proc Natl Acad Sci U S A*. 101:1427-8.
- Ferro, A.M., and B.M. Olivera. 1982. Poly(ADP-ribosylation) in vitro. Reaction parameters and enzyme mechanism. *J Biol Chem*. 257:7808-13.
- Fisher, A., H. Hohegger, S. Takeda, and K.W. Caldecott. 2007. Poly (ADP-ribose) Polymerase-1 Accelerates Single-Strand Break Repair in Concert with Poly (ADP-ribose) Glycohydrolase. *Mol Cell Biol*.
- Frank, G., J. Qiu, L. Zheng, and B. Shen. 2001. Stimulation of eukaryotic flap endonuclease-1 activities by proliferating cell nuclear antigen (PCNA) is independent of its in vitro interaction via a consensus PCNA binding region. *J Biol Chem*. 276:36295-302.
- Frank, K.M., J.M. Sekiguchi, K.J. Seidl, W. Swat, G.A. Rathbun, H.L. Cheng, L. Davidson, L. Kangaloo, and F.W. Alt. 1998. Late embryonic lethality and impaired V(D)J recombination in mice lacking DNA ligase IV. *Nature*. 396:173-7.
- Friedberg, E.C. 2003. DNA damage and repair. *Nature*. 421:436-40.
- Fuks, F., W.A. Burgers, A. Brehm, L. Hughes-Davies, and T. Kouzarides. 2000. DNA methyltransferase Dnmt1 associates with histone deacetylase activity. *Nat Genet*. 24:88-91.
- Fukuda, A., T. Nakadai, M. Shimada, T. Tsukui, M. Matsumoto, Y. Nogi, M. Meisterernst, and K. Hisatake. 2004. Transcriptional coactivator PC4 stimulates promoter escape and facilitates transcriptional synergy by GAL4-VP16. *Mol Cell Biol*. 24:6525-35.
- Gary, R., K. Kim, H.L. Cornelius, M.S. Park, and Y. Matsumoto. 1999. Proliferating cell nuclear antigen facilitates excision in long-patch base excision repair. *J Biol Chem*. 274:4354-63.
- Gaudet, F., J.G. Hodgson, A. Eden, L. Jackson-Grusby, J. Dausman, J.W. Gray, H. Leonhardt, and R. Jaenisch. 2003. Induction of tumors in mice by genomic hypomethylation. *Science*. 300:489-92.
- Gaudet, F., W.M. Rideout, 3rd, A. Meissner, J. Dausman, H. Leonhardt, and R. Jaenisch. 2004. Dnmt1 expression in pre- and postimplantation embryogenesis and the maintenance of IAP silencing. *Mol Cell Biol*. 24:1640-8.

- Ge, H., and R.G. Roeder. 1994. Purification, cloning, and characterization of a human coactivator, PC4, that mediates transcriptional activation of class II genes. *Cell*. 78:513-23.
- Ge, H., Y. Zhao, B.T. Chait, and R.G. Roeder. 1994. Phosphorylation negatively regulates the function of coactivator PC4. *Proc Natl Acad Sci U S A*. 91:12691-5.
- Goetz, J.D., T.A. Motycka, M. Han, M. Jasin, and A.E. Tomkinson. 2005. Reduced repair of DNA double-strand breaks by homologous recombination in a DNA ligase I-deficient human cell line. *DNA Repair (Amst)*. 4:649-54.
- Gottfredi, V., K. McKinney, M.V. Poyurovsky, and C. Prives. 2004. Decreased p21 levels are required for efficient restart of DNA synthesis after S phase block. *J Biol Chem*. 279:5802-10.
- Gradwohl, G., J.M. Menissier de Murcia, M. Molinete, F. Simonin, M. Koken, J.H. Hoeijmakers, and G. de Murcia. 1990. The second zinc-finger domain of poly(ADP-ribose) polymerase determines specificity for single-stranded breaks in DNA. *Proc Natl Acad Sci U S A*. 87:2990-4.
- Grawunder, U., M. Wilm, X. Wu, P. Kulesza, T.E. Wilson, M. Mann, and M.R. Lieber. 1997. Activity of DNA ligase IV stimulated by complex formation with XRCC4 protein in mammalian cells. *Nature*. 388:492-5.
- Green, C.M., and G. Almouzni. 2003. Local action of the chromatin assembly factor CAF-1 at sites of nucleotide excision repair in vivo. *Embo J*. 22:5163-74.
- Groth, A., W. Rocha, A. Verreault, and G. Almouzni. 2007. Chromatin challenges during DNA replication and repair. *Cell*. 128:721-33.
- Guo, G., W. Wang, and A. Bradley. 2004. Mismatch repair genes identified using genetic screens in Blm-deficient embryonic stem cells. *Nature*. 429:891-5.
- Hauptner, A., S. Dietzel, G.A. Drexler, P. Reichart, R. Krucken, T. Cremer, A.A. Friedl, and G. Dollinger. 2004. Microirradiation of cells with energetic heavy ions. *Radiat Environ Biophys*. 42:237-45.
- Hauptner, A., R. Krucken, C. Greubel, V. Hable, G. Dollinger, G.A. Drexler, M. Deutsch, R. Lowe, A.A. Friedl, S. Dietzel, H. Strickfaden, and T. Cremer. 2006. DNA-repair protein distribution along the tracks of energetic ions. *Radiat Prot Dosimetry*. 122:147-9.
- Hoege, C., B. Pfander, G.L. Moldovan, G. Pyrowolakis, and S. Jentsch. 2002. RAD6-dependent DNA repair is linked to modification of PCNA by ubiquitin and SUMO. *Nature*. 419:135-41.
- Hoeijmakers, J.H. 2001. Genome maintenance mechanisms for preventing cancer. *Nature*. 411:366-74.
- Holmes, A.M., and J.E. Haber. 1999. Double-strand break repair in yeast requires both leading and lagging strand DNA polymerases. *Cell*. 96:415-24.
- Houtsmuller, A.B., S. Rademakers, A.L. Nigg, D. Hoogstraten, J.H. Hoeijmakers, and W. Vermeulen. 1999. Action of DNA repair endonuclease ERCC1/XPF in living cells. *Science*. 284:958-61.
- Jackson-Grusby, L., C. Beard, R. Possemato, M. Tudor, D. Fambrough, G. Csankovszki, J. Dausman, P. Lee, C. Wilson, E. Lander, and R. Jaenisch. 2001. Loss of genomic methylation causes p53-dependent apoptosis and epigenetic deregulation. *Nat Genet*. 27:31-9.
- Jaenisch, R., and A. Bird. 2003. Epigenetic regulation of gene expression: how the genome integrates intrinsic and environmental signals. *Nat Genet*. 33 Suppl:245-54.

- Jakob, B., M. Scholz, and G. Taucher-Scholz. 2002. Characterization of CDKN1A (p21) binding to sites of heavy-ion-induced damage: colocalization with proteins involved in DNA repair. *Int J Radiat Biol.* 78:75-88.
- Jakob, B., M. Scholz, and G. Taucher-Scholz. 2003. Biological imaging of heavy charged-particle tracks. *Radiat Res.* 159:676-84.
- Janicki, S.M., T. Tsukamoto, S.E. Salghetti, W.P. Tansey, R. Sachidanandam, K.V. Prasanth, T. Ried, Y. Shav-Tal, E. Bertrand, R.H. Singer, and D.L. Spector. 2004. From silencing to gene expression: real-time analysis in single cells. *Cell.* 116:683-98.
- Jasin, M. 1996. Genetic manipulation of genomes with rare-cutting endonucleases. *Trends Genet.* 12:224-8.
- Jiricny, J. 2006. The multifaceted mismatch-repair system. *Nat Rev Mol Cell Biol.* 7:335-46.
- Johnson, R.E., G.K. Kovvali, S.N. Guzder, N.S. Amin, C. Holm, Y. Habraken, P. Sung, L. Prakash, and S. Prakash. 1996. Evidence for involvement of yeast proliferating cell nuclear antigen in DNA mismatch repair. *J Biol Chem.* 271:27987-90.
- Kaiser, K., and M. Meisterernst. 1996. The human general co-factors. *Trends Biochem Sci.* 21:342-5.
- Kaiser, K., G. Stelzer, and M. Meisterernst. 1995. The coactivator p15 (PC4) initiates transcriptional activation during TFIIA-TFIID-promoter complex formation. *Embo J.* 14:3520-7.
- Kerppola, T.K. 2006. Visualization of molecular interactions by fluorescence complementation. *Nat Rev Mol Cell Biol.* 7:449-56.
- Kim, J.S., T.B. Krasieva, V. LaMorte, A.M. Taylor, and K. Yokomori. 2002. Specific recruitment of human cohesin to laser-induced DNA damage. *J Biol Chem.* 277:45149-53.
- Kim, M., B.N. Trinh, T.I. Long, S. Oghamian, and P.W. Laird. 2004. Dnmt1 deficiency leads to enhanced microsatellite instability in mouse embryonic stem cells. *Nucleic Acids Res.* 32:5742-9.
- Knaus, R., R. Pollock, and L. Guarente. 1996. Yeast SUB1 is a suppressor of TFIIB mutations and has homology to the human co-activator PC4. *Embo J.* 15:1933-40.
- Kretzschmar, M., K. Kaiser, F. Lottspeich, and M. Meisterernst. 1994. A novel mediator of class II gene transcription with homology to viral immediate-early transcriptional regulators. *Cell.* 78:525-34.
- Kubota, Y., R.A. Nash, A. Klungland, P. Schar, D.E. Barnes, and T. Lindahl. 1996. Reconstitution of DNA base excision-repair with purified human proteins: interaction between DNA polymerase beta and the XRCC1 protein. *Embo J.* 15:6662-70.
- Kulczyk, A.W., J.C. Yang, and D. Neuhaus. 2004. Solution structure and DNA binding of the zinc-finger domain from DNA ligase IIIalpha. *J Mol Biol.* 341:723-38.
- Lan, L., S. Nakajima, Y. Oohata, M. Takao, S. Okano, M. Masutani, S.H. Wilson, and A. Yasui. 2004. In situ analysis of repair processes for oxidative DNA damage in mammalian cells. *Proc Natl Acad Sci U S A.* 101:13738-43.
- Leonhardt, H., and M.C. Cardoso. 2000. DNA methylation, nuclear structure, gene expression and cancer. *J Cell Biochem Suppl.* Suppl 35:78-83.
- Leonhardt, H., A.W. Page, H.U. Weier, and T.H. Bestor. 1992. A targeting sequence directs DNA methyltransferase to sites of DNA replication in mammalian nuclei. *Cell.* 71:865-73.

- Levin, D.S., A.E. McKenna, T.A. Motycka, Y. Matsumoto, and A.E. Tomkinson. 2000. Interaction between PCNA and DNA ligase I is critical for joining of Okazaki fragments and long-patch base-excision repair. *Curr Biol.* 10:919-22.
- Li, E., C. Beard, and R. Jaenisch. 1993. Role for DNA methylation in genomic imprinting. *Nature.* 366:362-5.
- Li, E., T.H. Bestor, and R. Jaenisch. 1992. Targeted mutation of the DNA methyltransferase gene results in embryonic lethality. *Cell.* 69:915-26.
- Li, R., G.J. Hannon, D. Beach, and B. Stillman. 1996. Subcellular distribution of p21 and PCNA in normal and repair-deficient cells following DNA damage. *Curr Biol.* 6:189-99.
- Limoli, C.L., and J.F. Ward. 1993. A new method for introducing double-strand breaks into cellular DNA. *Radiat Res.* 134:160-9.
- Lisby, M., U.H. Mortensen, and R. Rothstein. 2003. Colocalization of multiple DNA double-strand breaks at a single Rad52 repair centre. *Nat Cell Biol.* 5:572-7.
- Lukas, J., and J. Bartek. 2004. Watching the DNA repair ensemble dance. *Cell.* 118:666-8.
- Mackenney, V.J., D.E. Barnes, and T. Lindahl. 1997. Specific function of DNA ligase I in simian virus 40 DNA replication by human cell-free extracts is mediated by the amino-terminal non-catalytic domain. *J Biol Chem.* 272:11550-6.
- Mackey, Z.B., C. Niedergang, J.M. Murcia, J. Leppard, K. Au, J. Chen, G. de Murcia, and A.E. Tomkinson. 1999. DNA ligase III is recruited to DNA strand breaks by a zinc finger motif homologous to that of poly(ADP-ribose) polymerase. Identification of two functionally distinct DNA binding regions within DNA ligase III. *J Biol Chem.* 274:21679-87.
- Maga, G., and U. Hubscher. 2003. Proliferating cell nuclear antigen (PCNA): a dancer with many partners. *J Cell Sci.* 116:3051-60.
- Malik, S., and R.G. Roeder. 2000. Transcriptional regulation through Mediator-like coactivators in yeast and metazoan cells. *Trends Biochem Sci.* 25:277-83.
- Martin, I.V., and S.A. MacNeill. 2002. ATP-dependent DNA ligases. *Genome Biol.* 3:REVIEWS3005.
- Masson, M., C. Niedergang, V. Schreiber, S. Muller, J. Menissier-de Murcia, and G. de Murcia. 1998. XRCC1 is specifically associated with poly(ADP-ribose) polymerase and negatively regulates its activity following DNA damage. *Mol Cell Biol.* 18:3563-71.
- Masutani, M., T. Nozaki, E. Nishiyama, T. Shimokawa, Y. Tachi, H. Suzuki, H. Nakagama, K. Wakabayashi, and T. Sugimura. 1999. Function of poly(ADP-ribose) polymerase in response to DNA damage: gene-disruption study in mice. *Mol Cell Biochem.* 193:149-52.
- Matsumoto, Y., K. Kim, J. Hurwitz, R. Gary, D.S. Levin, A.E. Tomkinson, and M.S. Park. 1999. Reconstitution of proliferating cell nuclear antigen-dependent repair of apurinic/apyrimidinic sites with purified human proteins. *J Biol Chem.* 274:33703-8.
- Matunis, M.J. 2002. On the road to repair: PCNA encounters SUMO and ubiquitin modifications. *Mol Cell.* 10:441-2.
- McDonald, E.R., 3rd, G.S. Wu, T. Waldman, and W.S. El-Deiry. 1996. Repair Defect in p21 WAF1/CIP1 $-/-$ human cancer cells. *Cancer Res.* 56:2250-5.
- Meisterernst, M., A.L. Roy, H.M. Lieu, and R.G. Roeder. 1991. Activation of class II gene transcription by regulatory factors is potentiated by a novel activity. *Cell.* 66:981-93.

- Melo, J.A., J. Cohen, and D.P. Toczyski. 2001. Two checkpoint complexes are independently recruited to sites of DNA damage in vivo. *Genes Dev.* 15:2809-21.
- Menissier de Murcia, J., M. Ricoul, L. Tartier, C. Niedergang, A. Huber, F. Dantzer, V. Schreiber, J.C. Ame, A. Dierich, M. LeMeur, L. Sabatier, P. Chambon, and G. de Murcia. 2003. Functional interaction between PARP-1 and PARP-2 in chromosome stability and embryonic development in mouse. *Embo J.* 22:2255-63.
- Miyawaki, A. 2003. Visualization of the spatial and temporal dynamics of intracellular signaling. *Dev Cell.* 4:295-305.
- Moggs, J.G., P. Grandi, J.P. Quivy, Z.O. Jonsson, U. Hubscher, P.B. Becker, and G. Almouzni. 2000. A CAF-1-PCNA-mediated chromatin assembly pathway triggered by sensing DNA damage. *Mol Cell Biol.* 20:1206-18.
- Moldovan, G.L., B. Pfander, and S. Jentsch. 2007. PCNA, the maestro of the replication fork. *Cell.* 129:665-79.
- Mone, M.J., T. Bernas, C. Dinant, F.A. Goedvree, E.M. Manders, M. Volker, A.B. Houtsmuller, J.H. Hoeijmakers, W. Vermeulen, and R. van Driel. 2004. In vivo dynamics of chromatin-associated complex formation in mammalian nucleotide excision repair. *Proc Natl Acad Sci U S A.* 101:15933-7.
- Montecucco, A., E. Savini, F. Weighardt, R. Rossi, G. Ciarrocchi, A. Villa, and G. Biamonti. 1995. The N-terminal domain of human DNA ligase I contains the nuclear localization signal and directs the enzyme to sites of DNA replication. *Embo J.* 14:5379-86.
- Mortusewicz, O., U. Rothbauer, M.C. Cardoso, and H. Leonhardt. 2006. Differential recruitment of DNA Ligase I and III to DNA repair sites. *Nucleic Acids Res.* 34:3523-32.
- Mortusewicz, O., L. Schermelleh, J. Walter, M.C. Cardoso, and H. Leonhardt. 2005. Recruitment of DNA methyltransferase I to DNA repair sites. *Proc Natl Acad Sci U S A.* 102:8905-9.
- Okano, M., D.W. Bell, D.A. Haber, and E. Li. 1999. DNA methyltransferases Dnmt3a and Dnmt3b are essential for de novo methylation and mammalian development. *Cell.* 99:247-57.
- Okano, M., S. Xie, and E. Li. 1998. Cloning and characterization of a family of novel mammalian DNA (cytosine-5) methyltransferases. *Nat Genet.* 19:219-20.
- Pan, Z.Q., H. Ge, A.A. Amin, and J. Hurwitz. 1996. Transcription-positive cofactor 4 forms complexes with HSSB (RPA) on single-stranded DNA and influences HSSB-dependent enzymatic synthesis of simian virus 40 DNA. *J Biol Chem.* 271:22111-6.
- Pan, Z.Q., J.T. Reardon, L. Li, H. Flores-Rozas, R. Legerski, A. Sancar, and J. Hurwitz. 1995. Inhibition of nucleotide excision repair by the cyclin-dependent kinase inhibitor p21. *J Biol Chem.* 270:22008-16.
- Panning, B., and R. Jaenisch. 1996. DNA hypomethylation can activate Xist expression and silence X-linked genes. *Genes Dev.* 10:1991-2002.
- Papouli, E., S. Chen, A.A. Davies, D. Huttner, L. Krejci, P. Sung, and H.D. Ulrich. 2005. Crosstalk between SUMO and ubiquitin on PCNA is mediated by recruitment of the helicase Srs2p. *Mol Cell.* 19:123-33.
- Parrish, J.R., K.D. Gulyas, and R.L. Finley, Jr. 2006. Yeast two-hybrid contributions to interactome mapping. *Curr Opin Biotechnol.* 17:387-93.
- Perucca, P., O. Cazzalini, O. Mortusewicz, D. Necchi, M. Savio, T. Nardo, L.A. Stivala, H. Leonhardt, M.C. Cardoso, and E. Prosperi. 2006. Spatiotemporal

- dynamics of p21CDKN1A protein recruitment to DNA-damage sites and interaction with proliferating cell nuclear antigen. *J Cell Sci.* 119:1517-27.
- Petrini, J.H., Y. Xiao, and D.T. Weaver. 1995. DNA ligase I mediates essential functions in mammalian cells. *Mol Cell Biol.* 15:4303-8.
- Pfander, B., G.L. Moldovan, M. Sacher, C. Hoege, and S. Jentsch. 2005. SUMO-modified PCNA recruits Srs2 to prevent recombination during S phase. *Nature.* 436:428-33.
- Pleschke, J.M., H.E. Kleczkowska, M. Strohm, and F.R. Althaus. 2000. Poly(ADP-ribose) binds to specific domains in DNA damage checkpoint proteins. *J Biol Chem.* 275:40974-80.
- Podust, V.N., L.M. Podust, F. Goubin, B. Ducommun, and U. Hubscher. 1995. Mechanism of inhibition of proliferating cell nuclear antigen-dependent DNA synthesis by the cyclin-dependent kinase inhibitor p21. *Biochemistry.* 34:8869-75.
- Politi, A., M.J. Mone, A.B. Houtsmuller, D. Hoogstraten, W. Vermeulen, R. Heinrich, and R. van Driel. 2005. Mathematical modeling of nucleotide excision repair reveals efficiency of sequential assembly strategies. *Mol Cell.* 19:679-90.
- Reik, W. 2007. Stability and flexibility of epigenetic gene regulation in mammalian development. *Nature.* 447:425-32.
- Robertson, K.D. 2002. DNA methylation and chromatin - unraveling the tangled web. *Oncogene.* 21:5361-79.
- Robinett, C.C., A. Straight, G. Li, C. Wilhelm, G. Sudlow, A. Murray, and A.S. Belmont. 1996. In vivo localization of DNA sequences and visualization of large-scale chromatin organization using lac operator/repressor recognition. *J Cell Biol.* 135:1685-700.
- Rogakou, E.P., C. Boon, C. Redon, and W.M. Bonner. 1999. Megabase chromatin domains involved in DNA double-strand breaks in vivo. *J Cell Biol.* 146:905-16.
- Rountree, M.R., K.E. Bachman, and S.B. Baylin. 2000. DNMT1 binds HDAC2 and a new co-repressor, DMAP1, to form a complex at replication foci. *Nat Genet.* 25:269-77.
- Ruan, S., M.F. Okcu, J.P. Ren, P. Chiao, M. Andreeff, V. Levin, and W. Zhang. 1998. Overexpressed WAF1/Cip1 renders glioblastoma cells resistant to chemotherapy agents 1,3-bis(2-chloroethyl)-1-nitrosourea and cisplatin. *Cancer Res.* 58:1538-43.
- Savio, M., L.A. Stivala, A.I. Scovassi, L. Bianchi, and E. Prosperi. 1996. p21waf1/cip1 protein associates with the detergent-insoluble form of PCNA concomitantly with disassembly of PCNA at nucleotide excision repair sites. *Oncogene.* 13:1591-8.
- Schermelleh, L., A. Haemmer, F. Spada, N. Rosing, D. Meilinger, U. Rothbauer, M. Cristina Cardoso, and H. Leonhardt. 2007. Dynamics of Dnmt1 interaction with the replication machinery and its role in postreplicative maintenance of DNA methylation. *Nucleic Acids Res.*
- Schreiber, V., J.C. Ame, P. Dolle, I. Schultz, B. Rinaldi, V. Fraulob, J. Menissier-de Murcia, and G. de Murcia. 2002. Poly(ADP-ribose) polymerase-2 (PARP-2) is required for efficient base excision DNA repair in association with PARP-1 and XRCC1. *J Biol Chem.* 277:23028-36.
- Schreiber, V., F. Dantzer, J.C. Ame, and G. de Murcia. 2006. Poly(ADP-ribose): novel functions for an old molecule. *Nat Rev Mol Cell Biol.* 7:517-28.
- Schreiber, V., M. Ricoul, J.C. Amé, F. Dantzer, V.S. Meder, C. Spenlehauer, P. Stiegler, C. Niedergang, L. Sabatier, V. Favaudon, J. Ménissier-de Murcia,

- and G. de Murcia. 2004. PARP-2, structure-function relationship. *In poly(ADP-ribose)ylation*. A. Burkle, editor. Landes.
- Sekar, R.B., and A. Periasamy. 2003. Fluorescence resonance energy transfer (FRET) microscopy imaging of live cell protein localizations. *J Cell Biol.* 160:629-33.
- Sheikh, M.S., Y.Q. Chen, M.L. Smith, and A.J. Fornace, Jr. 1997. Role of p21Waf1/Cip1/Sdi1 in cell death and DNA repair as studied using a tetracycline-inducible system in p53-deficient cells. *Oncogene.* 14:1875-82.
- Shivji, K.K., M.K. Kenny, and R.D. Wood. 1992. Proliferating cell nuclear antigen is required for DNA excision repair. *Cell.* 69:367-74.
- Shivji, M.K., E. Ferrari, K. Ball, U. Hubscher, and R.D. Wood. 1998. Resistance of human nucleotide excision repair synthesis in vitro to p21Cdn1. *Oncogene.* 17:2827-38.
- Shivji, M.K., S.J. Grey, U.P. Strausfeld, R.D. Wood, and J.J. Blow. 1994. Cip1 inhibits DNA replication but not PCNA-dependent nucleotide excision-repair. *Curr Biol.* 4:1062-8.
- Solomon, D.A., M.C. Cardoso, and E.S. Knudsen. 2004. Dynamic targeting of the replication machinery to sites of DNA damage. *J Cell Biol.* 166:455-63.
- Soutoglou, E., J.F. Dorn, K. Sengupta, M. Jasin, A. Nussenzweig, T. Ried, G. Danuser, and T. Misteli. 2007. Positional stability of single double-strand breaks in mammalian cells. *Nat Cell Biol.*
- Spada, F., A. Haemmer, D. Kuch, U. Rothbauer, L. Schermelleh, E. Kremmer, T. Carell, G. Langst, and H. Leonhardt. 2007. DNMT1 but not its interaction with the replication machinery is required for maintenance of DNA methylation in human cells. *J Cell Biol.* 176:565-71.
- Sporbert, A., P. Domaing, H. Leonhardt, and M.C. Cardoso. 2005. PCNA acts as a stationary loading platform for transiently interacting Okazaki fragment maturation proteins. *Nucleic Acids Res.* 33:3521-8.
- Sporbert, A., A. Gahl, R. Ankerhold, H. Leonhardt, and M.C. Cardoso. 2002. DNA polymerase clamp shows little turnover at established replication sites but sequential de novo assembly at adjacent origin clusters. *Mol Cell.* 10:1355-65.
- Stelter, P., and H.D. Ulrich. 2003. Control of spontaneous and damage-induced mutagenesis by SUMO and ubiquitin conjugation. *Nature.* 425:188-91.
- Suter, B., D. Auerbach, and I. Stagljar. 2006. Yeast-based functional genomics and proteomics technologies: the first 15 years and beyond. *Biotechniques.* 40:625-44.
- Tashiro, S., J. Walter, A. Shinohara, N. Kamada, and T. Cremer. 2000. Rad51 accumulation at sites of DNA damage and in postreplicative chromatin. *J Cell Biol.* 150:283-91.
- Taylor, R.M., J. Whitehouse, E. Cappelli, G. Frosina, and K.W. Caldecott. 1998a. Role of the DNA ligase III zinc finger in polynucleotide binding and ligation. *Nucleic Acids Res.* 26:4804-10.
- Taylor, R.M., B. Wickstead, S. Cronin, and K.W. Caldecott. 1998b. Role of a BRCT domain in the interaction of DNA ligase III-alpha with the DNA repair protein XRCC1. *Curr Biol.* 8:877-80.
- Thomas, M.C., and C.M. Chiang. 2006. The general transcription machinery and general cofactors. *Crit Rev Biochem Mol Biol.* 41:105-78.
- Thompson, L.H., K.W. Brookman, L.E. Dillehay, A.V. Carrano, J.A. Mazrimas, C.L. Mooney, and J.L. Minkler. 1982. A CHO-cell strain having hypersensitivity to mutagens, a defect in DNA strand-break repair, and an extraordinary baseline frequency of sister-chromatid exchange. *Mutat Res.* 95:427-40.

- Timson, D.J., M.R. Singleton, and D.B. Wigley. 2000. DNA ligases in the repair and replication of DNA. *Mutat Res.* 460:301-18.
- Tom, S., L.A. Henricksen, and R.A. Bambara. 2000. Mechanism whereby proliferating cell nuclear antigen stimulates flap endonuclease 1. *J Biol Chem.* 275:10498-505.
- Trucco, C., F.J. Oliver, G. de Murcia, and J. Menissier-de Murcia. 1998. DNA repair defect in poly(ADP-ribose) polymerase-deficient cell lines. *Nucleic Acids Res.* 26:2644-9.
- Tsukamoto, T., N. Hashiguchi, S.M. Janicki, T. Tumber, A.S. Belmont, and D.L. Spector. 2000. Visualization of gene activity in living cells. *Nat Cell Biol.* 2:871-8.
- Tumber, T., G. Sudlow, and A.S. Belmont. 1999. Large-scale chromatin unfolding and remodeling induced by VP16 acidic activation domain. *J Cell Biol.* 145:1341-54.
- Umar, A., A.B. Buermeyer, J.A. Simon, D.C. Thomas, A.B. Clark, R.M. Liskay, and T.A. Kunkel. 1996. Requirement for PCNA in DNA mismatch repair at a step preceding DNA resynthesis. *Cell.* 87:65-73.
- van Attikum, H., and S.M. Gasser. 2005. The histone code at DNA breaks: a guide to repair? *Nat Rev Mol Cell Biol.* 6:757-65.
- Vazquez, J., A.S. Belmont, and J.W. Sedat. 2001. Multiple regimes of constrained chromosome motion are regulated in the interphase Drosophila nucleus. *Curr Biol.* 11:1227-39.
- Vodenicharov, M.D., F.R. Sallmann, M.S. Satoh, and G.G. Poirier. 2000. Base excision repair is efficient in cells lacking poly(ADP-ribose) polymerase 1. *Nucleic Acids Res.* 28:3887-96.
- Volker, M., M.J. Mone, P. Karmakar, A. van Hoffen, W. Schul, W. Vermeulen, J.H. Hoeijmakers, R. van Driel, A.A. van Zeeland, and L.H. Mullenders. 2001. Sequential assembly of the nucleotide excision repair factors in vivo. *Mol Cell.* 8:213-24.
- Walter, J., T. Cremer, K. Miyagawa, and S. Tashiro. 2003. A new system for laser-UVA-microirradiation of living cells. *J Microsc.* 209:71-5.
- Wang, H., B. Rosidi, R. Perrault, M. Wang, L. Zhang, F. Windhofer, and G. Iliakis. 2005. DNA ligase III as a candidate component of backup pathways of nonhomologous end joining. *Cancer Res.* 65:4020-30.
- Wang, J.Y., A.H. Sarker, P.K. Cooper, and M.R. Volkert. 2004. The single-strand DNA binding activity of human PC4 prevents mutagenesis and killing by oxidative DNA damage. *Mol Cell Biol.* 24:6084-93.
- Wang, K.Y., and C.K. James Shen. 2004. DNA methyltransferase Dnmt1 and mismatch repair. *Oncogene.* 23:7898-902.
- Wang, Z.Q., L. Stingl, C. Morrison, M. Jantsch, M. Los, K. Schulze-Osthoff, and E.F. Wagner. 1997. PARP is important for genomic stability but dispensable in apoptosis. *Genes Dev.* 11:2347-58.
- Warbrick, E. 2000. The puzzle of PCNA's many partners. *Bioessays.* 22:997-1006.
- Wei, Y.F., P. Robins, K. Carter, K. Caldecott, D.J. Pappin, G.L. Yu, R.P. Wang, B.K. Shell, R.A. Nash, P. Schar, and et al. 1995. Molecular cloning and expression of human cDNAs encoding a novel DNA ligase IV and DNA ligase III, an enzyme active in DNA repair and recombination. *Mol Cell Biol.* 15:3206-16.
- Werten, S., and D. Moras. 2006. A global transcription cofactor bound to juxtaposed strands of unwound DNA. *Nat Struct Mol Biol.* 13:181-2.

-
- Werten, S., G. Stelzer, A. Goppelt, F.M. Langen, P. Gros, H.T. Timmers, P.C. Van der Vliet, and M. Meisterernst. 1998. Interaction of PC4 with melted DNA inhibits transcription. *Embo J.* 17:5103-11.
- Wu, S.Y., and C.M. Chiang. 1998. Properties of PC4 and an RNA polymerase II complex in directing activated and basal transcription in vitro. *J Biol Chem.* 273:12492-8.
- Xu, G.L., T.H. Bestor, D. Bourc'his, C.L. Hsieh, N. Tommerup, M. Bugge, M. Hulten, X. Qu, J.J. Russo, and E. Viegas-Pequignot. 1999. Chromosome instability and immunodeficiency syndrome caused by mutations in a DNA methyltransferase gene. *Nature.* 402:187-91.



5. CURRICULUM VITAE

Name: **Oliver Mortusewicz**
Address: Ludwig Maximilians University, Dept. Biology II,
Biocenter, Großhaderner Str. 2,
82152 Planegg-Martinsried, Germany
Date of Birth: 10/ 01/ 1978
Place of Birth: Giessen

Education:

1998 Allgemeine Hochschulreife (grade 1.7)
Hanns-Seidel-Gymnasium
Hösbach, Germany

1999-2002 Intermediate Diploma (grade 1.3)
University of Kaiserslautern
Kaiserslautern, Germany

2002-2005 Diploma in Biology (grade 1.1)
Ludwig Maximilians University Munich
Munich, Germany

2005- PhD in Biology
Ludwig Maximilians University Munich
Munich, Germany

Positions and teaching:

2005 student assistant in the group of Prof. H. Leonhardt
2005-present graduate student in the group of Prof. H. Leonhardt
2006-2007 supervision of basic and advanced practical courses
2007 co-supervision of the diploma thesis of Regina Kleinhans

Conference contributions and talks:

September, 2005, **Oliver Mortusewicz**, Lothar Schermelleh, Joachim Walter, M. Cristina Cardoso and Heinrich Leonhardt , “Recruitment of genetic and epigenetic repair factors in living cells.” Poster at the *19th International Workshop on The Cell Nucleus (The Wilhelm Bernhard Workshop)*, Münsterschwarzach Abbey, Germany

December, 2005, **Oliver Mortuserwicz**, “Recruitment of genetic and epigenetic repair factors in living cells.” Talk at the *Workshop on Cell Biology and Microscopy*, Altleinigen, Germany

July, 2006, **Oliver Mortusewicz**, Lothar Schermelleh, Ulrich Rothbauer, M. Cristina Cardoso and Heinrich Leonhardt, “Analysis of the recruitment of genetic and epigenetic repair factors in living cells.” Poster at the *International Symposium on Optical Analysis of Biomolecular Machines*, Berlin, Germany

January, 2007, **Oliver Mortusewicz**, “Recruitment of repair factors to DNA damage sites in living cells.” Invited talk at the *Ecole Supérieure de Biotechnologie de Strasbourg*, Strasbourg, France

List of publications:

Mortusewicz, O., L. Schermelleh, J. Walter, M.C. Cardoso, and H. Leonhardt. 2005. Recruitment of DNA methyltransferase I to DNA repair sites.

Proc Natl Acad Sci U S A. 102:8905-9.

Perucca, P., O. Cazzalini, **O. Mortusewicz**, D. Necchi, M. Savio, T. Nardo, L.A. Stivala, H. Leonhardt, M.C. Cardoso, and E. Prosperi. 2006. Spatiotemporal dynamics of p21CDKN1A protein recruitment to DNA-damage sites and interaction with proliferating cell nuclear antigen. *J Cell Sci. 119:1517-27.*

Mortusewicz, O., U. Rothbauer, M.C. Cardoso, and H. Leonhardt. 2006. Differential recruitment of DNA Ligase I and III to DNA repair sites. *Nucleic Acids Res. 34:3523-32.*

Mortusewicz, O., and H. Leonhardt. 2007. XRCC1 and PCNA are loading platforms with distinct kinetic properties and different capacities to respond to multiple DNA lesions. *BMC Mol Biol. 8:81.*

Mortusewicz, O., Amé, J.-C., Schreiber, V. and Leonhardt, H. Feedback regulated poly(ADP-ribosyl)ation by PARP-1 is required for rapid response to DNA damage in living cells. *Nucleic Acids Res.*

Mortusewicz, O., Roth, W., Cardoso M.C., Meisterernst, M and Leonhardt, H. Recruitment of RNA Polymerase II cofactor PC4 to DNA repair sites. *Under Revision at the Journal of Cell Biology*

Zolghadr, K., **Mortusewicz, O.**, Rothbauer, U., Kleinhans, R., Göhler, H., Wanker, E., Cardoso, M.C. and Leonhardt, H. A fluorescent two-hybrid (F2H) assay for direct visualization of protein interactions in living cells. *Submitted to Nature Methods.*